MERCURY AT THE TERRESTRIAL-AQUATIC INTERFACE: THE BIOGEOCHEMICAL CYCLING OF MERCURY IN WETLANDS OF DIFFERENT HYDROGEOLOGIC SETTING, AND DURING SNOWMELT IN A FORESTED HEADWATER STREAM

A Dissertation

Presented to the Faculty of the Graduate School

of Cornell University

in Partial Fulfillment of the Requirements for the Degree of

Doctor of Philosophy

by

Jason D. Demers

May 2009

MERCURY AT THE TERRESTRIAL-AQUATIC INTERFACE: THE BIOGEOCHEMICAL CYCLING OF MERCURY IN WETLANDS OF DIFFERENT HYDROGEOLOGIC SETTING, AND DURING SNOWMELT IN A FORESTED HEADWATER STREAM

Jason D. Demers, Ph.D.

Cornell University 2009

Anthropogenic emissions of mercury into the atmosphere have increased mercury deposition that, in turn, has led to a large legacy of mercury accumulation in terrestrial ecosystems and increased mercury contamination of surface waters. Despite efforts to control anthropogenic emissions of mercury, it is possible that release of mercury historically deposited to forests and wetlands will moderate the recovery of aquatic ecosystems. This research examined the biogeochemical cycling of mercury in different wetland types in the Adirondack region of New York and in a forested headwater catchment during snowmelt at the Hubbard Brook Experimental Forest (HBEF) in the White Mountains of New Hampshire.

Mercury pool size varied across the upland-wetland interface, among wetland types, across individual wetland transects, and along depth profiles in soils of forests and wetlands of the Adirondack region. In mineral horizons of uplands and shallow peat riparian wetlands, mercury was strongly correlated with carbon ($p=0.002$, $r^2=0.73$), and nitrogen ($p<0.001$, $r^2=0.82$), but not sulfur. In contrast, there was a strong correlation between mercury and sulfur in peat of headwater wetlands ($p<0.0001$, $r^2=0.60$). Flux estimates suggest a mean residence time of 590 years (SE =

69) for mercury in headwater wetlands and shallow peat riparian wetlands, and >10,000 years in deep peat riparian wetlands.

Concentrations of mercury and methyl mercury in wetland peat porewater and streams varied seasonally and among wetland types. Differences in mercury:carbon stoichiometry among wetland types suggested that the supply of mercury was limited relative to DOC binding sites in headwater wetlands, whereas mercury:carbon ratios converged toward a maximum in riparian wetlands, a condition suggestive of mercury saturation. High dissolved methyl mercury concentrations in peat porewater occurred at low nitrate concentrations ($p<0.0001$), suggesting redox reactions associated with nitrate can inhibit microbial methylation of mercury.

At the HBEF, dissolved organic carbon mobilized from shallow organic soils during snowmelt resulted in the mobilization of mercury from these same sources. Overall, this research on the biogeochemistry of mercury highlights the linkages between hydrological processes and organic matter dynamics that function as master variables influencing the ultimate fate of a large legacy of mercury accumulation in forest and wetland ecosystems.

BIOGRAPHICAL SKETCH

Jason D. Demers was born on November 22, 1972, in Dover, New Hampshire. He graduated from Dover High School in 1991. Having become interested in chemistry and biology, Jason began his pre-med studies as a Granite State Fellowship recipient at the University of New Hampshire. Determined to prepare himself for a medical career, he enrolled in an Emergency Medical Technician course, and quickly learned that spending time in hospitals resulted in his loss of consciousness. Thus, he refocused his academic pursuits on ecology and ecosystem science, and completed a senior thesis studying sugar maple distribution along elevational gradients in the White Mountains of New Hampshire. Jason graduated summa cum laude with a bachelor of science in general biology from the University of New Hampshire in 1995.

In June 1996, Jason began a temporary research technician job with the Institute of Ecosystem Studies at the Hubbard Brook Experimental Forest in New Hampshire. The two-month appointment became three months, three months drifted into six months, and six months blurred into five years. Amidst his tenure at IES, Jason hiked the Appalachian Trail in 1997 and traveled to the mountains of the Dominican Republic in 2000 to study forest ecology. Jason started his master of science degree in the Department of Natural Resources at Cornell University in July 2001, where he began studying mercury biogeochemistry and actively participated in Cornell's Program in Biogeochemistry. Within weeks, he requested to change his degree goals from M.S. to M.S./Ph.D. Jason completed the degree of master of science in natural resources at Cornell University in 2005, and immediately continued on in his pursuit of a doctoral degree.

ACKNOWLEDGMENTS

The work contained herein could not have been accomplished without the encouragement and wisdom of those I have encountered along the way.

I thank my parents, Alfred and Carolyn, for always encouraging me in my academic pursuits, as well as not too often asking when I would be finished.

Two teachers from Dover High School were particularly influential in my development as a scientist. Walter Bullock taught me the foundations of chemistry, the first principles of which I find myself returning to on a daily basis. Linda Albright taught me the foundations of biology and wisely advised me to focus on the basics of chemistry to better prepare myself for college, and inadvertently, the rest of my career.

Tom Lee, my undergraduate honors thesis advisor, initiated me into the discipline of ecology and began teaching me to approach scientific research in a logical, professional manner. He instilled in me the belief that it is crucial to get out into the field, ramble about, and truly observe the world that we are attempting to understand and interpret. Perfecting that art will always be a work in progress.

My experiences at the Hubbard Brook Experimental Forest have been, and continue to be, pivotal. Sandy Tartowski hired me for my first technician position at the HBEF, and kept me on despite the fact that I broke my ankle on the second day of my first summer field season. Her insightfulness, intellect, and zest for science remain an inspiration. Don Buso was instrumental in developing my skills in the field. Peter Groffman remains one of the best supervisors and mentors with whom I have worked.

Many friends and assistants have helped with this research in the field and in the lab over the past several years, including Darren James, Ava Goodale, Sara Cohen, Christine Voyer, Melanie Hayn, Sophia Montesdeoca, and Janet Towse. I thank them all for maintaining a sense of humor amidst the mayhem and tedium of the field and lab.

Mario Montesdeoca has tirelessly shared his technical laboratory expertise and management savvy. The QCQA and technical research skills I have learned from Mario have made me a more capable and confident research scientist. His friendship and his humor, especially amidst difficulty, has been a welcome relief. Thank you.

My fellow graduate students have tremendously enriched my experience at Cornell. The members of F-House, the Bruckner Group, and the Biogeochemistry Program have pushed my thinking to be broader and deeper, generously passing along the wisdom they themselves had gained through their own toil. I thank them all for the many (often late night) scientific exchanges, their infinite willingness to review proposals and manuscripts, and especially for their camaraderie.

I am greatly appreciative of the funding sources that have contributed to this research. This research is partially based upon work supported under a National Science Foundation Graduate Research Fellowship. Any opinions, findings, conclusions, or recommendations expressed in this publication are those of the author and do not necessarily reflect the views of the National Science Foundation. This research was also supported with funding from a fellowship for continuing students and from the Small Grants Program within the NSF IGERT Program in Biogeochemistry and Environmental Biocomplexity at Cornell University. Additional funding was contributed by the Syracuse Center of Excellence 2006 Graduate Fellowship Program through a grant from the United States Environmental Protection Agency (No. X-83232501-0). The USDA Forest Service provided hydrologic and climatic data for the aspects of this research undertaken at the Hubbard Brook Experimental Forest, and their support has been invaluable to this study. Some data used in this research were obtained by scientists of the Hubbard Brook Ecosystem Study; this dissertation has not been reviewed by those scientists. The Hubbard Brook Experimental Forest is operated and maintained by the Northern Research Station,

U.S. Department of Agriculture, Newton Square, Pennsylvania. Other funding sources include the Kieckhefer Foundation, the Society of Wetland Scientists, Sigma Xi, the New York State Research and Development Authority, the U.S. Environmental Protection Agency, and the NSF Long-Term Ecological Research (No. 46222-7759) program at Hubbard Brook. Additionally, I would like to thank all of my committee members for their financial support for what has turned out to be a logistically difficult and expensive field of research.

I continue to be struck by the generosity and selflessness of my committee. As my committee chair, Joe Yavitt has helped me balance my quest for perfection with the reality of needing to finish my dissertation, and publish. I am grateful for his open-door policy, as many of our best conversations have occurred outside the confines of scheduled meetings. After nearly a decade since my college chemistry classes, Murray McBride initiated me upon my return to graduate school with his course *Environmental Chemistry of Soils*. His course and seemingly endless expertise was, no doubt, an awakening to the task that lay before me; a quite worn copy of his text is still never far from hand. During my first semester at Cornell, I also had the opportunity to serve as teaching assistant for Barbara Bedford's course *Wetland Ecology and Management*. This experience, in addition to the many conversations I continued to have with Barbara, provided a framework for the study of wetlands that served as a foundation for my research. Tim Fahey, through advice and example, has taught me to think and act more deliberately and (hopefully) with greater insight. Tim has also helped me to maintain perspective, and encouraged me to "keep my head down, and get my work done," which is advice that has and surely will continue to pay dividends. Charley Driscoll has enthusiastically incorporated me into his lab group at Syracuse University, invited me to participate in numerous research opportunities, and has provided unlimited access to his laboratory facilities, upon which all of my

research has depended. I will undoubtedly be paying these debts forward for the rest of my career. All of my committee members have given me the necessary autonomy that has allowed me to develop as an independent thinker and scientist, and have treated me as a colleague more often than they have treated me as a student. I look forward to continuing our collaborations.

TABLE OF CONTENTS

LIST OF FIGURES

LIST OF TABLES

PREFACE

Anthropogenic emissions of mercury into the atmosphere have increased mercury deposition that, in turn, has led to a large legacy of mercury accumulation in terrestrial soils and increased mercury contamination of aquatic ecosystems. This has resulted in the bioaccumulation of methyl mercury in fish tissue to concentrations that both exceed Environmental Protection Agency recommendations for human consumption and pose health risks to wildlife. Efforts to reduce anthropogenic emissions of mercury to the atmosphere are intended to reduce surface water mercury contamination. However, we do not know the rate at which mercury contaminated surface waters might recover in response to reduced atmospheric mercury deposition. Whereas some amount of initial recovery should be rapid, it is possible that chronic accumulation of mercury in soils of forests and wetlands will moderate recovery of aquatic ecosystems, as large repositories of historically deposited mercury are released to surface waters. Thus, the overarching objective of this dissertation was to improve our understanding of the ultimate fate of this mercury that has accumulated in forest and wetland soils.

The four chapters of this dissertation are linked by two themes: (1) the influence of hydrologic mechanisms on the biogeochemical cycling of mercury at the terrestrial-aquatic interface (i.e., in wetlands and headwater streams); and (2) the role of organic matter and inferred decomposition processes in the retention, transformation, release, transport, and residence time of mercury.

In the first three chapters, I quantify differences in the biogeochemistry of mercury among wetlands of different hydrogeologic setting in the Adirondack region of New York State. These chapters compare predominantly ombrotrophic headwater bogs influenced primarily by precipitation, with riparian wetlands that are strongly influenced by groundwater and surface water. The objective of Chapter 1 was to

quantify mercury pool size and stoichiometry with carbon, nitrogen, and sulfur in soils across upland-wetland transects. The objective of Chapter 2 was to quantify the concentration of mercury in porewater and stream water, and to estimate the flux and residence time of mercury and methyl mercury from wetlands of different hydrogeologic setting. In Chapter 2, I further discuss differences in mercury:carbon stoichiometry in porewater and stream water of these different wetland types. In Chapter 3, I present evidence supporting the inhibition of methyl mercury production by redox conditions in freshwater wetlands.

In Chapter 4, the research crosses into a more forested landscape, the Hubbard Brook Experimental Forest in the White Mountains of New Hampshire, and quantifies the hydrologic flow paths, source areas, and supply of dissolved organic carbon that link episodic acidification and mercury mobilization during snowmelt.

Overall, this dissertation highlights the linkages between hydrological processes and organic matter dynamics that function as master variables influencing the ultimate fate of vast pools of mercury accumulated in forest and wetland ecosystems.

CHAPTER ONE:
THE INFLUENCE OF HYDROGEOLOGIC SETTING ON MERCURY POOL SIZE AND STOICHIOMETRY WITH C, N, & S ACROSS UPLAND-WETLAND INTERFACES.

ABSTRACT

Elevated atmospheric deposition of mercury since the mid-1800s industrial revolution has led to a large legacy of mercury accumulation in wetlands. However, the influence of different wetland types on the retention and biogeochemical cycling of mercury within wetlands remains unclear. In this study, mercury pool sizes and stoichiometry with C, N, and S are quantified across upland-wetland transects and among wetlands of different hydrogeologic setting in the Adirondack region of New York State. The pool size of mercury varied across the upland-wetland interface, among wetland types, across individual wetland transects, and along depth profiles in soils of forests and wetlands of the Sunday Lake watershed. Total mercury pool size was greater in upland soils than in wetland soils (to 50 cm depth, $p<0.01$). Shallow peat riparian wetlands had greater mercury pool size (to 50 cm depth) than deep peat riparian or headwater wetlands ($p<0.099$, $p<0.046$). There was greater accumulation of mercury at the upland-wetland interface in deep peat riparian and headwater wetlands as compared to the overall wetland transect ($p=0.008$). In mineral horizons of the uplands and shallow peat riparian wetlands, mercury was strongly correlated with carbon ($p=0.002$, $r^2=0.73$), and nitrogen ($p<0.001$, $r^2=0.82$), but not sulfur. In deep peat riparian and headwater wetlands, there was no relationship between mercury and carbon or nitrogen; however, there was a strong correlation between mercury and sulfur in the peat of headwater wetlands ($p<0.0001$, $r^2=0.60$). Hydrogeologic setting influences decomposition processes, biogeochemical cycling of mercury, and

hydrologic transport that, in turn, govern the size, distribution, and stoichiometry of mercury pools across the upland-wetland interface, along peat depth profiles, and among different wetland types.

INTRODUCTION

In the Adirondack region of New York State, the current rate of mercury deposition is 3.5x the mercury deposition rate of the mid-1800s (Lorey and Driscoll 1999). This modern rate of mercury deposition has led to a large legacy of mercury accumulation in forest and wetland soils (e.g., Benoit et al. 1994, Grigal 2003). Current legislative efforts to decrease anthropogenic emissions of mercury into the atmosphere are intended to reduce surface water mercury contamination and subsequent bioaccumulation in fish and associated biota. However, we do not know the rate at which mercury contaminated surface waters might recover in response to reduced atmospheric mercury deposition. While it is possible that recovery will be rapid, it is also possible that chronic accumulation of mercury in forests and wetland soils will moderate recovery of aquatic ecosystems as large repositories of historically deposited mercury are transformed to bioavailable methyl mercury and exported to surface waters. However, because of the complex cycling and speciation of mercury in the environment, the ultimate fate of mercury retained in wetlands is difficult to predict.

Wetlands function as ecological and biogeochemical linkages between terrestrial and aquatic ecosystems; and biogeochemical mass-balance studies traditionally classify wetlands as sources or sinks with respect to the cycling of nutrients and other chemical components in the environment. Whether a wetland functions as a source or sink depends upon relative rates of inputs and outputs. The rate at which changing inputs translates into altered source/sink dynamics is controlled

by pool size and residence time (Aber and Mellilo 2001). Thus, the degree to which observed changes in mercury outputs from wetlands will lag behind changes in mercury loading should be more dependent upon pool size and residence time than on current rates of mercury deposition. Most studies concerning the fate of total mercury (i.e., all forms of mercury) and methyl mercury (i.e., the neurotoxic bioaccumulating form of mercury) at the interface of wetland and aquatic ecosystems have focused on only the present day flux of mercury and methyl mercury, and have seldom considered the pool size and residence time of mercury within the wetlands. This study quantifies pool sizes of mercury and possible mechanisms for retention of that mercury in different wetland types; quantifying pool sizes is a critical first step toward estimating the residence time of mercury in wetlands.

Wetlands are traditionally defined by their hydrology, physicochemical environment, and biota (Mitch and Gosselink 2000). However, hydrogeologic setting has been recognized as a primary factor influencing wetland structure and function (Winter 1988, 1992, Brinson 1993, Bedford 1996, 1999). In essence, the distribution of wetlands and varying wetland types across the landscape is a manifestation of local and regional hydrological processes, and the interaction of those hydrological processes with geological characteristics. The hydrogeologic setting of a wetland links landscape position and surficial geology to the resulting hydrologic regime, water chemistry, and the chemistry and accumulation of wetland soils (Winter 1988, Winter and Woo 1990, 1992, Bedford 1996, Hill and Devito 1997, 1999). In this study, I use hydrogeologic setting (Winter 1988, 1992, Bedford 1996, 1999) as a framework within which to assess differences in the biogeochemical cycling of mercury in wetlands across a post-glacial Adirondack landscape. Hydrogeologic setting of a wetland influences water table level and fluctuation and thus the duration of soil saturation, as well as the supply of nutrients and electron acceptors. Together,

these hydrological and geochemical factors influence the rate of production and decomposition of organic matter, the balance of which controls the formation and rate of accumulation of peat. These hydrological and geochemical factors also influence the biogeochemical pathways of decomposition; soil saturation results in anoxic conditions, and the availability of alternate electron acceptors influences which anaerobic decomposition pathways dominate (e.g., denitrification, sulfate reduction). Given the importance of organic matter in the retention of mercury (e.g., Mieli 1991, Grigal 2003) these hydrogeologically linked factors likely influence the fate of mercury within different wetland types.

Connectivity between terrestrial and aquatic ecosystems has emerged as an important characteristic influencing mercury supply to surface waters, and hydrogeologic setting places a large emphasis on the placement of a wetland within the landscape and the hydrologic connectivity between the upland and the wetland (Bedford 1996, 1999). Understanding the role of wetlands in this upland-wetland-surface water linkage becomes increasingly important as we attempt to predict the rate of recovery of surface waters following reductions in mercury loading. Not only does hydrogeologic setting enable one to consider wetlands within the context of the broader landscape, but the influence of hydrogeologic setting on the biogeochemical cycling of mercury may provide a more mechanistic framework within which to interpret and predict the role of varying wetland types in mediating upland-surface water connectivity and the retention of mercury within wetland ecosystems.

The objective of this study was to quantify mercury pool size and stoichiometry with carbon, nitrogen, and sulfur in wetlands of different hydrogeologic setting across upland-wetland transects in a glaciated landscape. I compared ombrotrophic headwater bogs influenced primarily by precipitation, and riparian wetlands that are strongly influenced by groundwater and surface water, to evaluate

the role of hydrogeologic settings in determining the quantity of mercury and the character of mercury-element interactions in soils. I hypothesized that differences in the hydrology and associated mode of decomposition would result in characteristic differences in the distribution and elemental stoichiometry of mercury along upland-wetland transects and among wetlands of different hydrogeologic setting.

METHODS

Site description

This research was conducted in the Sunday Lake watershed located near the Stillwater Reservoir along the southwestern boundary of the Adirondack region of New York, USA (43°51'40" N, 74°06'07"W). Average precipitation is ~1300 mm/yr (1971-2000 mean), with about 30% delivered as snow (data from Big Moose Station and available online at http://climod.nrcc.cornell.edu). Sunday Lake has two inlets, with combined watershed area of ~1273 ha. Vegetation cover is typical north temperate mixed deciduous and coniferous forest, with the coniferous forests predominantly surrounding ponds, wetlands, and stream corridors. The upland soils of this watershed are mostly well drained spodosols (Typic Haplorthods) with a sandy loam to loamy sand texture overlying glacial till or glacial outwash (Demers 2007). Eskers are a distinctive feature of the landscape in the vicinity of Sunday Lake and provide a complex series of ridges and depressions resulting in myriad wetlands and numerous wetland types, which reflect differences in hydrogeologic setting. The highest density of wetlands occurs amidst the esker terrain; however, numerous wetlands also occur in areas of the watershed underlain by glacial till, especially along stream corridors and in the headwaters of each sub-watershed. I selected two hydrogeologic settings that result in different wetland structure and function.

At one end of the hydrologic gradient were two “headwater wetlands”. In terms of the physiographic settings framed by Winter (1988, 1992), these are depressional wetlands typical of Wisconsinan-age glacial terrain of the north-central and northeastern United States. These headwater wetlands are perched in depressions formed by eskers and are elevated above the lower stream valleys within the watershed; thus they have no inlet streams and very small watersheds that influence only edges of the wetlands. Away from the upwelling gradients associated with the break in slope at the edges of these headwater wetlands, the central portions of these headwater wetlands are ombrotrophic bogs with strong recharge gradients and hydrologic inputs dominated by precipitation (Appendix A, Appendix B). Both headwater wetland sites are dominated by sphagnum moss (*Sphagnum* spp.); one headwater wetland site has an open central pond and a scrub-forest fringe dominated by red spruce (*Picea rubens* Sarg.), black spruce (*Picea mariana* Mill.), and American larch (*Larix laricina* Du Roi), whereas the second headwater wetland site is more densely forested. The water table is near the surface of the peat in both headwater wetlands throughout the year, resulting in permanently saturated conditions, and peat accumulation that has reached ~ 7 m in depth.

At the other end of the hydrologic gradient were four “riparian wetlands”, which I further differentiated into two “deep peat riparian” and two “shallow peat riparian” wetlands. In the terms of Winter (1988, 1992), these riparian wetlands occur in a physiographic setting of steep slopes adjacent to narrow lowlands, typical in mountainous terrain but common at both large and small scales. Thus, the riparian wetlands result from discontinuities in the slope of the water table and land surface, and can be influenced by groundwater, surface water, and precipitation inputs. Stratigraphy within the riparian wetlands differentiates the shallow and deep peat riparian wetlands, and influences the flow of water through them. Both the shallow

and deep peat riparian wetlands are influenced by local upwelling (discharge) zones at the break in slope at the upland-wetland interface (Appendix A, Appendix B). However, movement of subsurface water across the deep peat riparian wetlands is limited by the low hydraulic conductivity of the peat (*see* Chapter 2). In the shallow peat riparian wetlands, subsurface water movement across the wetland is less restricted, and underflow of subsurface water originating from both the adjacent slope and the adjacent stream interacts with the shallow peat. The deep peat riparian wetlands ranged from ~5-6m maximum peat depth, and were dominated by sedges (*Carex* spp), broad leaved deciduous shrubs (e.g., *Myrica gale*), and occasional occurrence of spruce and larch. The shallow peat riparian wetlands seldom exceeded peat depths of ~35cm, but were also dominated by sedge species, with speckled alder (*Aldus rugosa*) present in dense patches, and occasional occurrence of red spruce and American larch. The water table fluctuates more in the riparian wetlands than in the headwater wetlands, episodically rising to the surface of the peat and seasonally dropping more than 50 cm below the surface of the peat in shallow peat riparian wetlands.

Sampling procedures

An upland-wetland transect was established across the entirety of each of the six study wetlands. Transect length ranged ~10-20 m in the shallow peat riparian wetlands, to ~60-80 m in the deep peat riparian wetlands, and ~75 – 135 m in the headwater wetlands. Along each transect, at least six wetland soil sampling points were established between the upland-wetland interface and the outlet or riparian stream (a greater number of cores were taken from longer transects). An upland soil sampling point was located 1m upslope of the upland-wetland interface of each wetland.

Wetland soil cores were obtained with a stainless-steel hemispherical peat corer (5.5 cm diameter) in order to minimize compaction of peat samples. The top 50 cm of each wetland core was sectioned into 5 cm increments. An additional 10 cm increment of each peat core was sampled at a depth of 90-100 cm, and at each additional meter of depth throughout the entire wetland peat profile. Upland soil cores were obtained with acid-washed split PVC cores (5.2 cm diameter), horizons (forest floor, A, E, B) were delineated in the field and the depth of each horizon was verified by "in-hole" measurements. All soil samples were double-bagged in Ziploc bags, frozen immediately upon return from the field, and freeze-dried in preparation for analysis.

Sample analysis

Soil samples were analyzed for total mercury using a hot refluxing nitric:sulfuric (3:7) acid digestion, followed by dilution and analysis with a Tekran 2600 Cold Vapor Atomic Fluorescence Spectrometer (CVAFS; Tekran, Toronto, Ontario, Canada). Soil carbon, nitrogen, and sulfur were analyzed with an Elemental Combustion System, Model ECS 4010 (Costech Analytical Technologies, Valencia, California, USA). Samples were analyzed in batches with quality control that included field blanks and duplicates; independent primary and secondary source standards; method detection limit check standards; analysis of appropriate certified reference materials; matrix spike and matrix spike duplicate samples to verify the absence of sample matrix interferences; as well as initial and ongoing calibration verification standards, initial and ongoing calibration blanks, and intitial and ongoing precision and recovery standards.

Pool size and stoichiometric calculations

Total pool size of mercury, carbon, nitrogen and sulfur in the top 50 cm of soils was based on measured concentrations, cross sectional area of the core, and total dry soil weight. In the wetland soils, pool size calculations were made separately for each 5 cm increment, and then summed over a depth of 50 cm. Wetland soil pool size beyond 50 cm in depth was determined by averaging pool size estimates at the top and bottom of each additional 1m segment and then extrapolating that value to each additional 1m segment. In the upland soils, pool size calculations were made separately for each soil horizon, and then summed over a depth of 50 cm.

Molar ratios of mercury with carbon, nitrogen, and sulfur were calculated based on the total pool size of each element within the top 50 cm of soil in the headwater and deep peat riparian wetlands. In the upland and shallow peat riparian soils, molar ratios were calculated separately for the organic and mineral soil horizons. Additionally, within the top 50 cm of each core, I assessed elemental correlations within individual wetland soil core segments and upland soil horizon samples in order to show the variability within molar ratios described for bulk soil pools.

Statistical procedures

Statistical procedures were performed with SAS (SAS Institute 1999). Difference in total mercury pool size between upland and wetland soils, and among wetland types was analyzed using balanced, fixed effects models (PROC GLM, SAS Institute 1999). All wetland soil cores across each individual wetland transect were averaged to obtain a single estimate of pool size for each wetland; thus, differences among wetland types were more difficult to detect because of a low number of replicate wetlands ($n = 2$ for each wetland type) and p-values < 0.1 were interpreted to indicate statistically significant differences. Differences between the pool size of

mercury at the upland-wetland edge of each wetland and the average pool size across the wetland transect were assessed with a paired t-test (PROC Means, SAS Institute 1999). Differences in the Hg:C, Hg:N, and Hg:S ratio between upland mineral and organic soil horizons, mineral soil horizons in the uplands and shallow peat riparian wetlands, upland organic horizon and peat at the wetland edge, and among wetland types were also determined using balanced, fixed effects models (PROC GLM, SAS Institute 1999). Correlation between mercury and carbon, mercury and nitrogen, and mercury and sulfur concentrations in individual samples was assessed using a regression model (PROC GLM, SAS Institute 1999); a multiple regression analysis was utilized to determine variability in mercury concentration that could be uniquely explained by carbon or nitrogen (PROC GLM, SAS Institute 1999).

RESULTS

Mercury pool size in forest soil and wetland peat

Total mercury pool size to a depth of 50 cm was greater in upland soils than in wetland soils on an areal basis (Figure 1.1; $p < 0.01$, $n = 12$). Among wetland types in this study, shallow peat riparian wetlands had a greater mercury content than deep peat riparian wetlands or headwater wetlands (Figure 1.1; $p < 0.099$, $p < 0.046$, respectively; $n = 2$ for each wetland site).

Much of the mercury pool in uplands and shallow peat riparian wetlands was associated with mineral soil horizons that have been enriched with organic matter from the overlying forest floor and wetland sedge peat, respectively. In contrast, there was no evidence of mineral soil in the top 50 cm of the deep peat riparian and headwater wetlands. The accumulation of mercury in the organic horizon alone (to a depth of 50 cm) did not differ among sites; however, including the entire peat profile mercury pool from deep peat riparian and headwater wetlands increased total wetland

mercury pool size. Mineral soil horizon samples from the uplands and shallow peat riparian wetlands were high in mercury concentration; whereas the mineral soils underlying deep peat sites were low in mercury concentration.

The accumulation of mercury in wetland soils varied across wetland transects, with a greater accumulation of mercury occurring at the upland-wetland interface in deep peat riparian and headwater wetlands (Figure 1.1; $p = 0.008$; $n=4$). However, there was no difference in the mercury pool at the edge of shallow peat riparian wetlands in comparison to the rest of the wetland transect, as the edge effect apparent in other wetland types appeared to extend across the entire transect in the (narrow) shallow peat riparian wetlands.

Stoichiometry of mercury, carbon, nitrogen, and sulfur

Molar ratios in soil pools. Molar ratios of mercury with carbon, nitrogen, and sulfur were quantified using total elemental pools in the top 50 cm of upland soil and in each wetland type. The molar ratio of mercury to carbon (Hg:C) varied between mineral and organic soil horizons and among wetland types. Within the upland soils, Hg:C ratio was almost 2x greater in the mineral horizon than in the organic horizon (Figure 1.2; $p = 0.0464$, $n = 6$ for each soil horizon). There was no consistent difference in Hg:C between the mineral soils of the upland versus that in shallow peat riparian wetlands. There was also no consistent difference between the Hg:C ratio in the upland organic horizon and peat at the wetland edge in all wetland types. However, the mean molar ratio of Hg:C from across the entire shallow peat riparian transect was greater than the mean Hg:C ratio across deep peat riparian and headwater wetland transects, regardless of edge effects (Figure 1.2, $p < 0.01$, $n = 2$ for each wetland type).

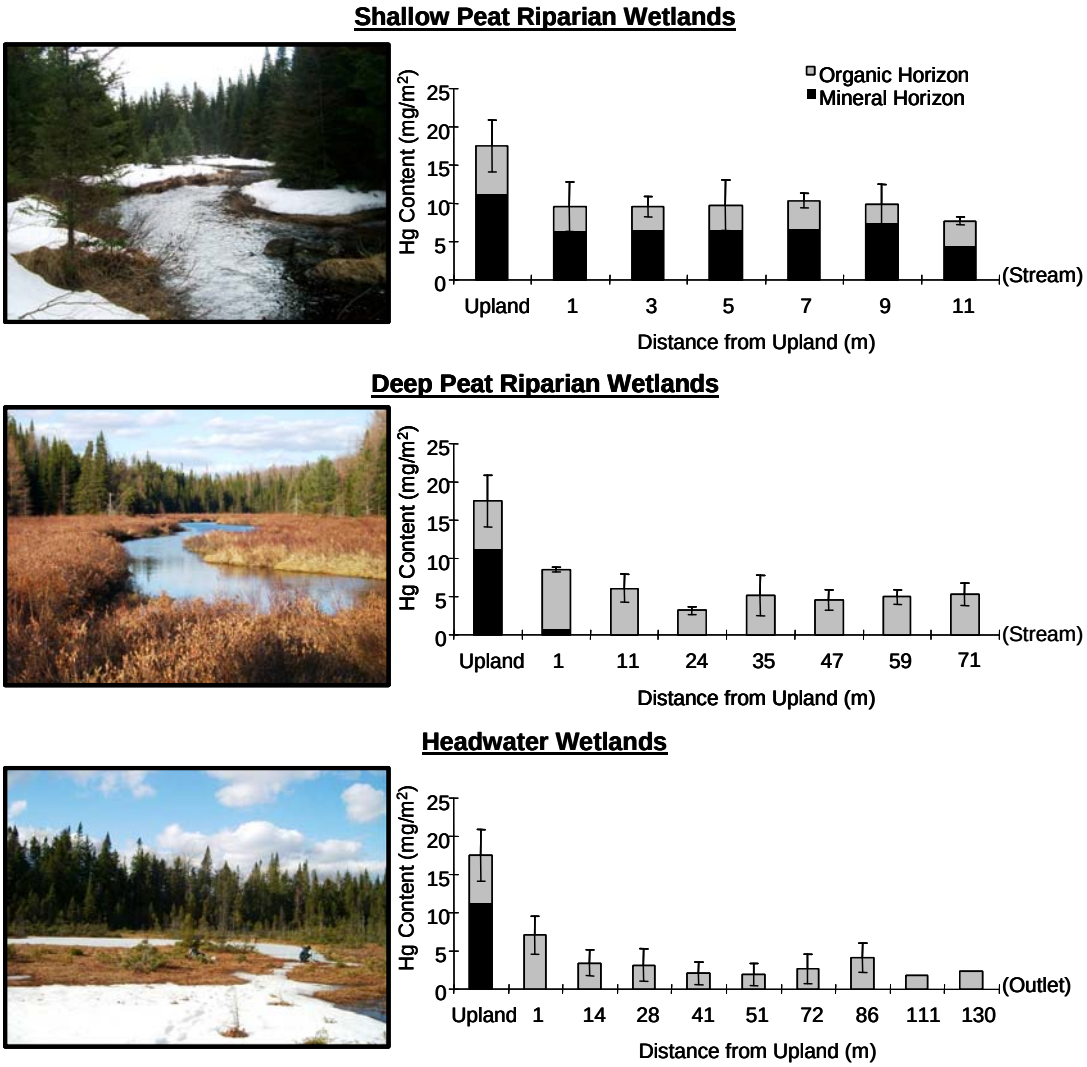

Figure 1.1. Mercury pool size in soil substrates along transects across different wetland types of the Sunday Lake watershed in the western Adirondack region of New York State. Bars represent mean total Hg pool in the top 50 cm of soil (n = 6 for upland; n = 2 for each wetland type). Error bars show +/- 1SE of total mercury pool in upland soils, whereas bars show the range of total mercury content along transects in individual wetlands. Distances along these generalized transects are approximate.

Figure 1.2. Mean accumulation of mercury per unit carbon, mercury per unit nitrogen, and mercury per unit sulfur in organic and mineral soil substrates of uplands and different wetland types in the Sunday Lake watershed located in the western Adirondack region of New York State. Upland samples were taken 1m from the wetland edge, wetland edge samples were taken 1m from the upland edge, wetland mean represents mean accumulation across wetland transects. Error bars associated with uplands show +/-1SE (n=6). Error bars associated with wetlands show range (n=2).

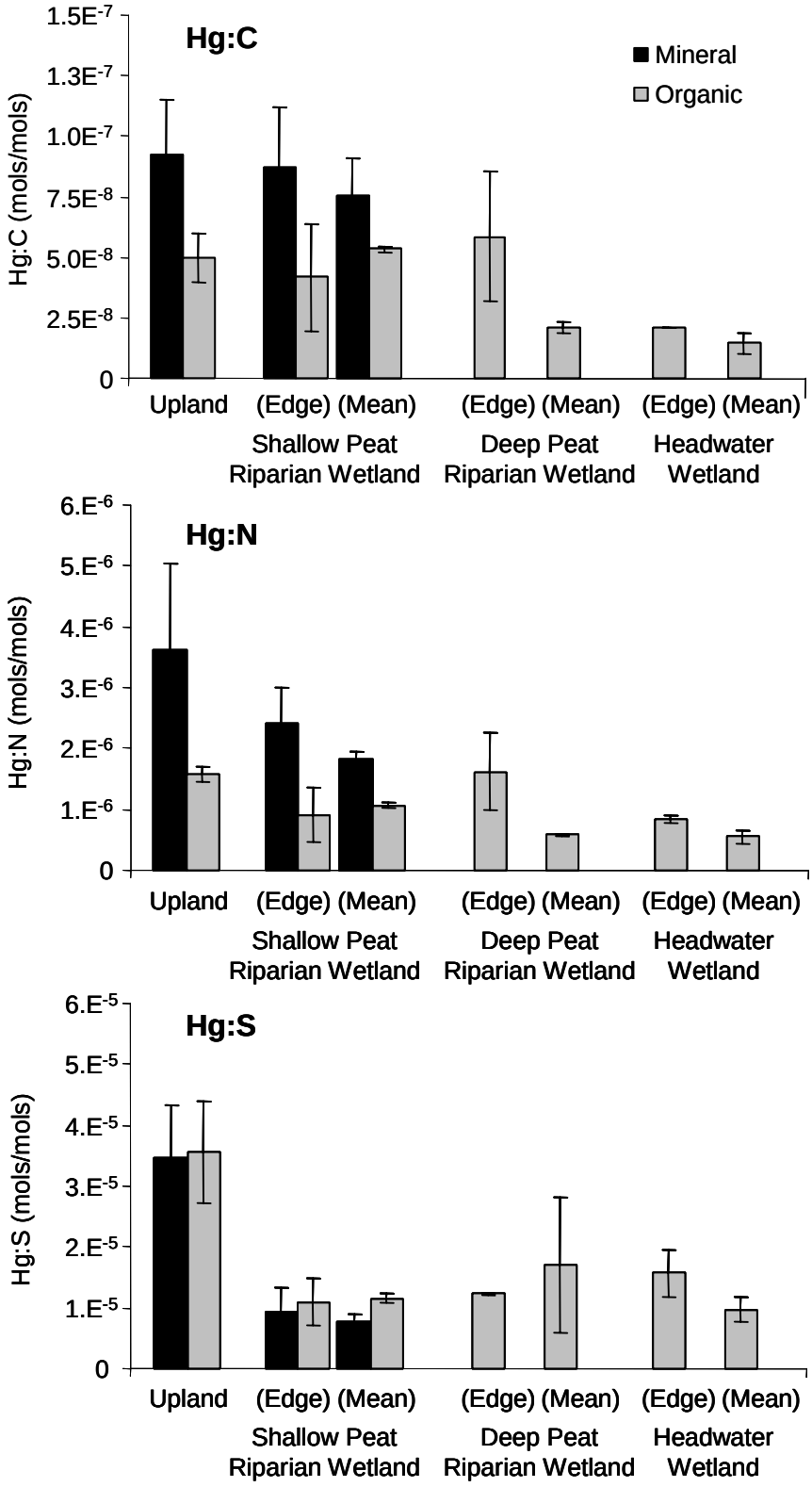
Hg:C
Mineral
Organic
Hg:C (mols/mols)
1.5E-7
1.3E-7
1.0E-7
7.5E-8
5.0E-8
2.5E-8
0
Upland
(Edge) (Mean)
(Edge) (Mean)
(Edge) (Mean)
Shallow Peat Riparian Wetland
Deep Peat Riparian Wetland
Headwater Wetland
Hg:N
Hg:N (mols/mols)
6.E-6
5.E-6
4.E-6
3.E-6
2.E-6
1.E-6
0
Upland
(Edge) (Mean)
(Edge) (Mean)
(Edge) (Mean)
Shallow Peat Riparian Wetland
Deep Peat Riparian Wetland
Headwater Wetland
Hg:S
Hg:S (mols/mols)
6.E-5
5.E-5
4.E-5
3.E-5
2.E-5
1.E-5
0
Upland
(Edge) (Mean)
(Edge) (Mean)
(Edge) (Mean)
Shallow Peat Riparian Wetland
Deep Peat Riparian Wetland
Headwater Wetland

The spatial patterns of Hg:N across the study sites were similar to those for Hg:C. The molar ratio of mercury to nitrogen (Hg:N) also varied in organic versus mineral soil horizons, and among wetland types (Figure 1.2). Within upland soils, the Hg:N ratio was greater in the mineral soil horizon than in the organic soil horizon (Figure 1.2; $p = 0.090$, $n = 6$ for each soil horizon). There was no consistent difference in Hg:N in the mineral horizons of the upland and shallow peat riparian wetlands. The only exception to the similarity of spatial patterns of Hg:N and Hg:C was that, on average, the Hg:N ratio in the upland organic horizon was greater than in peat at the upland-wetland interface (i.e., the wetland edge; $p = 0.070$, $n = 12$) and across the entire wetland transect ($p < 0.001$, $n = 12$; Figure 1.2). Among wetland types, and similar to Hg:C patterns, the mean molar ratio of Hg:N across shallow peat riparian wetlands was greater than the mean molar ratio of Hg:N across deep peat riparian and headwater wetlands, regardless of edge effects (Figure 1.2; $p < 0.05$, $n = 2$ for each wetland type).

In contrast to Hg:C and Hg:N, the molar ratio of mercury to sulfur (Hg:S) did not vary between organic and mineral soil horizons nor among wetlands (Figure 1.2). However, Hg:S was much greater in the uplands than in the wetlands overall (Figure 1.2).

Elemental correlations within individual samples. Correlations between mercury and carbon, mercury and nitrogen, and mercury and sulfur in individual samples across wetland transects and along peat depth profiles (Figure 1.3) clarified the variability of molar ratios described for soil pools (Figure 1.2) by showing how elemental relationships differ within the uplands and different wetland types in this study.

In the uplands, mercury in the A horizon and the B horizon was strongly correlated with carbon (Figure 1.3.a; $p = 0.002$, $r^2 = 0.73$, $n=10$, and $p <0.001$, $r^2 =$

Figure 1.3. Relationship between mercury and carbon, nitrogen, and sulfur concentrations in soil substrates of (a) uplands, (b) shallow peat riparian wetlands, (c) deep peat riparian wetlands, and (d) headwater wetlands in the Sunday Lake watershed in the western Adirondack region of New York State. Wetland symbols that are closed represent areas not influenced by groundwater; whereas open symbols represent areas influenced by groundwater.

(a)

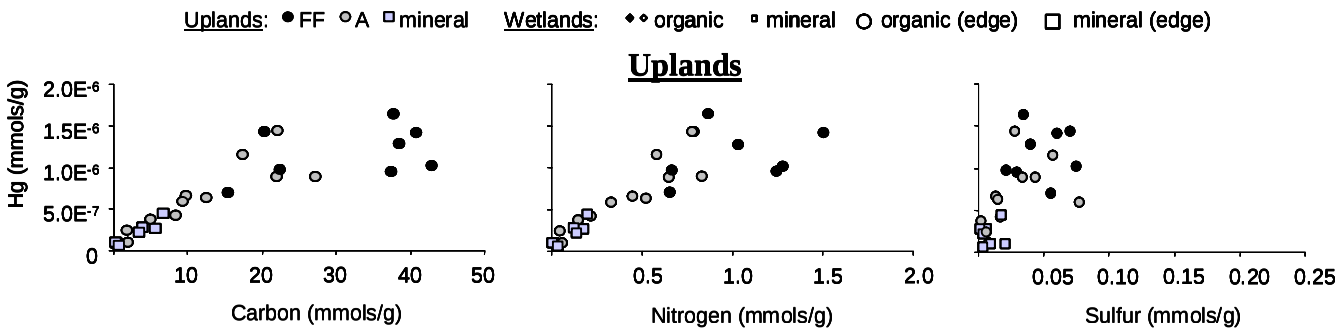
Uplands: FF A mineral
Wetlands: organic mineral organic (edge) mineral (edge)
Uplands
Hg (mmols/g)
2.0E-6
1.5E-6
1.0E-6
5.0E-7
0
10
20
30
40
50
Carbon (mmols/g)
0.5
1.0
1.5
2.0
Nitrogen (mmols/g)
0.05
0.10
0.15
0.20
0.25
Sulfur (mmols/g)

(b)

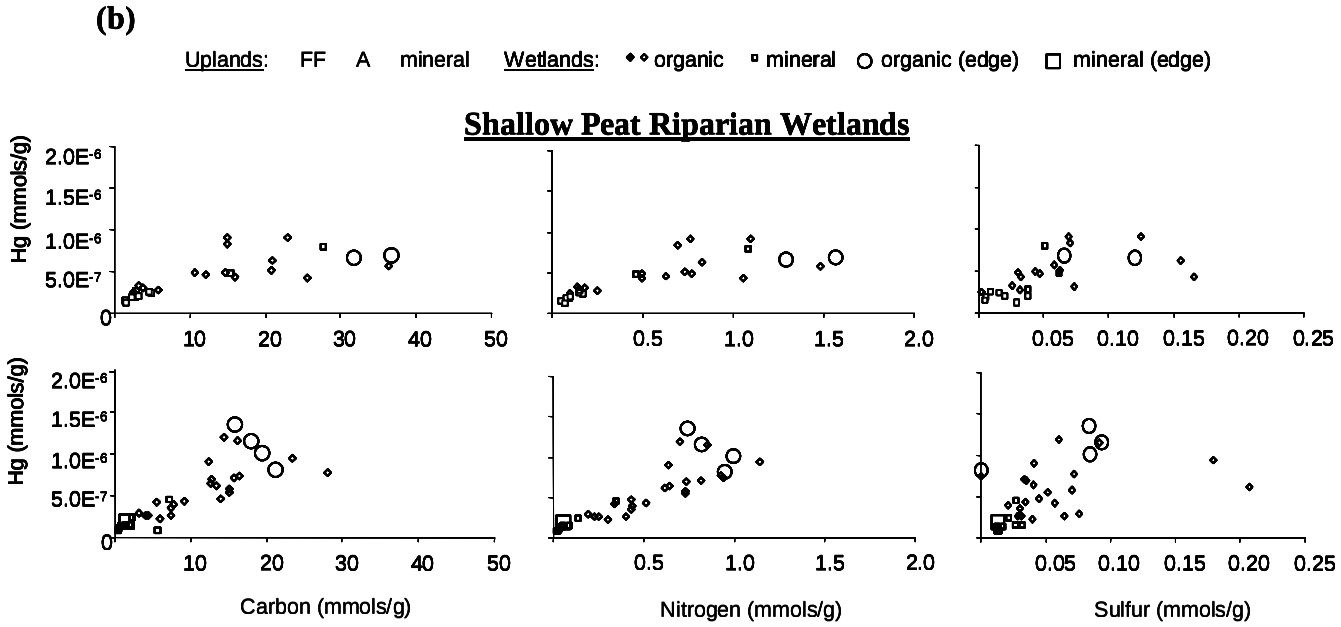
Uplands: FF A mineral
Wetlands: organic mineral organic (edge) mineral (edge)
Shallow Peat Riparian Wetlands
Hg (mmols/g)
2.0E-6
1.5E-6
1.0E-6
5.0E-7
0
10 20 30 40 50
0.5 1.0 1.5 2.0
0.05 0.10 0.15 0.20 0.25
Carbon (mmols/g)
Nitrogen (mmols/g)
Sulfur (mmols/g)

(c)

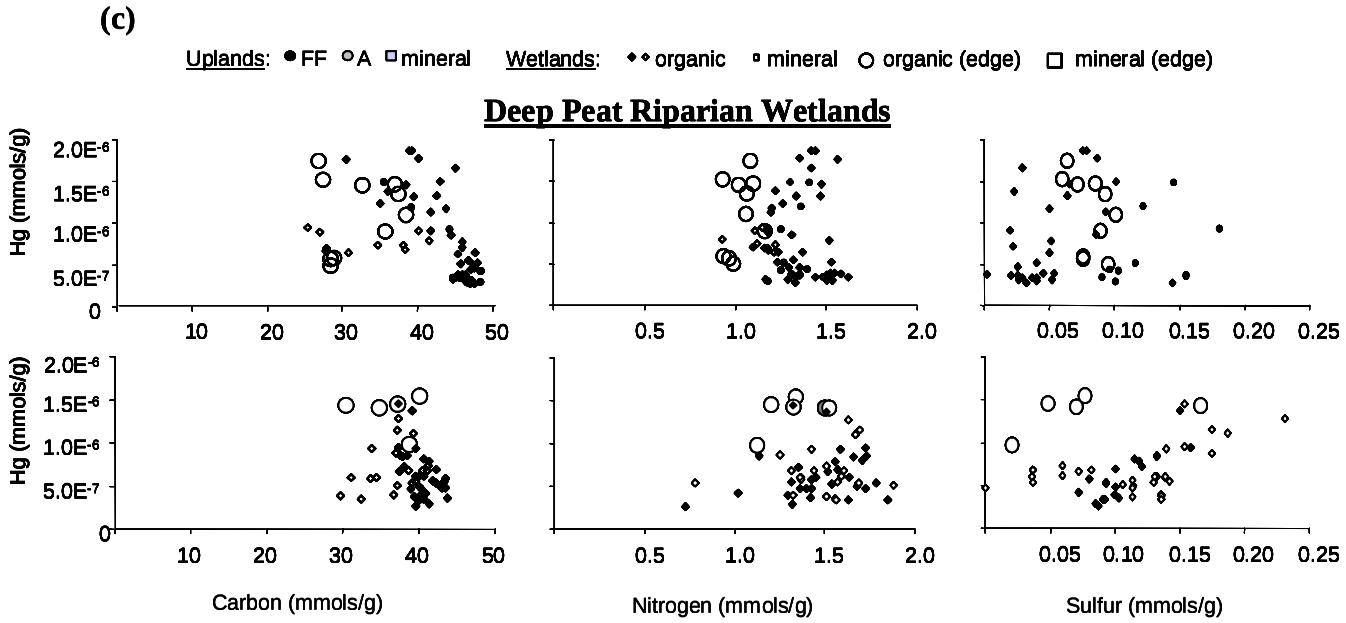
Uplands: FF A mineral
Wetlands: organic mineral organic (edge) mineral (edge)
Deep Peat Riparian Wetlands
Hg (mmols/g)
2.0E-6
1.5E-6
1.0E-6
5.0E-7
0
10 20 30 40 50
0.5 1.0 1.5 2.0
0.05 0.10 0.15 0.20 0.25
Carbon (mmols/g)
Nitrogen (mmols/g)
Sulfur (mmols/g)

(d)

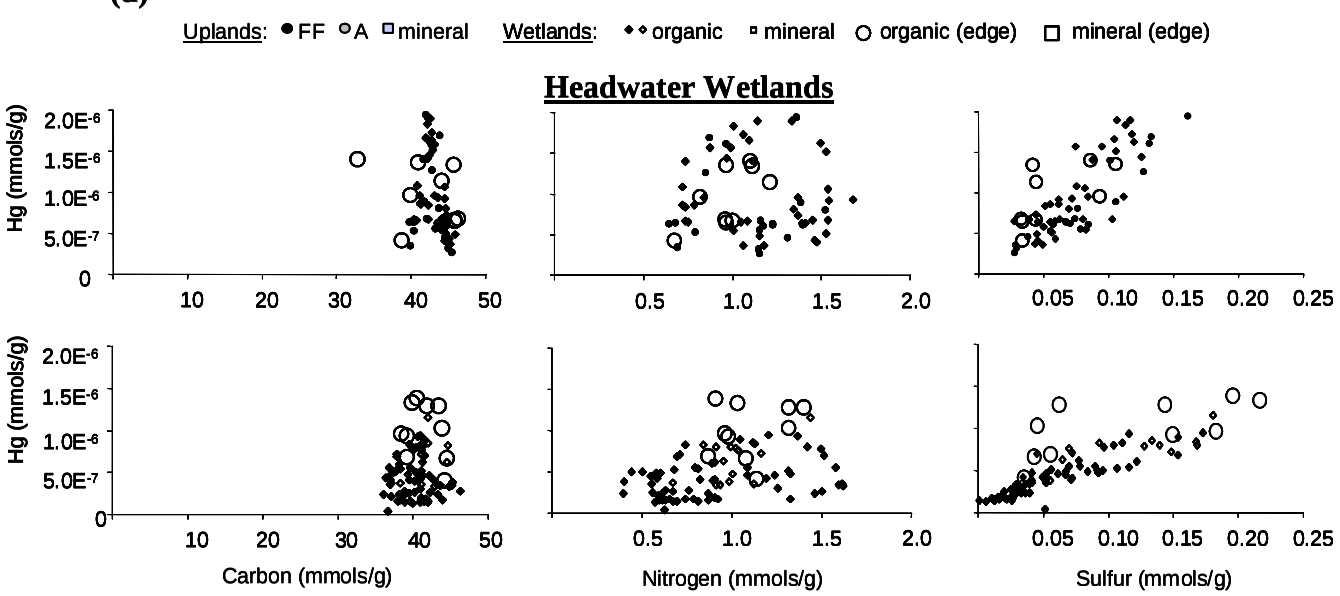
Uplands: FF A mineral
Wetlands: organic mineral organic (edge) mineral (edge)
Headwater Wetlands
Hg (mmols/g)
2.0E-6
1.5E-6
1.0E-6
5.0E-7
0
10 20 30 40 50
0.5 1.0 1.5 2.0
0.05 0.10 0.15 0.20 0.25
Carbon (mmols/g)
Nitrogen (mmols/g)
Sulfur (mmols/g)

0.96, n=8, respectively) and nitrogen (Figure 1.3.a; $p < 0.001$, $r^2 = 0.82$, n=10, and $p < 0.001$, $r^2 = 0.90$, n=8, respectively), but not with sulfur (Figure 1.3.a; $p = 0.14$, $r^2 = 0.25$, n=10, and $p=0.48$, $r^2 = 0.08$, n=8, respectively). A multiple regression analysis of the A and B horizon data together, revealed that carbon and nitrogen concentrations explained similar variability in the mercury concentrations, with only nitrogen explaining a unique portion of the variability ($r^2 = 0.87$), whereas carbon adds very little additional explanatory power (additional $r^2 < 0.01$). In contrast to the upland mineral horizons, there was no statistically significant correlation between mercury and carbon, mercury and nitrogen, nor mercury and sulfur in the organic horizon of the upland forest soils (Figure 1.3.a). When all of the upland soil data were considered together, the strong correlation between mercury and carbon, and between mercury and nitrogen, was lost at approximately ~15-20 mmols/g carbon and ~0.75-1.0 mmols/g nitrogen (Figure 1.3.a).

In the shallow peat riparian wetlands, the relationship between mercury and carbon, and mercury and nitrogen (Fig 1.3.b), were similar to those shown for the upland soils (Figure 1.3.a). Note that the relationship between mercury and carbon, and mercury and nitrogen, in one of the two shallow peat riparian wetlands did not plateau; however, in the range of carbon and nitrogen concentrations measured at that site (<20 mmols/g C, <1 mmols/g N, Figure 1.3.b), it remained consistent with the elemental relationship described for upland soils (Figure 1.3.a).

In the deep peat riparian and headwater wetlands, there was no statistically significant correlation between mercury and carbon, nor between mercury and nitrogen (Figure 1.3.c,d). There was also no clear relationship between mercury and sulfur in the deep peat riparian wetlands (Figure 1.3.c). In contrast, there was a strong correlation between mercury and sulfur in the peat of headwater wetlands (Figure 1.3.d; $p < 0.0001$, $r^2 = 0.60$, and $p < 0.0001$, $r^2=0.69$, respectively) and this

relationship improved when edge sites were excluded from the analysis ($r^2 = 0.78$). There was more mercury per unit sulfur in the forested headwater wetland (Slope $1.14E^{-5}$, SE = $1.14E^{-6}$) as compared to the non-forested headwater wetland (Slope $5.08E^{-6}$, SE = $3.72E^{-7}$). Peat samples from the wetland edges, where there is groundwater influence at the break in the hillslope, tended to be outliers in elemental correlations.

Depth profiles

Mercury concentrations decreased with increasing depth throughout all wetlands; however, peaks in mercury concentration in surficial substrates were more pronounced at the upland-wetland interface (Figure 1.4). Note that mercury concentrations measured along peat depth profiles at the wetland edge generally exceeded the concentration of mercury along peat depth profiles across the rest of the wetland (Figure 1.4).

In the shallow peat riparian wetlands, mercury concentrations were greater in predominantly organic surficial horizons (Figure 1.4). Carbon, nitrogen, and sulfur concentration also declined with depth as the percent organic matter declined; however, mercury, carbon, and nitrogen concentrations showed similar depth profiles, whereas sulfur did not.

In deep peat riparian and headwater wetlands, mercury concentration approached detection limit at depth. Carbon concentrations changed little with depth. Although nitrogen and sulfur did vary with depth in the top 50cm of peat substrate, only the sulfur profile in the headwater wetlands seemed similar to its associated mercury profile.

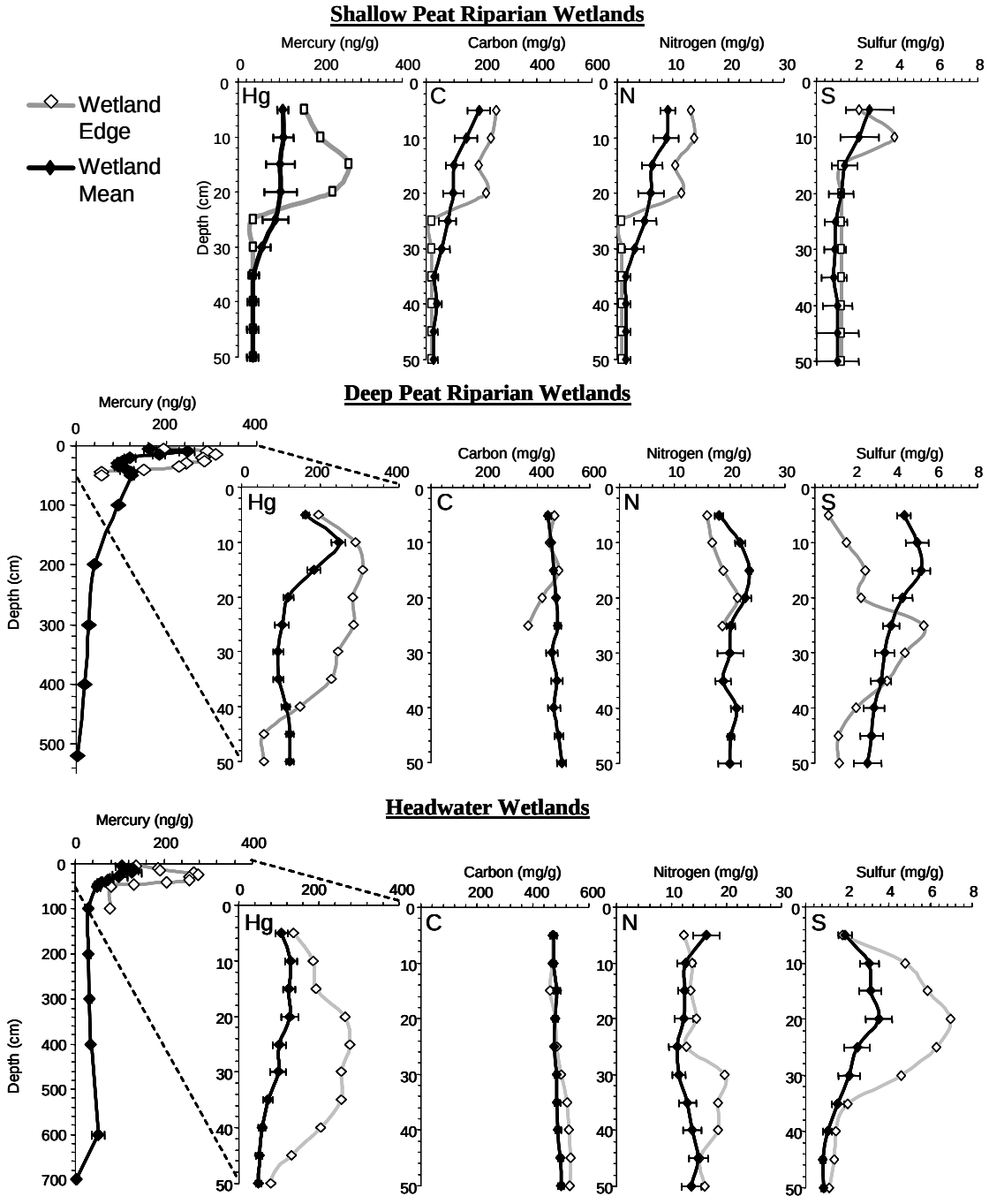

Figure 1.4. Depth profiles of mercury, carbon, nitrogen, and sulfur concentrations in representatives of different wetland types in the western Adirondack region of New York State. Hollow symbols show wetland depth profiles 1m from the upland interface. Solid symbols show mean concentration at each depth interval across wetland transects. Error bars show +/- 1SE.

DISCUSSION

A mechanistic framework for mercury retention and transport

The pool size of mercury varied across the upland-wetland interface, among wetland types, across individual wetland transects, and along depth profiles in soils of forests and wetlands of the Sunday Lake watershed. The residence time of mercury in soils is long (i.e., at least tens to hundreds of years) and most soil ecosystems are not at steady state with respect to the biogeochemical cycling of mercury (Lindqvist et al. 1991, Grigal et al. 2000, Schwesig and Matzner 2000). Rates of input exceed rates of release, and soil mercury pool sizes are increasing. Accumulated differences in the pool size of mercury across upland-wetland transects and along depth profiles results from differences in net retention (i.e., inputs - outputs) over long periods of time. Differences in the mechanisms controlling the retention of mercury within soils ultimately contribute to differences in the pool size and stoichiometry of mercury among ecosystems.

The chemical properties of mercury influence the mode of its transport and retention. Mercury is a soft acid (a type B metal) and bonds strongly with soft ligands such as thiol (-SH) and sulfide (S^{2-}), and organic S (cysteine) and N (lysine, histidine) (Stumm and Morgan 1995). Thus, mercury transport and retention is often closely linked to organic matter (e.g., Meili 1991, Mierle and Ingram 1991), although specific mechanisms for the retention of mercury in natural soils might vary across hydrologic gradients. In well drained, predominantly oxic soils, Hg(II) is predominantly bound to particulate and dissolved organic matter (e.g., Khwaja et al. 2006, and references therein). Direct evidence from EXAFS shows that humic acids derived from forest soil organic horizons form bidentate complexes with mercury, with Hg(II) coordinating with one reduced sulfur (e.g., thiol) and one oxygen or nitrogen hetero-atom (Xia et al. 1999, Skyllberg et al. 2000).

In poorly drained or saturated anoxic soils, equilibrium calculations involving inorganic ligands predict that mercury sulfide complexation and precipitation should dominate the distribution of mercury between the aqueous and solid phase, thus limiting the mobility of mercury (Hurley et al. 1998b, Benoit et al. 1999, Drexel et al. 2002, Benoit et al. 2003). However, studies from the Florida Everglades have demonstrated that strong Hg(II) binding sites in peat actually compete with inorganic sulfide species (Drexel et al. 2002). At environmentally relevant concentrations of mercury and realistically low Hg:DOM ratios, Hg-DOM complexes have greater conditional stability constants than Hg-inorganic sulfide complexes (Skyllberg et al. 2000, Drexel et al. 2002, Haitzer et al. 2002, Ravichandran 2004). Moreover, DOM has been shown to enhance the dissolution of cinnabar (HgS) (Ravichandran et al. 1998, Ravichandran et al. 1999, Reddy and Aiken 2001, Waples et al. 2005). Based on the strength of estimated Hg-DOM stability constants and the results of dissolution experiments of HgS by DOM, it appears that organic matter is capable of out-competing sulfide for mercury in anoxic environments. Thus, the retention and transport of mercury can be mechanistically coupled to organic matter in both uplands and wetlands of different hydrogeologic settings.

Forest soil mercury pool: Evidence of mercury saturation?

The pool size of mercury in the top 50 cm of forest soils was greater than the mercury pool size in the top 50 cm of wetland soils; however, most of this mercury was associated with the mineral horizons underlying the organic horizon in the forest soils (Figure 1.1; also, see *Results*). Atmospheric deposition of mercury to terrestrial ecosystems is greatly enhanced by the forest canopy (Rea et al. 2000, 2001, St Louis et al. 2001, Rea et al. 2002, Miller et al. 2005). In the Sunday Lake watershed, mercury inputs to the forest floor are roughly 3-6x atmospheric mercury deposition to

open sites (Demers et al. 2007). These mercury inputs are approximately 1.5-3x greater than mercury export from the forest floor, and more than an order of magnitude greater than leaching losses from mineral soil horizons (Demers et al. 2007). Whereas the residence time of mercury in the forest organic soil pool is on the order of 100s of years, the residence time of the mercury in the forest mineral soil pool is on the order of 1000s of years (Demers et al. 2007).

Mercury entering the forest floor via leaf litter or throughfall is already associated with particulate or dissolved organic matter. During decomposition of organic matter in forest organic horizons, the concentration of mercury increases (Hall and Louis 2004, Demers et al. 2007). Eventually, decomposition of organic matter releases dissolved organic matter (along with its complexed mercury), which is hydrologically transported into the mineral soil where it is immobilized through the process of podzolization. Thus, the distribution of mercury in forest soils is an emergent property of the interaction of multiple processes: decomposition, hydrologic transport, and the physicochemical fractioning of organic matter between the dissolved and adsorbed phases (*sensu* Schuster 1991).

Despite known mechanisms of mercury retention by reduced sulfur groups in organic matter, there was no correlation between mercury and sulfur either in the organic or mineral soils of the upland forest soils. Note that only a fraction of the total sulfur in organic matter is reduced sulfur (e.g., Xia et al. 1999, Skyllberg et al. 2000, Ravichandran 2004) and only a fraction of the reduced sulfur is available for binding with mercury (e.g., Skyllberg et al. 2000). There was also no correlation between mercury and carbon, nor mercury and nitrogen in the forest soil organic horizon. Nonetheless, this lack of elemental correlations with mercury does not necessarily mean that mercury retention is not associated with organic matter or reduced sulfur

content, but simply that the over-abundance of available binding sites poses no limit on the amount of mercury bound with the organic matter (Hurley et al. 1998a).

In contrast, mercury was highly correlated with both carbon and nitrogen within the mineral soils of the upland forests (Figure 1.3). These observations lend support to the hypothesis that mercury is involved in bidentate complexation with one reduced sulfur and one nitrogen hetero-atom (e.g., Skyllberg et al. 2000, Hesterberg et al. 2001). As suggested by Skyllberg (2000), the quantity of reduced sulfur binding sites actually occurring in close proximity to reduced nitrogen binding sites may significantly reduce the quantity of strongest binding sites available to complex with mercury.

Numerous calculations over the past decade have demonstrated that the quantity of reduced sulfur sites present in organic matter is multiple orders of magnitude greater than environmentally relevant concentrations of mercury (Ravichandran 2004). However, the distinct patterns in elemental stoichiometry (Hg:C, Hg:N; Figure 1.3) observed in the upland forest soils challenge the notion that the binding capacity of organic matter cannot be saturated under natural environmental conditions. In the upland forest organic soil horizon, mercury is not well correlated with carbon, nor nitrogen. Lack of elemental correlation in these predominantly organic horizons suggests that the supply of mercury is limited relative to the numerous potential binding sites for mercury. Applying similar logic to the mineral soil horizon leads us to the opposite conclusion, that the quantity of potential binding sites for mercury in the mineral soil horizon is limited relative to the supply of mercury (i.e., binding sites appear saturated). However, as previously discussed, mercury accumulating in the mineral horizon is likely transported to depth along with DOM, with which it was already complexed in the organic soil horizon. As decomposition proceeds, the concentration of mercury associated with the dissolved

organic matter that is produced and released from the organic soil horizon appears to converge upon an Hg:C and Hg:N ratio that serves as an upper limit to Hg:C and Hg:N ratios throughout the forest soil profile. Thus, the observed patterns in the mineral soil horizon could result, in part, from a relatively fixed stoichiometry associated with decomposition products.

Cross site comparison of forest soil mercury pools

Mercury concentrations measured in the forest floor (mean = 235 ng/g, SE = 22 ng/g, n = 8), A horizon (mean = 135 ng/g, SE = 27 ng/g, n = 10), and B horizon (mean = 52 ng/g, SE = 14 ng/g SE, n = 8) in this study were nearly double the mean mercury concentration in the forest floor (140 ng/g) and mineral soils (20 ng/g) reported for the north-central USA, and were greater than the mode for natural and arable soils from Europe (Grigal 2003). In my study, the mean ratio of Hg:C was ~2.5x greater in the mineral soil (mean of B horizon = 10.3×10^{-8}, SE = 2.9×10^{-8}) than in the organic horizon (mean of FF horizon = 4.0×10^{-8}, SE = 5.2×10^{-9}); this is similar to the nearly 2-2.5x greater Hg:SOM ratio in the mineral versus organic horizons reported by Grigal (2003) for the north-central USA and Sweden. These data also show that the variability in that relationship is much less in the mineral soil than in the overlying organic matter. Grigal (2003) suggests that these patterns result from C mineralization at a greater rate than mercury. However, decomposition also has been shown to concentrate mercury in leaf litter (and organic horizons), increasing the mass of mercury beyond what can be accounted for by deposition alone (Demers et al. 2007). Both mineralization of carbon, and translocation to and immobilization of mercury in the organic horizon, together, are mechanisms that would result in the concentration of mercury and increase the Hg:C ratio of decomposition products released from the forest floor and transported into mineral horizons.

Grigal (2003) emphasizes the close relationship between Hg and SOM with a review of forest soil organic horizons from Sweden, Norway, and the north-central USA, indicating that similar changes in Hg concentration with changes in SOM occurred at all sites, with the Swedish data having the highest intercept and the data from the USA having the greatest slope. However, data from the organic horizon of forest soils in my study showed no statistically significant relationship between mercury and carbon. In my study, the correlation between mercury and carbon became significant through the transition from the organic horizon to the underlying mineral horizons (A and B horizon), with the strongest correlation in the mineral B horizon.

Grigal (2003) does point out that the slope of the relationship between Hg and SOM is widely variable, with the slope value in the forest floor (0.29) being less than the slope value in the mineral horizon (0.44). Stoichiometry also varied with depth, with Hg:C increasing with depth. His review found that the average ratio for surface organic horizons was (4.2×10^{-8} mol Hg per mol C), increasing in the A, B, and C horizons (9.0×10^{-8}, 15.0×10^{-8}, and 22.8×10^{-8} mol Hg per mol C, respectively; units converted for data in Grigal 2003, and references therein). The stoichiometry of mercury and carbon was similar in my study, increasing with depth from the forest floor (4.0×10^{-8} mol Hg per mol C) to the mineral A and B horizons (6.6×10^{-8}, and 10.3×10^{-8} mol Hg per mol C, respectively). Grigal (2003) suggests that vertical variation in the Hg-SOM stoichiometry may be related to historical loading, degree of mineralization, or the relative amount of reduced sulfur groups. However, note that despite differences in regional mercury deposition and soil concentrations across the world, Hg:C converge toward similar values. This seems somewhat unlikely if historic loading alone was responsible for the pattern. Thus, this cross-site comparison is consistent with the possibility that biological processes (e.g. carbon

mineralization and mercury immobilization during decomposition) governs the concentration of mercury in organic horizons and its release to the mineral soils with DOC.

The stoichiometry between mercury and sulfur varies. Data from the north-central USA show a more constant relationship between Hg-S than Hg-SOM, and Hg-S stoichiometry of the organic and mineral horizon did not differ, implying that differences in Hg concentration simply reflected changes in S concentration. In my study, soil pool data showed a similar relationship between Hg-S in the upland organic and mineral soil (Figure 1.2), and the Hg-S ratio within and among wetlands did not vary, though it was much lower than the Hg-S ratio of the uplands (Figure 1.2). However, in the uplands, mercury and sulfur were not correlated at the scale of individual samples, whereas mercury and nitrogen were strongly correlated.

Wetland mercury soil pool: Importance of wetland type and hydrogeologic setting

The presence of wetlands and the occurrence of different wetland types are a function of the landscape and hydrological processes. Given the close coupling of mercury with organic matter, and the apparent influence of decomposition on the transport and fate of mercury observed in upland soils, it is possible that hydrogeologically driven differences in decomposition in different wetland types also influence the retention and transport of mercury in wetland soils.

Shallow peat riparian wetlands. Shallow peat riparian wetlands had larger mercury pool sizes than deep peat riparian and headwater wetlands (to a depth of 50cm). Patterns of mercury retention within the shallow peat riparian wetlands resembled patterns of retention within the upland soils, rather than patterns of retention in the other (more hydrologically saturated) wetlands. As observed for the forest soils, much of the mercury pool within shallow peat riparian wetlands was

within mineral soils underlying the organic peat soils. In comparison to other wetlands in this study, these riparian wetlands have a shallow accumulation of peat (not exceeding ~35cm). Although anoxic conditions do exist in these shallow peat riparian soils (as evidenced by the presence of reduced iron and sulfide in porewaters; *see* Chapter 3), the hydrology is both seasonally and episodically dynamic, and much of the organic horizon is not permanently saturated, thus promoting (fast, efficient) aerobic decomposition. Furthermore, upwelling groundwater provides a supply of alternate electron acceptors (e.g., nitrate, sulfate, iron) and the fluctuating water table provides a mechanism for the recycling of electron acceptors between their reduced and oxidized forms. Thus, I suggest that organic matter decomposition is relatively rapid in the shallow peat riparian wetlands, and decomposition of organic matter within the peat is a source of dissolved organic carbon and associated mercury that can be transported to the underlying mineral soil horizons. The coarse matrix of soils below the shallow riparian peat is enriched in organic matter contributed from the overlying peat, and mercury associated with this organic matter may be more hydrologically mobile than the mercury retained in podzolized upland soils.

Elemental stoichiometry in the shallow peat riparian wetlands resembled elemental stoichiometry observed in the upland forest soils. Mercury was well correlated to carbon and nitrogen concentrations within the mineral soil, and in general, the correlation was strong in soils with a carbon content of less than ~15 - 20 mmol C/g and a nitrogen content of less than ~0.75 – 1.0 mmols N/g. Whereas there was no statistically significant correlation between mercury and sulfur in the upland forest soils, Hg:S followed similar patterns as Hg:C and Hg:N in the shallow peat riparian wetlands, although the correlation was weaker than for carbon and nitrogen. Thus, similar mechanisms might control the distribution of mercury in upland forest soils and shallow peat riparian wetlands: predominantly aerobic decomposition of

organic matter and subsequent transport and retention of decomposition products and associated mercury into the mineral horizon.

Headwater wetlands. Overall, mercury pool size was smallest in the headwater wetlands (to a depth of 50 cm). Deep peats form as a result of slow decomposition (relative to primary production); and this slow decomposition is the result of a consistently high water table that maintains saturated, anoxic conditions within the peat and promotes (slow, inefficient) anaerobic decomposition (Mitch and Gosselink 2000). Moreover, these headwater wetlands are predominantly ombrotrophic (away from their edges), and thus limited groundwater contributions constrain the supply of alternate electron acceptors, further limiting microbial decomposition. Thus, the hydrogeologic setting of the headwater wetlands provides a fundamentally different environment for the biogeochemical cycling of elements that influences both the rate and mode of decomposition, and perhaps, the biogeochemical cycling of mercury.

Elemental stoichiometry of mercury, carbon, nitrogen, and sulfur in the deep peat of the headwater wetlands was distinctly different from elemental stoichiometry in uplands and shallow peat riparian wetlands. In contrast to the shallow peat riparian and upland soils, there was no correlation between mercury and carbon, nor mercury and nitrogen, in the peat of the headwater wetlands. However, there was a strong correlation between mercury and sulfur in the headwater wetlands. There are at least two alternative mechanisms that could explain these patterns. One possible mechanism is the co-deposition of sulfur and mercury from the atmosphere, which are subsequently immobilized together within the peat. Benoit et al. (1994) suggested that, on the basis of inorganic mercury speciation, mercury was immobile within the peat profile; however, recent isotopic evidence indicates that sulfur is not immobile within the peat profile, migrating vertically down through the peat subsequent to

deposition (Novak et al. 2005). Thus, a simple model of co-deposition and immobilization as inorganic mercury sulfide alone does not seem to be a complete explanation for the strong correlation between mercury and sulfur in the headwater peat.

Another possible mechanism for the strong correlation between mercury and sulfur in wetland peat involves the biogeochemical cycling of sulfur, in conjunction with strong mercury-DOM binding. The proportion of total sulfur as organic sulfur in sphagnum peat wetlands typically exceeds 90% (Germida 2005) with 90% of the organic sulfur typically involved in carbon-sulfur bonds; however, available sulfate rapidly cycles via microbial sulfate reduction (Wieder and Lang 1988). Turnover of the sulfate and inorganic sulfur pool is rapid (i.e., hours and days, respectively), whereas the turnover of carbon bonded sulfur is slow (i.e., years, Wieder and Lang 1988). Thus, most inorganic additions of sulfur are eventually incorporated into the organic sulfur pool. Net sulfur immobilization dominates when the substrate molar ratio of C:S >400, whereas net sulfur mineralization dominates when the substrate molar ratio of C:S < 200 (Germida 2005). In addition to the significant correlation between mercury and sulfur in headwater wetland peat (Figure 1.3), mercury concentration increases exponentially with decreasing C:S ratio (Figure 1.5). The rate of increase in mercury concentration becomes markedly greater between a C:S ratio of 200-400, and asymptotes as the C:S ratio approaches 200, the theoretical break-point for net microbial sulfur mineralization (Figure 1.5).

The strong correlation between mercury and the C:S ratio suggests a biological influence on the retention of mercury in the headwater wetlands; however, the mechanism ultimately controlling retention may be either biotic or abiotic, or the interaction of both. As the C:S ratio decreases, mercury binding site density increases. As sulfur mineralization becomes dominant, more inorganic sulfur would enter into

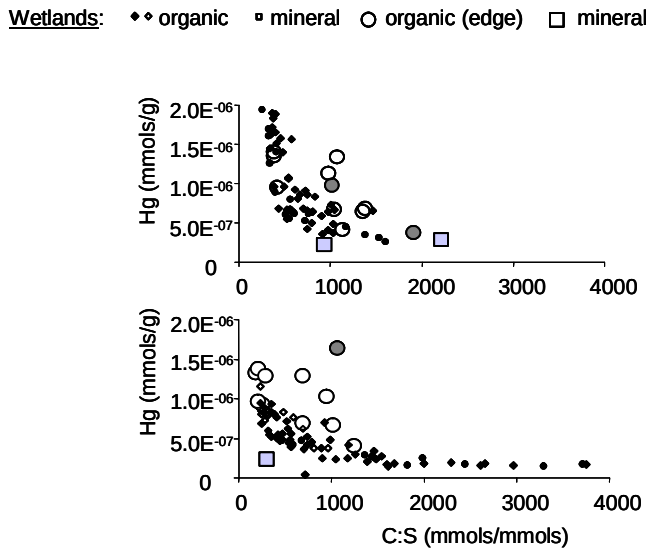

Figure 1.5. Relationship between mercury and C:S ratio in headwater wetland peat in the Sunday Lake watershed in the Adirondack region of New York State. Wetland symbols that are closed represent areas not influenced by groundwater; whereas open symbols represent areas influenced by groundwater.

the rapidly cycling inorganic sulfur pool, possibly promoting formation of HgS complexes and precipitates. As sulfur rapidly cycles through inorganic sulfur pools via biologically mediated reduction and oxidation, some of this sulfur reacts with organic matter to form C-S bonded sulfur with a much longer turnover time. Wieder and Lang (1988) suggest that organic S formation by dissimalatory reduction of sulfate to H_2S and subsequent reaction of H_2S with organic matter dominates over organic S formation by assimilatory reduction. Moreover, recent research shows that dissolved organic matter can compete with cinnabar in binding mercury (e.g. Drexel et al. 2002), and that much of the mercury in organic-rich environments may indeed be associated with the organic sulfur pool, even in the presence of sulfides. It is possible that the cycling of mercury through inorganic and organic pools also results in the predominance of binding association of mercury with organic sulfur. Retention, mobility, and transport of mercury in saturated wetland peat is likely a complex interaction between inorganic and organic pools of sulfur and associated mercury; further research quantifying these complex interactions between the inorganic and organic biogeochemical cycling of sulfur and mercury is a critical next step for understanding the future fate of the large pools of mercury stored in wetland environments.

Edge effects and evidence of upland-wetland connectivity

Differences in mercury pool size across upland-wetland transects is suggestive of wetland retention of mercury inputs derived from the uplands. This edge effect, the increased mercury pool size at the upland-wetland interface, is likely the result of a combination of different mercury fluxes including: (1) increased atmospheric deposition along the forest-edge (e.g., Weathers et al. 2000, Weathers et al. 2001); (2) direct inputs of litter from the forest canopy to the adjacent wetland (St Louis et al.

2001); (3) shallow lateral interflow from forested hillslopes into wetlands (Branfireun et al. 1998); and (4) upwelling of groundwater at the break in slope at the upland-wetland interface (e.g., Winter 1988, 1992) that may contribute DOC and associated mercury (Krabbenhoft and Babiarz 1992).

Increased mercury pool size at the upland-wetland interface was most evident in the deep peat riparian and headwater wetlands, possibly due to lower hydraulic conductivity or lower hydrologic flux through these zones, thus limiting mobility of deposited mercury. In the shallow peat riparian wetlands, the total pool size at the upland-wetland interface was similar to the mercury pool size across the rest of the wetland transect, whereas mercury concentrations at shallow depths alone (dominated by organic matter rather than mineral soil) were greater at the upland-wetland edge. This pattern reflects that pool sizes in the shallow peat riparian wetland were strongly influenced by the mineral soil horizon. The edge-effect apparent in the organic horizon is likely influenced by increased deposition (throughfall and litter) at the forest-edge. Shallow lateral interflow and upwelling groundwater would likely have a stronger influence on the mineral soil mercury pool throughout the wetland.

Edge effects also influenced elemental stoichiometry. In the uplands and shallow peat riparian wetlands where apparent edge-effects influenced most of the narrow wetland corridor, the elemental stoichiometry of edge samples was similar to the stoichiometry in samples from across the remainder of the wetland. However, in deep peat riparian and headwater wetlands, the stoichiometry of samples from edges tended to be outliers when compared to the samples from across the remainder of the wetland transect (Figure 1.3).

Differences in mercury pool sizes among wetlands of a single wetland type, or within an individual wetland could be further explained by differences in groundwater hydrology and vegetation. Differences in mercury accumulation within deep peat

riparian wetlands coincided with differences in groundwater hydrology. Transect points within the deep peat riparian wetlands that were associated with discharge gradients (i.e., upwelling) accumulated more mercury in surficial peat substrates than transect points with recharge gradients (i.e., downwelling; Appendix A, Appendix B). Differences in mercury pool size in peat substrates of the headwater wetlands coincided with differences in vegetation, with the sphagnum-dominated bog accumulating less mercury than its forested counterpart. Also, greater mercury accumulation in headwater wetland peat appeared to coincide with increases in forest canopy cover along an individual transect.

CONCLUSIONS AND IMPLICATIONS

Wetlands of differing hydrogeologic setting differ in the magnitude of the pool size and elemental stoichiometry of accumulated mercury. If process can be inferred from pattern, then it is likely that the mechanism responsible for the retention of mercury in uplands and varying wetland types also differs. Hydrology governs the rate and mode of decomposition in wetlands of differing hydrogeologic setting by influencing the extent and duration of saturation, and the supply of nutrients and alternate electron acceptors. The resulting differences in decomposition processes, biogeochemical cycling and recycling of mercury, and the extent of subsequent hydrologic transport influences the size, distribution, and stoichiometry of mercury pools across the upland-wetland interface, along peat depth profiles, and among wetlands of varying hydrogeologic setting. This research illustrates the importance of considering wetland type in our assessments and modeling of terrestrial effects on mercury in surface waters at landscape scales.

Upland-wetland connectivity appears to influence the quantity of mercury in wetland soil pools, and the distribution of those pools along depth profiles and across

the wetland landscape. It is possible that the connectivity evidenced by differences in pool sizes of mercury might also affect mercury transformations within, or mercury fluxes from, wetlands of varying hydrogeologic setting. Quantifying mercury transformations within and fluxes from these different wetland types is a critical next step in determining the ultimate effect of this upland-wetland connectivity upon the loading of mercury from terrestrial and wetland ecosystems to surface waters and is necessary to improve predictions of the response of those surface waters to decreases in mercury emissions and deposition.

REFERENCES

Aber, J. D., and J. M. Mellilo. 2001. Terrestrial Ecosystems (2nd Ed.). Academic Press.

Bedford, B. L. 1996. The need to define hydrologic equivalence at the landscape scale for freshwater wetland mitigation. Ecological Applications **6**:57-68.

Bedford, B. L. 1999. Cumulative effects on wetland landscapes: Links to wetland restoration in the United States and southern Canada. Wetlands **19**:775-788.

Benoit, J. M., W. F. Fitzgerald, and A. W. H. Damman. 1994. Historical Atmospheric Mercury Deposition in the Mid-Continental U.S. as Recorded in an Ombrotrophic Peat Bog. Pages 187-202 *in* J. W. Huckabee, editor. Mercury Pollution: Integration and Synthesis. Lewis Publishers.

Benoit, J. M., C. C. Gilmour, A. Heyes, R. P. Mason, and C. L. Miller. 2003. Geochemical and biological controls over methylmercury production and degradation in aquatic ecosystems. Biogeochemistry of Environmentally Important Trace Elements **835**:262-297.

Benoit, J. M., C. C. Gilmour, R. P. Mason, and A. Heyes. 1999. Sulfide controls on mercury speciation and bioavailability to methylating bacteria in sediment pore waters. Environmental Science & Technology **33**:951-957.

Branfireun, B. A., D. Hilbert, and N. T. Roulet. 1998. Sinks and sources of methylmercury in a boreal catchment. Biogeochemistry **41**:277-291.

Brinson, M. M. 1993. A hydrogeomorphic classification for wetlands. Technical Report WRP-DE-4, U.S. Army Engineer Waterways Experiment Station, Vicksburg, Mississippi, USA.

Demers, J. D., C. T. Driscoll, T. J. Fahey, and J. B. Yavitt. 2007. Mercury cycling in litter and soil in different forest types in the Adirondack region, New York, USA. Ecological Applications **17**:1341-1351.

Drexel, R. T., M. Haitzer, J. N. Ryan, G. R. Aiken, and K. L. Nagy. 2002. Mercury(II) sorption to two Florida Everglades peats: Evidence for strong and weak binding and competition by dissolved organic matter released from the peat. Environmental Science & Technology **36**:4058-4064.

Germida, J. J. 2005. Transformations of Sulfur. Pages 433-462 *in* D. A. Zuberer, editor. Principles and Applications of Soil Microbiology. Prentice-Hall, Upper Saddle River, New Jersey.

Grigal, D. F. 2003. Mercury sequestration in forests and peatlands: A review. Journal of Environmental Quality **32**:393-405.

Grigal, D. F., R. K. Kolka, J. A. Fleck, and E. A. Nater. 2000. Mercury budget of an upland-peatland watershed. Biogeochemistry **50**:95-109.

Haitzer, M., G. R. Aiken, and J. N. Ryan. 2002. Binding of mercury(II) to dissolved organic matter: The role of the mercury-to-DOM concentration ratio. Environmental Science & Technology **36**:3564-3570.

Hall, B. D., and V. L. S. Louis. 2004. Methylmercury and total mercury in plant litter decomposing in upland forests and flooded landscapes. Environmental Science & Technology **38**:5010-5021.

Hesterberg, D., J. W. Chou, K. J. Hutchison, and D. E. Sayers. 2001. Bonding of Hg(II) to reduced organic, sulfur in humic acid as affected by S/Hg ratio. Environmental Science & Technology **35**:2741-2745.

Hill, A. R., and K. J. Devito. 1997. Hydrological-chemical interactions in headwater forest wetlands. Pages 213-230 *in* J. K. Jeglum, editor. Northern Forested Wetlands: Ecology and Management. Lewis Publishers, Boca Raton, Florida, USA.

Hurley, J. P., S. E. Cowell, M. M. Shafer, and P. E. Hughes. 1998a. Tributary loading of mercury to Lake Michigan: Importance of seasonal events and phase partitioning. Science of the Total Environment **213**:129-137.

Hurley, J. P., D. P. Krabbenhoft, L. B. Cleckner, M. L. Olson, G. R. Aiken, and P. S. Rawlik. 1998b. System controls on the aqueous distribution of mercury in the northern Florida Everglades. Biogeochemistry **40**:293-310.

Khwaja, A. R., P. R. Bloom, and P. L. Brezonik. 2006. Binding constants of divalent mercury (Hg2+) in soil humic acids and soil organic matter. Environmental Science & Technology **40**:844-849.

Krabbenhoft, D. P., and C. L. Babiarz. 1992. The role of groundwater transport in aquatic mercury cycling. Water Resources Research **28**:3119-3128.

Lindqvist, O., K. Johansson, M. Aastrup, A. Andersson, L. Bringmark, G. Hovsenius, L. Hakanson, A. Iverfeldt, M. Meili, and B. Timm. 1991. Mercury in the Swedish Environment - Recent Research on Causes, Consequences and Corrective Methods. Water Air and Soil Pollution **55**:R11-&.

Lorey, P., and C. T. Driscoll. 1999. Historical trends of mercury deposition in Adirondack lakes. Environmental Science & Technology **33**:718-722.

Meili, M. 1991. The Coupling of Mercury and Organic-Matter in the Biogeochemical Cycle - Towards a Mechanistic Model for the Boreal Forest Zone. Water Air and Soil Pollution **56**:333-347.

Mierle, G., and R. Ingram. 1991. The role of humic substances in the mobilization of mercury from watersheds. Water Air and Soil Pollution **56**:349-357.

Miller, E. K., A. Vanarsdale, G. J. Keeler, A. Chalmers, L. Poissant, N. C. Kamman, and R. Brulotte. 2005. Estimation and mapping of wet and dry mercury deposition across northeastern North America. Ecotoxicology **14**:53-70.

Mitch, W. J., and J. G. Gosselink. 2000. Wetlands, Third edition. John Wiley & Sons, Inc., New York.

Novak, M., M. Adamova, R. K. Wieder, and S. H. Bottrell. 2005. Sulfur mobility in peat. Applied Geochemistry **20**:673-681.

Ravichandran, M. 2004. Interactions between mercury and dissolved organic matter - A review. Chemosphere **55**:319 - 331.

Ravichandran, M., G. R. Aiken, M. M. Reddy, and J. N. Ryan. 1998. Enhanced dissolution of cinnabar (mercuric sulfide) by dissolved organic matter isolated from the Florida Everglades. Environmental Science & Technology **32**:3305 - 3311.

Ravichandran, M., G. R. Aiken, J. N. Ryan, and M. M. Reddy. 1999. Inhibition of precipitation and aggregation of metacinnabar (mercuric sulfide) by dissolved organic matter isolated from the Florida Everglades. Environmental Science & Technology **33**.

Rea, A. W., S. E. Lindberg, and G. J. Keeler. 2000. Assessment of dry deposition and foliar leaching of mercury and selected trace elements based on washed foliar and surrogate surfaces. Environmental Science & Technology **34**:2418-2425.

Rea, A. W., S. E. Lindberg, and G. J. Keeler. 2001. Dry deposition and foliar leaching of mercury and selected trace elements in deciduous forest throughfall. Atmospheric Environment **35**:3453-3462.

Rea, A. W., S. E. Lindberg, T. Scherbatskoy, and G. J. Keeler. 2002. Mercury accumulation in foliage over time in two northern mixed-hardwood forests. Water Air and Soil Pollution **133**:49-67.

Reddy, M. M., and G. R. Aiken. 2001. Fulvic acid-sulfide binding competition for mercury ion binding in the in the Florida Everglades. Water Air and Soil Pollution **132**:89-104.

SAS Institute, I. 1999. SAS OnlineDoc. Version 8. *in*, Cary, North Carolina, USA.

Schuster, E. 1991. The Behavior of mercury in the soil with special emphasis on complexation and adsorption processes - A review of the literature. Water Air and Soil Pollution **56**:667-680.

Schwesig, D., and E. Matzner. 2000. Pools and fluxes of mercury and methylmercury in two forested catchments in Germany. Science of the Total Environment **260**:213-223.

Skyllberg, U., K. Xia, P. R. Bloom, E. A. Nater, and W. F. Bleam. 2000. Binding of mercury(II) to reduced sulfur in soil organic matter along upland-peat soil transects. Journal of Environmental Quality **29**:855-865.

St Louis, V. L., J. W. M. Rudd, C. A. Kelly, B. D. Hall, K. R. Rolfhus, K. J. Scott, S. E. Lindberg, and W. Dong. 2001. Importance of the forest canopy to fluxes of methyl mercury and total mercury to boreal ecosystems. Environmental Science & Technology **35**:3089-3098.

Stumm, W., and J. J. Morgan. 1995. Aquatic Chemistry. John Wiley and Sons, New York, New York, USA.

Waples, J. S., K. L. Nagy, G. R. Aiken, and J. N. Ryan. 2005. Dissolution of cinnabar (HgS) in the presence of natural organic matter. Geochimica et Cosmochimica Acta **69**:1575-1588.

Weathers, K. C., M. L. Cadenasso, and S. T. A. Pickett. 2001. Forest edges as nutrient and pollutant concentrators: Potential synergisms between fragmentation, forest canopies, and the atmosphere. Conservation Biology **15**:1506-1514.

Weathers, K. C., G. M. Lovett, G. E. Likens, and R. Lathrop. 2000. The effect of landscape features on deposition to Hunter Mountain, Catskill Mountains, New York. Ecological Applications **10**:528-540.

Wieder, R. K., and G. E. Lang. 1988. Cycling of Inorganic and Organic Sulfur in Peat from Big Run Bog, West-Virginia. Biogeochemistry **5**:221-242.

Winter, T. C. 1988. Conceptual framework for assessment of cumulative impacts on the hydrology of non-tidal wetlands. Environmental Management **12**:605-620.

Winter, T. C. 1992. A physiographic and climatic framework for hydrologic studies of wetlands. Pages 127-148 *in* M. L. Bothwell, editor. Aquatic ecosystems in semi-arid regions: implications for resource management. Environment Canada, Saskatoon, Sasketchewan, Canada.

Winter, T. C., and M. K. Woo. 1990. Hydrology of lakes and wetlands. Pages 159-187 *in* H. C. Riggs, editor. The geology of North America. The Geological Society of America, Boulder, Colorado, USA.

Xia, K., U. L. Skyllberg, W. F. Bleam, P. R. Bloom, E. A. Nater, and P. A. Helmke. 1999. X-ray absorption spectroscopic evidence for the complexation of Hg(II) by reduced sulfur in soil humic substances. Environmental Science & Technology **33**:257-261.

CHAPTER TWO:
THE INFLUENCE OF HYDROGEOLOGIC SETTING ON THE CONCENTRATION, FLUX, AND RESIDENCE TIME OF MERCURY AND METHYL MERCURY IN DIFFERENT WETLAND TYPES.

ABSTRACT

Wetlands influence the supply of mercury and methyl mercury to aquatic ecosystems. However, the influence of different wetland types on the transformation, release, and transport of mercury to surface waters remains unclear. This study quantifies the hydrology; the concentration and flux of methyl mercury; and the concentration, flux, and residence time of total mercury in wetlands of different hydrogeologic setting in the Adirondack region of New York State. Headwater wetlands were characterized by a consistently high water table and strong recharge gradients; whereas riparian wetlands were characterized by a more dynamically fluctuating water table and moderate discharge gradients. Total mercury and methyl mercury concentrations in peat porewater, outlets, and streams peaked during late summer, when water table elevations were low and soil water temperatures were high. In April and June, total mercury and methyl mercury concentrations were greater in headwater wetland peat porewater and stream water as compared to shallow peat riparian wetlands. In August, total mercury concentrations remained greater in headwater wetlands than in shallow peat riparian wetlands, whereas methyl mercury concentrations in riparian wetlands increased to concentrations similar to the methyl mercury concentrations in headwater wetlands. By November, when water tables had risen and temperatures had decreased, headwater outlet concentrations of mercury and methyl mercury again exceeded concentrations in riparian streams; however, peat porewater concentrations remained similar.

Flow path analysis revealed a decrease in mercury and methyl mercury stream water concentrations from headwater wetland outlets through a series of riparian corridors through the watershed, suggesting a dilution effect from the contribution of groundwater lower in mercury concentrations, or the degradation of methyl mercury.

The stoichiometry of mercury with organic carbon differed in porewater and stream water among wetland types. Differences in stoichiometry suggested that the supply of mercury was limited relative to DOC binding sites in headwater wetlands , whereas mercury:carbon ratios converged toward a maximum in riparian wetlands , a condition suggestive of mercury saturation.

Seepage flux estimates of mercury and methyl mercury were similar in headwater and shallow peat riparian wetlands (mean Hg_d = 5.4 ug*yr^{-1}, SE = 2.4 ug*yr^{-1}; mean $MeHg_d$ = 1.01 ug*yr^{-1}, SE = 0.56 ug*yr-1; Table 2.2); whereas the fluxes of Hg_d and $MeHg_d$ from deep peat riparian wetlands were relatively small (mean Hg_d = 0.6 ug*yr^{-1}, SE = 0.6 ug*yr^{-1}; mean $MeHg_d$ = 0.16 ug*yr^{-1}, SE = 0.16 ug*yr^{-1}; Table 2.2). These fluxes suggest a mean residence time for mercury of 590 years (SE = 69) for headwater wetlands and shallow peat riparian wetlands; whereas the mean residence time was >10,000 years for deep peat riparian wetlands. Seepage flux estimates and the associated residence time of mercury were more strongly dependent upon hydrological parameters than differences in mercury concentrations in different wetland types. Because these estimates of seepage flux were two orders of magnitude smaller than previously measured stream water export from the watershed to the lake, it suggests that preferential flow paths, or deeper flow paths, or both, may contribute to mercury release and transport from wetlands to aquatic ecosystems in the Sunday Lake watershed. Whereas hydrogeologic setting may not result in large differences in fluxes of mercury from wetlands to surface waters, hydrogeologic

setting does fundamentally influence the mechanisms responsible for retention, release, and transport of mercury from different wetland types.

INTRODUCTION

Anthropogenic emissions of mercury to the atmosphere have increased mercury deposition that, in turn, has increased mercury contamination of surface waters (Mason et al. 1994, Lorey and Driscoll 1999, Kamman and Engstrom 2002). In many regions around the world, including the Adirondack region of New York State, this has resulted in the bioaccumulation of methyl mercury (MeHg) in fish tissue to concentrations that exceed EPA recommendations for human consumption and pose health risks to wildlife (Driscoll et al. 1994, Evers and Clair 2005).

Wetlands have been identified as a feature of mercury-sensitive landscapes because they influence the supply of total mercury and methyl mercury to adjacent surface waters (Driscoll et al. 2007, Evers et al. 2007). In general, the role of wetlands has been inferred from watershed-scale studies that correlate the abundance of wetlands within terrestrial ecosystems to concentrations of mercury and methyl mercury in down-gradient aquatic ecosystems (Mierle 1990, Driscoll et al. 1995, Hurley et al. 1995, Babiarz et al. 1998). However, fewer studies have attempted to quantify the influence of different wetland types across the landscape. St Louis et al. (1996) found no consistent differences in yields of total mercury related to wetland type, percentage wetland area, or annual water yield in the boreal forest of the Experimental Lakes Area (Ontario, Canada). That investigation did find that a basin wetland consistently had the greatest flux of methyl mercury and suggested that differences among wetland types stemmed from differences in the internal hydrology of the wetlands (St Louis et al. 1996). Studies that have compared fluxes from different wetland types, or have related mercury concentration or flux in stream water

to the areal extent of wetlands within watersheds, provide a near consensus that hydrological processes are a primary factor influencing the transformation and fate of mercury across upland-wetland landscapes. However, few studies have attempted to quantify the hydrological factors that may underlie wetland influence on mercury supply to surface waters, and the influence of different wetland types on the biogeochemical cycling of mercury remains unclear.

In this study, we use hydrogeologic setting as a framework within which to quantify differences in the biogeochemical cycling of mercury among different wetland types in the Adirondack region of New York State. The distribution of different wetlands types across the landscape is a manifestation of local and regional hydrological processes, and the interaction of those hydrological processes with geological characteristics (*see* Chapter 1). Thus, the hydrogeologic setting of a wetland links landscape position and surficial geology to the resulting hydrologic regime and water chemistry, as well as the chemistry and accumulation of wetland soils (*as summarized in* Chapter 1, Winter 1988, Winter and Woo 1990, Winter 1992, Bedford 1996, Hill and Devito 1997, Bedford 1999). A more detailed articulation of the concept of hydrogeologic setting, as well as the application of this concept to the wetlands of the Sunday Lake watershed can be found elsewhere (i.e., Bedford 1996, Bedford 1999, see Chapter 1, respectively). The hydrogeologic setting of a wetland influences hydrologic flux to and through wetlands, water table level and fluctuation, and thus the duration of soil saturation, as well as the supply of nutrients and electron acceptors. Together, these hydrological and geochemical factors influence the biogeochemical pathways of decomposition; soil saturation results in anoxic conditions and the availability of alternate electron acceptors influences which anaerobic decomposition pathways dominate (e.g., denitrification, iron reduction, sulfate reduction). Mercury methylation is commonly attributed to bacterial sulfate

reduction (Benoit et al. 2003), and mercury transport is commonly attributed to the transport of dissolved organic carbon (Driscoll et al. 2007); thus, hydrogeologically linked factors ultimately control mercury transformations, and the production and release of dissolved organic matter (DOM) on which mercury transport to surface waters is dependent.

The objective of this study was to quantify the concentration, flux, and residence time of mercury within wetlands of different hydrogeologic settings. I compare predominantly ombrotrophic headwater bogs influenced primarily by precipitation, with riparian wetlands that are strongly influenced by groundwater and surface water. By focusing on these hydrogeologically disparate wetlands within a single watershed, I contrast the role of different wetland settings in determining mercury and methyl mercury concentrations in peat porewater, and the release of mercury and methyl mercury from wetlands to surface waters.

METHODS

Site description

The Sunday Lake watershed (~1273 ha) is located along the southwestern boundary of the Adirondack region of New York State, USA (43°51'40" N, 74°06'07"W). Average precipitation is ~1300 mm/yr (1971-2000 mean, with about 30% delivered as snow; data from Big Moose Station and online at http://climod.nrcc.cornell.edu; *see* Chapter 1). The upland soils are mostly well drained spodosols (Typic Haplorthods) with sandy loam to loamy sand texture overlying glacial till or glacial outwash (*see* Chapter 1). Eskers are a distinct feature of the landscape in the Sunday Lake watershed, forming a complex series of ridges and depressions and resulting in the occurrence of numerous wetlands. A more

detailed description of the Sunday Lake watershed and its wetlands is available elsewhere (*see* Chapter 1).

Wetland transects and instrumentation

Nested clusters of water table wells and piezometers were placed along upland-wetland transects previously established for wetland peat coring (*see* Chapter 1). In riparian wetlands, one nested well cluster was placed one meter into the wetland from the upland-wetland interface, a second nested well cluster was placed midway between the upland-wetland interface and the stream channel, and a third nested well cluster was placed one meter from the edge of the stream. In headwater wetlands, additional clusters were used to quantify the influence of open water and changes in overstory vegetation along each transect.

Each nested well cluster was comprised of two water table wells and two piezometers. Each water table well extended to 50 cm depth, and was slotted long its entire length from the surface of the peat to its tip. One water table well was made of Teflon, for sampling porewater chemistry. The second water table well was used for hydrological measurements. The two piezometers were at different depths. The tip of one piezometer was placed at the midway point between the peat surface and the underlying mineral soil. The tip of the second piezometer was placed into the mineral soil below the accumulation of organic peat in each wetland. Each piezometer was slotted along a 10 cm segment at its tip. A staff gauge was installed at each headwater outlet and in each stream to monitor water level.

Hydrologic measurements

Water table wells, piezometers, and staff gauges were surveyed in order to determine their relative elevation in each wetland. During each sampling period,

water level heights were recorded in water table wells, piezometers, and at staff gauges. Water level data were used to determine water table elevation and calculate piezometric gradients across each wetland. Hydrologic data were summarized in longitudinal cross sections of each wetland transect and flow nets were constructed in order to characterize hydrologic flow through each wetland. Hydraulic conductivity was measured at each nested well cluster with a Horslev piezometer test (i.e., bail tests, Freeze and Cherry 1979).

Sampling procedures

Peat porewater, headwater outlets, and streams associated with riparian sites were sampled seasonally (April, June, August, September, November/December). Peat porewater samples were pumped from Teflon water table wells at each well cluster in each wetland. Samples were pumped through Teflon tubing into a borosilicate glass reservoir, and then transferred to Teflon bottles in the field, using clean procedures (USEPA 1996). Separate tubing and reservoir equipment was used for each wetland. All tubing and reservoirs were thoroughly rinsed with ultra-pure de-ionized water and cleaned in a 20% hot nitric acid bath between seasonal sampling periods. Glass reservoirs were stored with 1% hydrochloric acid, rinsed with ultra-pure de-ionized water prior to sampling campaigns, and additionally rinsed with sample water in the field. Outlet and streamwater samples were collected directly into Teflon bottles, using clean procedures (USEPA 1996). Water samples were double bagged, with labels attached to only the outer bag. Samples for analysis of dissolved organic carbon (DOC) were collected in high-density polyethylene sample bottles and filled to minimize headspace. Samples were packed in coolers with ice packs, and returned to the laboratory for processing. Sample filtering and preservation occurred upon arrival at Syracuse University within 48 hours of sampling.

Sample analyses

Samples for analysis of mercury and methyl mercury were filtered through a clean 0.45 µm Teflon membrane. For outlet and stream water samples, both filtered and unfiltered aliquots were acidified to 0.4% with hydrochloric acid and stored in the dark at 4C until analysis. For porewater samples, only the filtered fraction was preserved and stored for analysis. The concentration of total mercury (all forms of mercury) was determined for both unfiltered (Hg_t) and filtered (Hg_d) samples, and the concentration of particulate bound mercury (Hg_p) was estimated by difference (i.e., $Hg_p = Hg_t - Hg_d$). Prior to analysis for Hg_t, samples were subjected to UV light treatment to remove measurement interferences (i.e., high concentrations of DOC). Mercury concentrations were quantified according to EPA Method 1631 using automated CVAFS (Tekran, Toronto, Ontario, Canada, USEPA 1998). The concentration of methyl mercury was also determined for both unfiltered ($MeHg_t$) and filtered ($MeHg_d$) samples. Methyl mercury samples were distilled and analyzed following EPA Method 1630 (USEPA 2001, Revision E). Dissolved organic carbon concentrations were determined for filtered samples (0.7 µm glass fiber filter, pre-baked at 450^{o}C) with a Dohrmann Phoenix 8000 Analyzer using the persulfate-ultraviolet oxidation method (APHA 1998). Samples were analyzed in batches with quality control that included field blanks and duplicates, independent primary and secondary source standards, method detection limit check standards, analysis of appropriate certified reference materials, matrix spike and matrix spike duplicate samples to verify the absence of sample matrix interferences, as well as initial and ongoing calibration verification standards, initial and ongoing calibration blanks, and initial and ongoing precision and recovery standards.

Wetland peat leaching experiment

The amount of mercury available for immediate release from different wetland types to downstream environments was quantified using a simple repeat leaching experiment of wetland peat soils and a synthetic precipitation as an extractant. One peat core (50 cm depth) was collected adjacent to the headwater outlet or riparian stream in each wetland. Each core was homogenized, and extracted repeatedly (10 cycles) using a synthetic precipitation of similar pH and ionic strength to precipitation measured at Huntington Forest, Newcomb, New York. Synthetic precipitation was acidified to pH 4.9 with sulfuric acid, and brought to the correct ionic strength (6.1 x 10^{-5} mols/L) with calcium chloride. Extraction slurries were 2L in volume, with a 2:1 ratio of extractant volume to sample volume. Each cycle of the extraction was shaken for 12 hours at 4-8 ^{o}C, and peat samples were kept cold and in the dark throughout the experiment. Extractions were not kept strictly anaerobic; however, extractant solution and headspace of each Teflon extraction unit were sealed and degassed with ultra-pure nitrogen at the beginning of each leaching cycle. Each leaching cycle lasted approximately 2 days; at the end of each 2-day cycle, samples were pressure filtered through a 0.45um teflon membrane filter. Subsamples for mercury analysis were transferred to teflon bottles and acidified to 0.4% with hydrochloric acid; subsamples for DOC analysis were transferred to glass vials with no headspace. Mercury and DOC analyses were analyzed as described for field collected samples (see Methods, *Sample Analyses*).

Flux and residence time calculations

Hydrologic fluxes were calculated as seepage face fluxes (e.g., Dunne and Leopold 1978) at the outlet in headwater wetlands and at streamside in riparian wetlands according to Darcy's Law:

$$Q = AK(\Delta h/\Delta l) \quad (2.1)$$

where Q is the rate of flow (m^3/day), A is the cross sectional area of flow (m^2), K is the hydraulic conductivity (m/day), Δh is the difference in water table elevation across the wetland transect, Δl is the distance between measurement points along the flowpath, and thus ($\Delta h/\Delta l$) represents the hydraulic gradient of the water table (Dunne and Leopold 1978). Because we hypothesized that the less decomposed and more biologically active surface peat (i.e., the acrotelm) would be more hydrologically conductive than deeper accumulations of wetland peat, we limited our per meter width cross sectional area to a depth of 50 cm. This corresponds to the same depths over which water table wells were sampled for peat porewater chemistry. These seepage face flux estimates assume that horizontal flow dominates hydrologic fluxes and do not account for preferential flow. Thus, flux estimates from different wetland types may be comparable in a relative sense, but they likely do not represent total hydrological or chemical fluxes from different wetland types.

Residence time of mercury in different wetland types was calculated from seepage face fluxes (as estimated above) and mercury pool sizes quantified for these upland-wetland transects and described in detail elsewhere (*see* Chapter 1).

RESULTS AND DISCUSSION

Hydrologic characteristics of wetlands of different hydrogeologic setting

Hydrologic characteristics varied among wetland types, across individual wetland transects, and with season; water table elevation and piezometric gradients were more dynamic in riparian zones as compared to headwater wetlands (Table 2.1, Appendix A, Appendix B). Overall, wetland hydrology was typical for each wetland type. Headwater wetlands were characterized by a consistently high water table and

strong recharge gradients; whereas, riparian wetlands were characterized by a more dynamically fluctuating water table and patterns of piezometric head potential that were dominated by discharge gradients.

Specifically, in the headwater wetlands, the water table remained near the surface of the peat throughout the year, rising above the surface during winter, spring, and fall (mean maximum = 5.7 cm, SE = 2.3 cm) and falling below the surface of the peat during summer (mean minimum = -7.4 cm, SE = 0.4 cm; Table 2.1). Both the deep peat riparian and the shallow peat riparian wetlands had greater seasonal fluctuations in the water table (Table 2.1). The water table in the shallow peat riparian wetlands remained below the surface of the peat during all seasonal sampling periods (mean maximum = -4.9 cm, SE = 2.4 cm), falling to a mean depth of -30.4 cm (SE = 9.1 cm) below the surface of the peat during summer. However, observations of sand and gravel deposited throughout shallow peat riparian soil profiles and on the surface of organic horizons are indicative of occasional over-bank flooding. Whereas nearly the entire peat profile of the headwater wetlands remained saturated throughout the year, the water table in the shallow peat riparian wetlands declined into the mineral horizons underlying the organic horizons (*see* Chapter 1), thus exposing the entire peat profile to unsaturated, oxidizing conditions (Table 2.1, Appendix A, Appendix B). Piezometric head potential varied more in magnitude and direction in the riparian wetlands as compared to the headwater wetlands (Figure 2.1a,b,c, Appendix A, Appendix B). Recharge gradients dominated the hydrology of headwater wetlands during all seasonal sampling periods (Figure 2.1a). Only at the upland edge of the headwater wetlands did we detect a weak discharge gradient (Figure 2.1a). The piezometric head potential gradients in the riparian wetlands were spatially and temporally more variable. In the deep peat riparian wetlands, weak discharge zones were common at the streamside and at the upland-wetland interface during spring and

Table 2.1. Water table level maximum, minimum, and range (max-min) across wetland transects in headwater (HW), deep peat riparian (DPR), and shallow peat riparian (SPR) wetlands in the Sunday Lake watershed. Water table levels relative to ground surface were back-calculated from surveyed reference points. Additional letters after wetland type abbreviations denote individual wetlands.

		Water Table Relative to Ground Surface		
Wetland	Transect Distance (m)	Max (cm)	Min (cm)	Max-Min (cm)
HW_P	1	0.9	-16.8	17.7
HW_P	45	2.7	-4.9	7.6
HW_P	60	5.5	-6.9	12.4
HW_P	80	2.2	-6.4	8.6
HW_P	100	5.7	-0.3	6.0
HW_P	Outlet	9.2	-0.3	9.5
HW_H	1	8.5	-6.6	15.1
HW_H	37	6.9	-9.4	16.3
HW_H	75	8.3	-7.5	15.8
HW_H	Outlet	-6.7	-29.6	22.9
DPR_MR	1	-5.3	-19.5	14.2
DPR_MR	40	1.0	-20.7	21.7
DPR_MR	81	5.2	-4.7	9.9
DPR_MR	Stream	-11.3	-20.1	8.8
DPR_BR	1	-13.9	-33.6	19.7
DPR_BR	30	-8.6	-30.7	22.1
DPR_BR	60	-0.5	-26.6	26.1
DPR_BR	Stream	-5.6	-33.1	27.5
SPR_HR	1	-10.6	-49.8	39.2
SPR_HR	9	-8.8	-35.5	26.7
SPR_HR	18	-2.4	-33.0	30.6
SPR_HR	Stream	-5.8	-38.8	33.0
SPR_SLR	1	0.6	-14.3	14.9
SPR_SLR	5	-0.7	-19.2	18.5
SPR_SLR	10	-7.5	-30.0	22.5
SPR_SLR	Stream	-13.3	-39.8	26.5

Figure 2.1.a. Concentrations of dissolved mercury (Hg_d) and dissolved methyl mercury ($MeHg_d$) in peat porewater from across transects within two individual shallow peat riparian wetlands of the Sunday Lake watershed. Particulate bound mercury (Hg_p) is shown only for stream samples. The distance from the upland-wetland edge along each transect is noted below each sampling point. The two arrows below each sampling point represent measured piezometric gradients. The top arrow at each sampling point represents the piezometric gradient measured by the mid-depth piezometer; the bottom arrow at each sampling point represents the piezometric gradient measured by the piezometer within mineral sediments below the wetland. Upward pointing arrows represent discharge gradients; downward pointing arrows represent recharge gradients. Arrows represent weak gradients (<10 cm difference in head potential compared to the water table), the dash represents no detectable gradient; n.v. means that no value was available.

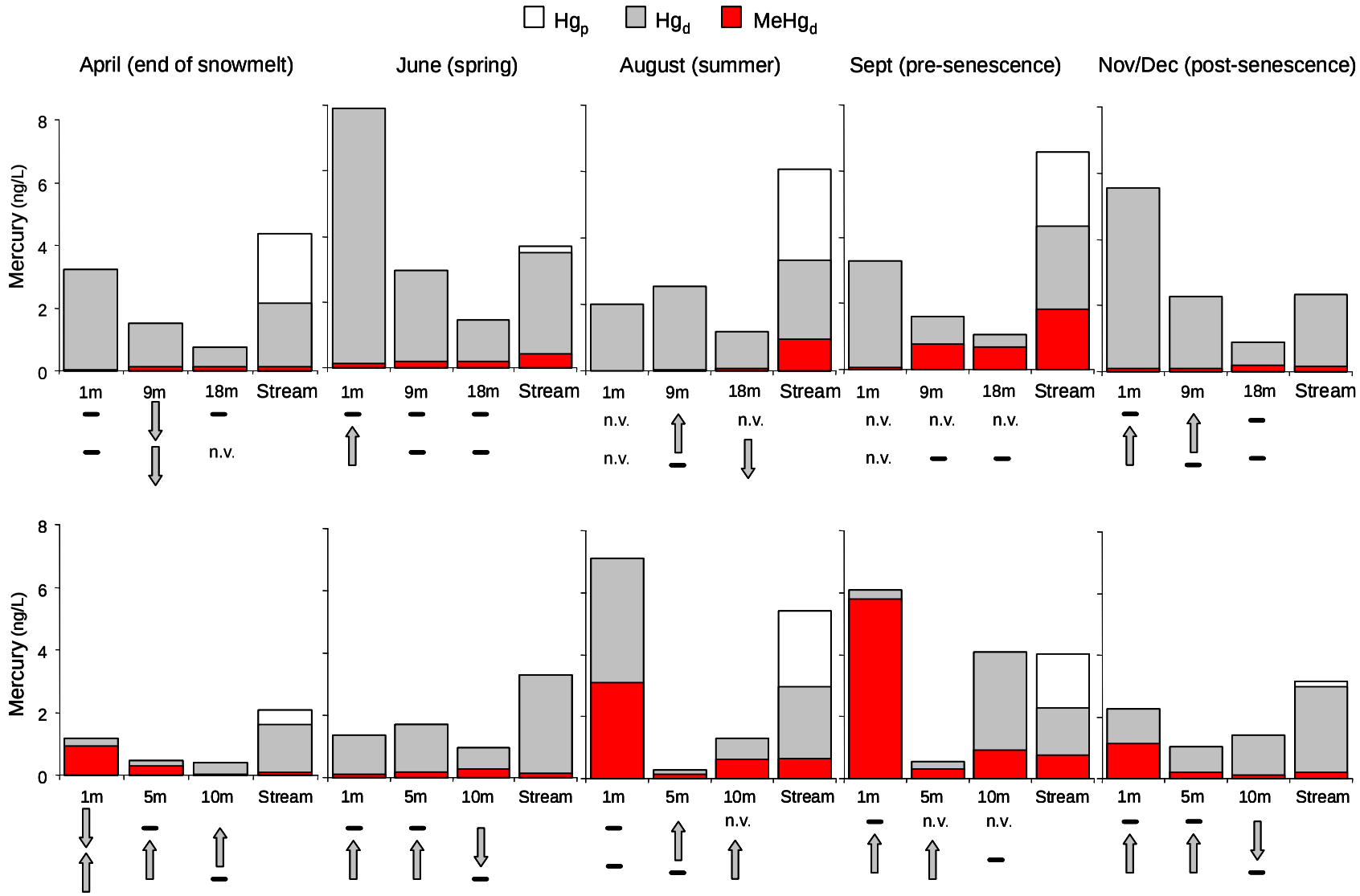
Hg$_p$
Hg$_d$
MeHg$_d$
April (end of snowmelt)
June (spring)
August (summer)
Sept (pre-senescence)
Nov/Dec (post-senescence)
Mercury (ng/L)
0
2
4
6
8
1m
9m
18m
5m
10m
Stream
n.v.

Figure 2.1.b. Concentrations of dissolved mercury (Hg_d) and dissolved methyl mercury ($MeHg_d$) in peat porewater from across transects within two individual deep peat riparian wetlands of the Sunday Lake watershed. Particulate bound mercury (Hg_p) is shown only for riparian stream samples. The distance from the upland-wetland edge along each transect is noted below each sampling point. The two arrows below each sampling point represent measured piezometric gradients. The top arrow at each sampling point represents the piezometric gradient measured by the mid-depth piezometer; the bottom arrow at each sampling point represents the piezometric gradient measured by the piezometer within mineral sediments below the wetland. Upward pointing arrows represent discharge gradients; downward pointing arrows represent recharge gradients. Large arrows represent strong gradients (>10 cm difference in head potential compared to the water table); small arrows represent weak gradients (<10 cm difference in head potential compared to the water table), the dash represents no detectable gradient; n.v. means that no value was available.

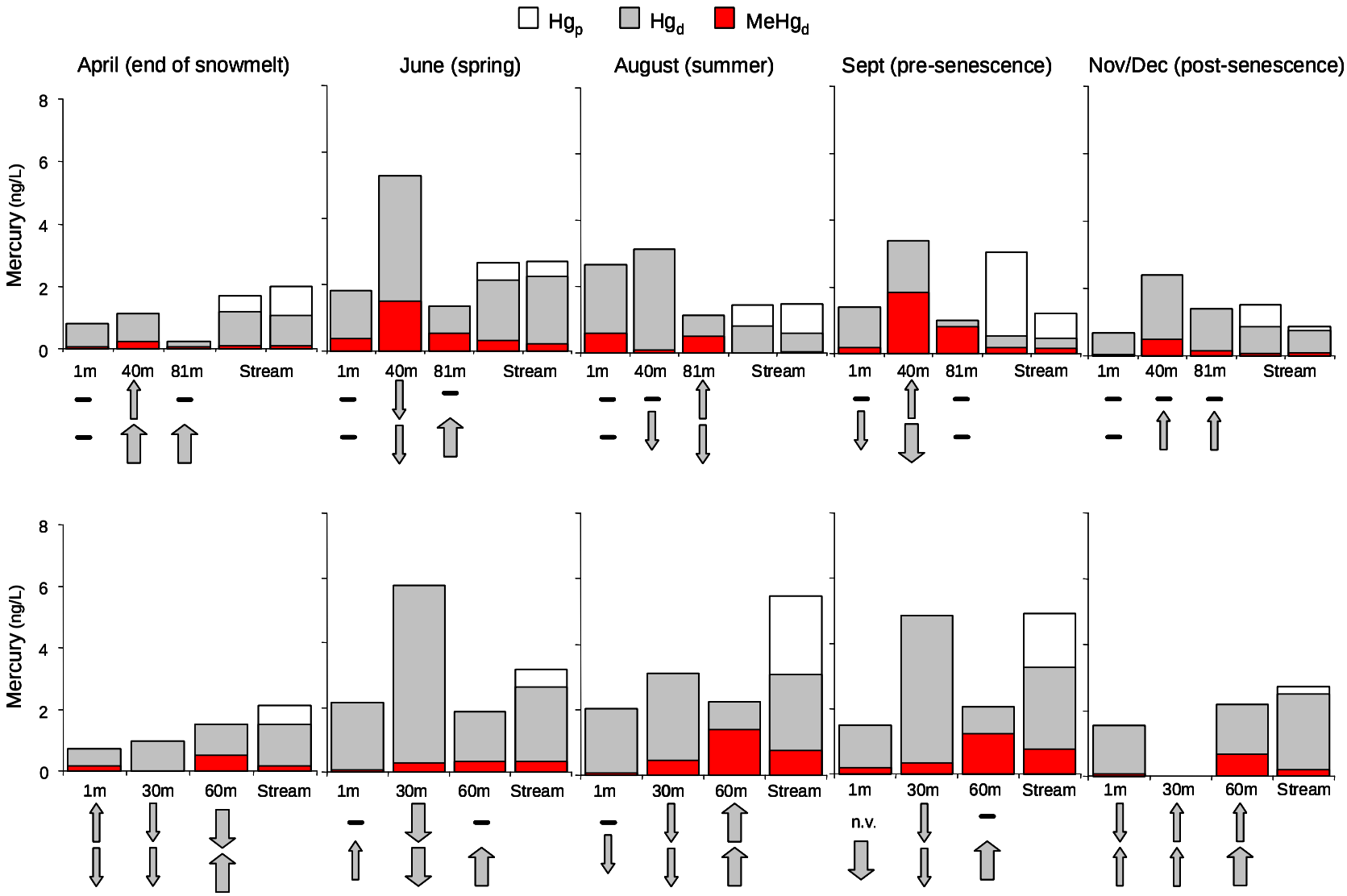
Hg$_p$
Hg$_d$
MeHg$_d$
April (end of snowmelt)
June (spring)
August (summer)
Sept (pre-senescence)
Nov/Dec (post-senescence)
Mercury (ng/L)
0
2
4
6
8
1m
40m
81m
30m
60m
Stream
n.v.

Figure 2.1.c. Concentrations of dissolved mercury (Hg_d) and dissolved methyl mercury ($MeHg_d$) in peat porewater from across transects within two individual headwater wetlands of the Sunday Lake watershed. Particulate bound mercury (Hg_p) is shown only for outlet samples. The distance from the upland-wetland edge along each transect is noted below each sampling point. The two arrows below each sampling point represent measured piezometric gradients. The top arrow at each sampling point represents the piezometric gradient measured by the mid-depth piezometer; the bottom arrow at each sampling point represents the piezometric gradient measured by the piezometer within mineral sediments below the wetland. Upward pointing arrows represent discharge gradients; downward pointing arrows represent recharge gradients. Large arrows represent strong gradients (>10 cm difference in head potential compared to the water table); small arrows represent weak gradients (<10 cm difference in head potential compared to the water table), the dash represents no detectable gradient; n.v. means that no value was available.

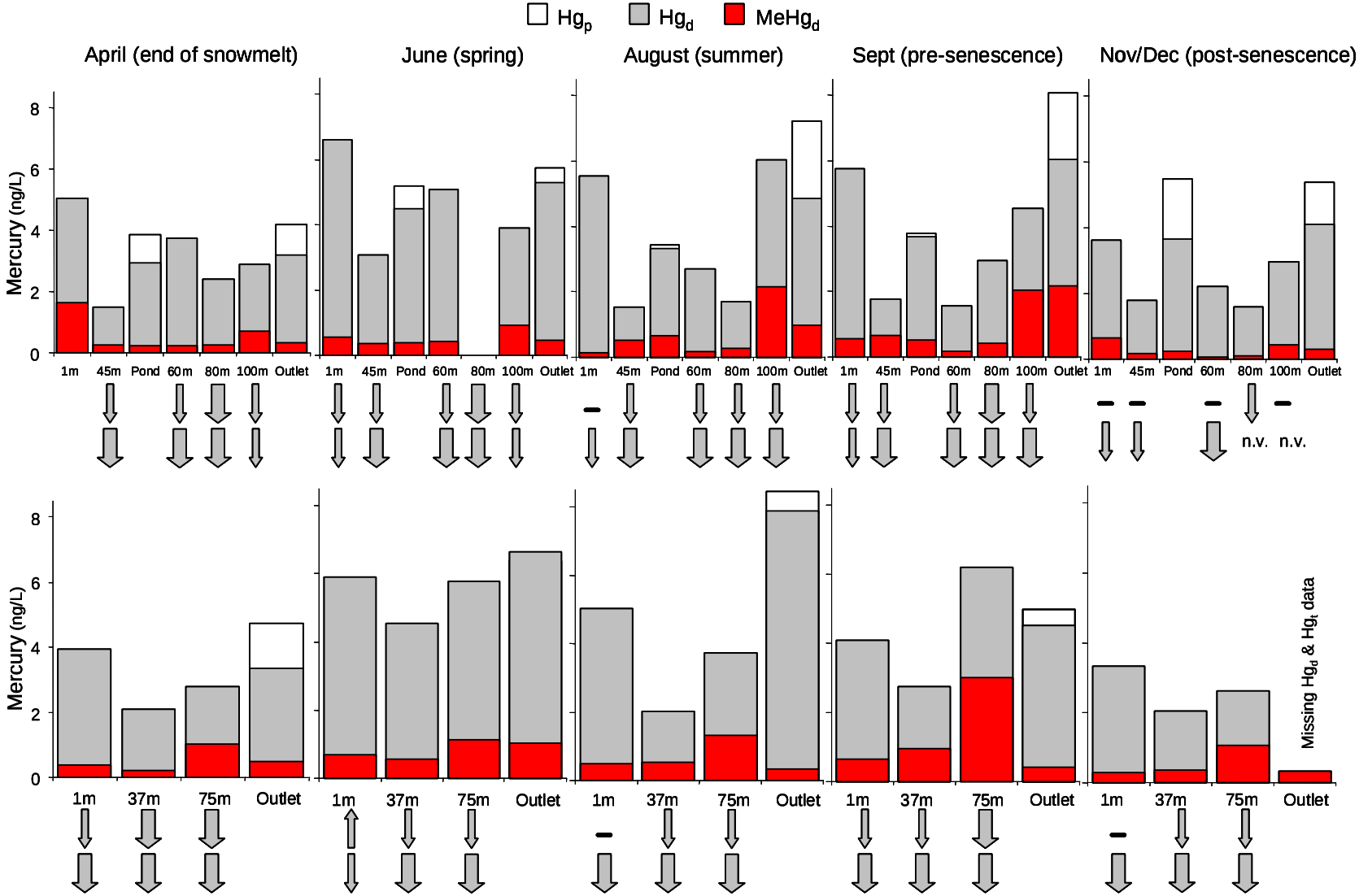
Hg_p
Hg_d
MeHg_d
April (end of snowmelt)
June (spring)
August (summer)
Sept (pre-senescence)
Nov/Dec (post-senescence)
Mercury (ng/L)
0
2
4
6
8
1m
45m
Pond
60m
80m
100m
Outlet
n.v.
n.v.
37m
75m
Missing Hg_d & Hg_t data

fall (Figure 2.1b). In contrast, recharge gradients dominated the central portions of the deep peat riparian wetlands, especially during summer (Figure 2.1b). In shallow peat riparian wetlands, piezometric head potentials were difficult to detect due, in part, to the shallow placement of piezometers relative to the water table. Thus, shallow peat riparian wetlands tended to lack clear recharge and discharge gradients. Nonetheless, we detected discharge gradients far more frequently than recharge gradients in shallow peat riparian wetlands (71% overall, 86% at upland edge, 78% at the center, and 40% at stream edge; Figure 2.1c).

Mercury and methyl mercury concentrations

Seasonality. Dissolved mercury (Hg_d) and $MeHg_d$ concentrations varied by season. Peaks in Hg_d concentration occurred in wetland porewater, outlets, and associated streams of all wetland types during June, August, and September as temperatures increased and water table elevations declined (Figure 2.2, Table 2.1, Table 2.2). This pattern likely results from two interactions: (1) high temperature increases decomposition that releases mercury associated with dissolved organic matter (DOM); and (2) increased evapotranspiration concentrates mercury in residual porewater. In headwater wetland porewater and outlet streamwater, $MeHg_d$ concentrations increased in June and August (as compared to April), and were greatest in late summer (i.e., September). Deep peat riparian porewater concentrations of $MeHg_d$ also increased in June and August (as compared to April) and were also greatest in late summer (i.e., September). Peak $MeHg_d$ concentrations in shallow peat riparian porewater and stream water were delayed until August and September. Thus, in the shallow peat riparian wetlands, peaks in $MeHg_d$ concentrations tended to occur later in the summer season (i.e., August, September), lagging behind peaks in Hg_d concentrations. This pattern suggests that mercury methylation responds to the supply

Figure 2.2. Average concentrations of dissolved mercury (Hg_d) and dissolved methyl mercury ($MeHg_d$) in peat porewater of headwater and riparian wetlands, and Hg_d, $MeHg_d$, and particulate bound mercury (Hg_p) in headwater wetland outlets and riparian wetland streams of the Sunday Lake watershed during five seasonal sampling periods. Total height of each bar represents total mercury (Hg_t). Error bars show range in concentrations of mercury (n = 2 for each wetland type). Wetland types are headwater wetlands (HW), deep peat riparian wetlands (DPR), and shallow peat riparian wetlands (SPR).

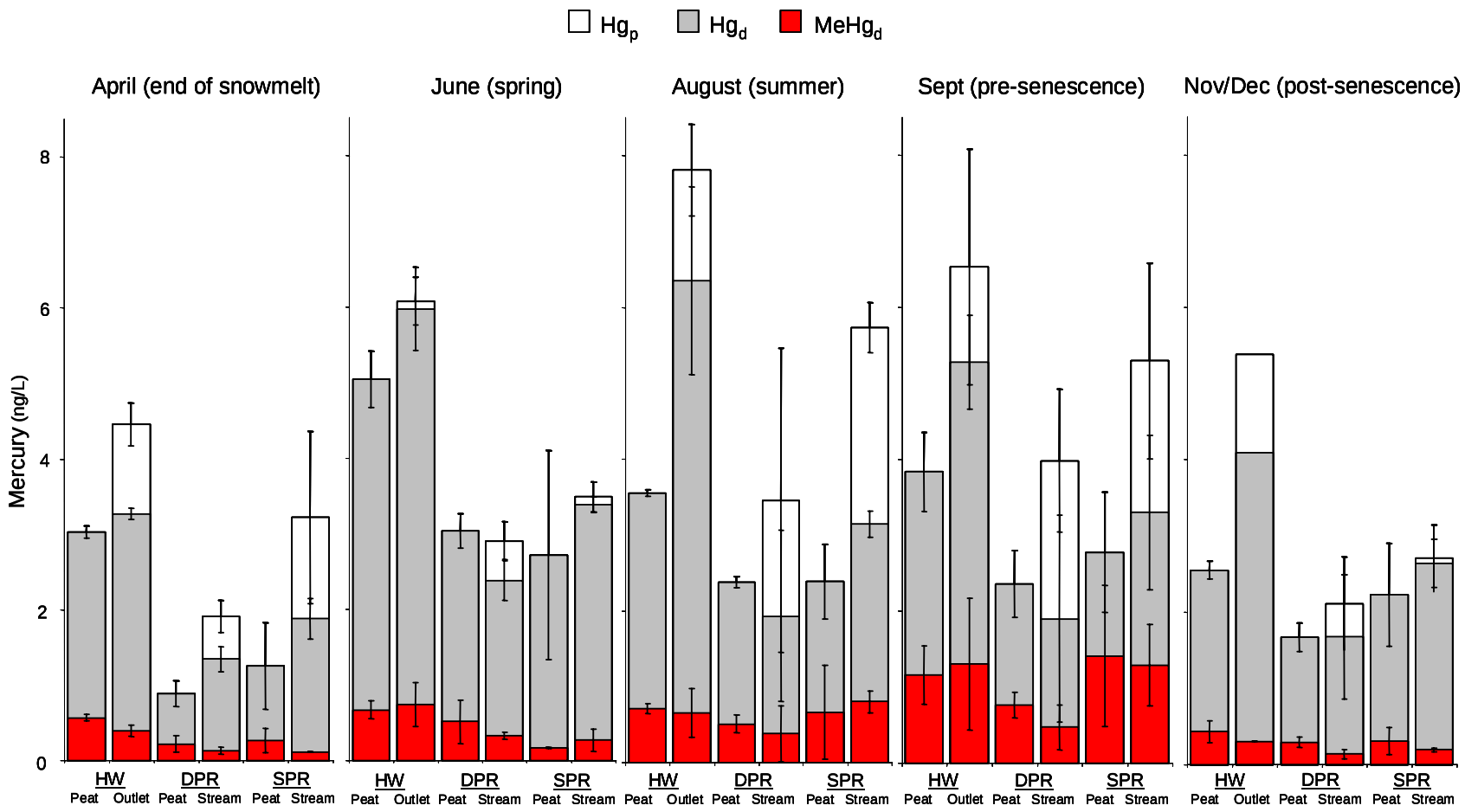
Hg$_p$
Hg$_d$
MeHg$_d$
April (end of snowmelt)
June (spring)
August (summer)
Sept (pre-senescence)
Nov/Dec (post-senescence)
Mercury (ng/L)
0
2
4
6
8
HW
DPR
SPR
Peat
Outlet
Stream

Table 2.2. Flux and residence time of mercury in (a) different wetland types and (b) individual wetlands of the Sunday Lake watershed. Fluxes calculated for each seasonal sampling period have been composited to represent a single annual flux from each wetland. Water fluxes were calculated with Darcy's Law, and are seepage fluxes through a per meter width cross sectional area of the peat profile to 50 cm depth (representing the acrotelm). Streamside flux estimates were calculated with hydraulic conductivity measurements taken from within one meter of stream; average flux estimates were calculated with an average hydraulic conductivity from measurements made at each water table well located along the wetland transect. Residence times were calculated with (streamside or average) seepage fluxes and total soil pool of organic horizons within the top 50 cm of each wetland. Values in parentheses show 1 SE. For shallow peat riparian wetlands, values in [brackets]* show the residence time for total soil pool to 50 cm, including mineral horizons.

(a) Flux and mean residence time for wetland types.

		Streamside		Average	
Wetland		Flux ug/yr	Residence Time (yrs)	Flux ug/yr	Residence Time (yrs)
HW	Hg_d	10.6 (1.5)	268 (117)	5.6 (3.7)	614 (114)
	$MeHg_d$	1.35 (<0.01)		1.11 (0.81)	
DPR	Hg_d	0.4 (0.3)	>10,000 (>10,000)	0.6 (0.6)	>10,000 (>10,000)
	$MeHg_d$	0.15 (0.12)		0.16 (0.16)	
SPR	Hg_d	2.4 (2.1)	4006 (3098)	5.3 (2.0)	566 (3)
	$MeHg_d$	0.45 (0.39)		0.91 (0.53)	

(b) Flux and mean residence time for individual wetlands.

		Streamside		Average	
Wetland		Flux ug/yr	Residence Time (yrs)	Flux ug/yr	Residence Time (yrs)
HW_P	Hg_d	9.11	151	1.9	728
	$MeHg_d$	1.36		0.30	
HW_H	Hg_d	12.09	385	9.3	500
	$MeHg_d$	1.35		1.93	
DPR_MR	Hg_d	0.69	4967	1.3	2724
	$MeHg_d$	0.27		0.32	
DPR_BR	Hg_d	0.08	>10,000	0.04	>10,000
	$MeHg_d$	0.03		0.01	
SPR_HR	Hg_d	4.48	908 [2378]*	7.2	562 [1473]*
	$MeHg_d$	0.83		0.39	
SPR_SLR	Hg_d	0.27	7103 [>10,000]*	3.3	569 [2252]*
	$MeHg_d$	0.06		1.44	

of inorganic mercury and thus is limited by its availability in shallow peat riparian wetlands.

Mercury associated with the particulate phase (Hg_p) varied widely; however streamwater concentrations of Hg_p tended to be greatest during late summer, especially in the riparian streams. In late summer during low stream flow, riparian streambeds developed a thick biofilm, contributing organic floc to the water column (*personal observation*). This agrees with other streamwater mercury measurements during monthly monitoring at the Sunday Lake watershed that found peak Hg_t concentrations occur during summer low flow at the lake inlet (Selvendiran et al. *in press*). The prevalence of the particulate mercury fraction at low flow is in contrast to findings from large rivers and higher gradient streams that report that the greatest particulate transport of mercury occurs during snowmelt and other high flow events.

Differences among wetland types. There were few consistent differences in mercury and methyl mercury concentrations in peat porewater and stream water among different wetland types (Figure 2.2). In April and June, concentrations of Hg_d and $MeHg_d$ in porewater, as well as Hg_d, $MeHg_d$, and Hg_t in stream water, were greater in headwater wetlands as compared to shallow peat riparian wetlands (Figure 2.2). In August, porewater Hg_d, as well as stream water Hg_d and Hg_t, remained greater in headwater wetlands as compared to shallow peat riparian wetlands; however, $MeHg_d$ concentrations in porewater and stream water in headwater wetlands were no different than concentrations in shallow peat riparian wetlands (Figure 2.2). Thus, the net methylation efficiency (i.e., the percentage of Hg_d occurring as $MeHg_d$, or %MeHg) in the shallow peat riparian wetlands increased during summer when temperatures were warm and the water table was low. By September, the only remaining difference in mercury concentrations among wetland types was that the stream water Hg_d concentrations of the headwater outlets were greater than the Hg_d

concentration of the riparian wetland streams. By November, when water table levels had risen to near their maximum, the headwater wetland outlet concentrations of Hg_d, $MeHg_d$, and Hg_t again exceeded that of the riparian streams; however, porewater concentrations of Hg_d and $MeHg_d$ remained no different. Thus, the only consistent difference among wetland types was that headwater wetland outlets exhibited higher Hg_d concentrations than riparian streams.

Comparing porewater to streamwater. Average peat porewater concentrations of Hg_d in headwater wetlands were generally lower than concentrations in associated outlet streams (Figure 2.2). This pattern suggests that not all areas equally contribute to Hg_d concentrations at the outlet, or that only a certain fraction of the DOC, and thus, only a certain fraction of the mercury in headwater wetlands is mobile. This sort of phenomenon would be consistent with the previous findings of Kolka (2001) which suggested that much of the mercury exported from a bog in Minnesota originated from the lag zone.

Shallow peat riparian wetlands showed a similar pattern with generally lower Hg_d concentrations in porewater than in adjacent stream water. However, in riparian wetlands, differences between porewater and stream water concentrations of mercury are difficult to interpret because riparian stream water is a composite of sources from the adjacent riparian wetland and the watershed upstream of the sampling location. Thus, it is unclear if different areas of the riparian wetlands contribute equally to stream water mercury concentrations. Depending upon which areas of the riparian wetlands are contributing to the stream, the riparian porewater may be either increasing or diluting the concentration of mercury in the adjacent stream (Figure 2.1, Figure 2.2).

In deep peat riparian wetlands, the relationship between porewater and stream water concentrations of Hg_d was variable; porewater concentrations of Hg_d in deep

riparian wetlands tended to be greater than stream water concentrations during the summer sampling periods (June, August, September), and less than or equal to stream water concentrations during the spring and fall (April, November/December; Figure 2.1b; Figure 2.2). In the deep peat riparian wetlands, the hydrologic flux from the wetland to the riparian stream was minimal compared to other wetland types in this study (see *Results and Discussion: Differences in mercury flux and residence time among wetland types*); thus, the deep peat riparian wetland porewater likely has little influence on stream water concentrations of Hg_d or $MeHg_d$. Seasonal fluctuations in porewater concentrations of Hg_d in these deep peat riparian wetlands are likely due to evaporative and dilution effects, the balance between deposition and revolatilization of mercury, and the release of mercury from peat to porewater in association with the processing of organic matter.

Seasonal fluctuation of $MeHg_d$ concentrations in porewater are also likely influenced by the balance of *in situ* methylation and demethylation processes (*sensu* Marvin-Dipasquale and Oremland 1998, Marvin-DiPasquale et al. 2000). It is unclear what percentage of $MeHg_d$ present during periods of peak net $MeHg_d$ production in wetlands is actually transported to aquatic ecosystems before it is demethylated.

In contrast to Hg_d, average peat porewater concentrations of $MeHg_d$ were greater than or equal to average concentrations of $MeHg_d$ in associated headwater outlets and riparian streams in all wetlands during all sampling periods (Figure 2.2). Thus, it would appear that all wetlands of the Sunday Lake watershed have the potential to increase the concentration of $MeHg_d$ transported from watersheds to downstream surface waters. This pattern is consistent with watershed level observations suggesting that wetlands are important sources of methyl mercury to surface waters (Driscoll et al. 1994, Driscoll et al. 1998). However, individual wetland transects also show that porewater $MeHg_d$ concentrations are both spatially

and temporally variable within individual wetlands (Figure 2.1a,b,c). During all sampling periods in headwater wetlands and deep peat riparian wetlands, at least some areas of the wetland were capable of contributing concentrations of $MeHg_d$ great enough to drive outlet concentrations (Figure 2.1a,b). In contrast, shallow peat riparian wetlands did not consistently have porewater $MeHg_d$ concentrations greater than $MeHg_d$ concentrations in associated riparian streams (Figure 2.1c). Thus, the importance of shallow peat riparian wetlands for increasing $MeHg_d$ concentrations to downstream surface waters is highly variable among individual wetlands, and is dependent upon the relative $MeHg_d$ concentration of upstream sources.

Flow path analysis. The arrangement of the wetlands along one section of the watershed allowed us to evaluate patterns of mercury concentrations along the flow path of water through the catchment, utilizing one headwater wetland and three of the riparian wetlands (Figure 2.3). In all seasons, total unfiltered mercury concentrations (Hg_t), Hg_d, and $MeHg_d$ tended to be highest in the headwater outlets and to decrease along the flow path of the stream (Figure 2.3). Differences in mercury and methyl mercury concentrations between the last two sampling points along the flow path were generally small, and the final station tended to be slightly elevated during spring and fall. This observation may result from this entire section of the stream being lined with riparian wetlands, the inputs of which might gradually increase stream water concentrations of Hg_d, or from the contribution of a tributary draining a small sub-watershed containing a large complex of headwater wetlands. However, the range in porewater Hg_d concentrations in the riparian wetlands were less than stream water concentrations during these sampling periods, which suggests that increases in the stream water Hg_d concentration resulted from the contributions of the tributary.

Figure 2.3. Stream water concentrations of total mercury (Hg_t), dissolved mercury (Hg_d), and dissolved methyl mercury ($MeHg_d$) along the flow path of the stream through different wetland types of the Sunday Lake watershed during five seasonal sampling periods. Peat porewater concentrations of dissolved mercury (Hg_d), and dissolved methyl mercury ($MeHg_d$) are shown associated with mercury concentrations in stream water. Error bars show the range of peat porewater mercury concentrations in each wetland (n = 5 in headwater peat porewater, n = 3 in riparian peat porewater).

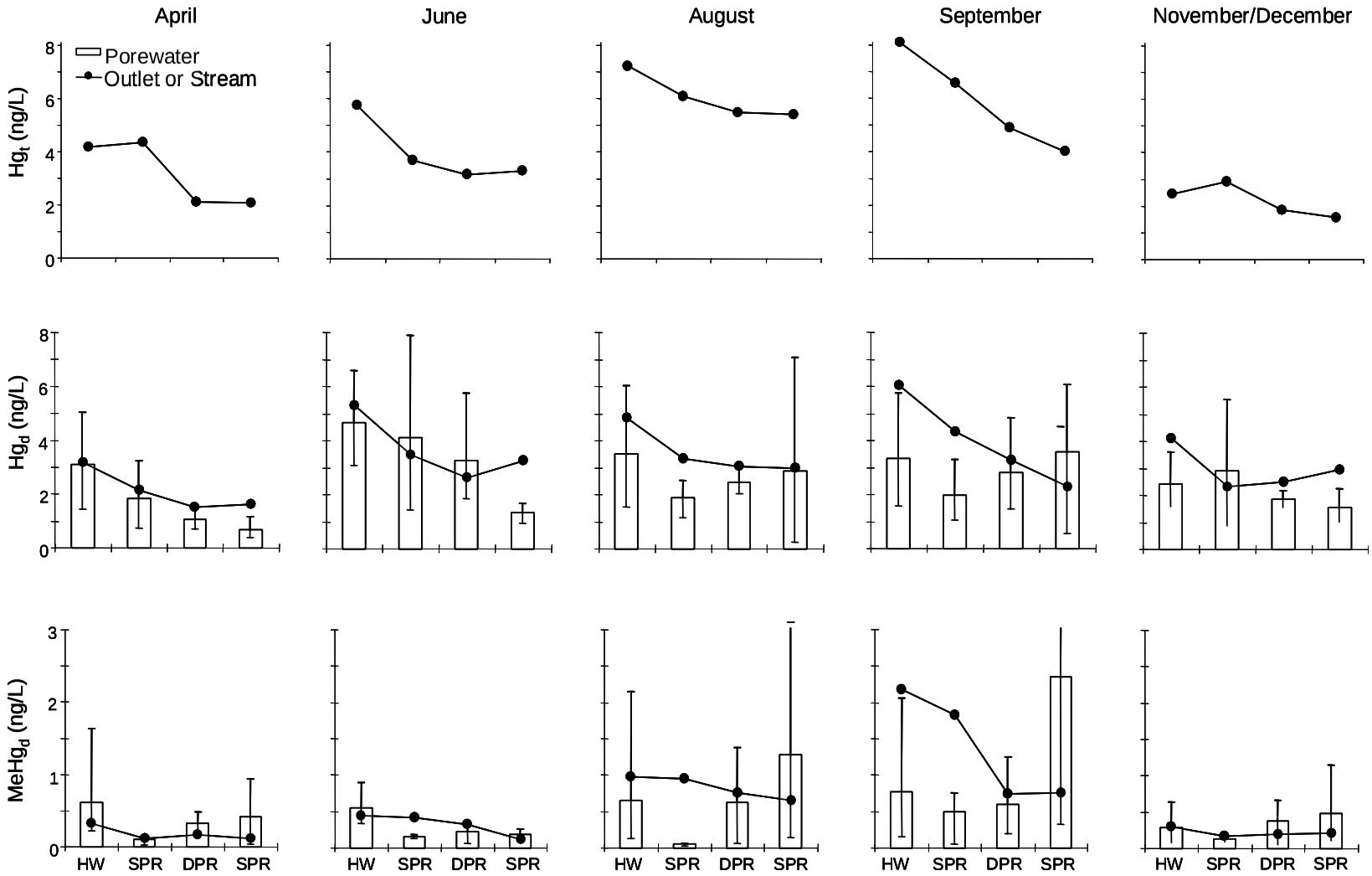
April
June
August
September
November/December
Porewater
Outlet or Stream
Hg_t (ng/L)
Hg_d (ng/L)
$MeHg_d$ (ng/L)
0
2
4
6
8
1
3
HW
SPR
DPR
SPR

Overall, mercury concentrations were likely diluted along the flow path by groundwater concentrations low in mercury; whereas methyl mercury concentrations could have decreased as a result of dilution or degradation. Because total water flow increases substantially along the flow path, total flux of mercury and methyl mercury also likely increase along the flow path despite decreases in concentration.

Mercury release and transport

Mercury:carbon stoichiometry. The relationship between mercury and organic carbon differed both in peat porewater, as well as in stream water, among different wetland types (Figure 2.4). Peat porewater Hg_d was weakly correlated with DOC in deep and shallow peat riparian wetlands ($r^2 = 0.44$; $r^2 = 0.46$, respectively; Figure 2.4a); Hg_d was not correlated with DOC in porewater of headwater wetlands (Figure 2.4a). Nonetheless, mercury was transported in association with DOC in both headwater wetland outlets and riparian streams ($r^2 = 0.63$, $r^2 = 0.80$, respectively; Figure 2.4b). However, the slope of the Hg_d:DOC relationship was 3x lower in the headwater outlets versus the riparian streams, reflecting differences in porewater Hg_d:DOC relationships. Thus, among wetland type differences in stream water and porewater chemistry reflect differences in peat chemistry (*see* Chapter 1, Figure 1.3d,g,p,s). The observed lack of correlation between mercury and organic carbon in the peat and porewater chemistry of headwater wetlands (*see* Chapter 1, Figure 1.3p,s; Figure 2.4a) suggests that the Hg:DOC relationship may be limited by the supply of mercury rather than by the availability of Hg-DOC binding sites in headwater wetlands (Figure 2.4a,b). As suggested previously for differences in porewater and outlet concentrations, the slight slope of the Hg:C relationship in the headwater outlets may indicate that either the source of mercury to the outlet does not equally reflect

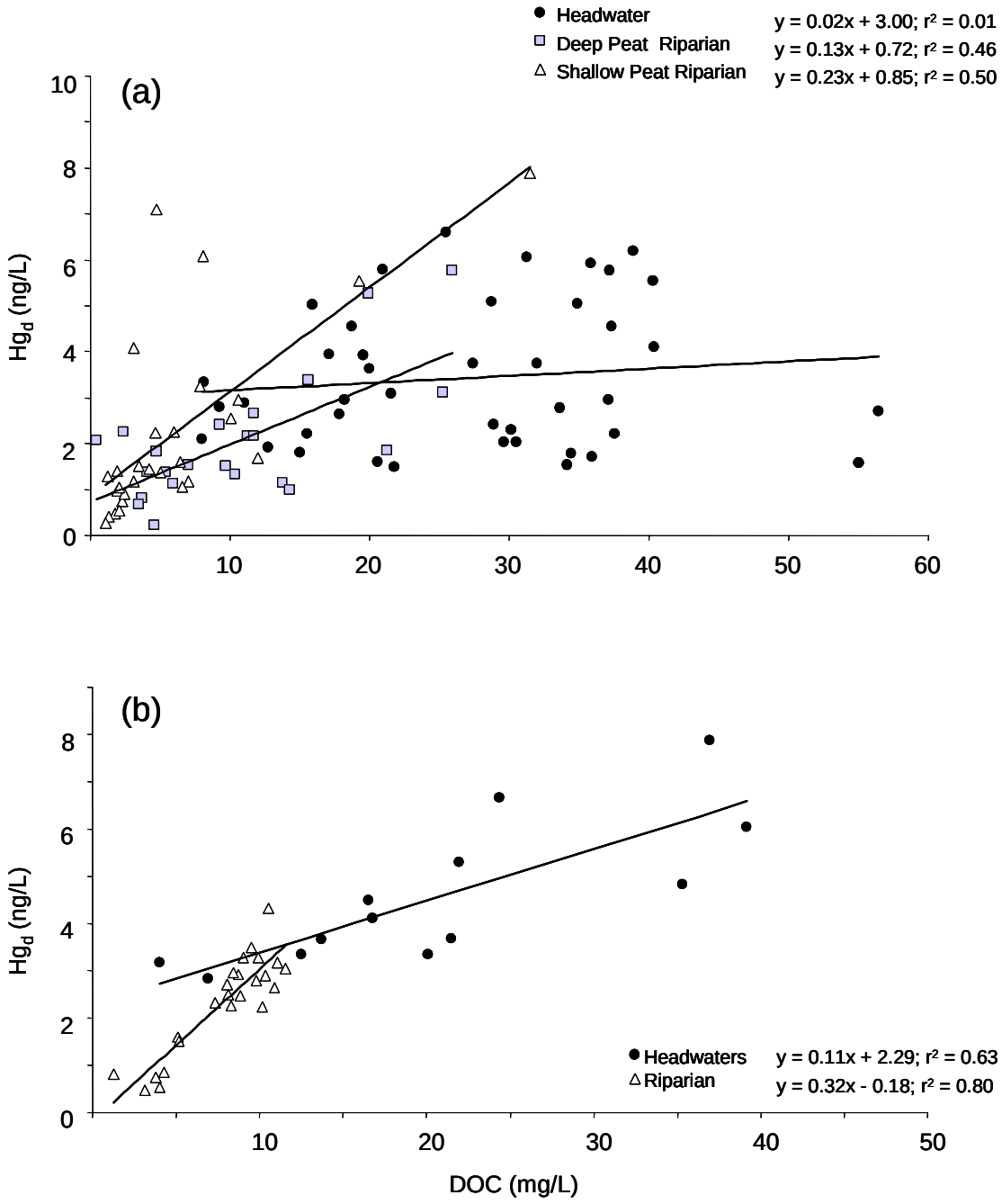

Figure 2.4. Scatterplots showing the relationship between dissolved mercury (Hg_d) and dissolved organic carbon (DOC) in (a) wetland peat porewater, and (b) headwater outlets and riparian streams. Note that there was no significant difference in the slope and intercept of the deep and shallow riparian regression lines; thus all riparian stream data were combined.

average wetland porewater, or that only a fraction of DOC in the headwater wetland porewater is mobile.

Riparian porewater also had a lower (and more variable) Hg:C ratio than riparian stream water. Nonetheless, the strong correlation between mercury and carbon in riparian stream water (Figure 2.4b) suggests that the mercury transported in riparian streams is limited by DOC binding and transport, and resembles the strong correlation between mercury and organic carbon observed in both shallow peat riparian wetland soils and upland mineral soil horizons (Figure 2.4b; *see* Chapter 1, Figure 1.3a,d,g).

Convergence of Hg:C stoichiometry. In Chapter 1, it was postulated that the Hg:C ratio in mineral soil horizons of forests results from decomposition, hydrologic transport, and the physicochemical fractioning of organic matter between the dissolved and adsorbed phases (*sensu* Schuster 1991). Data suggested that as dissolved organic matter is released from the organic soil horizon during organic matter decomposition, the Hg:C ratio converges upon an upper limit to Hg:C ratios found throughout the forest soil profile (*see* Chapter 1). Thus, Chapter 1 concluded that the observed patterns of Hg:C in the mineral soil horizon could result from a relatively fixed stoichiometry associated with decomposition products. Based on the slope of the Hg:DOC relationship of various sources (Figure 2.5), it appears that riparian streams are a composite of upland and riparian sources (which are similar) and headwater wetland sources. It also appears that headwater sources may have a strong influence on the Hg:C composition in riparian streams.

Wetland peat leaching experiment. In a simple repeat leaching experiment of wetland peat soils using a synthetic precipitation as an extractant, I quantified the amount of mercury and DOC in different wetland types that was available for immediate release to downstream environments. DOC was released during all

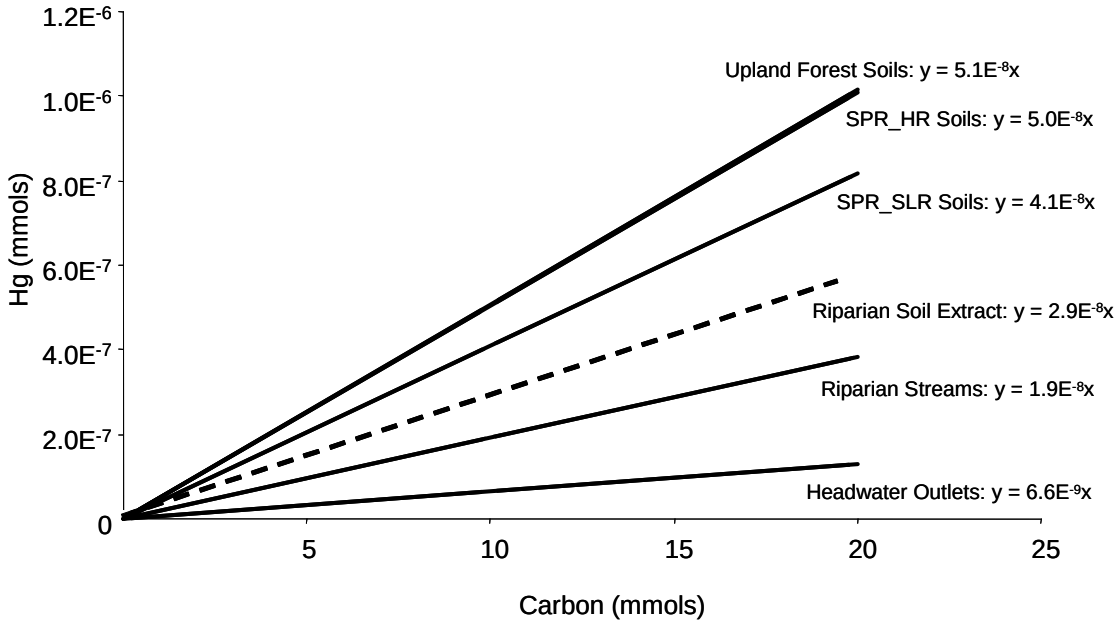

Figure 2.5. Slopes representing the molar stoichiometry between mercury and carbon in upland soils, shallow peat riparian wetland soils, riparian soil extracts, riparian wetland streams, and headwater wetland outlets. Molar stoichiometry of Hg:C in upland soils are from a previous study (*see* Chapter 1, Figure 1.3a,d,g). All mercury and carbon units were converted to mmols per gram (for soil) and mmols per liter (for stream water).

wetland peat extractions, and the quantity of DOC released declined over 10 extraction cycles, suggesting that the rate of decomposition or oxidation of organic matter during the experiment was minimized (Figure 2.6). Dissolved mercury (Hg_d) was consistently released from the shallow peat riparian soils, where it was correlated with the release of DOC ($r^2 = 0.78$; Figure 2.7a). Although equal or greater amounts of DOC were released from headwater wetlands, mercury was released only sporadically (Figure 2.6). Mercury concentrations from headwater wetland leachate was lower than expected based on DOC concentrations of the leachate in comparison to DOC concentrations observed in field sampling of headwater wetland outlets and peat porewater.

The results of this leaching study corroborate field observations of differences in the Hg:C stoichiometry of peat, peat porewater, and stream water of shallow peat riparian and headwater wetlands. Differences in the Hg:DOC relationship between headwater wetlands and shallow peat riparian wetlands further emphasize that there is likely a functional difference in DOC character among wetland types that influences the release and transport of mercury. These differences may result from the mode and degree of decomposition that results from differences in hydrogeologic setting of the different wetland types. The lack of correlation between Hg and DOC in headwater wetland extraction solutions supports our earlier suggestions that mercury in headwater wetland outlets is not contributed equally from all areas of the wetland, or that all DOC fractions are not equally mobilized from the peat porewater to the outlet. Ultimately, decomposition and hydrology control the production and release of dissolved organic matter that can be subsequently mobilized and transported to surface waters, along with associated mercury.

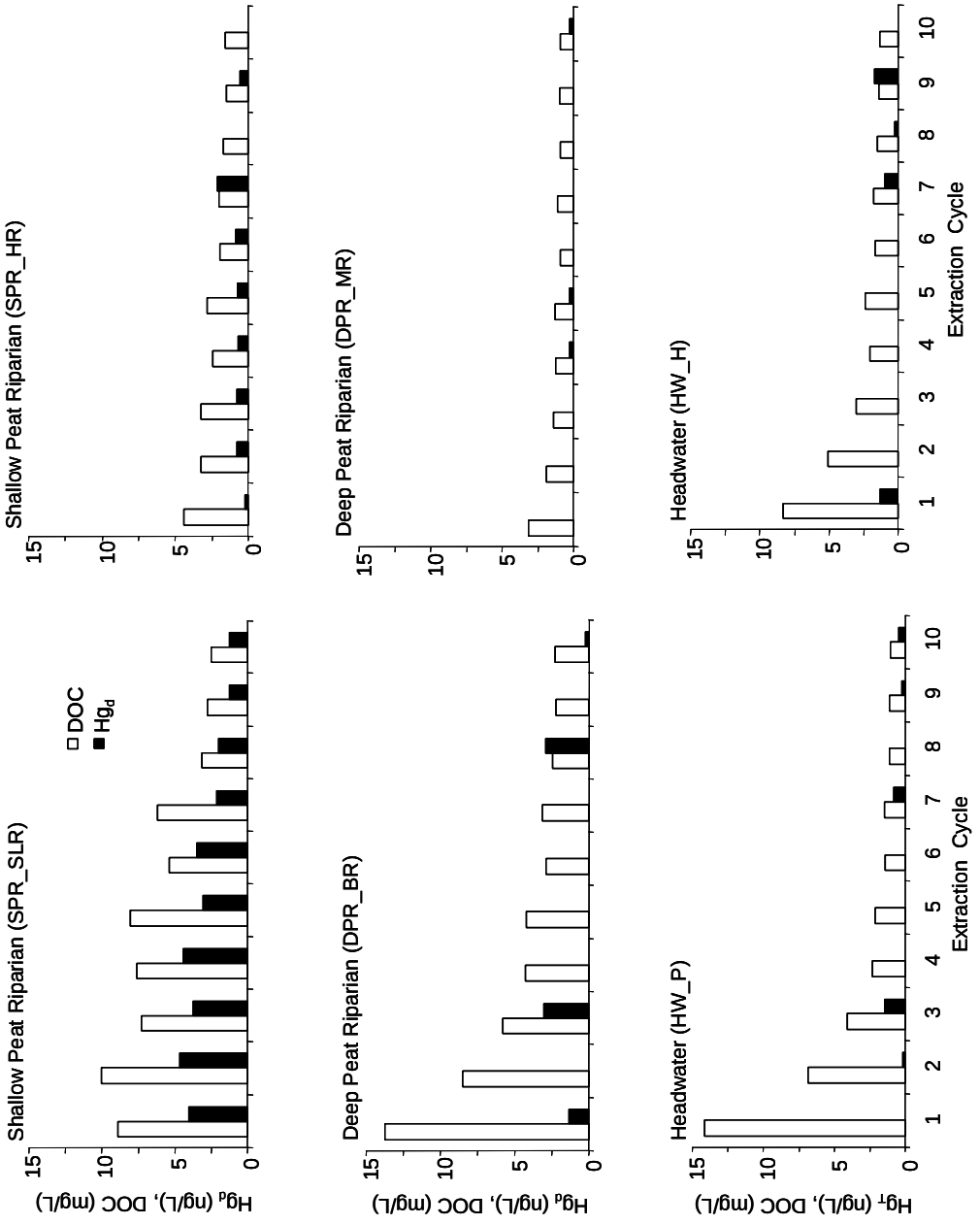

Figure 2.6. Dissolved mercury (Hg_d) and dissolved organic carbon (DOC) extracted from wetland peat soils by a synthesized rain water equivalent. Ten extraction cycles are shown for each of six wetland soil cores from different wetland types within the Sunday Lake watershed.

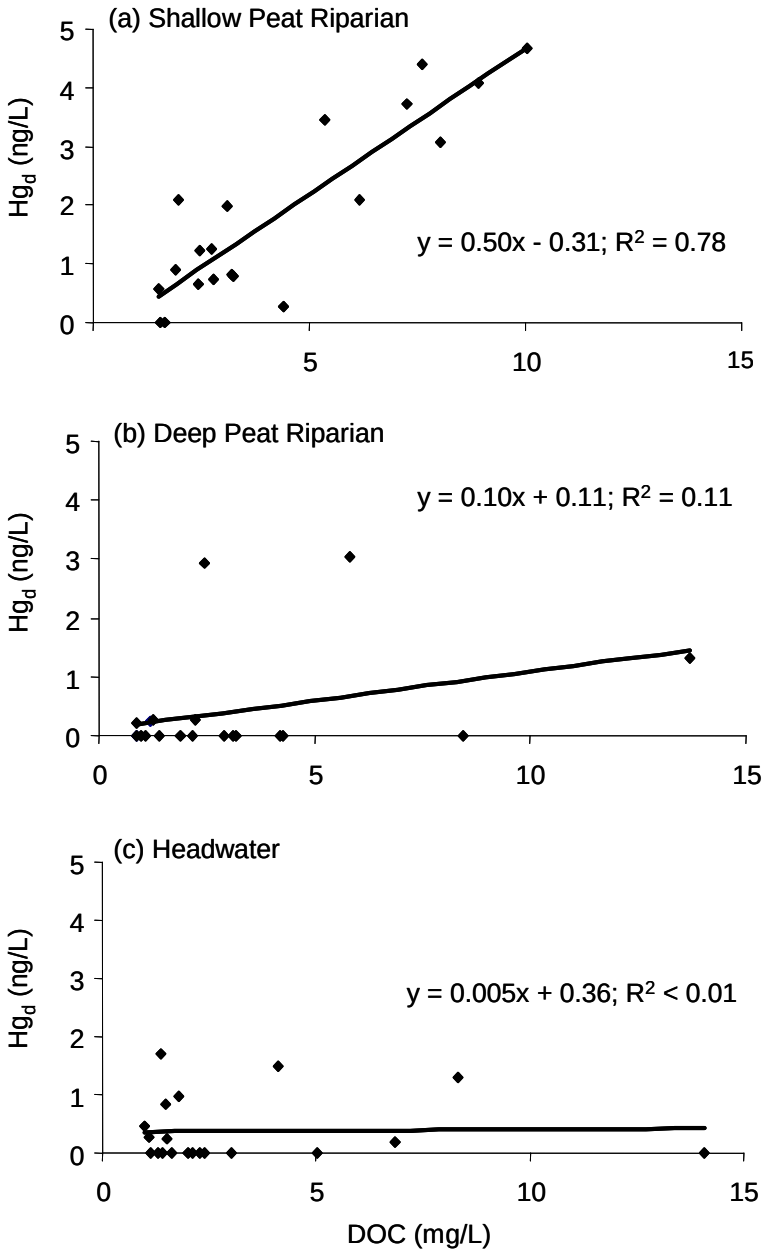

Figure 2.7. Scatterplots showing the relationship between dissolved mercury (Hg_d) and dissolved organic carbon (DOC) in soil extracts leached from (a) shallow peat riparian wetlands, (b) deep peat riparian wetlands, and (c) headwater wetlands in the Sunday Lake watershed.

Differences in mercury flux and residence time among wetland types

The fluxes of Hg_d of $MeHg_d$ from headwater wetland and shallow peat riparian wetland soils were similar, based on Darcy law calculations of seepage flux across an assumed one meter wide, 50 cm deep seepage face in each wetland (mean Hg_d = 5.4 $ug*yr^{-1}$, SE = 2.4 $ug*yr^{-1}$; mean $MeHg_d$ = 1.01 $ug*yr^{-1}$, SE = 0.56 ug*yr-1; Table 2.2); whereas the fluxes of Hg_d and $MeHg_d$ from deep peat riparian wetlands were relatively small (mean Hg_d = 0.6 $ug*yr^{-1}$, SE = 0.6 $ug*yr^{-1}$; mean $MeHg_d$ = 0.16 $ug*yr^{-1}$, SE = 0.16 $ug*yr^{-1}$; Table 2.2). These fluxes suggest a mean residence time for mercury of 590 years (SE = 69) for headwater wetlands and shallow peat riparian wetlands; whereas the mean residence time was >10,000 years for deep peat riparian wetlands (Table 2.2). Including the mineral soil mercury pool (to a depth of 50 cm) in the shallow peat riparian wetlands increased the mean residence time to thousands of years (Table 2.2).

Flux and residence time calculations were more strongly influenced by the hydrology characteristic of each wetland than by the peat porewater mercury chemistry. The hydraulic conductivity of the peat and the hydraulic gradient of the water table were the key drivers of seepage face flux estimates and subsequent mean residence time calculations. Estimates of hydrologic flux across a seepage face are likely more appropriate for the riparian wetlands that have a larger horizontal component of flow, whereas, headwater wetlands have strong vertical recharge gradients (Appendix B) that are not considered in calculations using Darcy's Law. Thus, actual export fluxes of water (and mercury) from headwater wetlands are dependent upon the strength of vertical hydraulic gradients, differences in hydraulic conductivity throughout the peat profile that may function as aquitards (*sensu* Freeze and Cherry 1979), and the occurrence of preferential flow paths. Actual export fluxes of water (and mercury) from riparian wetlands are also dependent upon the strength of

upwelling gradients, differences in hydraulic conductivity throughout the peat profile (especially within the underlying sand, gravel, and cobble matrix), and the occurrence of preferential flow paths. Furthermore, per meter width seepage flux estimates more easily scale to watershed-wide contributions to streamwater from riparian wetlands than from headwater wetlands having substantial recharge gradients and a single outlet point. The effect of alternate flow paths would likely increase estimated fluxes, and decrease estimated residence times of mercury, especially in shallow peat riparian wetlands. Note that these annual flux estimates are based on seasonal sampling snapshots, and do not include snowmelt and storm flow effects, which can be substantial (Shanley et al. 2005, Mitchell et al. 2008, *also see* Chapter 4).

Overall, estimates of fluxes from wetlands to down-gradient surface waters could be greatly improved through more sophisticated hydrological modeling, and the gauging of headwater outlets. An alternative method of establishing an upper limit for hydrologic fluxes from wetlands would be to calculate the total amount of precipitation to the wetland watershed, subtract out average evaporative losses for the region, and scale the resulting hydrologic flux to the concentrations of mercury within each wetland; this would assume all vertical mercury fluxes were eventually delivered to surface waters with Hg:DOC complexes intact. The relative importance of mercury fluxes from different wetland types in a watershed is thus dependent upon both the areal extent and the internal hydrology of different wetland types, and may be less dependent upon differences in porewater concentrations of mercury.

Comparing wetland and watershed fluxes. In a recent mass balance study of Sunday Lake, Selvendiran et al. (*in press*) calculated that inlet streams transported 30.1 g yr^{-1} Hg_t and 3.14 g yr^{-1} $MeHg_t$ from the watershed to the lake. Note that neither the flux of mercury from wetlands to streams (this study), nor the flux of mercury from inlet to lake (Selvendiran et al. *in press*) accounted for storm flow, and are thus

representative of similar flow conditions. Assuming all stream reaches were bounded by riparian wetlands, estimates of seepage fluxes of mercury and methyl mercury from the top 50 cm of shallow peat riparian wetlands alone were still two orders of magnitude lower than estimates of mercury and methyl mercury entering the lake in stream flow. Thus, the discrepancy between mercury fluxes contributed from wetlands and fluxes transported by streams presents a bit of an enigma. Apparently, simple models of wetland fluxes do not quantitatively capture the role of wetlands in supplying mercury to surface waters. As discussed, it is likely that the Darcy Law based flux calculations in this study grossly under-estimate hydrologic contributions from wetlands to surface waters. It is possible that both preferential flow and deeper flow paths that account for a greater amount of the hydrologic flux may be more important than previously estimated (e.g., Krabbenhoft and Babiarz 1992), especially in substrates with high hydraulic conductivities and relatively limited ability to retain DOC, such as the glacial outwash that underlies wetlands of the Sunday Lake watershed.

Canham et al. (2004) used an inverse modeling technique to show that, on average, about 70% of DOC in Adirondack lakes was contributed by forested uplands rather than by wetlands. However, that contribution varied substantially depending on the percentage wetland area in the watershed. For example, Muir Lake (a high-DOC lake with 27% watershed area as wetlands) was modeled to have 66% of DOC inputs contributed from wetlands (compare to the 30% of DOC inputs contributed from wetlands on average, Canham et al. 2004). The modeling of Canham et al. (2004) presented a number of observations concerning DOC transport through watersheds that are particularly salient with regard to potential watershed sources and transport of mercury through the ecosystem. First, their model indicated that watersheds are "well-plumbed" such that all areas of the watershed are capable of contributing DOC

to lakes (and streams). Second, once DOC entered into groundwater, little further decay occurred until the DOC reached open water and was exposed to sunlight, and transit time in small Adirondack streams was too short for much degradation to occur during stream transport of DOC to lakes. Third, the high fraction of carbon entering rivers that has been found to be ancient (>1000 years) also suggests limited decomposition during transit in groundwater (Gron et al. 1992, Canham et al. 2004). Finally, Canham et al. (2004) emphasize that although soil adsorption removes much DOC from soil water as it passes through upper soil horizons (e.g., McDowell and Wood 1984, McDowell and Likens 1988), their spatially explicit model suggests that there is little further adsorption or decomposition during transport to lakes (and streams) via groundwater flow paths. Thus, if mercury passes into the mineral soils in association with DOC, and if that DOC is relatively stable in groundwater and small streams during transit to lakes, then it is reasonable to surmise that deeper flow paths from wetlands may be important to mercury transport to surface waters.

CONCLUSIONS AND IMPLICATIONS

Hydrogeologic setting was a successful framework for predicting hydrological characteristics associated with different wetland types; that is, headwater wetlands were characterized by a consistently high water table and strong recharge gradients, whereas riparian wetlands were characterized by a more dynamically fluctuating water table and discharge gradients. However, differences in hydrogeologic setting resulted in only small differences in mercury and methyl mercury concentrations within wetland porewater. Thus, differences in mercury and methyl mercury flux from different wetland types, as calculated using Darcy's Law, were driven more by the hydrologic parameters of hydraulic gradient and hydraulic conductivity than by the relatively small differences in porewater concentrations. As revealed by a comparison

of individual scale wetland flux estimates (this study) and whole watershed stream export estimates (Selvendiran et al. *in press*), preferential flow and deeper flow paths through wetlands are likely important fluxes of mercury from wetlands to surface waters. Flow path analysis suggests that headwater (and riparian) wetland contributions to streamwater mercury are likely diluted by groundwater originating from the uplands, and improved estimates of both surface and sub-surface hydrological fluxes from wetlands to surface waters are necessary to determine the contribution of mercury from different wetland types to total watershed stream export of mercury.

Nonetheless, wetlands represent large pools of mercury that may be available for release to surface waters. As suggested by Munthe et al. (2007), there may be some initial amount of rapid recovery of surface waters that results from decreases in atmospheric deposition of mercury directly to those surface waters; however, further recovery will likely be buffered by exports of mercury from the terrestrial ecosystem, including wetlands. Note that Selvendiran et al. (*in press*) estimated that direct atmospheric deposition to the surface of Sunday Lake was 0.6 $g*yr^{-1}$, whereas contributions from the watershed were 30.1 $g*yr^{-1}$ (i.e., 98% of inputs to the lake are from the watershed).

Mercury:DOC relationships controlling the release and transport of mercury differed markedly among wetland types. In headwater wetlands, transport of mercury with DOC appeared to be more limited by mercury than by the availability of mercury:DOC binding sites; this follows the accepted paradigm that the quantity of mercury binding sites on DOC is virtually unlimited in relation to environmentally relevant concentrations of mercury. However, the tight relationship between mercury and organic carbon in riparian streams, and the apparent convergence toward a maximum ratio of Hg:C upon decomposition in soils of forests and shallow peat

riparian wetlands appears to be a condition suggestive of mercury saturation of DOC binding sites within the products of decomposition.

Differences in hydrogeologic setting influence the rate and mechanism of decomposition of organic matter as well as the release of organic matter from wetlands to surface waters. Whether wetlands will continue to contribute mercury to surface waters may depend on whether old mercury incorporated in peat is actually available for release to down-gradient surface waters. Simple leaching experiments using a synthetic precipitation to extract mercury from wetland peat cores suggest that mercury may be more available for release from shallow peat riparian wetland soils than from the peat of either deep peat riparian or headwater wetlands. Ultimately decomposition dynamics and hydrology will control the magnitude and mode of transformation and release of mercury accumulated in wetlands (and forests). Thus, environmental change that alters the hydrologic regime and associated mode of decomposition will likely have a larger and more rapid effect on the transformation and release of mercury from wetlands than would changes in the rate of atmospheric mercury deposition.

REFERENCES

APHA. 1998. Standard methods for the examination of water and wastewater, 20th edition, American Public Health Association: Washington, D.C., USA.

Babiarz, C. L., J. P. Hurley, J. M. Benoit, M. M. Shafer, A. W. Andren, and D. A. Webb. 1998. Seasonal influences on partitioning and transport of total and methylmercury in rivers from contrasting watersheds. Biogeochemistry **41**:237-257.

Bedford, B. L. 1996. The need to define hydrologic equivalence at the landscape scale for freshwater wetland mitigation. Ecological Applications **6**:57-68.

Bedford, B. L. 1999. Cumulative effects on wetland landscapes: Links to wetland restoration in the United States and southern Canada. Wetlands **19**:775-788.

Benoit, J. M., C. C. Gilmour, A. Heyes, R. P. Mason, and C. L. Miller. 2003. Geochemical and biological controls over methylmercury production and degradation in aquatic ecosystems. Biogeochemistry of Environmentally Important Trace Elements **835**:262-297.

Canham, C. D., M. L. Pace, M. J. Papaik, A. G. B. Primack, K. M. Roy, R. J. Maranger, R. P. Curran, and D. M. Spada. 2004. A spatially explicit watershed-scale analysis of dissolved organic carbon in Adirondack lakes. Ecological Applications **14**:839-854.

Driscoll, C. T., V. Blette, C. Yan, C. L. Schofield, R. Munson, and J. Holsapple. 1995. The Role of Dissolved Organic-Carbon in the Chemistry and Bioavailability of Mercury in Remote Adirondack Lakes. Water Air and Soil Pollution **80**:499-508.

Driscoll, C. T., Y. J. Han, C. Y. Chen, D. C. Evers, K. F. Lambert, T. M. Holsen, N. C. Kamman, and R. K. Munson. 2007. Mercury contamination in forest and freshwater ecosystems in the Northeastern United States. Bioscience **57**:17-28.

Driscoll, C. T., J. Holsapple, C. L. Schofield, and R. Munson. 1998. The chemistry and transport of mercury in a small wetland in the Adirondack region of New York, USA. Biogeochemistry **40**:137-146.

Driscoll, C. T., C. Yan, C. L. Schofield, R. Munson, and J. Holsapple. 1994. The Mercury Cycle and Fish in the Adirondack Lakes. Environmental Science & Technology **28**:A136-A143.

Dunne, T., and L. B. Leopold. 1978. Water in Environmental Planning. W.H. Freeman and Company, New York.

Evers, D. C., and T. A. Clair. 2005. Mercury in northeastern North America: A synthesis of existing databases. Ecotoxicology **14**:7-14.

Evers, D. C., Y. J. Han, C. T. Driscoll, N. C. Kamman, M. W. Goodale, K. F. Lambert, T. M. Holsen, C. Y. Chen, T. A. Clair, and T. Butler. 2007. Biological mercury hotspots in the northeastern United States and southeastern Canada. Bioscience **57**:29-43.

Freeze, R. A., and J. A. Cherry. 1979. Groundwater. Prentice-Hall, Englewood Cliffs.

Gron, C., J. Torslov, H. J. Albrechtsen, and H. M. Jensen. 1992. Biodegradability of Dissolved Organic-Carbon in Groundwater from an Unconfined Aquifer. Science of the Total Environment **118**:241-251.

Hill, A. R., and K. J. Devito. 1997. Hydrological-chemical interactions in headwater forest wetlands. Pages 213-230 *in* J. K. Jeglum, editor. Northern Forested Wetlands: Ecology and Management. Lewis Publishers, Boca Raton, Florida, USA.

Hurley, J. P., J. M. Benoit, C. L. Babiarz, M. M. Shafer, A. W. Andren, J. R. Sullivan, R. Hammond, and D. A. Webb. 1995. Influences of Watershed Characteristics on Mercury Levels in Wisconsin Rivers. Environmental Science & Technology **29**:1867-1875.

Kamman, N. C., and D. R. Engstrom. 2002. Historical and present fluxes of mercury to Vermont and New Hampshire lakes inferred from Pb-210 dated sediment cores. Atmospheric Environment **36**:1599-1609.

Kolka, R. K., D. F. Grigal, E. A. Nater, and E. S. Verry. 2001. Hydrologic cycling of mercury and organic carbon in a forested upland-bog watershed. Soil Science Society of America Journal **65**:897-905.

Krabbenhoft, D. P., and C. L. Babiarz. 1992. The role of groundwater transport in aquatic mercury cycling. Water Resources Research **28**:3119-3128.

Lorey, P., and C. T. Driscoll. 1999. Historical trends of mercury deposition in Adirondack lakes. Environmental Science & Technology **33**:718-722.

Marvin-DiPasquale, M., J. Agee, C. McGowan, R. S. Oremland, M. Thomas, D. Krabbenhoft, and C. C. Gilmour. 2000. Methyl-mercury degradation pathways: A comparison among three mercury-impacted ecosystems. Environmental Science & Technology **34**:4908-4916.

Marvin-Dipasquale, M. C., and R. S. Oremland. 1998. Bacterial methylmercury degradation in Florida Everglades peat sediment. Environmental Science & Technology **32**:2556-2563.

Mason, R. P., W. F. Fitzgerald, and F. M. M. Morel. 1994. The Biogeochemical Cycling of Elemental Mercury - Anthropogenic Influences. Geochimica Et Cosmochimica Acta **58**:3191-3198.

McDowell, W. H., and G. E. Likens. 1988. Origin, Composition, and Flux of Dissolved Organic-Carbon in the Hubbard Brook Valley. Ecological Monographs **58**:177-195.

McDowell, W. H., and T. Wood. 1984. Podzolization - Soil Processes Control Dissolved Organic-Carbon Concentrations in Stream Water. Soil Science **137**:23-32.

Mierle, G. 1990. Aqueous inputs of mercury to Precambrian Shield Lakes in Ontario. Environmental Toxicology and Chemistry **9**:843-851.

Mitchell, C., B. Branfireun, and R. Kolka. 2008. Total mercury and methylmercury dynamics in upland-peatland watersheds during snowmelt. Biogeochemistry **90**:225-241.

Munthe, J., R. A. Bodaly, B. A. Branfireun, C. T. Driscoll, C. C. Gilmour, R. Harris, M. Horvat, M. Lucotte, and O. Malm. 2007. Recovery of mercury-contaminated fisheries. Ambio **36**:33-44.

Schuster, E. 1991. The Behavior of mercury in the soil with special emphasis on complexation and adsorption processes - A review of the literature. Water Air and Soil Pollution **56**:667-680.

Selvendiran, P., C. T. Driscoll, M. R. Montesdeoca, H. Choi, and T. M. Holsen. in press. Mercury dynamics and transport in two Adirondack Lakes. Limnology and Oceanography.

Shanley, J. B., N. C. Kamman, T. A. Clair, and A. Chalmers. 2005. Physical controls on total and methylmercury concentrations in streams and lakes of the northeastern USA. Ecotoxicology **14**:125-134.

St Louis, V. L., J. W. M. Rudd, C. A. Kelly, K. G. Beaty, R. J. Flett, and N. T. Roulet. 1996. Production and loss of methylmercury and loss of total mercury from boreal forest catchments containing different types of wetlands. Environmental Science & Technology **30**:2719-2729.

USEPA. 1996. Method 1669. United States Environmental Protection Agency, Office of Water, Office of Science and Technology, Engineering and Analysis Division (4303), Washington, D.C., USA.

USEPA. 1998. Method 1631. United States Environmental Protection Agency, Office of Water, Office of Science and Tachnology, Engineering and Analysis Division (4303), Washington, D.C., USA.

USEPA. 2001, Revision E. Method 1630. United States Environmental Protection Agency, Office of Water, Office of Science and Tachnology, Engineering and Analysis Division (4303), Washington, D.C., USA.

Winter, T. C. 1988. Conceptual framework for assessment of cumulative impacts on the hydrology of non-tidal wetlands. Environmental Management **12**:605-620.

Winter, T. C. 1992. A physiographic and climatic framework for hydrologic studies of wetlands. Pages 127-148 *in* M. L. Bothwell, editor. Aquatic ecosystems in semi-arid regions: implications for resource management. Environment Canada, Saskatoon, Sasketchewan, Canada.

Winter, T. C., and M. K. Woo. 1990. Hydrology of lakes and wetlands. Pages 159-187 *in* H. C. Riggs, editor. The geology of North America. The Geological Society of America, Boulder, Colorado, USA.

CHAPTER THREE:
INHIBITION OF METHYL MERCURY PRODUCTION BY REDOX CONDITIONS IN FRESHWATER WETLANDS.

ABSTRACT

Wetlands are hotspots of methyl mercury production and sources of bioavailable methyl mercury to aquatic ecosystems; however, there is much spatial and temporal variability in methyl mercury concentrations within and among wetlands. Sulfate reducing bacteria (SRB) are important methylators of mercury under reducing conditions, and the suite of factors controlling net methyl mercury production by SRB are complex. Here we show that nitrate and ferrous iron are associated with the inhibition of net methyl mercury production in riparian wetlands, and that abiotic methylation via a DOC mechanism may be important in headwater ombrotrophic bogs under natural background environmental conditions.

INTRODUCTION

Wetlands are hotspots of methyl mercury (MeHg) production (e.g., Branfireun et al. 1998, Mitchell et al. 2008b) and are sources of MeHg to down-gradient aquatic ecosystems where it is bioaccumulated to toxic concentrations in fish and wildlife (e.g., Driscoll et al. 2007, Evers et al. 2007). Although wetlands are considered hotspots of MeHg production relative to the broader landscape, there is much spatial and temporal variability in MeHg concentrations and the percentage of total mercury as MeHg (%MeHg) within and among different wetlands (%MeHg is a surrogate for net MeHg production, Mitchell et al. 2008b, see also Chapter 2). The factors controlling the methylation of mercury in natural environments are somewhat elusive, in part, because there are multiple mechanisms (both biological and abiotic) that

directly and indirectly influence net MeHg production (Barkay and Wagner-Dobler 2005, and references therein).

The most commonly documented pathway of biological MeHg production in laboratory experiments and the natural environment is methylation of ionic mercury during sulfate reduction to sulfide by sulfate reducing bacteria (SRB), although not all SRB methylate mercury (e.g., Compeau and Bartha 1985, Gilmour and Henry 1992, King et al. 1999, King et al. 2000). Numerous studies have investigated the controls on mercury methylation by SRB. The availability of sulfate (as an electron acceptor for SRB) has been shown to stimulate MeHg production during controlled laboratory studies and field experiments (e.g., Gilmour et al. 1992, Branfireun et al. 1999, Galloway and Branfireun 2004, Jeremiason et al. 2006, Mitchell et al. 2008a). Dissolved organic carbon has also been shown to increase the methylation of mercury (e.g., Barkay et al. 1997); Mitchell (2008a) showed that sulfate and DOC additions together increased net MeHg production more than did sulfate additions alone.

The presence of sulfide has been shown to either stimulate or to suppress net methylation of mercury, depending on concentration. Low concentrations of sulfide result in a greater proportion of dissolved mercury sulfide complexes occurring as neutral dissolved mercury sulfide complexes that easily pass through bacterial cell walls, whereas at high concentrations dissolved sulfide complexes are mostly charged and react with mercury to form insoluble precipitates. Sulfide concentrations optimal for the production of MeHg in laboratory experiments with freshwater sediment have been shown to be in the range of 2 -100 μM (Benoit et al. 2003, and references therein). Within this range of low sulfide concentrations, increasing the sulfide concentration may increase the overall quantity of mercury substrate (i.e., ionic mercury, Hg[II]) available for methylation; whereas, above this range of sulfide

concentrations, increasing the sulfide concentration decreases the quantity of mercury substrate available for methylation (Benoit et al. 2003, and references therein).

The inhibition of SRB activity by redox conditions (i.e., inhibition of SRB in anoxic sediments by the presence of a different dominant terminal electron acceptor such as iron or nitrate) has received little attention as a possible control limiting the biological methylation of mercury by SRB in the natural environment. Warner et al. (2003) showed that potential rates of mercury methylation in anoxic wetland slurries were similar under methanogenic and sulfate-reducing conditions but suppressed under iron-reducing conditions. However, they were unable to determine whether net MeHg suppression was the result of low inorganic mercury availability due to sorption to iron (III) oxide surfaces, or the inability of SRB to compete with iron-reducers for substrates.

Mehrotra et al. (2003) showed that ferrous iron (reduced iron, Fe[II]) amendments to sediment-free cultures decreased net MeHg production more than four-fold over a 72 hour incubation period; ferrous iron amendments to cultures containing a model wetland sediment decreased net MeHg production more than three-fold. Mehrotra et al. (2003) suggested that suppression of net MeHg production in their study resulted from a decrease in sulfide concentration that led to a decrease in the overall concentration of dissolved mercury sulfide complexes (both charged and uncharged). However, when normalized to sulfate reduction and initial filterable Hg(II) concentrations, net MeHg concentrations increased with increasing Fe(II) likely because the fraction of dissolved Hg(II) occurring as neutral mercury sulfide complexes increases with decreased free sulfide concentrations (which occur as Fe(II) increases; Mehrotra et al. 2003). Thus, these ferrous iron experiments both support and contradict the findings of Benoit et al. (2003). On one hand, substantial mercury methylation under the experimental sulfide concentrations used by Mehrotra et al.

(2003; 500-5000 uM) occurred at sulfide concentrations well above the optimal range for mercury methylation described by Benoit et al. (2003). In fact, Benoit et al.(2003) showed that methylation was strongly inhibited at sulfide concentrations above 100 uM. On the other hand, the normalized dataset (Mehrotra et al. 2003) supports the hypothesis that neutral mercury sulfide complexes become more prevalent as sulfide concentrations decrease, despite that Benoit et al. (2003) demonstrated that neutral complexes should be nearly absent at sulfide concentrations above 100 uM. Clearly, the range of sulfide concentrations that result in either the formation of neutral mercury sulfide complexes or the inhibition of methylation need to be evaluated for surface waters of various composition, and Mehrotra et al (2003) noted the need to test the efficacy of ferrous iron to suppress mercury methylation by SRB under field conditions.

In this study, we examined how redox conditions and DOC concentrations influence the occurrence of MeHg in pristine freshwater wetlands of the Adirondack region of New York State. We hypothesized that nitrate and ferrous iron would suppress the production of MeHg in wetland peat porewater, and that high concentrations of DOC would increase net MeHg production. We also hypothesized that the mechanisms influencing mercury methylation would differ in wetlands of different hydrogeologic setting, as different wetland types are influenced by differences in solute chemistry and inferred differences in decomposition processes that result from differences in hydrogeologic setting.

METHODS

Site description

This study was conducted at the Sunday Lake watershed (~1273 ha), which is located along the southwestern boundary of the Adirondack region of New York, USA

(43°51'40"N, 74°06'07"W), and is the site of ongoing research investigating the influence of hydrogeologic setting on the biogeochemical cycling of mercury within and among wetland types. Average precipitation is ~1300 mm/yr, with about one third delivered as snow. The upland soils are mostly well drained spodosols (Typic Haplorthods) with sandy loam to loamy sand texture overlying glacial till and outwash (*see* Chapter 1). This watershed contains numerous wetlands (~20% of total watershed area), which are formed within the complex series of ridges and depressions resulting from glacial stream bed loads that remain as eskers. A more detailed description of the Sunday Lake watershed and its wetlands is available elsewhere (*see* Chapter 1).

Sampling procedures

Peat porewater (to a depth of 50 cm), headwater wetland outlets, and riparian streams were sampled seasonally (April, June, August, September, November/December) from water table well transects previously established across wetlands of different hydrogeologic setting (*see* Chapter 2). Teflon and borosilicate glass equipment was used for all mercury sampling, and clean procedures were followed (USEPA 1996). Mercury samples were double bagged, with labels on the outer bag only. Water samples for ancillary solute chemistry were collected in high-density polyethylene bottles and filled to minimize head space. Samples were packed in coolers with ice packs, and returned to the laboratory for processing. Sample filtering and preservation occurred upon arrival at Syracuse University within 48 hours of sampling.

Several chemical parameters were measured in the field. Temperatures were measured with a digital probe placed at the peat surface, 5 cm depth, and 15 cm depth in the soil. Conductivity and pH were measured in the field using separate aliquots of

samples removed from water table wells or streams. Samples for the analysis of sulfide and reduced iron were obtained only for the August and September sampling periods. Sulfide and reduced iron samples were carefully removed from water table wells and streams with a syringe attached to a long Teflon straw, which avoided mixing sample water with air. Sulfide and iron samples were then injected into appropriate reagents within 20 ml glass vials, releasing samples only after the syringe tip extension had been submerged in solution (see *Methods: Sample Analyses* for details concerning reagents and chemical analyses). Once fixed, sulfide and iron samples were tightly capped and kept at ambient temperature in a dark box until spectrometric analysis (within 24 hours); the colorimetric products were found to be stable for at least 24 hours and required no additional processing.

Sample analysis

Mercury and methyl mercury samples were filtered through a clean 0.45um Teflon membrane. For outlet and stream water samples, both filtered and unfiltered aliquots were acidified to 0.4% HCl and stored in the dark at 4^{o}C until analysis. For porewater samples, only the filtered fraction was analyzed. The concentration of total mercury (all forms of mercury) was determined for unfiltered (Hg_t) and filtered (Hg_d) samples. Prior to analysis for total mercury, samples were UV light treated to remove measurement interferences (i.e., DOC, Olson et al. 1997). Total mercury concentrations were analyzed using automated CVAFS (Tekran, Toronto, Ontario, Canada, USEPA 1998). Methyl mercury samples were distilled and analyzed following EPA Method 1630 (USEPA 2001, Revision E).

Standard methods were used for the analysis of ancillary chemical parameters. The pH and acid neutralizing capacity (ANC) were determined for bulk (unfiltered, unpreserved) samples. The pH was measured in both the field and laboratory using a

glass combination electrode after calibration using pH 4.00 and pH 7.00 buffer solutions; pH measurements in the laboratory were made on a 50 ml aliquot of sample just prior to analysis of ANC. ANC was determined by titration using a glass electrode and a Brinkmann Metrohm 716 DMS Titrino auto-analyzer, followed by a modified Gran analysis of the resulting data (Gran 1952, Kramer 1984). Anions (F^-, Cl^-, NO_3^-, SO_4^{2-}) were analyzed by ion chromatography with chemical suppression of eluent conductivity using an Ion-Pac AS18 column (Dionex). DOC concentrations were determined for filtered samples (0.7 µm glass fiber filter, pre-baked at 450^oC) with a Dohrmann Phoenix 8000 Analyzer using the persulfate-ultraviolet oxidation method (APHA 1998). Ferrous iron (Fe[II]) was measured colorimetrically using ferrozine (*sensu* Stookey 1970, Lovely and Phillips 1987). Sulfide was measured colorimetrically using the methylene blue method (APHA 1998 Method 4500 - Sulfide d., Spectronic 20 Genesys Spectrophotometer). Samples were analyzed in batches with quality control (*see* Chapter 1, Chapter 2).

Statistical procedures

Statistical procedures were performed with SAS (SAS Institute 1999). Regression analysis was used to determine the significance of predictive models overall as well as the significance of individual predictor variables, using the f-test and (type III) simultaneous sums of squares. Non-significant predictor variables were eliminated from the models. The significance of the slope of the relationship between response and predictor variables was tested with a one-way t-test (SAS, PROC GLM, SAS Institute 1999). Response and predictor variables were transformed as necessary to satisfy linearity requirements. Assumptions of linearity between response and predictor variables as well as between residuals and predictor variables, equal variance of residuals, and normality of residuals were satisfied for all results presented.

Outliers were identified by assessing leverage plots and Cook's Distance; where outliers were identified, results are presented for models with and without the outlier observations.

RESULTS AND DISCUSSION

Solute chemistry of wetland peat porewater

Solute chemistry varied markedly among wetland types, and reflected differences in hydrogeologic setting (Table 3.1). Headwater wetlands receive a majority of their solute inputs from precipitation and are thus relatively dilute; whereas, riparian wetlands receive a substantial quantity of solutes from upwelling groundwater. As compared to riparian wetlands, headwater wetlands in this study were characterized by low concentrations of inorganic electron acceptors (e.g., nitrate, sulfate) and reduced species (e.g., reduced iron, sulfide), negative ANC values indicative of low concentrations of base cations, low pH (circa pH 4.1), and high concentrations of DOC (Table 3.1). Deep peat and shallow peat riparian wetlands had similar concentrations of nitrate and sulfate; whereas deep peat riparian wetlands had lower reduced iron concentrations but higher sulfide concentrations than shallow peat riparian wetlands (Table 3.1). The pH also differed between the deep peat and shallow peat riparian wetlands (pH 4.9 and 5.6, respectively). DOC concentrations in deep peat riparian wetlands were double those of the shallow peat riparian wetlands. ANC was most positive in the shallow peat riparian wetlands, reflecting contribution of base cations from the predominance of groundwater discharge zones.

Methyl mercury concentrations in peat porewater varied among wetland types, within wetland types, and with season (*see* Chapter 2, Figure 2.1a,b,c, Figure 2.2). Although solute chemistry associated with differences in the hydrogeologic setting of different wetland types may influence the mode and efficiency of mercury

Table 3.1. Wetland peat porewater solute chemistry from 50 cm depth water table wells and soil water temperature in different wetland types in the Sunday Lake watershed.

		Headwater Wetlands				Deep Peat Riparian Wetlands				Shallow Peat Riparian Wetlands			
		Mean (SE), n	n	Min	Max	Mean (SE)	n	Min	Max	Mean (SE)	n	Min	Max
NO_3^-	(umol/L)	0.47 (0.33)	43	0.01	14.0	12.6 (2.7)	24	0.82	52.9	9.9 (2.6)	37	0.05	68.1
SO_4^{-2}	(umol/L)	7.58 (1.17)	43	1.78	44.8	35.0 (4.9)	24	4.8	86.3	43.8 (3.0)	37	0.41	76.01
Fe^{+2}	(umol/L)	10.37 (2.97)	16	0.36	44.0	78.7 (16.8)	10	17.6	182.3	150.0 (53.8)	12	1.61	595.2
S^{-2}	(umol/L)	1.94 (0.48)	16	<0.01	5.93	16.9 (9.7)*	10	1.53	103.0*	3.8 (1.0)	12	0.03	9.2
DOC	(mg/L)	27.3 (1.8)	43	8.0	56.4	10.5 (1.5)	24	0.45	25.9	5.3 (1.0)	37	1.1	31.5
pH (air eq)		4.1 (<0.1)	43	3.9	4.7	4.9 (0.1)	24	4.4	6.1	5.6 (0.1)	37	4.2	7.0
ANC	(ueq/L)	-80.3 (5.2)	43	-143.5	-4.4	26.4 (18.8)	24	-30.8	311.0	79.6 (20.2)	37	-47.4	415.3
In Field Measurements:													
pH (field)		4.1 (0.1)	43	3.8	5.6	4.8 (0.1)	24	4.2	5.9	5.5 (0.1)	37	4.1	6.8
Conductivity	(uS/cm)	39.1 (2.2)	43	13.8	97.8	31.1 (2.8)	24	13.7	78.3	29.6 (1.8)	37	13.7	54.8
Groundwater Temperature:													
	Apr	no data				no data				no data			
	Jun	11.5 (0.3)	7			10.6 (1.1)	5			12.6 (0.4)	7		
	Aug	no data				no data				no data			
	Sep	16.9 (1.0)	9			14.5 (0.1)	2			17.6 (1.6)	4		
	Dec	no data*				3.9 (0.1)	2			4.1 (0.5)	8		

* Excluding one outlier sulfide concentration (103.0 umol/L), Mean(SE) = 7.4 (1.8) umol/L, n = 9, Max = 18.8 umol/L.

transformation to methyl mercury, broad scale factors such as wetland type, location along the wetland transect, and seasonality alone were poor predictors of methyl mercury concentrations.

Mercury supply and net mercury methylation

High concentrations of Hg_d provided the potential "substrate" from which high concentrations of $MeHg_d$ could be produced in the porewater of all wetland types (<0.5 to 7.89 ng/L Hg_d , <0.02 to 5.79 ng/L $MeHg_d$; Figure 3.1a); that is $MeHg_d$ increased with increasing concentrations of Hg_d (ln transformed response variable, n=100, $p<0.0001$). In contrast, net methyl mercury production (as inferred from $\%MeHg_d$) increased with decreasing Hg_d concentration (ln transformed response variable, n=100, p=0.0129). However, only the slope of the relationship between Hg_d and $MeHg_d$ in the shallow peat riparian wetland was significantly different from zero when data from individual wetlands were considered (ln transformed response variable, n= 34, p=0.0192; Figure 3.1b). Across all wetlands, $\%MeHg_d$ ranged from 0 to 95% in wetland peat porewater, with 68% of all values exceeding $10\%MeHg_d$, 35% of all values exceeding $25\%MeHg_d$, and 13% of all values exceeding $50\%MeHg_d$ (Figure 3.1b). Not surprisingly, this extent of net methylmercury production was much higher than %MeHg values observed for stream water within this watershed (Figure 3.1c), and exceeds most porewater and stream water %MeHg values reported in the literature. In comparison, Shanley et al. (2005) reported a methylation efficiency of 3.9% for 177 stream water measurements in the Norhteastern USA. Microbial ecology research using soils from shallow riparian wetlands in this watershed shows a complete lack of demethylation potential (M. Hines, *personal communication*), and this could help explain observed high rates of net methylmercury production (%MeHg) in the shallow peat riparian wetlands.

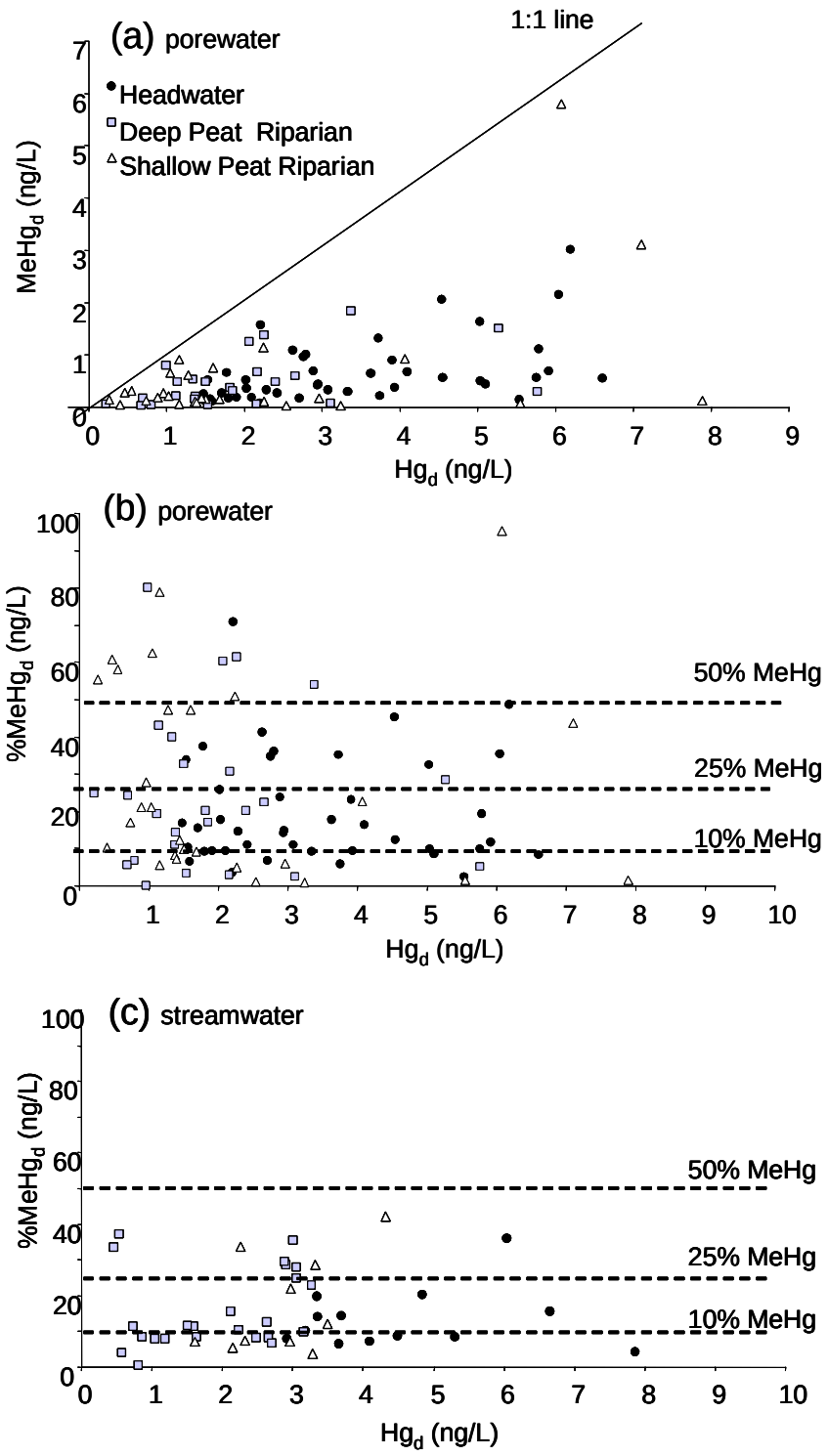

Figure 3.1. Scatterplots showing the relationship between (a) dissolved mercury (Hg_d) and methylmercury ($MeHg_d$) in wetland peat porewater, (b) Hg_d and $\%MeHg_d$ in wetland peat porewater, and (c) Hg_d and $\%MeHg_d$ in stream water of different wetland types of the Sunday Lake watershed.

Evidence of redox inhibition of mercury methylation in riparian wetlands

The activity of anaerobic microbial communities under reducing conditions is, to some extent, controlled by redox conditions. Based on the energetic efficiency of anaerobic microbial respiration using various electron acceptors (e.g., nitrate, iron, sulfate), nitrate reducers should inhibit both iron reducers and sulfate reducers, and iron reducers should inhibit sulfate reducers (in the range of ~pH4 to pH7, Richardson and Vepraskas 2001). Thus, the presence of nitrate should inhibit the microbial methylation of mercury by both iron and sulfate reducers, and the presence of oxidized iron, in the presence of iron reducers, should inhibit microbial methylation by sulfate reducers.

In this study, high $MeHg_d$ concentrations occurred at low nitrate concentrations (ln transformed response and predictor variables, n=100, $p<0.0001$), suggesting that nitrate inhibits the microbial methylation of mercury by iron and sulfate reducers (Figure 3.2a). However, only the slope of the relationship in the shallow peat riparian wetland was significantly different from zero when data from individual wetlands were considered (ln transformed response variable, n= 34, p=0.0153; Figure 3.2a). Similarly, high $MeHg_d$ concentrations occurred at low Fe(II) concentrations (ln transformed response variable, n=32, p=0.0394, with two data points at the origin removed). As was the case for the relationship between $MeHg_d$ and nitrate, only the slope of the relationship between $MeHg_d$ and Fe(II) for the shallow peat riparian wetlands was different from zero at a moderately significant level (ln transformed response and predictor variable, n = 10, p=0.0595, with one observation at the origin removed; Figure 3.2b). Because Fe(II) was only measured in August and September, the resulting smaller sample size and range of data make it difficult to demonstrate statistical significance of observed patterns. Nevertheless, the inverse relationship between $MeHg_d$ and Fe(II) could be interpreted in two ways: (1) that the presence of

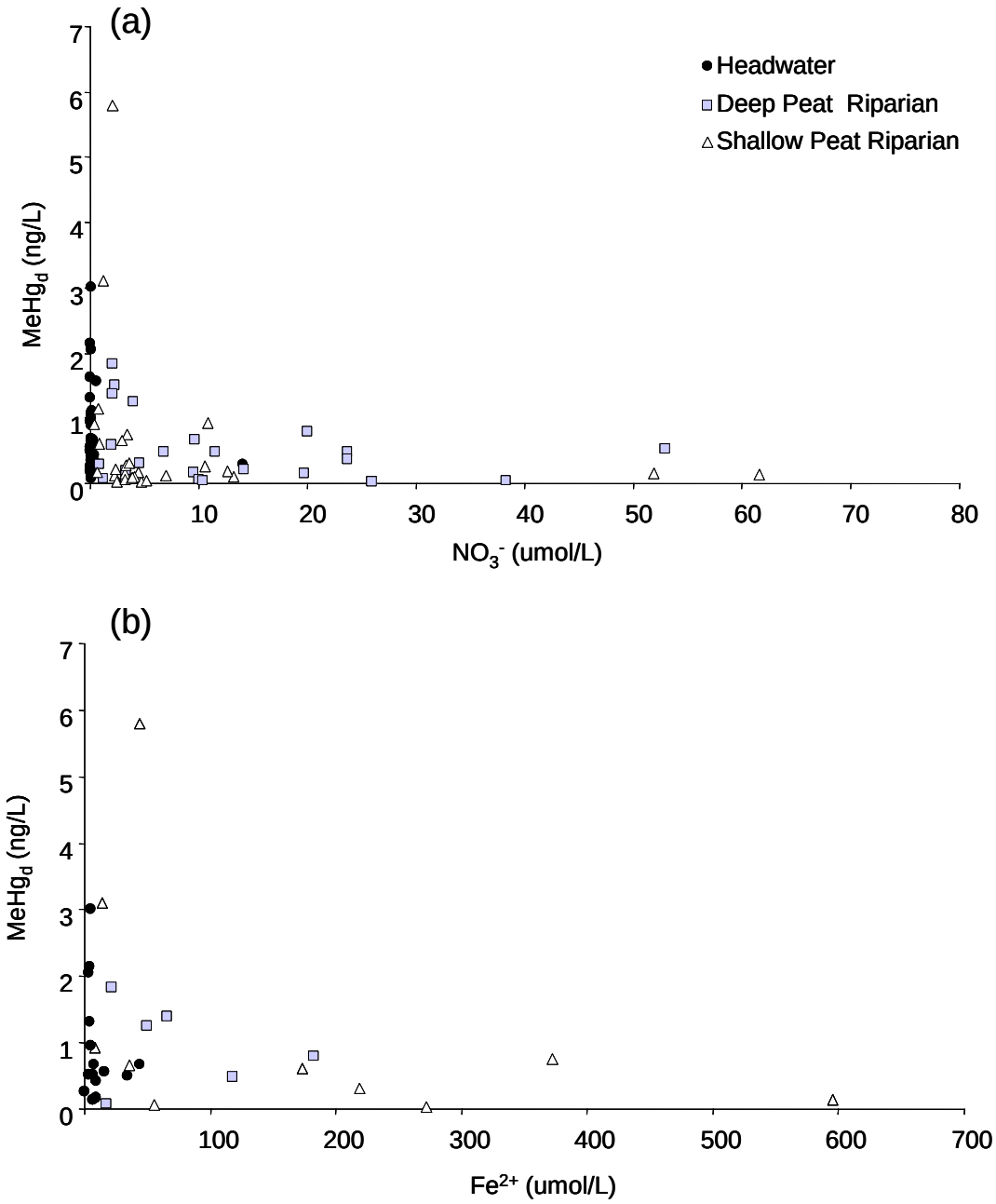

Figure 3.2. Scatterplots showing the relationship between (a) nitrate (NO_3^-) and dissolved methyl mercury ($MeHg_d$), and (b) reduced iron (Fe^{2+}) and methyl mercury ($MeHg_d$) in wetland peat porewater of different wetland types of the Sunday Lake watershed.

iron reducers also inhibits the biological methylation of mercury by sulfate reducers; or (2), that the ferrous iron suppresses net methylmercury production by decreasing overall sulfide activity and thus decreasing the total dissolved mercury concentrations (i.e., neutral dissolved mercury sulfide complexes, sensu Mehrotra et al. 2003). Note that there was no significant relationship between ferrous iron and sulfide, even though the highest sulfide concentrations appeared to occur at low [Fe(II)] (Figure 3.3). Thus, the presence of mercury, sulfate, sulfate reducing bacteria, adequate carbon substrate, and anoxic conditions may not always induce high methyl mercury concentrations, as microbial sulfate reduction may be inhibited by competing biological processes such as denitrification and iron reduction, as well as the potential lowering of dissolved mercury sulfide activity through ferrous iron interactions with sulfide.

Although it is tenuous to infer the production of methyl mercury by sulfate reduction from the consumption of sulfate in field studies, our data do show patterns of increasing $MeHg_d$ concentrations with decreasing sulfate concentrations within wetland porewater across all wetland types (ln transformed response variable, n=102, p=0.0001; Figure 3.4a). However, when wetland types are analyzed separately, this inverse relationship holds only for the deep peat riparian (ln transformed response variable, n=24, p=0.0080) and combined deep peat riparian and shallow peat riparian dataset (ln transformed response variable, n= 60, p=0.0077, wetland type differences were not significant). Sulfide concentrations also increased with decreasing sulfate concentrations in shallow peat riparian porewater (non-transformed data, n = 12, p=0.0019) and for a combined deep peat riparian and shallow peat riparian porewater dataset (non-transformed data, n=17, p=0.0002, wetland type differences were not significant; the small deep peat riparian dataset alone yielded only a moderately significant result, p=0.0875).

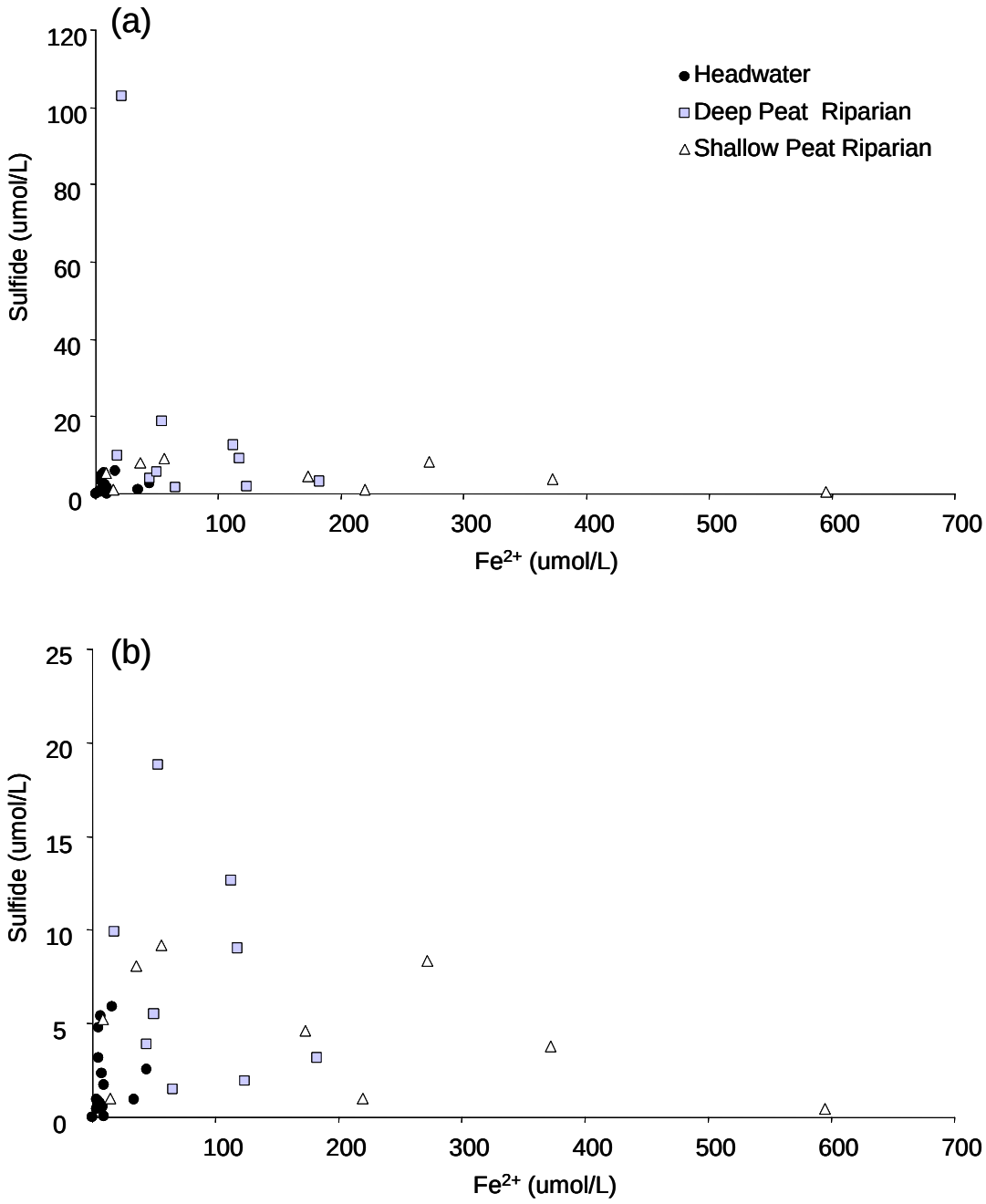

Figure 3.3. Scatterplots showing the relationship between ferrous iron (Fe^{2+}) and sulfide (S^{2-}) in wetland peat porewater of different wetland types of the Sunday Lake watershed. Two different scales are shown in order to demonstrate the relationship both with and without the outlier at sulfide concentration 103 umol/L.

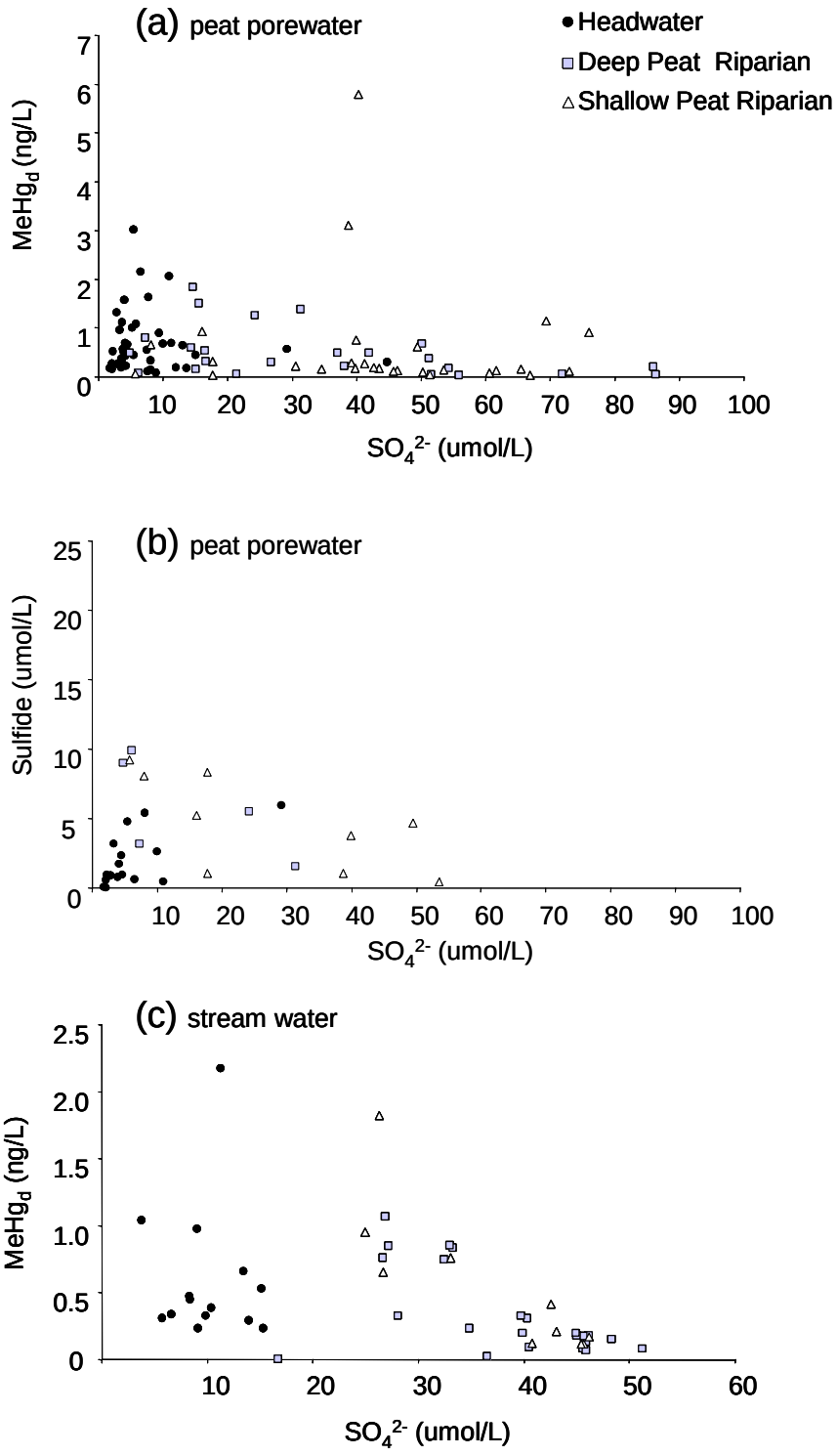

Figure 3.4. Scatterplots showing the relationship between sulfate (SO_4^{2-}) and (a) dissolved methyl mercury ($MeHg_d$) in peat porewater, (b) sulfide in peat porewater, and (c) $MeHg_d$ in stream water in different wetland types in the Sunday Lake watershed.

These results suggest that sulfate reduction is likely responsible, in part, for the observed high net methyl mercury production (Figure 3.1a,b). $MeHg_d$ concentration in stream water of the deep and shallow peat riparian wetlands also peaked at low sulfate concentrations (ln transformed response and predictor variable, n=10, p=0.0003 for shallow peat riparian stream water; ln transformed response and predictor variable, n = 20, p=0.0001, for the deep peat riparian stream water with one outlier removed to satisfy model assumptions; Figure 3.4c). The absence of this inverse relationship between $MeHg_d$ and sulfate within the headwater wetland porewater may suggest that mercury methylation by sulfate reducing bacteria is less important in headwater wetlands, or that the SRB community in headwater wetlands is less active (precipitation inputs of sulfate to the headwater wetlands are small), or that demethylation is more important to net methyl mercury production in headwater wetlands than in the riparian wetlands (Figure 3.4c).

DOC and net mercury methylation

The relationship between DOC and MeHg concentration, and between DOC and %MeHg, appear to differ among wetland types (Figure 3.5a,b,c, Figure 3.6a,b,c). However, only two of the observed patterns showed any statistically significant result. In shallow peat riparian wetlands, %MeHg concentrations increased with decreasing DOC concentration (ln transformed response variable, n=32, p=0.0003; Figure 3.6a); whereas, MeHg concentrations increased with increasing DOC concentration in headwater wetlands (ln transformed response variable, n=40, P=0.0383, with two outliers between 50-60 mg/L DOC removed; p=0.6490 with no outliers removed). Evidence of redox inhibition of mercury methylation was conspicuously absent from headwater wetlands. However, headwater wetlands had low concentrations of both nitrate and iron (Table 3.1), and thus the conditions under which inhibition would

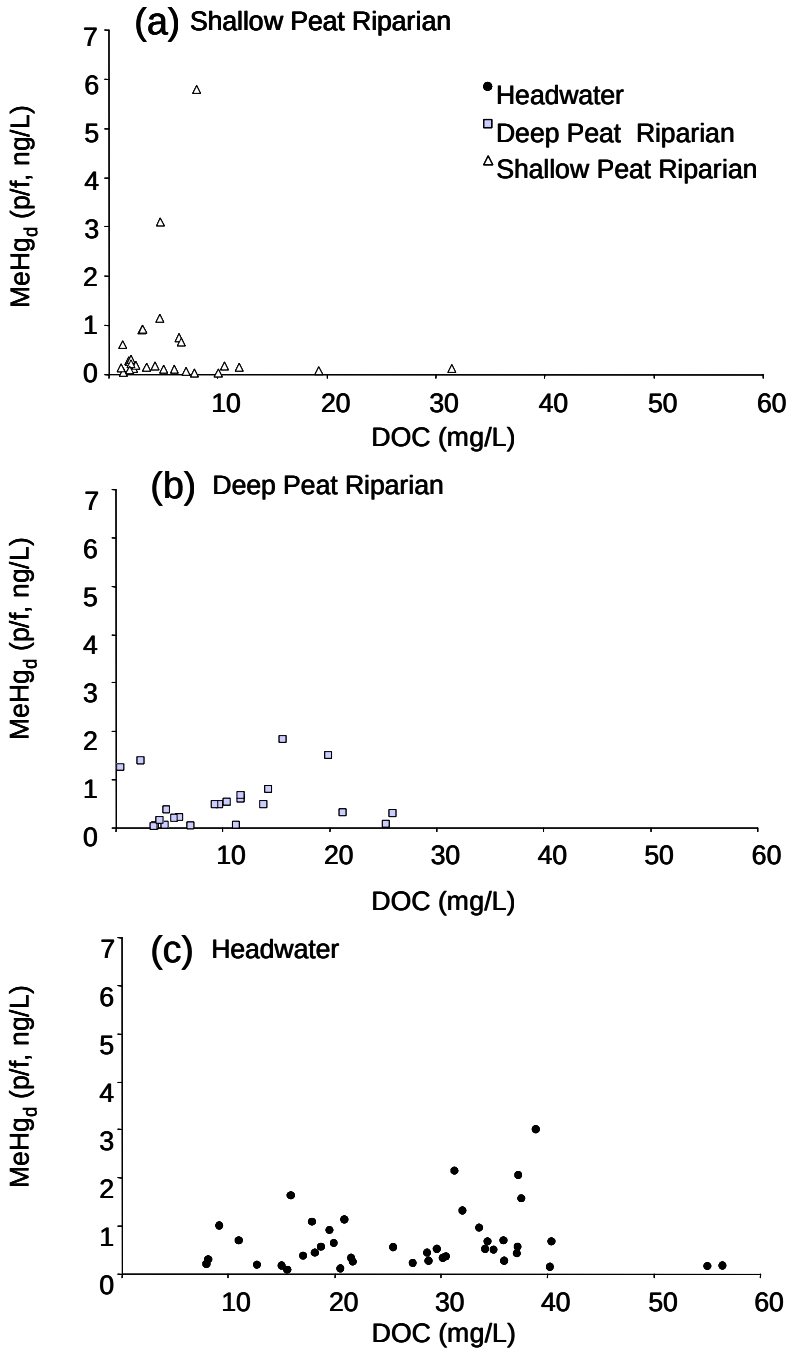

Figure 3.5. Scatterplots showing the relationship between dissolved organic carbon (DOC) and dissolved methyl mercury ($MeHg_d$) in (a) shallow peat riparian wetlands, (b) deep peat riparian wetlands, and (c) headwater wetlands in the Sunday Lake watershed.

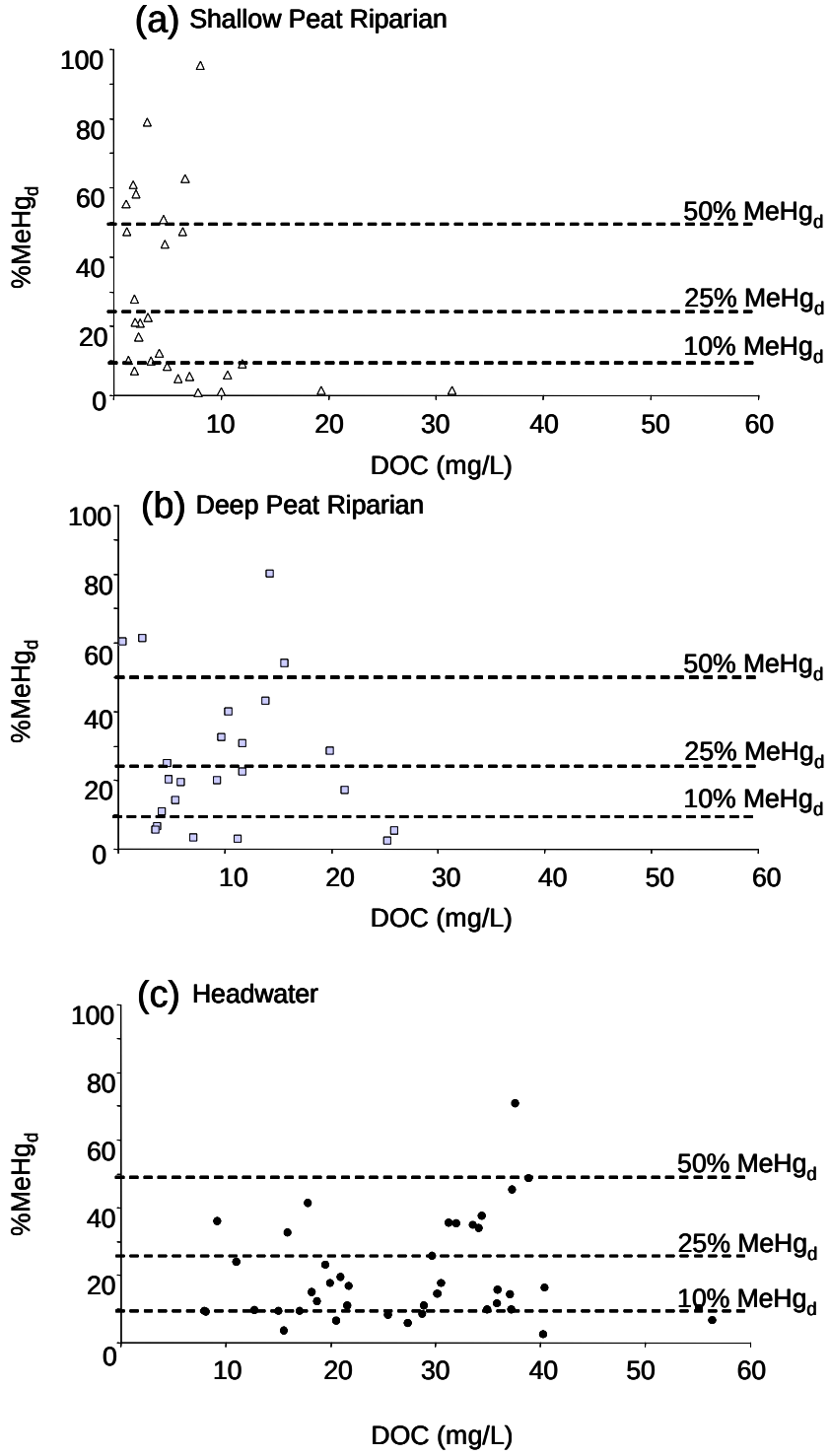

Figure 3.6. Scatterplots showing the relationship between dissolved organic carbon (DOC) and $\%MeHg_d$ in (a) shallow peat riparian wetlands, (b) deep peat riparian wetlands, and (c) headwater wetlands in the Sunday Lake watershed.

occur were not present in these wetlands. Despite the lack of inhibiting processes, neither $MeHg_d$ concentrations nor %MeHg in the headwater wetlands were consistently higher than in the riparian wetlands. In fact, net methylation increased disproportionately in the shallow peat riparian wetlands during August and September when water tables were low and soil water temperatures were high (see Chapter 2, Figure 2.2, Table 3.1).

It is possible that processes other than mercury methylation by microbial sulfate reduction contribute to methyl mercury production within the headwater wetlands. Both iron and sulfate concentrations were low in the porewater of headwater wetlands (Table 3.2), and there was only limited evidence of sulfate consumption in association with high concentrations of $MeHg_d$ in the headwater wetlands (Figure 3.6c). Note that this finding cannot entirely rule out the role of sulfate reduction in the methylation of mercury in the headwater wetlands; that is, sulfur cycling and re-cycling in this low sulfate ombrotrophic bog may be rapid, as has been shown to be the case in high sulfate ombrotrophic bogs (Wieder and Lang 1988). However, given the lack of clear redox control over net methyl mercury production (Figure 3.2a,b) and the increased potential for high $MeHg_d$ concentrations that occurs with increases in DOC concentrations in headwater wetlands (Figure 3.5c), it is possible that DOC-mediated abiotic methylation of mercury contributes to high net methyl mercury concentrations observed in headwater wetlands (*sensu* Weber 1993, Loseto et al. 2004).

CONCLUSIONS

Hydrogeologic setting influences the solute chemistry and the mode of decomposition in different wetland types, and these differences may suggest differences in the mechanism responsible for mercury methylation in these different

wetland environments. In shallow peat riparian wetlands, maximum net methyl mercury production appears to result from high rates of methylation by active sulfate reducer communities in conjunction with low rates of demethylation. Nitrate and iron appear to inhibit methyl mercury production. In the headwater wetlands, there is little evidence that microbial sulfate reduction alone is responsible for the observed patterns in net methyl mercury production. It is possible that abiotic methylation contributes to the pattern of net methyl mercury production in headwater wetlands, along with reduced activity of sulfate reducers and greater rates of methyl mercury demethylation. Much research is needed to elucidate the in situ controls on net mercury methylation in different wetland types across the landscape.

REFERENCES

APHA. 1998. Standard methods for the examination of water and wastewater, 20th edition, American Public Health Association: Washington, D.C., USA.

Barkay, T., M. Gillman, and R. R. Turner. 1997. Effects of dissolved organic carbon and salinity on bioavailability of mercury. Applied and Environmental Microbiology **63**:4267-4271.

Barkay, T., and I. Wagner-Dobler. 2005. Microbial transformations of mercury: Potentials, challenges, and achievements in controlling mercury toxicity in the environment. Advances in Applied Microbiology, Vol 57 **57**:1-52.

Benoit, J. M., C. C. Gilmour, A. Heyes, R. P. Mason, and C. L. Miller. 2003. Geochemical and biological controls over methylmercury production and degradation in aquatic ecosystems. Biogeochemistry of Environmentally Important Trace Elements **835**:262-297.

Branfireun, B. A., D. Hilbert, and N. T. Roulet. 1998. Sinks and sources of methylmercury in a boreal catchment. Biogeochemistry **41**:277-291.

Branfireun, B. A., N. T. Roulet, C. A. Kelly, and J. W. M. Rudd. 1999. In situ sulphate stimulation of mercury methylation in a boreal peatland: Toward a link between acid rain and methylmercury contamination in remote environments. Global Biogeochemical Cycles **13**:743-750.

Compeau, G. C., and R. Bartha. 1985. Sulfate-Reducing Bacteria - Principal Methylators of Mercury in Anoxic Estuarine Sediment. Applied and Environmental Microbiology **50**:498-502.

Driscoll, C. T., Y. J. Han, C. Y. Chen, D. C. Evers, K. F. Lambert, T. M. Holsen, N. C. Kamman, and R. K. Munson. 2007. Mercury contamination in forest and freshwater ecosystems in the Northeastern United States. Bioscience **57**:17-28.

Evers, D. C., Y. J. Han, C. T. Driscoll, N. C. Kamman, M. W. Goodale, K. F. Lambert, T. M. Holsen, C. Y. Chen, T. A. Clair, and T. Butler. 2007. Biological mercury hotspots in the northeastern United States and southeastern Canada. Bioscience **57**:29-43.

Galloway, M. E., and B. A. Branfireun. 2004. Mercury dynamics of a temperate forested wetland. Science of the Total Environment **325**:239-254.

Gilmour, C. C., and E. A. Henry. 1992. Mercury Methylation by Sulfate-Reducing Bacteria - Biogeochemical and Pure Culture Studies. Abstracts of Papers of the American Chemical Society **203**:140-Geoc.

Gilmour, C. C., E. A. Henry, and R. Mitchell. 1992. Sulfate Stimulation of Mercury Methylation in Fresh-Water Sediments. Environmental Science & Technology **26**:2281-2287.

Gran, G. 1952. Determination of the Equivalence Point in Potentiometric Titrations. Analytical Chemistry **24**:1519-1519.

Jeremiason, J. D., D. R. Engstrom, E. B. Swain, E. A. Nater, B. M. Johnson, J. E. Almendinger, B. A. Monson, and R. K. Kolka. 2006. Sulfate addition increases methylmercury production in an experimental wetland. Environmental Science & Technology **40**:3800-3806.

King, J. K., J. E. Kostka, M. E. Frischer, and F. M. Saunders. 2000. Sulfate-reducing bacteria methylate mercury at variable rates in pure culture and in marine sediments. Applied and Environmental Microbiology **66**:2430-2437.

King, J. K., F. M. Saunders, R. F. Lee, and R. A. Jahnke. 1999. Coupling mercury methylation rates to sulfate reduction rates in marine sediments. Environmental Toxicology and Chemistry **18**:1362-1369.

Kramer, J. R. 1984. Modified Gran analysis for acid base titrations. McMaster University, Hamilton, Ontario, Canada.

Loseto, L. L., S. D. Siciliano, and D. R. S. Lean. 2004. Methylmercury production in High Arctic wetlands. Environmental Toxicology and Chemistry **23**:17-23.

Lovely, D. R., and E. J. P. Phillips. 1987. Rapid assay for microbially reducible ferric iron in aquatic sediments. Applied and Environmental Microbiology **53**:1536-1540.

Mehrotra, A. S., A. J. Horne, and D. L. Sedlak. 2003. Reduction of net mercury methylation by iron in Desulfobulbus propionicus (1pr3) cultures: Implications for engineered wetlands. Environmental Science & Technology **37**:3018-3023.

Mitchell, C. P. J., B. A. Branfireun, and R. K. Kolka. 2008a. Assessing sulfate and carbon controls on net methylmercury production in peatlands: An in situ mesocosm approach. Applied Geochemistry **23**:503-518.

Mitchell, C. P. J., B. A. Branfireun, and R. K. Kolka. 2008b. Spatial characteristics of net methylmercury production hot spots in peatlands. Environmental Science & Technology **42**:1010-1016.

Olson, M. L., L. B. Cleckner, J. P. Hurley, D. P. Krabbenhoft, and T. W. Heelan. 1997. Resolution of matrix effects on analysis of total and methyl mercury in aqueous samples from the Florida Everglades. Fresenius Journal of Analytical Chemistry **358**:392-396.

Richardson, J. L., and M. J. Vepraskas. 2001. Wetland Soils: Genesis, Hydrology, Landscapes, and Classification. CRC Press.

Shanley, J. B., N. C. Kamman, T. A. Clair, and A. Chalmers. 2005. Physical controls on total and methylmercury concentrations in streams and lakes of the northeastern USA. Ecotoxicology **14**:125-134.

Stookey, L. L. 1970. Ferrozine - a New Spectrophotometric Reagent for Iron. Analytical Chemistry **42**:779-&.

USEPA. 1996. Method 1669. United States Environmental Protection Agency, Office of Water, Office of Science and Technology, Engineering and Analysis Division (4303), Washington, D.C., USA.

USEPA. 1998. Method 1631. United States Environmental Protection Agency, Office of Water, Office of Science and Tachnology, Engineering and Analysis Division (4303), Washington, D.C., USA.

USEPA. 2001, Revision E. Method 1630. United States Environmental Protection Agency, Office of Water, Office of Science and Tachnology, Engineering and Analysis Division (4303), Washington, D.C., USA.

Warner, K. A., E. E. Roden, and J. C. Bonzongo. 2003. Microbial mercury transformation in anoxic freshwater sediments under iron-reducing and other electron-accepting conditions. Environmental Science & Technology **37**:2159-2165.

Weber, J. H. 1993. Review of Possible Paths for Abiotic Methylation of Mercury(Ii) in the Aquatic Environment. Chemosphere **26**:2063-2077.

Wieder, R. K., and G. E. Lang. 1988. Cycling of Inorganic and Organic Sulfur in Peat from Big Run Bog, West-Virginia. Biogeochemistry **5**:221-242.

CHAPTER FOUR:
HYDROLOGIC FLOW PATHS, SOURCE AREAS, AND SUPPLY OF DISSOLVED ORGANIC CARBON LINK EPISODIC ACIDIFICATION AND MERCURY MOBILIZATION DURING SNOWMELT.

ABSTRACT

I quantified hydrologic source areas and flow paths, acid-base and aluminum chemistry, dissolved organic carbon dynamics, and mercury mobilization during snowmelt at the Hubbard Brook Experimental Forest (HBEF), NH USA. This study shows: (1) episodic acidification during snowmelt at the HBEF is controlled by multiple mechanisms (base cation dilution, nitrate and aluminum acidity, and natural organic acids) and persists despite long-term decreases in acidic deposition; (2) episodic acidification continues to result in mobilization of inorganic monomeric aluminum to concentrations toxic to fish; (3) DOC mobilized from shallow organic soils during snowmelt results in the mobilization of mercury from these same sources; (4) methyl mercury may be produced in the forest floor over winter and flushed from soils during snowmelt; (5) the amount of mercury released during snowmelt likely represents a large portion of annual mercury export; and (6) hydrologic source areas and flow paths, and DOC dynamics, strongly influence episodic acidification and the mobilization of mercury, even in a watershed with low stream water DOC concentrations and export.

INTRODUCTION

Environmental perturbations such as acid and mercury deposition do not occur in isolation, and ecosystem recovery from such perturbations will likely have some degree of interdependence. Hydrological processes and dissolved organic carbon

(DOC) dynamics that link terrestrial and aquatic ecosystems are, in part, drivers of episodic acidification, aluminum mobilization, and mercury transport from terrestrial to aquatic ecosystems. Although previous stream research has demonstrated a strong relationship between mercury concentration and discharge (e.g., Schuster et al. 2008, Balogh et al. 2006, Shanley et al. 2005, Shanley et al. 2002, Babiarz et al. 1998, Scherbatskoy et al. 1998, Bishop et al. 1995), and between mercury and water column carbon (i.e., POC, DOC; e.g., Meili 1991, Shanley et al. 2002, Kolka et al. 2001), no previous studies have made detailed multi-solute observations of acid-base and aluminum chemistry in conjunction with mercury species across event hydrographs. By quantifying mercury mobilization within the context of episodic acidification, the objective of this study was to improve understanding of hydrologic and biogeochemical controls governing mercury transport from terrestrial to aquatic ecosystems.

Terrestrial ecosystems mediate the transport of atmospheric deposition to and thus the ultimate effects of atmospheric deposition on surface waters. The degree to which acid deposition acidifies surface waters is a function of watershed characteristics, including elevation, forest type, bedrock, soil depth, base saturation, and hydrologic flow paths (e.g., Lovett et al. 1996, Schaefer et al. 1990, Driscoll et al. 1987, Newton et al. 1987, Chen et al. 1984). Acidification of these drainage waters, in turn, facilitates the export of labile (inorganic) monomeric aluminum (Al_i; Driscoll and Postek 1995, Driscoll et al. 1985, Johnson et al. 1981). Watersheds additionally mediate surface water acidification and aluminum mobilization through the supply of natural organic solutes (i.e., dissolved organic carbon, DOC) (Driscoll et al. 1994, Cirmo and Driscoll 1993, Driscoll et al. 1989, Driscoll et al. 1988). Thus, the mode and magnitude of surface water acidification and aluminum mobilization is a function

of both atmospheric deposition, and the hydrological and biogeochemical processes characteristic of individual watersheds.

Similarly, terrestrial ecosystems also mediate the transport of mercury, influencing the amount, timing, and chemical form that is ultimately delivered to aquatic ecosystems. Watershed characteristics affect the amount of mercury deposited to the landscape as well as the form of mercury that is delivered to surface waters. In general, forests enhance mercury deposition to terrestrial ecosystems (St Louis et al. 2001, Rea et al. 2002), and there is some evidence that forest type influences the magnitude and form of mercury deposited (Demers et al. 2007, Miller et al. 2005). Despite enhanced deposition of mercury, upland forest watersheds generally exhibit lower export of mercury than agricultural and wetland dominated watersheds, due to lower particulate mercury losses in comparison to agricultural ecosystems and lower dissolved mercury losses in comparison to wetland ecosystems. The strong retention of mercury in soils of upland ecosystems is linked to organic matter (Grigal 2002, 2003, Yin et al. 1997, Meili 1991), likely associated with reduced sulfur and nitrogen groups (i.e., thiols, amines; Khwaja et al., 2006; Drexel et al., 2002; Skyllberg et al., 2000). Subsequent mobilization of mercury is dependent upon decomposition and erosional processes that release dissolved and particulate organic matter. Wetlands also influence the form of mercury released to surface waters, and the amount of methyl mercury in fish has been correlated with the percentage of wetlands within the entire watershed (Driscoll et al., 1995), as ionic mercury is transformed to methyl mercury within anoxic wetland soils (Branfireun et al., 1998; St. Louis et al., 1996). Thus, the magnitude and form of mercury mobilized from the terrestrial ecosystem to surface waters is also a function of both the atmospheric deposition, and the hydrological and biogeochemical processes as influenced by watershed characteristics.

Terrestrial ecosystems that have been previously impacted by acid deposition may subsequently limit recovery of affected aquatic ecosystems following reductions in inputs. Recovery of acid-impacted watersheds is dependent upon not only reductions in acidic deposition, but also the rate of chemical weathering that will re-supply base cations leached during soil acidification and the net loss of sulfur stored from a legacy of elevated atmospheric sulfur deposition (Driscoll et al., 2001). Recovery of surface waters (and associated fisheries) from mercury contamination is, in part, dependent upon the rate at which mercury is transferred from the uplands to downstream aquatic ecosystems; that is, the residence time of mercury in the terrestrial soil environment. Because mercury transport has been linked to DOC transport, changes in the mobilization of DOC that may occur in concert with environmental change or recovery from acidification may significantly affect mercury transport. In order to predict the recovery of surface waters from elevated atmospheric acid and mercury deposition (e.g., acidification and associated aluminum toxicity, mercury contamination), it is imperative to not only understand the biogeochemical processes and hydrologic connectivity governing chemical transfer between terrestrial and aquatic ecosystems, but also how recovery from environmental perturbations may be linked through those biogeochemical processes and hydrologic controls.

Hydrologic connectivity between uplands and surface waters is dynamic, with changes in hydrologic flow paths being driven by storm events and seasonal fluctuations. As water tables rise, longer flow paths through deeper terrestrial soils can be short-circuited (e.g., Dittman et al. 2007, Chen et al. 1984). At sites where the rate of infiltration is high (as at HBEF, Pierce 1967) hydrologic events may result in shallow lateral flow through organic rich soils, thus promoting the transport of DOC to surface waters. In the absence of lateral flow, soil solutions migrate vertically through the soil profile, resulting in podzolization, as aluminum and iron are leached from

upper mineral horizons and immobilized in lower mineral horizons by organic acids derived from leaf litter and the forest floor (Driscoll and Postek 1995, Deconnick 1980). Thus, as flow paths and source areas shift in response to hydrologic events, a corresponding shift occurs in the composition of soil solutions contributed to surface waters.

Despite changes in flow paths during high flow events, Likens and Bormann (1995) show that the concentrations of many chemical components change little with increases in discharge at the Hubbard Brook Experimental Forest. In contrast, the concentration-discharge relationships for TSS, DOC, and mercury are more dynamic at the HBEF and at other sites (e.g., Shanley 2002, Scherbatskoy 1998, Bishop 1995, Likens and Bormann 1995) and result in an exponential increase in total flux as concentration increases with increasing discharge. In dilute systems, even small changes in concentration-discharge dynamics can have important implications, especially where ecological effects may be threshold dependent. For example, high nitrate pulses during snowmelt can have deleterious effects on the water quality of downstream ecosystems (e.g., Sullivan et al. 1997, Schaefer et al. 1990, Driscoll et al. 1987, Driscoll and Schafran 1984), and associated increases of labile (inorganic) monomeric aluminum may be harmful to aquatic biota if toxic thresholds are exceeded (e.g., Baker et al. 1996, Van Sickle et al. 1996, Gagen et al. 1993,1994, Baker and Schofield 1982). Thus, knowledge of both the total annual load and the timing and distribution of the delivery of those loads from uplands to surface waters is important in assessing the recovery of aquatic ecosystems in response to decreases in the deposition of atmospheric pollutants to terrestrial watersheds.

High flow events are also important to the transfer of mercury from watersheds to surface waters (Schuster et al. 2008, Shanley et al. 2002, Scherbatskoy et al. 1998), and the quantity and form of mercury flux during high flow events is dependent upon

watershed characteristics (e.g., Babiarz et al. 1998, Hurley et al. 1998, Hurley et al. 1995, Bishop et al. 1995). Recent evidence suggests that mercury retention within terrestrial ecosystems of the midwestern and northeastern United States and Canada has declined from about 95% to 78% of annually deposited mercury (Engstrom and Swain 1997, Lorey and Driscoll 1999, Kamman and Engstrom 2002). However, there is currently a lack in understanding of the mechanisms that govern the release of mercury from terrestrial soils (Munthe et al. 2007). Hence, although it is important to constrain current estimates of mercury flux from the terrestrial landscape, it is also essential to strive for a mechanistic understanding of the hydrological and biogeochemical processes governing the transfer of mercury from soils to surface waters.

In this study I use base flow and soil solution chemistry as end-members from which to model event flow paths and contributing source areas during snowmelt in the reference watershed (W6) at the Hubbard Brook Experimental Forest. I provide detailed observations of acid-base and aluminum chemistry, DOC dynamics, and mercury mobilization across the snowmelt hydrograph. Based on observations of acid-base chemistry, DOC dynamics, and modeled hydrologic flowpaths, I infer source and process level controls on mercury mobilization. This study shows that the dynamics of episodic acidification, aluminum mobilization, and mercury transport are linked through hydrological and biogeochemical processes that influence the source and character of the DOC supply from terrestrial to aquatic ecosystems.

METHODS

Site description

In this study I quantified soil solution and stream chemistry in watershed 6 (W6) at the Hubbard Brook Experimental Forest (HBEF) in the southern White

Mountains of New Hampshire, USA (43°56' N, 71°45' W). Watershed 6 (W6), the biogeochemical reference watershed at the HBEF, is 13.2 hectares in area, located on the south facing slope (mean slope 15.8°, aspect S32°E), has an elevation ranging from ~540 m at the weir to ~800 m on the ridge, and is gauged with a modified San Dimas flume (Likens and Bormann 1995, www.hubbardbrook.org).

The climate of the HBEF is humid continental, with short, cool summers and long, cold winters (Likens and Bormann 1995). Average daily mean temperature (1956-2000) is 5.6°C, with mean monthly temperature increasing to 18.7°C in July, and decreasing to - 8.3°C in January (Bailey et al. 2003). Average annual precipitation at the HBEF (W6) is ~1,400 mm (Bailey et al. 2003), with ~30% delivered as snow (Likens and Bormann 1995). A snowpack develops and usually persists from mid-December through mid-April. At an elevation of ~560 m (reflecting low to mid elevation hardwoods on the south facing slope), peak snow depth (~1.0 -1.5 m) occurs in March, and has a snow water equivalent (SWE) of ~200 mm (Bailey et al. 2003). As a result of this snowpack, forest soils usually remain unfrozen throughout the winter (Likens and Bormann 1995). Annual estimated evapotranspiration is ~500 mm (Bailey et al. 2003). Precipitation is distributed evenly throughout the year, whereas approximately one third of total streamflow occurs during the snowmelt period (late March through early May). Soils at the HBEF are well-drained Spodosols, predominantly Haplorthods of sandy loam texture (Johnson et al. 2000; Likens and Bormann 1995). Precipitation (and snowmelt) infiltrates the soil rapidly, resulting in negligible overland flow (Detty 2008, Pierce 1967).

Stream chemistry at the weir during snowmelt was interpreted within the context of soil solutions and longitudinal stream samples taken from W6 on 28 April 2005. This snapshot characterization of acid-base chemistry and DOC dynamics along this elevational gradient was obtained from monthly monitoring ongoing at

HBEF since ~1984 (Johnson et al. 2000). Watershed 6 was initially divided into three subcatchments of roughly equal area based on elevation and topography (Figure 4.1); subsequently, W6 was divided into vegetation zones. The uppermost subcatchment (~710 m – 800 m) represents ~41% (5.4 ha) of the watershed (as calculated from grid map data at *www.hubbardbrook.org*). Within the uppermost elevational subcatchment, the spruce-fir-birch (SFB) and the high elevation hardwoods (HH) are the dominant vegetation zones. The dominant vegetation in the SFB zone includes red spruce (*Picea rubens* Sarg.), balsam fir (*Abies balsamea* L.), and white birch (*Betula papyrifera* var. *cordifolia* Marsh.). The SFB zone (1.6 ha, ~12% of total catchment area) occurs along the ridge in the northeastern corner of the watershed, where the topography is relatively flat, soils and till are shallow, and some bedrock is exposed. Soils in the SFB zone have a thick O horizon (~ 8.9 cm) and an average total depth of 42.8 cm to C horizon or bedrock (Johnson et al. 2000). The high hardwood zone (HH, 3.4 ha, ~26% of total catchment area) covers most of the rest of the upper subcatchment, and is dominated by American beech (*Fagus grandifolia* Ehrh.), yellow birch (*Betula allegheniensis* Britt.), and sugar maple (*Acer saccharum* Marsh.). Soils in the high hardwoods are generally deeper (~6.0 cm O horizon, ~64.5 cm total depth) but often lie directly on bedrock with no C horizon present (Johnson et al. 2000). The middle subcatchment (~625 m to 710 m, 4.5 ha) is mostly dominated by sugar maple and beech. The lower subcatchment (~540 m to 625 m, 3.1 ha) is a more equal mix of sugar maple, beech, and yellow birch. Together, the middle and lower subcatchments are collectively studied as the low hardwoods zone (LH, 7.9 ha, ~60% of total catchment area). The soils in the LH zone are deeper, and underlain by dense glacial till (~6.4 cm O horizon, ~60.5 cm total depth to C horizon), and the stream flows continuously at this elevation except in times of drought (Johnson et al. 2000).

Figure 4.1. Diagram of watershed 6 at the Hubbard Brook Experimental Forest (HBEF) in the White Mountains of New Hampshire, USA, showing elevational subcatchments and vegetation zones, soil solution lysimeter plots, and longitudinal stream sampling points (adapted from data online at www.hubbardbrook.org). Elevation at each grid corner available online. Abbreviations are SFB, high-elevation spruce-fir-birch; HH, high-elevation hardwood; LH, low-elevation hardwood. The location of the HBEF is denoted by the star on the inset map of the northeastern United States.

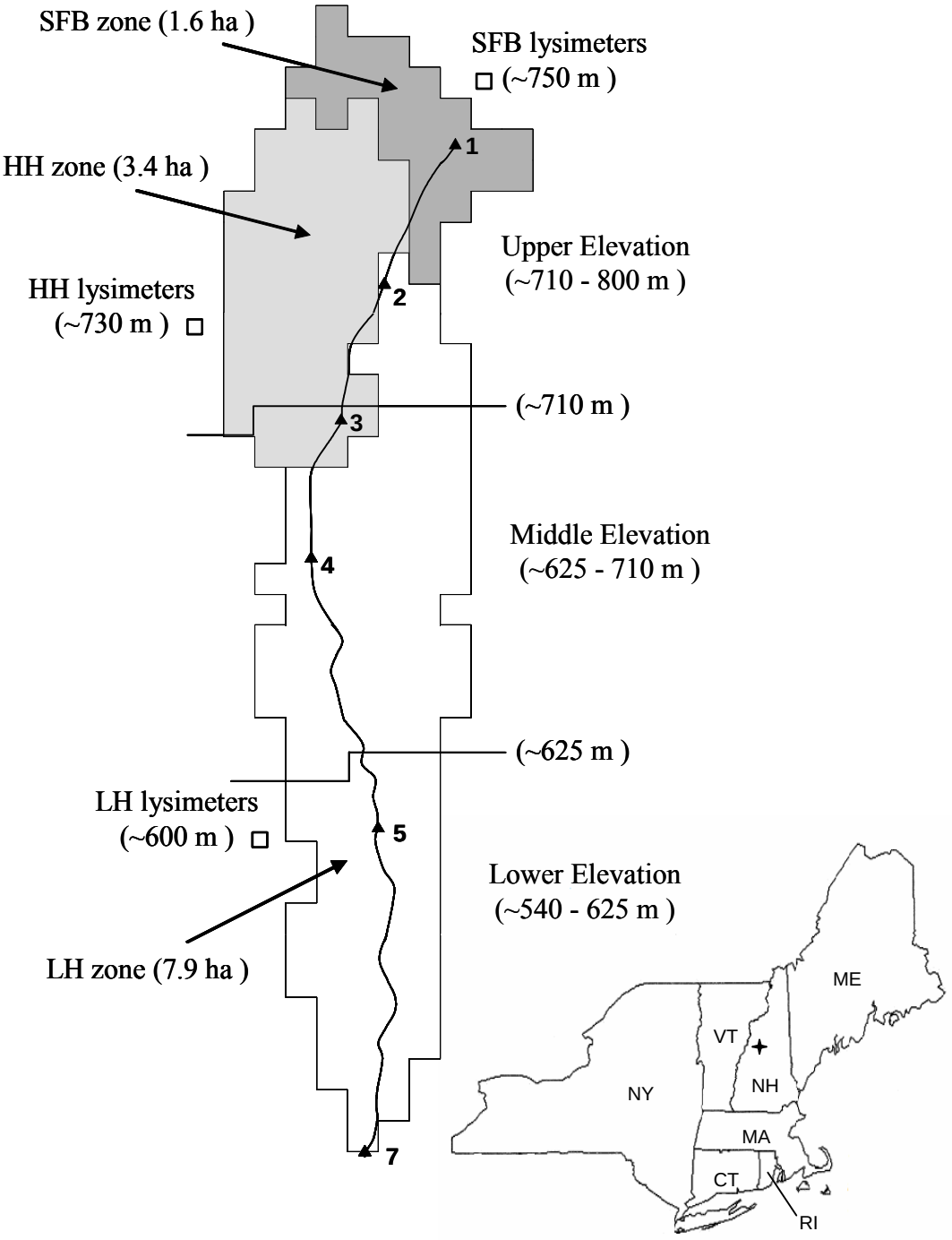
SFB zone (1.6 ha)
SFB lysimeters
(~750 m)
HH zone (3.4 ha)
1
Upper Elevation
(~710 - 800 m)
HH lysimeters
(~730 m)
2
(~710 m)
3
Middle Elevation
(~625 - 710 m)
4
(~625 m)
LH lysimeters
(~600 m)
5
Lower Elevation
(~540 - 625 m)
LH zone (7.9 ha)
7
ME
VT
NH
NY
MA
CT
RI

Sampling procedures

Stream samples obtained to characterize stream water chemistry across the snowmelt hydrograph were taken just above the weir in W6. Samples for mercury analyses were collected in new 2-L PETG bottles, using clean procedures (USEPA, 1996). Samples for analysis of dissolved organic carbon (DOC) and total suspended solids (TSS) were collected in clean, oven-baked 1L amber glass bottles. Stream water for the remaining chemical analyses was collected in polyethylene bottles and filled to minimize headspace. Samples were kept cold and in the dark until sample filtering and preservation was completed within 48 hours of sampling.

Soil solutions were collected during the snowmelt period from tension-free lysimeters installed in the Oa, Bh and Bs soil horizons at 3 sites adjacent to W6 at elevations of 750 m (SFB zone), 730 m (HH zone), and 600 m (LH zone). Additional information about lysimeter placement, construction, and installation is available (Johnson et al. 2000, Dahlgren and Driscoll 1994, Driscoll et al. 1988, and online at *www.hubbardbrook.org*).

Longitudinal stream samples were collected from 6 sites spaced along an elevational gradient between the stream origin and the weir in W6 (Figure 4.1), and were collected in conjunction with soil solutions. Stream sites 1 and 2 primarily drain the SFB zone, sites 3 and 4 primarily drain the SFB and HH zones, and sites 5 and 7 drain the combined SFB, HH, and LH zones (there is no site 6; Palmer et al. 2004). Snow depth and snow water equivalent (SWE) were measured weekly at elevations of 560 m and 760 m on the south facing slope at the HBEF, and reflect snow conditions at low to mid elevation hardwood forests and high elevation hardwood forests, respectively (Bailey et al. 2003; Bailey 2005, HBEF Snow Depth and Snow Water datasets online at *www.hubbardbrook.org*).

Chemical analyses

Standard procedures were used for the analysis of chemical parameters in stream water samples. The pH, acid neutralizing capacity (ANC), and dissolved inorganic carbon (DIC) were determined for bulk (unfiltered, unpreserved) samples. The pH was measured in the laboratory using a glass combination electrode after calibration using pH 4.00 and pH 7.00 buffer solutions; pH measurements were made on a 50 ml aliquot of sample just prior to analysis of ANC. In order to determine ANC, a separate 50 ml aliquot was subsequently titrated with 0.1N hydrochloric acid (HCl) using the same electrode and a Brinkmann Metrohm 716 DMS Titrino auto-analyzer and the Brinkmann Titrino Work Cell Version 4.3. Acid neutralizing capacity was determined by analyzing the titration data using a modified Gran analysis (Kramer 1982, Butler 1982, Kramer 1984, Gran 1952). DIC was measured in conjunction with the pH and ANC analyses by acidifying a separate 40 ml aliquot with phosphoric acid and purging the solution with nitrogen gas, thus converting and removing all carbonate species as carbon dioxide; the resulting CO_2 was quantified using a non-dispersive infrared detector on a Dohrmann Phoenix 8000 Analyzer.

Cations, anions, silica, and monomeric aluminum (Al_m) samples were syringe filtered (0.45 μm polypropylene) prior to analysis. Samples for analysis of cations (K^+, Na^+, Mg^{2+}, Ca^{2+}, Fe^{3+}, Mn^{2+}) were acidified to 1% nitric acid and analyzed on a Perkin Elmer ELAN 6100 ICP-MS, using U.S. EPA Method 200.8. Anions (F^-, Cl^-, NO_3^-, SO_4^{-2}) were analyzed by ion chromatography with chemical suppression of eluent conductivity using an Ion-Pac AS18 column (Dionex). Dissolved silica (SiO_2), ammonium (NH_4^+), and monomeric aluminum (Al_m) were analyzed colorometrically with a Bran & Luebbe Auto Analyzer. Dissolved silica was analyzed using an automated method for molybdate-reactive silica based on the heteropoly blue method (APHA 1998, 4-158 to 4-160). Ammonium (NH_4^+) was determined by the automated

phenate method (APHA 1998, 4-110). Total monomeric aluminum (Al_m) was determined by reaction with pyrocatechol violet (PCV, McAvoy et al.1992); organic (nonlabile) monomeric aluminum (Al_o) was determined by placing a cation-exchange column in the sample path to remove inorganic (labile) monomeric aluminum (Al_i); thus Al_i is determined by subtraction (i.e., $Al_i = Al_m - Al_o$; Driscoll 1984).

For determination of TSS, a one liter sample was filtered through a pre-weighed glass fiber filter (0.7 µm, pre-baked at 450^{o}C) into a clean flask. The filtrate was then sub-sampled for analysis of DOC with a Dohrmann Phoenix 8000 Analyzer using the persulfate-ultraviolet oxidation method (APHA 1998, 5-22, 5310C). The sample bottle was then rinsed thoroughly (3x) with de-ionized water and this rinse water was filtered through the same glass fiber filter, which was then dried and weighed to determine TSS (APHA 1998, 2-58, 2540D).

Samples for analysis of mercury were vacuum filtered through a 0.45 µm Teflon membrane following clean techniques. Filters were assembled in clean Teflon holders and pre-rinsed with 500 ml of 1% trace metal grade hydrochloric acid, followed by 500 ml of de-ionized water to remove residual acidity. Both filtered and unfiltered samples were poured into Teflon bottles subsequent to filtering, acidified to 0.4% with hydrochloric acid and stored in the dark at 4^{o}C until analysis. The concentration of total mercury (all forms of mercury) was determined for both unfiltered (Hg_t) and filtered (Hg_d) samples. The concentration of particulate bound mercury was estimated by difference (i.e., $Hg_p = Hg_t - Hg_d$). Total mercury in stream water was analyzed according to EPA Method 1631 using automated CVAFS (Tekran 2600, USEPA 1998). The concentration of methyl mercury (MeHg) was also determined for both unfiltered (MeHg) and filtered ($MeHg_d$) samples. Methyl mercury in stream water was distilled and analyzed using EPA Method 1630 (USEPA, 2001).

Samples were analyzed in batches with quality control that included field blanks and duplicates, procedural method blanks and duplicates, independent primary and secondary source standards, method detection limit check standards, analysis of appropriate certified reference materials, matrix spike and matrix spike duplicate samples to verify absence of sample matrix interferences, as well as initial and ongoing calibration verification standards, initial and ongoing calibration blanks, and initial and ongoing precision and recovery standards.

Acid-base calculations

Acid-base chemistry was summarized using the following equations; all components are expressed in μeq/L; base cations, metal cations, and inorganic acid anions are denoted by C_B, Me^{n+}, and C_A, respectively (Equation 4.1-4.6).

$$\text{Cations} = [C_B] + [Me^{n+}] + [H^+] \quad (4.1)$$

$$[C_B] = [Na^+] + [K^+] + [Mg^{2+}] + [Ca^{2+}] + [NH_4^+] \quad (4.2)$$

$$[Me^{n+}] = [Al^{3+}] + [Fe^{3+}] + [Mn^{2+}] \quad (4.3)$$

$$\text{Inorganic Anions} = [C_A] + [HCO_3^-] + [CO_3^{2-}] + [OH^-] \quad (4.4)$$

$$[C_A] = [NO_3^-] + [SO_4^{2-}] + [Cl^-] + [F^-] \quad (4.5)$$

$$\text{Calculated Alkalinity} = C_{ALK} = C_B - C_A \quad (4.6)$$

Organic acid anion $[A^-]$ was determined by charge balance discrepancy (Driscoll and Newton 1985, Driscoll et al. 1989, Driscoll et al. 1994, Equation 4.7). We determined the charge associated with inorganic monomeric aluminum (Al_i) and other metal cations from speciation calculations using the chemical equilibrium model CHEAQS Pro 2007.1 (CHemical Equilibria in Aquatic Systems, Wilko Verweij, available online at *http://home.tiscali.nl/cheaqs/index.html*). The proportion of strong acids (A_s) and

weak acids (A_w) were estimated (Munson and Gherini 1993, Equation 4.8, 4.9) and organic acid anion charge density was determined by dividing $[A^-]$ (μeq/L) by the concentration of DOC (μmol/L).

$$[A^-] = [C_B] + [Me^{n+}] - [C_A] - [HCO_3^-] + [H^+] \quad (4.7)$$

$$[A_s] = [C_B] + [Me^{n+}] - [C_A] - [ANC_{gran}] \quad (4.8)$$

$$[A_w] = [A^-] - [A_s] \quad (4.9)$$

Hydrograph separation

We performed a hydrograph separation for the snowmelt period by utilizing a principal components analysis (PCA, McCune and Grace 2002) combined with an end member mixing analysis (EMMA) model following Christophersen and Hooper (1992) as well as others (Burns et al. 2001, Wellington and Driscoll 2004). First, six solutes that appeared to mix conservatively were selected based on linear plots of pairwise combinations of solutes (i.e., mixing diagrams): F^-, SO_4^{2-}, Al_o, Na^+, Mg^{2+} and Ca^{2+}. Second, we performed a PCA on stream water data for these solutes using a correlation matrix (which standardizes data) to determine the number of end-members required to explain the variability in the data. PCA was performed on the correlation matrix using all six solutes, as well as combinations of five and four solutes. Based on PCA results, we selected a model that: (1) accounted for the greatest variability in stream chemistry with two principal components, implying 3 end members; and (2) was least likely due to chance based on broken stick eigenvalues (McCune and Grace 2002). Third, potential end members were standardized and projected into the space defined by the stream water PCA by multiplying the standardized values by the matrix of eigenvectors. Fourth, we chose the set of end members whose orthogonal projections best bounded the stream water observations. Fifth, we performed an end-

member mixing analysis using the orthogonal projections of these end members to determine their ability to reproduce the stream water concentrations. Finally, we used an EMMA model to calculate the contribution of each end member to stream discharge at the weir during snowmelt by solving the following simultaneous equations (Equations 4.10-4.12) (Christophersen and Hooper 1992, Burns et al. 2001; Wellington and Driscoll 2004).

$$Q_T = Q_{BF} + Q_{LH} + Q_{HH,SFB} \quad (4.10)$$

$$U1_T Q_T = U1_{BF} Q_{BF} + U1_{LH} Q_{LH} + U1_{HH,SFB} Q_{HH,SFB} \quad (4.11)$$

$$U2_T Q_T = U2_{BF} Q_{BF} + U2_{LH} Q_{LH} + U2_{HH,SFB} Q_{HH,SFB} \quad (4.12)$$

where Q is the discharge, U1 and U2 are the first and second principal component scores from the PCA, and subscript BF, LH, and HH/SFB denote base flow, lower hardwood zone, and the combined high hardwood and spruce-fir-birch zone, respectively.

RESULTS AND DISCUSSION

Snowmelt hydrograph

Snowmelt associated discharge (~357 mm) from 24 March through 7 May 2005 (DOY 83-127) accounted for ~30.5% percent of total annual discharge (1172 mm; Campbell and Bailey 2005, Daily Stream Flow dataset online at *www.hubbardbrook.com*). Overall, flow ranged from 1.3 L/s at base flow to 162 L/s during peak flow (Figure 4.2). Two rain-on-snow events dominated snowmelt discharge, the first on 3 April (71 mm, 162 L/s) likely representing a greater proportion of snowmelt from the lower elevations, and the second on 24 April (62 mm, 122 L/s) likely representing a greater proportion of snowmelt from higher

elevations (see *below for Hydrograph Separation*). These two high flow events coincided with 51 mm and 106 mm of rainfall respectively (Figure 4.2; Campbell and Bailey 2005, Daily Precipitation dataset online at *www.hubbardbrook.com*). Maximum snow depth in the low to mid elevation hardwoods (at 560 m) was 70.1 cm (SWE = 17.5 cm); this low elevation zone was snow-free by approximately 11 April. Maximum snow depth in the high hardwoods (at ~760 m) was 93.7 cm (SWE = 23.9 cm); this higher elevation zone was snow free by approximately 26 April (Bailey, 2005, Snow Depth and Snow Water datasets online at *www.hubbardbrook.org*). Snow depth, SWE, timing of snowmelt, the amount of precipitation during snowmelt, and snowmelt runoff were near average relative to the long term record at the HBEF (Table 4.1). Sampling coverage included two base flow samples prior to snowmelt (Q = 1.3, 1.4 L/s) and one base flow sample after snowmelt (Q=3.1 L/s; Figure 4.2); the remaining samples were obtained over a range of elevated flows (Q = 5.0 to 93.4 L/s), although the two largest discharge peaks were sampled only on their descending limbs. Overall, the snowmelt period was well characterized by the sampling effort across the hydrograph (Figure 4.2).

Hydrograph separation

A chemical separation of the hydrograph using principal components analysis (PCA) and an end member mixing analysis (EMMA) model revealed that a large proportion of stream discharge was derived from shallow soil water during the snowmelt period (Figure 4.2). This model result is in good agreement with previous research within this watershed (Dittman et al. 2007, Lawrence and Driscoll 1990, McDowell 1985). The first principal component appeared to represent variation between deep soil water and shallow soil water contributions to the stream, whereas the second principal component appeared to represent differences in soil solution

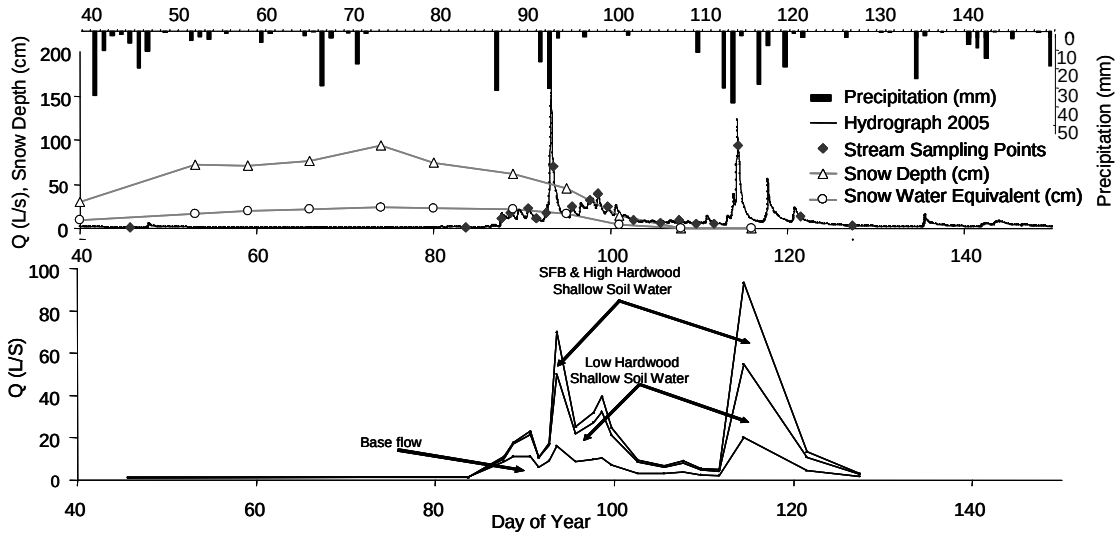

Figure 4.2. Snowpack, precipitation, discharge, and hydrograph separation based on PCA EMMA model during snowmelt at W6 at the Hubbard Brook Experimental Forest. Base flow represents deep soil water.

Table 4.1. Maximum snow depth, maximum snow water equivalent, date of completion of snowmelt, precipitation occurring during the snowmelt period, and snowmelt runoff for W6 at the Hubbard Brook Experimental Forest. Data are range, mean (+/- 1SE) for the 1985-1994 and 1995-2004 periods. For the purposes of this historic context, the snowmelt period was determined to begin at date of maximum snowpack in the low/mid elevation hardwoods and end at date of snowpack disappearance in the high elevation hardwoods. Summary data was compiled from data available online at *www.hubbardbrook.com* (Bailey 2005, Snow Depth and Snow Water datasets; Campbell and Bailey 2005, Daily Stream Flow and Daily Precipitation datasets).

	Low/Mid Elevation Hardwoods	High Elevation Hardwoods
Max Snow Depth (mm)		
1985 - 1994	343-892, 647 (66)	470-1057, 792 (76)
1995 - 2004	404-886, 633 (47)	599-1176, 833 (63)
2005	701	937
Max SWE (mm)		
1985 - 1994	89-226, 163 (15)	107-272, 214 (19)
1995 - 2004	97-249, 160 (17)	122-305, 213 (19)
2005	173	239
Completion of Melt (DOY)		
1985 - 1994	78-118, 103 (4)	78-122, 106 (4)
1995 - 2004	87-119,101 (3)	96-127, 109 (3)
2005	101	116
Snowmelt Precipitation (mm)		
1985 - 1994	45-252, 169 (19)	
1995 - 2004	67-385, 195 (34)	
2005	192	
Snowmelt Runoff (mm)		
1985 - 1994	169-363, 278 (21)	
1995 - 2004	149-448, 293 (32)	
2005	357	

chemistry along an elevational gradient within the watershed (Figure 4.3). The first principal component accounted for 69.7% of the variation in solute chemistry, whereas the second principal component accounted for an additional 19.0%, together explaining 88.7% of the variation in the model. Note that most studies differentiate source water contributions along a vertical gradient within the soil profile (i.e., principal component axis one) (e.g., Christopherson and Hooper 1992; Wellington and Driscoll 1994), whereas few separate sources among geographically distinct areas (Burns et al. 2001) or consider an elevational gradient of subcatchments (e.g., Johnson et al. 2000; Lawrence and Driscoll 1990; Driscoll et al. 1988). Conceptually, this reflects that subcatchment contributions to total watershed discharge are often approximated using relative watershed area. However, as subcatchments have differing amounts of accumulated snow and differ in their timing and rate of snowmelt along the elevational gradient, it is reasonable to expect that the relative contribution of each subcatchment along an elevational gradient might shift as the snowmelt period proceeds. Moreover, Lawrence and Driscoll (1990) showed that contributions from subcatchments along an elevational gradient differed in chemical composition. Thus, as the proportions of water originating from individual subcatchments vary, corresponding shifts in stream water chemistry will result.

Snowmelt hydrograph separations have also been performed in other watersheds at the HBEF. Hooper and Shoemaker (1986) used stable isotopes of water and dissolved silica to separate old and new water during snowmelt in W3, showing that the discharge was dominated by old water (i.e., water that was present in the watershed prior to snowmelt). Wellington and Driscoll (2004) used a PCA-EMMA to separate sources of stream water during snowmelt in W9 (a north facing conifer-dominated watershed), finding that shallow soil water was a dominant source of

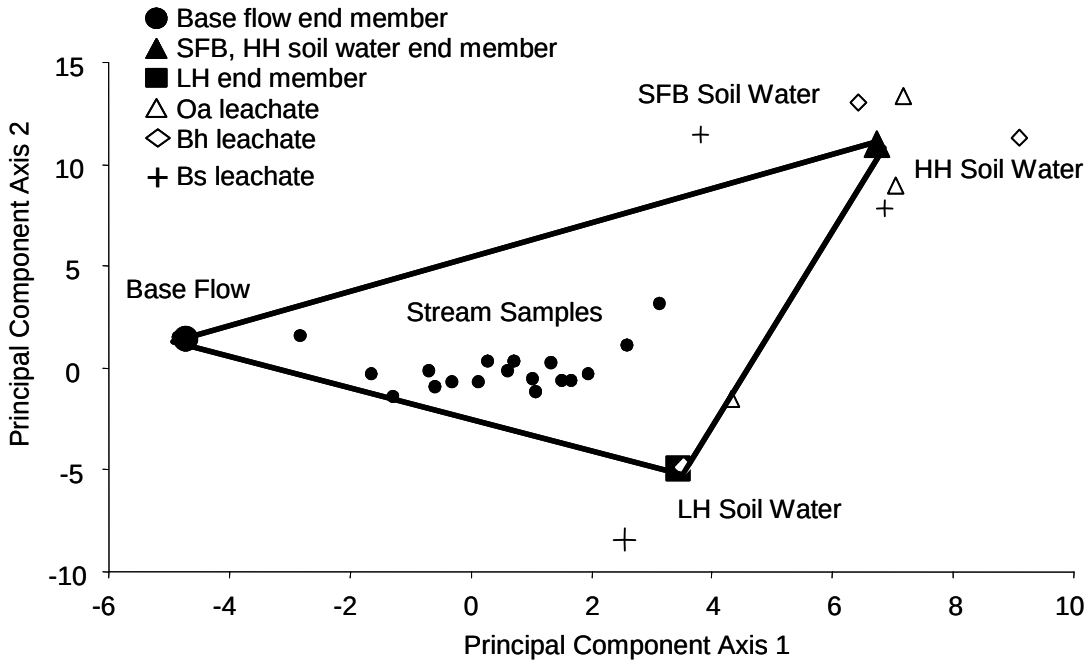

Figure 4.3. Mixing diagram generated with principal components analysis (PCA) showing snowmelt stream water scores bounded by deep soil water and shallow soil water end members. Principal component axis one represents the increasing contribution of shallow soil water as opposed to deep soil water (as represented by base flow); principal component axis two represents soil water contributions from different subcatchments along an elevational gradient within the watershed.

stream water during high flows. Neither of these previous studies at Hubbard Brook attempted to distinguish geographically distinct source areas within the watershed.

In this study, the PCA-EMMA showed that three distinct soil water end members bounded the chemical composition of stream water (Figure 4.3). The deep soil water end member was represented by pre-event stream base flow. Shallow soil water end members were represented by soil solution from lysimeters in subcatchments along an elevational gradient (Figure 4.1). The first shallow soil water end member was represented by the average soil water chemistry from the O_a, B_h, and B_s horizons in the LH subcatchment. Soil solution chemistry from the HH and SFB subcatchments clustered together during PCA, and thus their average solution chemistry was used for the second shallow soil water end member.

According to the PCA-EMMA model, the contribution of shallow soil water to total stream discharge ranged from 21% at the onset of snowmelt (10.9 L/s) to 78% at the sampled peaks in discharge (93.4 L/s, Figure 4.2). An analysis of the elevational component revealed that the contribution of shallow soil water from the HH and SFB subcatchments was more dynamic and occurred later during the snowmelt period (as snowmelt was delayed at elevation), contributing 29% and 42% of stream discharge during the two largest flows measured (Figure 4.2).

The EMMA model was a reasonably good predictor of stream solute chemistry. Solute chemistry predicted by the model was fairly well correlated with measured stream chemistry ($r = 0.90$, 0.81, 0.92, 0.85, 0.96, and 0.93 for F^-, SO_4^{2-}, Al_o, Na^+, Mg^{2+} and Ca^{2+}, respectively); however, the slope of the relationship between predicted and measured values varied (0.69, 1.69, 0.85, 2.78, 1.00, and 0.98 for F^-, SO_4^{2-}, Al_o, Na^+, Mg^{2+} and Ca^{2+}, respectively). The slope was closer to unity for Ca and Mg, solutes that were most associated with the first principal component and were expected to behave most conservatively.

Modeled soil water contributions also agreed qualitatively with the observed patterns in soil lysimeter and stream water chemistry not explicitly included in the model. Nitrate is known to peak during snowmelt (as it does in this study), and Campbell et al. (2006) used dual isotope analysis to demonstrate that this nitrate originates from shallow soils and has been processed prior to entry into the stream (i.e., nitrate is not directly contributed from meltwater). Dittman et al. (2007) also showed that shallow flow short-circuits deeper flow paths at higher elevations during high flow in this watershed. Moreover, soil solutions collected from lysimeters during the snowmelt period represent sources of nitrate and DOC that are available for export through shallow flow paths during high flow events, and nitrate and DOC concentrations in these soil solutions during snowmelt were high enough to contribute to peak concentrations observed in stream water (Table 4.2, 4.3, 4.4). Overall, modeled flow paths demonstrate a spatially and temporally dynamic connectivity between terrestrial and stream ecosystems.

Episodic acidification

Decreases in ANC and pH. Acid neutralizing capacity (ANC) and pH were lowest during episodes of high stream discharge, with the greatest depression in ANC during discharge peaks at the onset of snowmelt (Figure 4.4). The pH decreased to 4.85 from a baseflow pH of 5.25 during each of the two highest flow events (Figure 4.4). ANC decreased by 7.9 μeq/L during the initial high flow event (3 April, DOY 94) and 5.9 μeq/L during the latter high flow event (24 April, DOY 115; Table 2) to a minimum value of -1.6 μeq/L (Figure 4.4). These results are in agreement with previous studies of episodic acidification during snowmelt, which have shown that the largest pulses of acidification occur during the first flush of water from shallow soils

Table 4.2. Total concentration of components (μeq/L) during pre-snowmelt base flow, at two peak flows during snowmelt, and at post-snowmelt base flow. The pre-snowmelt base flow reference sample was taken 24 March 2005; the first and second peak flow events were sampled on 3 April and 24 April 2005; post-snowmelt base flow was sampled 7 May 2005. Change in concentration of components (μeq/L) from pre-snowmelt base flow conditions are shown in parentheses (i.e, Δ values).

Component	Pre-Snowmelt Base Flow (24 March)	Snowmelt 1st Peak Flow (3 April)	Snowmelt 2nd Peak Flow (24 April)	Post-Snowmelt Base Flow (7 May)
ANCgran	6.2	-1.6 (-7.9)	0.3 (-5.9)	2.5 (-3.8)
C_{ALK}	-7.3	-24.5 (-17.2)	-19.1 (-11.8)	-15.3 (-7.9)
Cations	101.2	101.3 (-0.1)	95.6 (-5.7)	94.8 (-6.5)
C_B	93.1	65.5 (-27.5)	62.2 (-30.9)	74.1 (-19.0)
nMen+	2.5	21.8 (19.3)	18.7 (16.2)	11.0 (8.5)
Inorg Anions	103.2	91.2 (-12.0)	82.1 (-21.0)	90.7 (-12.4)
C_A	100.4	90.1 (-10.3)	81.3 (-19.2)	89.4 (-11.0)
A^-	-1.9	10.2 (12.1)	13.4 (15.4)	4.1 (6.0)
HCO_3^-	2.7	1.1 (-1.7)	0.9 (-1.9)	1.3 (-1.4)
F^-	1.4	1.6 (0.2)	1.4 (0.0)	1.7 (0.2)
Cl^-	11.0	11.4 (0.5)	10.7 (-0.3)	10.9 (-0.1)
NO_3^-	2.0	15.2 (13.2)	6.0 (4.0)	0.3 (-1.7)
SO_4^{2-}	86.0	61.8 (-24.2)	63.1 (-22.9)	76.6 (-9.5)
Mn^{2+}	0.2	2.8 (2.6)	2.1 (1.9)	0.7 (0.5)
Fe^{n+}	0.0	0.1 (0.1)	0.2 (0.2)	0.1 (0.1)
Al_i^{n+}	2.2	18.8 (16.6)	16.4 (14.2)	9.7 (7.4)
H^+	5.7	14.0 (8.4)	14.7 (9.0)	9.7 (4.0)
NH_4^+	0.3	0.2 (-0.1)	0.7 (0.4)	0.5 (0.2)
K^+	3.9	9.5 (5.6)	8.0 (4.1)	4.8 (1.0)
Na^+	41.9	23.8 (-18.1)	22.9 (-19.0)	33.5 (-8.4)
Mg^{2+}	23.0	13.7 (-9.3)	12.6 (-10.4)	15.1 (-7.9)
Ca^{2+}	24.0	18.4 (-5.6)	18.0 (-6.1)	20.2 (-3.8)

Table 4.3. Soil solution chemistry during snowmelt in subcatchments along an elevational gradient in W6, the reference watershed at the HBEF. Samples were collected 28 April 2005. The spruce-fir-birch, high hardwood, and low hardwood subcatchments are represented by two, one, and three lysimeter pits, respectively; as complete data required to make organic acid anion calculations were missing from some lysimeter pits. Values in parentheses show one SE.

Site/Horizon	pH	ANC ueq/L	Al(m) umol/L	Al(i) umol/L	Al(o) umol/L	Al(i)/Al(m)	SO_4^{2-} umol/L	NO_3^- umol/L	DOC umol/L	$[A^-]$ ueq/L	As ueq/L	Aw ueq/L	Aw /$[A^-]$	$[A^-]$/DOC (ueq/L)/(umol/L)
Spruce-Fir-Birch														
Oa	4.20 (0.19)	-60.2 (35.2)	16.2 (0.20)	6.3 (0.3)	9.9 (0.2)	0.39	40.4 (3.3)	17.5 (14.8)	999.9 (79.8)	35.1 (2.0)	29.0 (6.9)	6.1 (4.9)	0.18 (0.15)	0.035 (0.001)
Bh	4.22 (0.06)	-54.3 (12.5)	20.4 (1.6)	9.5 (2.2)	10.9 (0.6)	0.47	47.1 (8.5)	33.2 (23.7)	888.6 (130.2)	7.9 (19.7)	9.5 (9.5)	4.3 (4.3)	0.16 (0.16)	0.006 (0.021)
Bs	4.65 (0.07)	-1.1 (7.1)	18.2 (2.1)	9.2 (3.4)	9.0 (1.3)	0.51	41.7 (0.6)	1.4 (1.2)	662.2 (157.4)	56.4 (37.1)	42.1 (38.6)	14.3 (1.5)	0.48 (0.34)	0.104 (0.081)
High Hardwood														
Oa	4.46	-24.8	20.5	14.1	6.4	0.69	35.3	10.3	435.4	14.2	7.1	7.2	0.51	0.033
Bh	4.34	-38.9	14.9	6.3	8.6	0.42	24.7	2.2	737.0	27.2	22.1	5.1	0.19	0.037
Bs	4.79	-2.7	19.0	14.9	4.1	0.78	33.6	0.2	277.2	-0.9	~	~	~	-0.003
Low Hardwood														
Oa	4.69 (0.07)	-12.8 (4.7)	10.9 (1.2)	7.1 (0.6)	3.8 (0.9)	0.65	33.8 (0.9)	6.7 (0.7)	288.2 (55.8)	9.8 (2.5)	4.6 (1.4)	5.2 (3.0)	0.42 (0.24)	0.033 (0.006)
Bh	4.85 (0.03)	-2.6 (1.4)	10.7 (0.1)	7.9 (0.2)	2.8 (0.04)	0.73	36.3 (2.3)	1.6 (0.2)	213.3 (11.2)	4.0 (0.1)	0.37 (0.37)	3.6 (0.2)	0.91 (0.10)	0.019 (0.002)
Bs	4.95 (0.06)	2.5 (2.3)	9.9 (1.4)	7.7 (1.4)	2.2 (0.1)	0.78	37.1 (2.8)	3.8 (1.3)	182.5 (4.4)	1.0 (4.2)	0	1.0 (4.2)	1.0	0.005 (0.024)

Table 4.4. Stream chemistry along an elevational gradient in W6, the reference watershed at the HBEF. Samples were collected 28 April 2005. Stream site locations are shown in Figure 1.

Stream Site #	pH	ANC ueq/L	Al(m) umol/L	Al(i) umol/L	Al(o) umol/L	Al(i)/Al(m)	SO_4^{2-} umol/L	NO_3^- umol/L	DOC umol/L	$[A^-]$ ueq/L	As ueq/L	Aw ueq/L	Aw /$[A^-]$	$[A^-]$/DOC (ueq/L)/(umol/L)
1	4.15	-61.6	9.2	1.6	7.5	0.17	25.3	0.4	1356.4	64.2	56.3	7.9	0.1	0.047
2	4.32	-40.7	10.7	3.6	7.1	0.34	29.3	4.9	803.3	23.4	16.2	7.2	0.3	0.029
3	4.49	-24.5	12.5	7.0	5.5	0.56	33.0	7.0	474.7	12.4	5.0	7.4	0.6	0.026
4	4.64	-17.7	12.5	9.0	3.6	0.72	35.8	5.1	286.8	4.4	0	4.4	1.0	0.015
5	4.74	-13.2	10.5	7.5	2.9	0.71	35.9	3.8	244.7	3.9	0	3.9	1.0	0.016
7	4.95	-5.4	7.7	5.5	2.2	0.71	37.4	2.2	197.5	-2.1	~	~	~	-0.01

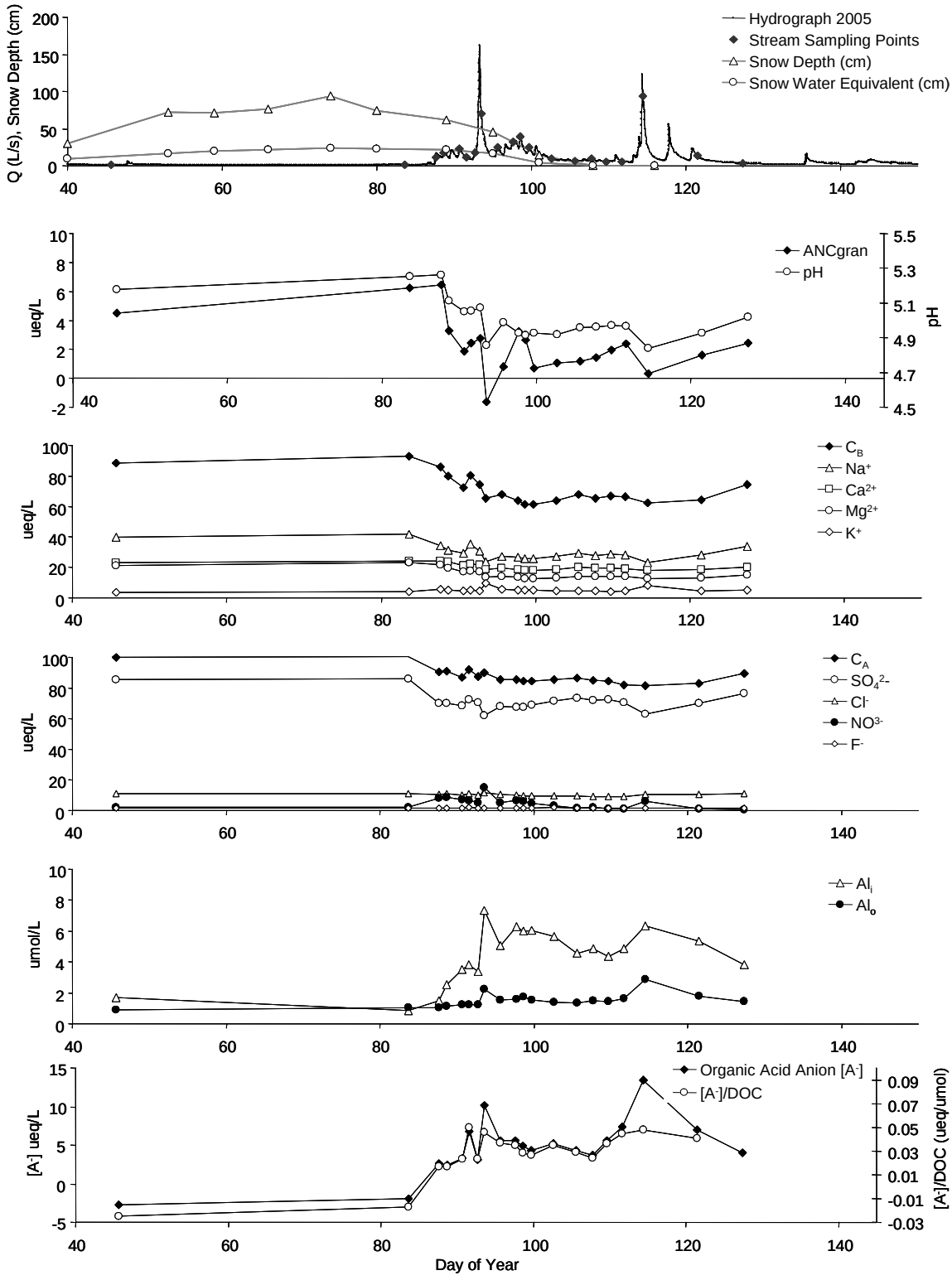

Figure 4.4. Snowpack, discharge, and stream concentrations of major solutes that regulate the acid-base status of W6 during snowmelt at the Hubbard Brook Experimental Forest.

of acid-impacted forested ecosystems (e.g., Wigington et al. 1996, and references therein).

Multiple mechanisms control episodic acidification during spring snowmelt in lakes and streams of the northeastern United States, driven in part by differences in hydrologic flow paths through the watershed (Schafran and Driscoll 1993; Schaefer et al. 1990; Wigington et al. 1996; and supported by data herein). Depression of ANC and pH in moderate/high ANC waters (associated with deep till and deep flow paths) results from meltwater dilution of groundwater-contributed base cations (Schaefer et al. 1990). Depression of ANC and pH in low ANC waters (associated with thin tills and shallow flow paths) coincide with pulses of nitrate, aluminum, and associated acidity from the forest floor to the stream during snowmelt (Schaefer et al. 1990). Sulfate acidity is more important to chronic baseline acidification and non-snowmelt driven acid episodes (Wigington et al. 1996). In lakes with ANC near 0 μeq/L (like HBEF stream water), Schaefer et al. (1990) showed that both C_B dilution and contributions of nitrate, aluminum, and associated acidity are important drivers of episodic acidification.

In this study, decreases in base cation concentrations in excess of decreases in inorganic strong acid anion concentrations were, in part, responsible for decreases in ANC (i.e., a C_B dilution mechanism; Figure 4.4). Overall, base cation patterns resulted from decreases in sodium, magnesium, and calcium ($\Delta Na^+ > \Delta Mg^{2+} > \Delta Ca^{2+}$; K^+ increased; Table 4.2). Patterns in total inorganic strong acid anions largely resulted from decreases in sulfate (from 86.0 to 61.8 μeq/L) that were only partially offset by increases in nitrate (from 1.9 to 15.2 μeq/L) (i.e., a nitrate supply mechanism). Note that these peak snowmelt nitrate concentrations (mean = 4.6 μeq/L [SE = 0.8]) are low relative to the historic record of volume weighted average monthly nitrate concentrations measured in W6 during the extended snowmelt period (March, April,

May), a time that is typically characterized by high nitrate pulses (Bernhardt et al. 2005). As predicted by Schaefer et al. (1990) for waters near 0 μeq/L ANC, episodic acidification at the HBEF appears to be under dual control (i.e., both C_B dilution and nitrate supply mechanisms). Base cation dilution remained important throughout the snowmelt period, as small decreases in C_B may represent a large proportion of the ANC in low ANC waters. Nitrate supply was important only in the initial high flow event of snowmelt, as the nitrate:sulfate equivalent ratio increased by an order of magnitude from base flow (~0.02 to 0.25, calculated from data in Table 4.2; Sullivan et al., 1997). This short-term contribution of nitrate is consistent with the initial flushing of mineralization by-products from soil during the early phase of snowmelt (Sebestyen et al., 2008).

Aluminum mobilization. Aluminum usually fluctuates in concert with nitrate during snowmelt driven acid episodes; however, in this study, stream concentrations of aluminum remained elevated after nitrate concentrations declined (Table 4.2). Thus, aluminum made up most of the deficit in positive charge due to dilution of base cation concentrations throughout snowmelt (Figure 4.4). Although aluminum mobilization buffers against decreases in ANC (Driscoll and Postek 1995), a large percentage of free acidity during snowmelt (29-36%), and in baseflow after snowmelt (43%), resulted from hydrolysis of mobile Al_i (the toxic form of aluminum).

Aluminum is mobilized from the forest floor by both strong inorganic and strong organic acids (e.g., David and Driscoll 1984, McDowell 1984, Driscoll et al. 1985, Driscoll and Postek 1995). Both Al_i and Al_m concentrations in soil solutions were equal to or greater than Al_i and Al_m concentrations in stream water (Table 4.3, Table 4.4). As DOC decreased vertically through the soil profile, with elevation down through subcatchments, and downstream during snowmelt, the proportion of Al_m as Al_i increased. At the weir, Al_i accounted for 44.6% of Al_m in pre-event baseflow, and

nearly doubled to 74.6% (SE = 2.0%) throughout the snowmelt period. In contrast, in a high DOC stream at HBEF (W9, a north facing conifer-dominated watershed), increases in Al_m were mainly due to increases in Al_o (Wellington and Driscoll 2004). Nonetheless, our results generally agree with other studies of aluminum speciation during high flow events showing that Al_i increases with decreases in pH (Driscoll et al. 1980, Driscoll et al. 1984, Driscoll and Postek 1995). This pattern suggests that episodic aluminum mobilization in dilute systems may result in high concentrations of Al_i due to limitations of DOC to bind Al_i.

Inorganic monomeric aluminum (Al_i) concentrations exceeded the ~2 μmol/L threshhold known to be toxic to fish when flows were still low at the onset of snowmelt, and Al_i remained elevated throughout the snowmelt period regardless of flow conditions (2.5-7.3 μmol/L, Q = 3.1-93.4 L/s; Figure 4.4; Baker et al. 1996, Van Sickle et al. 1996, MacAvoy and Bulger 1995, Gagen et al. 1994, Baker and Schofield 1982, Driscoll et al. 1980). Whereas decreases in volume weighted average monthly concentrations of Al_i (Palmer and Driscoll 2002), sulfate (Likens et al. 2002), nitrate (Bernhardt et al. 2005), and calculated alkalinity (C_{ALK}, Figure 4.5) exported from W6 during snowmelt over the historic record may be indicative of some recovery from soil acidification, observations of high stream Al_i and nitrate concentrations during snowmelt in this study somewhat contradict the notion of recovery from acidification.

Dissolved organic carbon, organic acid anions, and total suspended solids. Dissolved organic carbon (DOC), and organic acid anion (A^-) concentrations in stream water increased during snowmelt, despite the typically dilute nature of this system. TSS was nearly undetectable, but concentrations increased during the highest flows (4.4 and 17.0 mg/L TSS, at 70.2 and 93.4 L/s discharge, respectively; Figure 4.6). DOC concentrations ranged from 109.7 to 278.9 μmol C/L, and correlated strongly

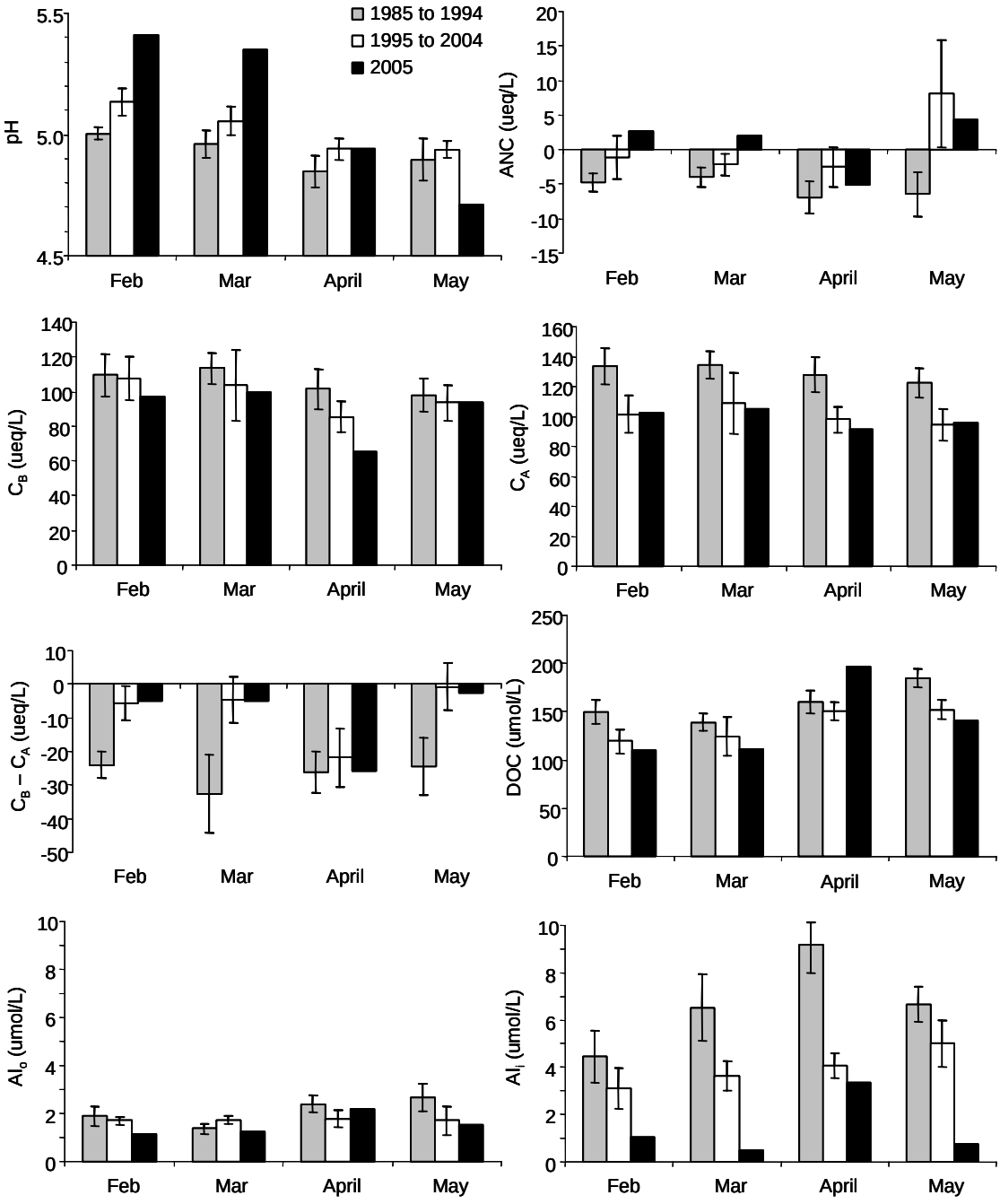

Figure 4.5. Historic record of stream water chemistry during snowmelt months at the weir in W6, the reference watershed at the HBEF. Data are average concentrations from monthly sampling. Error bars indicate +/- 1SE (C.T. Driscoll unpublished data, 1984 - 2005).

Figure 4.6. Snowpack, discharge, and stream concentrations of mercury species, DOC, and organic acid anions during snowmelt inW6 at the Hubbard Brook Experimental Forest.

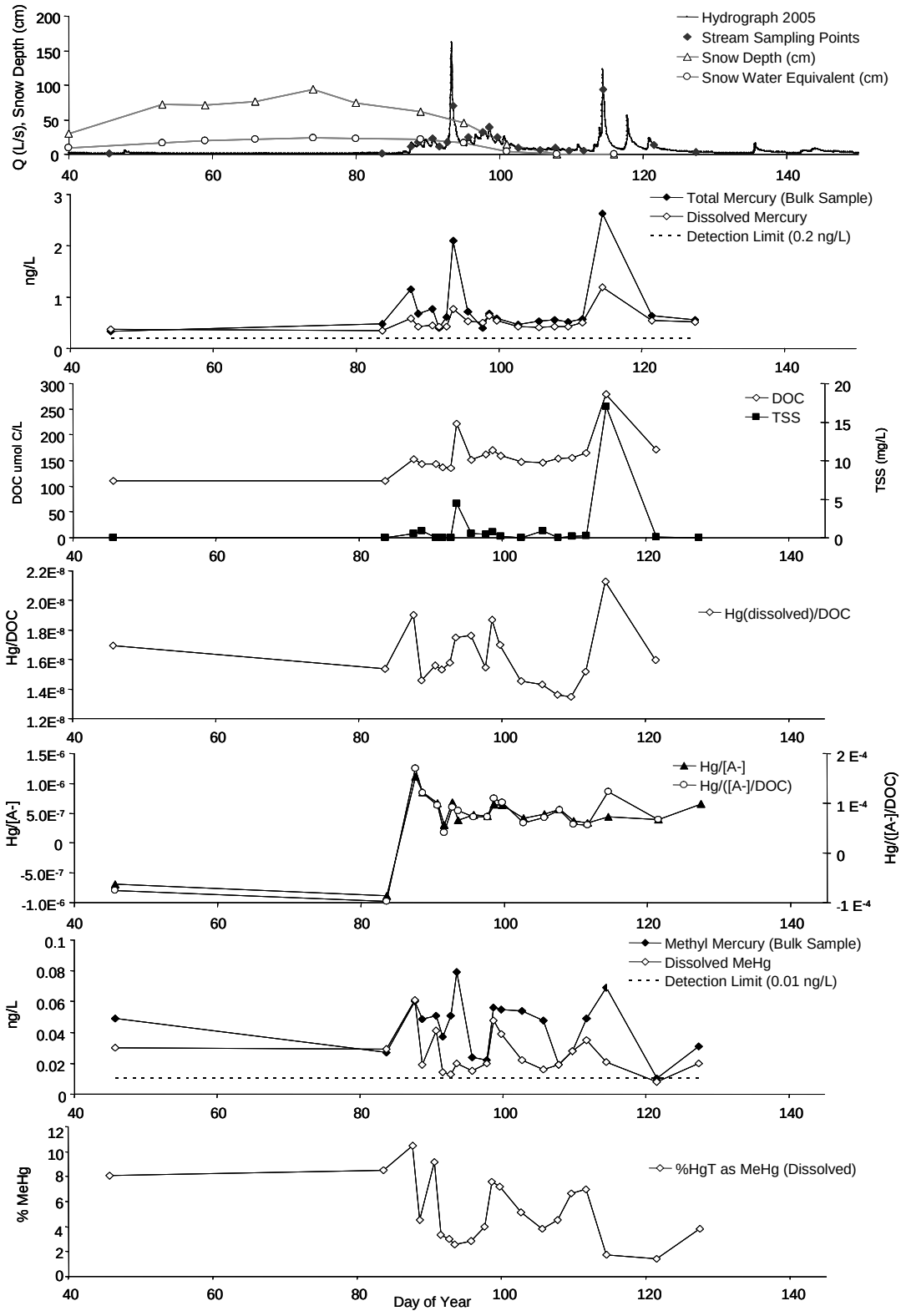
Q (L/s), Snow Depth (cm)
Hydrograph 2005
Stream Sampling Points
Snow Depth (cm)
Snow Water Equivalent (cm)
ng/L
Total Mercury (Bulk Sample)
Dissolved Mercury
Detection Limit (0.2 ng/L)
DOC umol C/L
TSS (mg/L)
DOC
TSS
Hg/DOC
Hg(dissolved)/DOC
Hg/[A-]
Hg/([A-]/DOC)
ng/L
Methyl Mercury (Bulk Sample)
Dissolved MeHg
Detection Limit (0.01 ng/L)
% MeHg
%HgT as MeHg (Dissolved)
Day of Year

with discharge ($r^2 = 0.82$, $p < 0.0001$; Figure 4.6). Not surprisingly, organic acid anion (A^-) concentrations increased with increases in DOC ($r^2 = 0.78$, $p < 0.0001$; Figure 4.4). With respect to acidification processes, organic acid anions were assumed to provide the balancing negative charge (Driscoll et al. 1989, Driscoll et al. 1994); this was reflected by the greater concentration of (A^-) released in the final high flow event (24 April, DOY 115) as the initial flushing of nitrate subsided and Al_i concentrations remained elevated. This pattern may suggest that aluminum was mobilized from within shallow soils by strong organic acids (especially late in snowmelt) in addition to being mobilized by strong inorganic acids (i.e., nitrate) which was more evident during early snowmelt.

All organic acids in stream water draining W6 during snowmelt were weakly acidic (as calculated with equations 4.7-4.9), a result somewhat inconsistent with research on the nature of organic acids in the northeastern United States. For example, Wellington and Driscoll (2004) found that most organic acids in W9 stream water were strongly acidic in nature (W9 is a north facing conifer-dominated watershed). In an Adirondack lake survey, Driscoll et al. (1994) found about one third of organic acids to be strongly acidic. Munson and Gherini (1993) showed that organic acidscontain a range of acidic functional groups (many of which display weak acid characteristics) with a substantial fraction as strong acids (i.e., $pK_a < 3$). Kramer et al. (1990) showed that organic acids at high elevation lakes (>530 m) in the USEPA's Eastern Lakes Study had a predominance of organic acids with low pK_a values, shifting to higher pK_a values (i.e., weaker organic acids) at lower elevations. Kramer et al. (1990) suggest that this shift results, in part, from degradation of low pK_a low molecular weight organic acids, and the production of stable phenolic compounds at lower elevations associated with increasing hydrologic residence times. Kramer et al. (1990) further suggest that the elevation and residence time patterns of DOC

degradation result from differences in flow paths through the watershed. The hypothesis of Kramer et al. (1990) is consistent with observations of organic acids along vertical gradients within the soil profile and along longitudinal stream gradients at Hubbard Brook (note W6 weir elevation at ~540 m). Specifically, the proportion of weak acids (i.e., $[A_w]/[A^-]$) generally increased with increasing soil depth (Table 4.3) and along the longitudinal gradient within the stream (Table 4.4). Thus, organic acids in solutions sampled from shorter more shallow hydrologic flow paths were less processed and more strongly acidic in nature than organic acids in solutions sampled from longer flow paths. Ultimately, the prevalence of weak acids in stream water at the weir suggests that DOC associated with shallow flow paths and strong organic acid anions at the top of the watershed is either diluted or rapidly processed, or both, before being delivered to the weir, even during the snowmelt period.

The charge density of organic acid anions ($[A^-]/[DOC]$, μeq/μmol) increased from -0.025 to 0.050 μeq/μmol (pH 4.8 – 5.3) across the hydrograph in conjunction with higher flows and greater concentrations of DOC. This pattern was likely due to changes in the character of stream DOC from different soil horizons and/or source areas of the watershed that became more hydrologically connected to the stream under high flow conditions (Dittman et al. 2007, Lawrence and Driscoll 1990, Hooper and Shoemaker 1986, see *Hydrograph Separation*).

Multiple mechanisms of episodic acidification. Multiple mechanisms influence episodic acidification across the snowmelt hydrograph in the dilute waters of the reference watershed at the HBEF. Dilution of base cations is important throughout the snowmelt period. Nitrate and aluminum acidity drove ANC to negative values only during the initial high flow event of snowmelt, whereas aluminum acidity persisted throughout the snowmelt event, even after nitrate concentrations declined. Finally, low concentrations of DOC and associated organic acids appeared to play a

key role in acidification processes throughout snowmelt, with the role of [A-] persisting and becoming proportionally more important after nitrate concentrations declined later in the event. These results mostly agree with the results from the Episodic Response Project (Wigington et al. 1996), which concluded that base cation dilution and organic acid production were the most important ion changes during episodic acidification (as based on absolute changes), with nitrate more important in snowmelt driven events and organic acids more important in coniferous and mixed deciduous forests. Thus, given that W6 at the HBEF is a mixed coniferous and deciduous forest with a substantial snowpack, and that stream water ANC is typically near 0 μeq/L, the three mechanisms hypothesized to be important based on these watershed characteristics all did influence acidification during snowmelt. Ultimately, differences in hydrologic source areas and flowpaths within (and among) watersheds are key drivers of differences in mechanisms resulting in episodic acidification.

Episodic mercury mobilization

Shifts in hydrologic source areas and flow paths that influence the source and character of the DOC supply to streams not only drives episodic acidification and aluminum mobilization, but also influences the transport of mercury from forest soils to aquatic ecosystems.

Mercury concentration and flux. Mercury concentrations observed in W6 stream water at the HBEF, even during high flow events, are low compared to concentrations of mercury in stream water from other watershed studies (Shanley et al. 2002, Barbiarz et al.1998, Hurley et al. 1998, Scherbatskoy et al. 1998, Bishop et al. 1995, Krabbenhoft et al. 1995). The low mercury concentrations are not surprising, as W6 has limited wetlands, few seeps, is dominated by upland deciduous forest (~ 85%), and exhibits low concentrations of TSS and DOC. Annual wet deposition of

mercury at the HBEF is ~8.7 μg/m^2-yr (MDN site NH02, available data spanned Feb 2004 through Feb 2005). Hydrologic connectivity between surficial terrestrial soils and the aquatic ecosystem is more spatially and temporally limited in this watershed than in watersheds with a greater percent area of wetlands, thus restricting transfer of dissolved mercury from forests to streams. Moreover, deciduous forests likely deposit less mercury to the forest floor than do conifer forests and deliver more of that mercury with leaf litter rather than in throughfall, which may affect the ultimate fate of mercury in the ecosystem (Demers et al. 2007). Thus, W6 at HBEF is an endmember watershed representing an ecosystem that should export limited mercury to streams and down-gradient aquatic ecosystems.

Average pre-event base flow stream concentrations of mercury were 0.41 ng/L for bulk samples and 0.36 ng/L for the dissolved fraction (<0.45 μm; Figure 4.6). Stream water concentrations of bulk total mercury (Hg_t) increased exponentially with flow (r^2=0.69, p<0.0001), reaching 2.6 ng/L at an instantaneous flow of 93.4 L/s; concentrations of dissolved mercury (Hg_d) also increased exponentially with flow to a maximum concentration of 1.2 ng/L (r^2=0.83, p<0.0001; PROC REG, SAS 1999; Figure 4.6). These patterns contrast with snowmelt at Sleepers River Vermont where Shanley et al. (2002) measured order of magnitude higher particulate mercury (Hg_p) concentrations (16 ng/L) and two times higher dissolved mercury concentrations (2 ng/L) compared to W6 at the HBEF. High flow conditions result in a range of responses in mercury export from wetland and forest ecosystems.

The exponential relationship between mercury concentration and discharge implies that a disproportionate amount of mercury export occurs during high flow events. The total amount of mercury exported from W6 during the snowmelt period (24 March – 7 May, 2005) was 59.8 mg. Estimated mercury fluxes from the two largest snowmelt peaks were 24.2 mg (DOY 92.3-95.4) and 13.3 mg (DOY 113.6-

117.2), respectively. Thus, nearly two-thirds (63%) of the mercury export from the entire snowmelt period occurred during two high discharge events that represented only a third of total discharge and 15% of total duration of the snowmelt.

Transport of mercury associated with both the dissolved and particulate fractions substantially contributed to mercury export during snowmelt. However, the dissolved fraction was more important during high flows at the HBEF than observed in Vermont for high flow events in forested ecosystems (e.g., Shanley et al. 2002, Scherbatskoy et al. 1998), with the particulate fraction dominating only at the highest flows (Figure 4.6). Across the entire snowmelt hydrograph, the percentage of Hg_t concentration accounted for by the dissolved fraction ranged from 37 to 100% of Hg_t concentrations (mean 77.5%, SE 5.8, n = 20). Dissolved mercury (Hg_d) accounted for 37% and 46% of Hg_t flux during the two highest snowmelt peaks, and was 53% of the total mercury flux during the entire snowmelt period. These fractions of Hg_d were large in comparison to the partitioning of mercury at peak snowmelt in Vermont (only 12.5% Hg_d, as calculated from data in Shanley et al. 2002). Moreover, mercury transported in the dissolved phase may be more bioavailable for methylation in downstream aquatic ecosystems than mercury associated with particulate matter (Munthe et al. 2007). Thus, both the particulate and dissolved phases of mercury are important contributions to Hg_t export during snowmelt at the HBEF.

Methyl mercury concentration and flux. In contrast with Hg_t, discharge explained only a moderate amount of the variability in particulate associated MeHg ($MeHg_p$; $r^2 = 0.34$, $p = 0.008$), and was not related to the variation in dissolved MeHg ($MeHg_d$) ($p = 0.81$; PROC REG, SAS 1999). Methyl mercury concentrations ranged from 0.01 to 0.08 ng/L in bulk samples (mean 0.04 ng/L, SE 0.007 ng/L, n = 20) and from <0.01 to 0.06 ng/L in the dissolved phase (mean 0.03 ng/L, SE 0.002 ng/L, n = 20); $MeHg_d$ accounted for 25 – 100% of the MeHg in bulk samples (Figure 4.6). The

percentage of Hg_t as MeHg was large, ranging from 1.6 – 14.5% in bulk samples and from 1.4 – 10.4% in filtered samples. Note that the %MeHg values are based on low MeHg and Hg_t concentrations, and should be interpreted with caution. Nonetheless, the percentage of Hg_d as MeHg (i.e., %MeHg) across the hydrograph revealed an intriguing pattern; the %MeHg peaked just after the first small snowmelt peak on the hydrograph (10.4% MeHg; 10.9 L/s; Figure 4.6). Proceeding from this first flush, and as discharge continued to increase, the %MeHg declined (Figure 4.6). Subsequent peaks in %MeHg tended to occur on rising limbs of the hydrograph, possibly as different hydrologic source areas in the watershed began to contribute shallow soil water to stream flow. This pattern may suggest that MeHg is produced within forest soils under winter conditions and that MeHg pools in soil solutions are diluted as flushing exceeds production. Alternate explanations for the observed patterns are possible (e.g., demethylation dynamics, or a spike in methylation at snowmelt); however, it is difficult to evaluate the mechanism responsible for these patterns without mercury data from within the forest soil pools.

Mercury, TSS, DOC, and organic acid anion charge density. Despite relatively low concentrations, DOC and TSS appear to influence mercury dynamics at the HBEF. Dissolved mercury (Hg_d) was more strongly correlated with DOC (r^2 = 0.91, $p<0.0001$) than particulate mercury (Hg_p) was with TSS ($r^2 = 0.40$, $p<0.01$; PROC REG, SAS 1999). As mercury has been shown to correlate with organic carbon (e.g., Meili, 1991), it is not surprising that peaks in Hg_p and Hg_d coincided with peaks in TSS and DOC, respectively (Figure 4.6). However, the quantity of mercury transported by DOC on a per mol basis (Hg_d/DOC) varied by more than 50% over the hydrograph (1.3×10^{-8} to 2.1×10^{-8}), and the ratio of Hg_d to organic acid anion charge density ($Hg_d/([A^-]/DOC)$) followed a similar pattern, varying by more than 300% across the hydrograph (Figure 4.6). Thus, increases in mercury transport may not

simply be due to increases in DOC concentration alone, but may also be influenced by the source and associated character of the DOC.

Statistical models that distinguish between hydrologic source areas within the watershed help explain fluctuations in (Hg_d/DOC), [Hg_d/([A^-]/DOC)], and Hg_d. Mercury transported per unit DOC on a per mol basis (Hg_d/DOC) was correlated with total discharge alone ($r^2 = 0.50$, $p<0.001$); however, when the discharge originating from specific hydrologic source areas was considered, the amount of discharge from shallow soils of the HH/SFB explained as much of the variation in (Hg_d/DOC) as did total discharge ($r^2 = 0.50$, $p<0.001$; PROC REG, SAS 1999). Also, mercury per unit charge density [Hg_d/([A^-]/DOC)] was not well correlated with total discharge alone ($r^2 = 0.17$, $p = 0.08$); whereas, a statistical model including total discharge and the percentage of total discharge originating from shallow soils in the LH and HH/SFB explained much more of the variation in Hg_d/([A^-]/DOC) ($r^2 = 0.86$, $p < 0.0001$; PROC REG, SAS 1999). Moreover, stream water Hg_d was also better explained by a model that distinguished between hydrologic source areas within the watershed; i.e., all of the variability in the spatially explicit model could be explained by the amount of discharge originating from shallow soils in the HH/SFB zone ($r^2 = 0.92$, $p < 0.0001$; PROC REG, SAS 1999). Thus, these discrete shifts in mercury density on DOC suggest the influence of DOC that varies both in character and contributing source area within the watershed.

Observed changes in the character of DOC corroborate changes in the hydrologic flow paths predicted by our hydrograph separation model. Soil solutions within the hardwood subcatchments show greater DOC concentrations, greater [A^-], and greater ([A-]/DOC) in more shallow soils (i.e., Oa and Bh horizons) than in lower mineral horizons (i.e., Bs horizon; Table 4.3). Soil solutions within the SFB subcatchment lack a distinct pattern along the soil depth profile; however, shallow soil

solutions in the HH and SFB zone have greater DOC and [A-] concentrations than soil solutions in corresponding horizons in the LH zone (Table 4.3). Along an elevational gradient within the stream, DOC concentrations, [A^-], and ([A-]/DOC) are greatest in the SFB zone at the top of the watershed, and decrease downstream (Table 4.4). This elevational pattern within the stream may, in part, be due to dilution effects or in-stream abiotic sorption of DOC, or both (McDowell, 1985). Whereas McDowell (1985) found biotic processing of DOC to be minimal in the stream draining W6, recent work in other regions suggest that DOC character may be microbially altered within the stream ecosystem (e.g. Frost et al. 2006; Young et al. 2004). Nevertheless, changes in DOC character across the hydrograph coincide with shifts in source areas and flow paths modeled by our hydrograph separation. Hydrologically induced changes in DOC character also have been demonstrated in other studies. In a small watershed associated with a fen wetland, Maurice et al. (2002) found that the contribution of soil pore water relative to groundwater influenced both the concentration and character of natural organic matter in streams. In the Colorado Rockies, Hood et al. (2005) showed that seasonal shifts in the chemical character of DOM resulted from changes in the source of that DOM. Dai et al. (2001) studied organic matter chemistry at the HBEF and concluded that variation in hydrologic flow paths are important in regulating the organic matter chemistry of stream water. Hence, increased mercury transport during high flow events is not simply due to an increase in the concentration of the same DOC that is exported at base flow, but instead there appears to be a shift in the source area and associated character of DOC (as inferred above from Hg:DOC ratios). Shanley et al. (2008) showed that the Hg:DOC ratio in stream water increased as snowmelt progressed at Sleepers River in Vermont and suggested that Hg was associated with a particular fraction of DOC. Clearly, the character and contributing source of DOC influences the transport of dissolved

mercury at Hubbard Brook and likely in other forested watersheds. Ultimately, differences in hydrology within (and among) watersheds determines contributing source areas and hydrologic flow paths that influence the concentration and character of DOC (and POC) which, in turn, drives concentrations and fluxes of dissolved (and particulate) mercury transported from terrestrial to aquatic ecosystems.

CONCLUSIONS AND IMPLICATIONS

DOC plays a key role in episodic acidification and mercury transport during snowmelt at the HBEF, even though DOC concentrations are relatively low. The supply of DOC that links episodic acidification by natural organic acids and mobilization of dissolved mercury is governed by shifts in hydrologic flow paths and contributing source areas. This research highlights the importance of spatially and temporally dynamic hydrologic connectivity between the uplands and the aquatic ecosystem, and this dynamic hydrologic connectivity influences how researchers should: (1) assess stream solute loads given the discharge dependent chemistry; and (2) consider the environmental consequences of the timing and distribution of the delivery of those loads to surface waters (e.g., pulses of toxic concentrations of labile (inorganic) monomeric aluminum and elevated loads of total mercury). Ultimately, terrestrial ecosystems mediate the transfer of atmospheric deposition from uplands to aquatic ecosystems, imposing lags upon the recovery of surface waters despite decreases in atmospheric emissions and deposition of pollutants.

Note that for this end member site representing: (1) limited recovery from acidification; (2) low concentrations of dissolved organic carbon; and (3) low mercury deposition and export, small increases in DOC export associated with high flows are linked to mercury export from terrestrial ecosystems to surface waters. Thus,

processes that generate and mobilize DOC within the watershed ultimately control mercury export dynamics from terrestrial ecosystems.

Recently, some watersheds in North America and Europe have begun to recover from chronic acid deposition (Stoddard et al. 1999, Skjelkvale et al. 2001, Driscoll et al. 2003). However, the degree of recovery of surface water pH and ANC has been less than expected with respect to measured declines in sulfate emissions and deposition, buffered in part by concomitant increases in DOC (Stoddard et al. 2003, Driscoll et al. 2003, Skjelkvale et al. 2001, 2005). It is possible that there also has been a concomitant increase in mercury export from forest ecosystems (i.e., based on DOC-Hg relationships), and this may be one possible mechanism explaining the long-term decrease in mercury retention within the forest ecosystem (Lorey and Driscoll 1999, Engstrom and Swain 1997, see *Introduction*). Increases in DOC export that might bind and therefore detoxify Al_i may, at the same time, exacerbate mercury mobilization. As ecosystems continue to recover from chronic acidification and respond to broader environmental change, shifting DOC dynamics will likely play an important role in the transfer of both aluminum and mercury loads from uplands to surface waters.

REFERENCES

[APHA] American Public Health Association. 1998. Standard methods for the examination of water and wastewater, 20th edition. American Public Health Association: Washington, D.C., USA.

Babiarz, C. L., J. P. Hurley, J. M. Benoit, M. M. Shafer, A. W. Andren, and D. A. Webb. 1998. Seasonal influences on partitioning and transport of total and methyl mercury in rivers from contrasting watersheds. Biogeochemistry **41**: 237-257.

Bailey, A.S., J.W. Hornbeck, J.L. Campbell, and C. Eager. 2003. Hydrometeorological database for Hubbard Brook Experimental Forest: 1955-2000. Gen. Tech. Rep. NE-305. Newton Square, PA:U.S. Department of Agriculture, Forest Service, Northeastern Research Station.

Baker, J. P., J. VanSickle, C. J. Gagen, D. R. DeWalle, W. E. Sharpe, R. F. Carline, B. P. Baldigo, P. S. Murdoch, D. W. Bath, W. A. Kretser, H. A. Simonin, and P. J. Wigington. 1996. Episodic acidification of small streams in the northeastern United States: Effects on fish populations. Ecological Applications **6**: 422-437.

Baker, J. P., and C. L. Schofield. 1982. Aluminum Toxicity to Fish in Acidic Waters. Water Air & Soil Pollution **18**: 289-309.

Balogh, S. J., E. B. Swain, and Y. H. Nollet. 2006. Elevated methylmercury concentrations and loadings during flooding in Minnesota rivers. Science of the Total Environment **368**:138-148.

Bernhardt, E. S., G. E. Likens, R. O. Hall, D. C. Buso, S. G. Fisher, T. M. Burton, J. L. Meyer, W. H. McDowell, M. S. Mayer, W. B. Bowden, S. E. G. Findlay, K. H. Macneale, R. Stelzer, and W. H. Lowe. 2005. Can't see the forest for the stream? - In-stream processing and terrestrial nitrogen exports. BioScience **55**: 219-230.

Bishop, K., Y. H. Lee, C. Pettersson, and B. Allard. 1995. Methyl mercury Output from the Svartberget Catchment in Northern Sweden During Spring Flood, Water Air & Soil Pollution **80**: 445-454.

Branfireun, B. A., D. Hilbert, and N. T. Roulet. 1998. Sinks and sources of methyl mercury in a boreal catchment, Biogeochemistry **41**: 277-291.

Burns, D. A., J. J. McDonnell, R. P. Hooper, N. E. Peters, J. E. Freer, C. Kendall, and K. Beven. 2001. Quantifying contributions to storm runoff through end-member mixing analysis and hydrologic measurements at the Panola Mountain Research Watershed (Georgia, USA). Hydrological Processes **15**: 1903-1924.

Butler, J. N. 1982. Carbon dioxide equilibria and their applications. Addison-Wesley Publications, Reading, Massachusetts.

Campbell, J. L., M. J. Mitchell, and B. Mayer. 2006. Isotopic assessment of NO_3^- and SO_4^{2-} mobility during winter in two adjacent watersheds in the Adirondack Mountains, New York. Journal of Geophysical Research **111**: G04007.

Chen, C. W., S. A. Gherini, N. E. Peters, P. S. Murdoch, R. M. Newton, and R. A. Goldstein. 1984. Hydrologic analyses of acidic and alkaline lakes. Water Resources Research **20**: 1875-1882.

Christophersen, N., and R. P. Hooper. 1992. Multivariate-analysis of stream water chemical-data - the use of principal components-analysis for the end-member mixing problem. Water Resources Research **28**: 99-107.

Cirmo, C. P., and C. T. Driscoll. 1993. Beaver pond biogeochemistry - acid neutralizing capacity generation in a headwater wetland. Wetlands **13**: 277-292.

Dahlgren, R.A., and C.T. Driscoll. 1994. The effects of whole-tree clear-cutting on soil processes at the Hubbard Brook Experimental Forest, New Hampshire, USA. Plant and Soil **158**: 239-262.

Dai, K.H., C.E. Johnson, and C.T. Driscoll. 2001. Organic matter chemistry and dynamics in clear-cut and unmanaged hardwood forest ecosystems. Biogeochemistry **54**: 51-83.

David, M.B., and C.T. Driscoll. 1984. Aluminum speciation and equilibria in soil solutions of a Haplorthod in the Adirondack Mountains (New York, U.S.A.). Geoderm **33**: 297-318.

Deconinck, F. 1980. Major mechanisms in formation of spodic horizons. Geoderma **24**: 101-128.

Demers, J.D., C.T. Driscoll, J.B. Yavitt, and T.J. Fahey. 2007. Mercury cycling in litter and soil in different forest types in the Adirondack region, New York, USA. Ecological Applications **17**: 1341–1351.

Detty, J. M. 2008. Patterns and Processes of Two States: Watershed Runoff as Determined by a Total Soil Water Threshold. M.S. Thesis, Plymouth State University.

Dittman, J.A., C.T. Driscoll, P.M. Groffman, and T.J. Fahey. 2007. Dynamics of nitrogen and dissolved organic carbon at the Hubbard Brook Experimental Forest. Ecology **88**: 1153-1166.

Drexel, R. T., M. Haitzer, J. N. Ryan, G. R. Aiken, and K. L. Nagy. 2002. Mercury(II) sorption to two Florida Everglades peats: Evidence for strong and weak binding and competition by dissolved organic matter released from the peat. Environmental Science & Technology **36**: 4058-4064.

Driscoll, C. T., J. P. Baker, J. J. Bisogni, and C. L. Schofield. 1980. Effect of aluminum speciation on fish in dilute acidified waters. Nature **284**: 161-164.

Driscoll, C. T. 1984. A procedure for the fractionation of aqueous aluminum in dilute acidic waters. International Journal of Environmental Analytical Chemistry **16**: 267-283.

Driscoll, C. T., J. P. Baker, J. J. Bisogni, and C. L. Schofield. 1984. Aluminum speciation and equilibria in dilute acidified surface waters of the Adirondack Region of New York State, in: Geological Aspects of Acid Deposition, edited by O.P. Bricker, pp. 55-75, Butterworth, Boston.

Driscoll, C.T. and Schafran. 1984. Short term changes in the base-neutralizing capacity of an acid Adirondack lake, New York. Nature **310**: 308-310.

Driscoll, C. T., and R. M. Newton. 1985. Chemical characteristics of Adirondack lakes. Environmental Sceince & Technology **19**: 1018-1024.

Driscoll, C. T., N. vanBreemen, and J. Mulder. 1985. Aluminum chemistry in a forested Spodosol, Soil Science Society of America Journal **49**: 437-444.

Driscoll, C. T., C. P. Yatsko, and F. J. Unangst. 1987. Longitudinal and temporal trends in the water chemistry of the north branch of the Moose River, Biogeochemistry **3**: 37-61.

Driscoll, C.T., R.D. Fuller, and D. M. Simone. 1988. Longitudinal variations in trace metal concentrations in a northern hardwood forested ecosystem. Journal of Environmental Quality **17**: 101-107.

Driscoll, C. T., R. D. Fuller, and W. D. Schecher. 1989. The role of organic-acids in the acidification of surface waters in the Eastern-United-States. Water Air & Soil Pollution **43**: 21-40.

Driscoll, C. T., M. D. Lehtinen, and T. J. Sullivan. 1994. Modeling the acid-base chemistry of organic solutes in Adirondack, New-York lakes. Water Resources Research **30**: 297-306.

Driscoll, C. T., V. Blette, C. Yan, C.L. Schofield, R. Munson, J.Holsapple. 1995. The role of dissolved organic carbon in the chemistry and bioavailability of mercury in remote Adirondack lakes. Water Air & Soil Pollution **80**: 499-508.

Driscoll, C.T. and K.M. Postek. 1995. The chemistry of aluminum in surface waters, in The Environmental Chemistry of Aluminum, edited by G. Sposito, Lewis Publishers, New York.

Driscoll, C. T., G. B. Lawrence, A. J. Bulger, T. J. Butler, C. S. Cronan, C. Eagar, K. F. Lambert, G. E. Likens, J. L. Stoddard, and K. C. Weathers. 2001. Acidic deposition in the northeastern United States: Sources and inputs, ecosystem effects, and management strategies. BioScience **51**: 180-198.

Driscoll, C. T., K. M. Driscoll, K. M. Roy, and M. J. Mitchell. 2003. Chemical response of lakes in the Adirondack region of New York to declines in acidic deposition. Environmental Science & Technology **37**: 2036-2042.

Frost, P.C., J.H. Larson, C.A. Johnston, K.C. Young, P.A. Maurice, G.A. Lamberti, and S. D. Bridgham. 2006. Landscape predictors of stream dissolved organic matter concentration and physicochemistry in a Lake Superior river watershed. Aquatic Science **68**: 40-51.

Engstrom, D. R., and E. B. Swain. 1997. Recent declines in atmospheric mercury deposition in the upper Midwest. Environmental Science & Technology **31**: 960-967.

Gagen, C. J., W. E. Sharpe, and R. F. Carline. 1994. Downstream movement and mortality of brook trout (*Salvelinus fontinalis*) exposed to acidic episodes in streams. Canadian Journal of Fisheries and Aquatic Sciences **51**: 1620-1628.

Gran, G. 1952. Determination of the equivalence point in potentiometric titrations. Analyst **77**: 661-671.

Grigal D.F. 2002. Inputs and outputs of mercury from terrestrial watersheds: a review. Environment Review **10**: 1-39.

Grigal, D. F. 2003. Mercury sequestration in forests and peatlands: A review. Journal of Environmental Quality **32**: 393-405.

Hood, E., M.W. Williams, and D.M. Mcknight. 2005. Sources of dissolved organic matter (DOM) in a Rocky Mountain stream using chemical fractionation and stable isotopes. Biogeochemistry **74**: 231-255.

Hooper, R. P., and C. A. Shoemaker. 1986. A comparison of chemical and isotopic hydrograph separation. Water Resources Research **22**: 1444-1454.

Hurley, J. P., J. M. Benoit, C. L. Babiarz, M. M. Shafer, A. W. Andren, J. R. Sullivan, R. Hammond, and D. A. Webb. 1995. Influences of watershed characteristics on mercury levels in Wisconsin rivers. Environmental Science & Technology **29**: 1867-1875.

Hurley, J. P., S. E. Cowell, M. M. Shafer, and P. E. Hughes. 1998. Tributary loading of mercury to Lake Michigan: Importance of seasonal events and phase partitioning. Science of the Total Environment **213**: 129-137.

Johnson, C.E., Driscoll, C.T., Siccama, T.G., and Likens, G.E. 2000. Element fluxes and landscape position in a northern hardwood forest watershed ecosystem. Ecosystems **3**: 159-184.

Johnson, N. M., C. T. Driscoll, J. S. Eaton, G. E. Likens, and W. H. McDowell. 1981. Acid-rain, dissolved aluminum and chemical-weathering at the Hubbard Brook Experimental Forest, New Hampshire. Geochimica Cosmochimica Acta **45**: 1421-1437.

Kamman, N.C., and D.R. Engstrom. 2002. Historical and present fluxes of mercury to Vermont and New Hampshire lakes inferred from 210Pb dated sediment cores, Atmospheric Environment **36**: 1599-1609.

Khwaja, A. R., P. R. Bloom, and P. L. Brezonik. 2006. Binding constants of divalent mercury (Hg^{2+}) in soil humic acids and soil organic matter. Environmental Science & Technology **40**: 844-849.

Kolka, R. K., D. F. Grigal, E. A. Nater, and E. S. Verry. 2001. Hydrologic cycling of mercury and organic carbon in a forested upland-bog watershed. Soil Science Society of America Journal **65**: 897-905.

Krabbenhoft, D. P., J. M. Benoit, C. L. Babiarz, J. P. Hurley, and A. W. Andren. 1995. Mercury cycling in the Allequash Creek watershed, northern Wisconsin. Water Air & Soil Pollution **80**: 425-433.

Kramer, J. R. 1982. Alkalinity and acidity, in Water Analysis, Volume 1 Inorganic Species, Part 1, edited by R. A. Minear and L. H. Keith, Academic Press, Orlando, Florida.

Kramer, J. R. 1984. Modified Gran analysis for acid base titrations. Environmental Geochemistry Report No. 1984-2, McMaster University, Hamilton, Ontario, Canada.

Kramer, J.R., P. Broussard, P. Collins, T.A. Clair, P Takats. 1990. Variability of organic acids in watersheds, in Organic acids in aquatic ecosystems, edited by E.M. Purdue and E.T. Gjessing, pp. 127-139, John Wiley, New York.

Lawrence, G. B., and C. T. Driscoll. 1990. Longitudinal patterns of concentration discharge relationships in stream water draining the Hubbard Brook Experimental Forest, New Hampshire. Journal of Hydrology **116**: 147-165.

Likens, G. E., C. T. Driscoll, D. C. Buso, M. J. Mitchell, G. M. Lovett, S. W. Bailey, T. G. Siccama, W. A. Reiners, and C. Alewell. 2002. The biogeochemistry of sulfur at Hubbard Brook. Biogeochemistry **60**: 235-316.

Likens G.E., and F.H. Bormann. 1995. Biogeochemistry of a forested ecosystem 2nd ed. New York: Springer Verlag.

Lorey, P., and C. T. Driscoll. 1999. Historical trends of mercury deposition in Adirondack lakes. Environmental Science & Technology **33**: 718-722.

Lovett, G. M., S. S. Nolan, C. T. Driscoll, and T. J. Fahey. 1996. Factors regulating throughfall flux in a New Hampshire forested landscape. Canadian Journal of Forest Research **26**: 2134-2144.

MacAvoy, S. E., and A. J. Bulger. 1995. Survival of brook trout (*Salvelinus fontinalis*) embryos and fry in streams of different acid sensitivity in Shenandoah National Park, USA. Water Air & Soil Pollution **85**: 445-450.

Maurice, P.A., S.E. Cabaniss, J. Drummond, and E. Ito. 2002. Hydrogeochemical controls on the variations in chemical characteristics of natural organic matter at a small freshwater wetland. Chemical Geology **187**: 59-77.

McCune, B. and J. B. Grace. 2002. Analysis of Ecological Communities, MjM Software, Gleneden Beach, Oregon, USA.

Mcavoy, D. C., R. C. Santore, J. D. Shosa, and C. T. Driscoll. 1992. Comparison between pyrocatechol violet and 8-hydroxyquinoline procedures for determining aluminum fractions. Soil Science Society of America Journal **56**: 449-455.

McDowell, W. H. 1985. Kinetics and mechanisms of dissolved organic carbon retention in a headwater stream. Biogeochemistry **1**: 329-352.

McDowell, W. H., and T. Wood. 1984. Podzolization - Soil processes control dissolved organic carbon concentrations in stream water. Soil Science **137**: 23-32.

Meili, M. 1991. The coupling of mercury and organic matter in the biogeochemical cycle - Towards a mechanistic model for the boreal forest zone. Water Air & Soil Pollution **56**: 333-347.

Miller, E.K., A. Vanarsdale, G.J. Keeler, A. Chalmers, L. Poissant, N.C. Kamman, and R. Brullotte. 2005. Estimation and mapping of wet and dry mercury deposition across northeastern North America. Ecotoxicology **14**: 53-70.

Munson, R. K., and S. A. Gherini. 1993. Influence of organic acids on the pH and acid neutralizing capacity of Adirondack lakes. Water Resources Research **29**: 891-899.

Munthe, J., R.A. Bodaly, B.A. Branfireun, C.T. Driscoll, C.C. Gilmour, R. Harris, M. Horvat, M. Lucotte, and O. Malm. 2007. Recovery of mercury-contaminated fisheries. Ambio **36**: 33-44.

Newton, R. M., J. Weintraub, and R. April. 1987. The relationship between surface water chemistry and geology in the north branch of the Moose river. Biogeochemistry **3**: 21-35.

Palmer, S. M., C. T. Driscoll, and C. E. Johnson. 2004. Long-term trends in soil solution and stream water chemistry at the Hubbard Brook Experimental Forest: relationship with landscape position. Biogeochemistry **68**: 51-70.

Palmer, S. M., and C. T. Driscoll. 2002. Acidic deposition - Decline in mobilization of toxic aluminium. Nature **417**: 242-243.

Pierce, R.S. 1967. Evidence of overland flow on forested watersheds, in: International Symposium of Forest Hydrology, edited by W.E. Sopper and H.W. Lull, pp. 247-253, Pergamon, Elmsford, New York.

Rea, A.W., S.E. Lindberg, T. Scherbatskoy, and G.J. Keeler. 2002. Mercury accumulation in foliage over time in two northern mixed-hardwood forests. Water Air & Soil Pollution **133**: 49-67.

SAS Institute Inc. 1999. SAS OnlineDoc. Version 8, Cary, North Carolina, USA.

Schafran, G. C., and C. T. Driscoll. 1993. Flow path composition relationships for groundwater entering an acidic lake. Water Resources Research **29**: 145-154.

Schaefer, D. A., C. T. Driscoll, R. Vandreason, and C. P. Yatsko. 1990. The episodic acidification of Adirondack lakes during snowmelt. Water Resources Research **26**: 1639-1647.

Scherbatskoy, T., J. B. Shanley, and G. J. Keeler. 1998. Factors controlling mercury transport in an upland forested catchment. Water Air & Soil Pollution **105**: 427-438.

Schuster, P.F., Shanley, J.B., Reddy, M.M., Aiken, G.R., Marvin-DiPasquale, M., Roth, D.A., Taylor, H.E., Krabbenhoft, D.P., Dewild, J.F. 2008. Mercury and organic carbon dynamics during runoff episodes from a northeastern USA watershed. Water Air & Soil Pollution **187**: 89-108.

Sebestyen, S. D., E. W. Boyer, J. B. Shanley, C. Kendall, D. H. Doctor, G. R. Aiken, and N. Ohte. 2008. Sources, transformations, and hydrological processes that control stream nitrate and dissolved organic matter concentrations during snowmelt in an upland forest. Water Resources Research **44**:1-14.

Shanley, J.B., P.F. Schuster, M.M. Reddy, D.A. Roth, H.E.Taylor, and G.R. Aiken. 2002. Mercury on the move during snowmelt in Vermont. Eos Transactions of the American Geophysical Union **83**: 45-8.

Shanley, J. B., N. C. Kamman, T. A. Clair, and A. Chalmers. 2005. Physical controls on total and methylmercury concentrations in streams and lakes of the northeastern USA. Ecotoxicology **14**: 125-134.

Shanley, J.B., M.A. Mast, D.H. Campbell, G.R. Aiken, D.P. Krabbenhoft, R.J. Hunt, J.F. Walker, P.F. Schuster, A. Chalmers, B.T. Aulenbach, N.E. Peters, M. Marvin-DiPasquale, D.W. Clow, and M.M. Shafer. 2008. Comparison of total mercury and methylmercury cycling at five sites using the small watershed approach. Environmental Pollution **154**: 143-154.

Skjelkvale, B. L., J. L. Stoddard, and T. Andersen. 2001. Trends in surface water acidification in Europe and North America (1989-1998). Water Air & Soil Pollution **130**: 787-792.

Skjelkvale, B. L., J. L. Stoddard, D. S. Jeffries, K. Torseth, T. Hogasen, J. Bowman, J. Mannio, D. T. Monteith, R. Mosello, M. Rogora, D. Rzychon, J. Vesely, J. Wieting, A. Wilander, and A. Worsztynowicz. 2005. Regional scale evidence for improvements in surface water chemistry 1990-2001. Environmental Pollution **137**: 165-176.

Skyllberg, U., K. Xia, P.R. Bloom, E.A. Nater, and W.F. Bleam. 2000. Binding of mercury(II) to reduced sulfur in organic matter along upland-peat soil transects. Journal of Environmental Quality **29**: 855-865.

St Louis, V. L., J. W. M. Rudd, C. A. Kelly, K. G. Beaty, R. J. Flett, and N. T. Roulet. 1996. Production and loss of methylmercury and loss of total mercury from boreal forest catchments containing different types of wetlands. Environmental Science & Technology **30**: 2719-2729.

St Louis, V. L., J. W. M. Rudd, C. A. Kelly, B. D. Hall, K. R. Rolfhus, K. J. Scott, S. E. Lindberg, and W. Dong. 2001. Importance of the forest canopy to fluxes of methyl mercury and total mercury to boreal ecosystems. Environmental Science & Technology **35**: 3089-3098.

Stoddard, J. L., D. S. Jeffries, A. Lukewille, T. A. Clair, P. J. Dillon, C. T. Driscoll, M. Forsius, M. Johannessen, J. S. Kahl, J. H. Kellogg, A. Kemp, J. Mannio, D. T. Monteith, P. S. Murdoch, S. Patrick, A. Rebsdorf, B. L. Skjelkvale, M. P. Stainton, T. Traaen, H. van Dam, K. E. Webster, J. Wieting, and A. Wilander. 1999. Regional trends in aquatic recovery from acidification in North America and Europe. Nature **401**: 575-578.

Stoddard, J.L., J.S. Kahl, F.A. Deviney, D.R. Dewalle, C.T. Driscoll, A.T. Herlihy, J.H. Kellogg, P.S. Murdoch, J.R. Webb, K.E. Webster. 2003. Response of surface water chemistry to the Clean Air Act Amendments of 1990. Report EPA 620/R-03/001, United States Environmental Protection Agency, North Carolina.

Sullivan, T.J., J.M. Eilers, B.J. Cosby, and K.B. Vache. 1997. Increasing role of nitrogen in the acidification of surface waters in the Adirondack mountains, New York. Water Air & Soil Pollution **95**: 313–336.

[USEPA] United States Environmental Protection Agency. 1996. Method 1669. USEPA, Office of Water, Office of Science and Technology, Engineering and Analysis Division (4303), 401 M Street SW, Washington, DC 20460.

[USEPA] United States Environmental Protection Agency. 1998. Method 1631. USEPA, Office of Water, Office of Science and Technology, Engineering and Analysis Division (4303), 401 M Street SW, Washington, DC 20460.

[USEPA] United States Environmental Protection Agency. 2001. Method 1630. Office of Water, Office of Science and Technology, Engineering and Analysis Division (4303), 401 M Street SW, Washington, DC 20460.

VanSickle, J., J. P. Baker, H. A. Simonin, B. P. Baldigo, W. A. Kretser, and W. E. Sharpe. 1996. Episodic acidification of small streams in the northeastern United States: Fish mortality in field bioassays. Ecological Applications **6**: 408-421.

Wellington, B. I., and C. T. Driscoll. 2004. The episodic acidification of a stream with elevated concentrations of dissolved organic carbon. Hydrological Processes **18**: 2663-2680.

Wigington, P. J., D. R. DeWalle, P. S. Murdoch, W. A. Kretser, H. A. Simonin, J. VanSickle, and J. P. Baker. 1996. Episodic acidification of small streams in the northeastern United States: Ionic controls of episodes. Ecological Applications **6**: 389-407.

Yin, Y. J., H. E. Allen, C. P. Huang, and P. F. Sanders. 1997. Interaction of Hg(II) with soil-derived humic substances. Analytica Chimica Acta 341: 73-82.

Young, K.C., P.A. Maurice, K.M. Docherty, and S.D. Bridgham. 2004. Bacterial degradation of dissolved organic matter from two northern Michigan streams. Geomicrobiology Journal **21**: 521-528.

APPENDIX A:

HYDROLOGIC DATA

Hydrologic data for each of six study wetlands during each of five seasonal sampling periods. Hydrologic data is separated by wetland type and seasonal sampling period: shallow peat riparian wetlands (A.1.a,b,c,d,e); deep peat riparian wetlands (A.2.a,b,c,d,e); and headwater wetlands (A.3.a,b,c,d,e). At each nested well cluster along each transect, WT denotes the water table well, Pz-Mid denotes the piezometer placed midway between the peat surface and the mineral soil below the wetland, and Pz-Bot denotes the piezometer placed in the mineral soil below the wetland. Error term of relative elevation (m) includes the propagation of surveying error throughout each site. Error term of water table relative to ground surface and piezometric head (m) includes both surveying error and water level measurement error. Based on the difference in water table elevation and the water level within piezometers, head potentials were split into five classes: strong recharge ($< {}^{-}0.10$ m), weak recharge (0 to $^{-}0.10$ m), strong discharge ($> {}^{+}0.10$ m), weak discharge (0 to $^{+}0.10$ m), and no gradient (not different from magnitude of error term). The term “below” denotes that water level was below the elevation of piezometer screening.

A.1.a. Shallow Peat Riparian Wetlands
Sampling Period: April (end of snowmelt)

Wetland	Transect Distance (m)		Relative Elevation (m)	Error	Water Table Relative to Ground Surface (m), Potentiometric Head (m)	Error	Classification of Potentiometric Head
SPR_HR	3m	Land-Surface	9.211				
		WT	9.077	0.005	-0.134	0.005	
		Pz-Mid	9.084	0.004	0.007	0.009	no gradient
		Pz-Bot	9.071	0.003	-0.006	0.008	no gradient
SPR_HR	9m	Land-Surface	8.926				
		WT	8.768	0.005	-0.158	0.005	
		Pz-Mid	8.720	0.003	-0.048	0.008	Weak Recharge
		Pz-Bot	8.731	0.004	-0.037	0.009	Weak Recharge
SPR_HR	18m	Land-Surface	8.803				
		WT	8.634	0.006	-0.169	0.006	
		Pz-Mid	Below	~	~	~	~
		Pz-Bot	8.631	0.004	-0.003	0.010	no gradient
SPR_HR	Stream	Land-Surface	8.803				
		WT	8.626	0.005	-0.177	0.005	
SPR_SLR	1m	Land-Surface	10.362				
		WT	10.368	0.005	0.006	0.005	
		Pz-Mid	10.346	0.006	-0.022	0.011	Weak Recharge
		Pz-Bot	10.387	0.005	0.019	0.010	Weak Discharge
SPR_SLR	5m	Land-Surface	10.29				
		WT	10.283	0.005	-0.007	0.005	
		Pz-Mid	10.280	0.006	-0.003	0.011	no gradient
		Pz-Bot	10.315	0.006	0.032	0.011	Weak Discharge
SPR_SLR	10.5m	Land-Surface	9.764				
		WT	9.651	0.006	-0.113	0.006	
		Pz-Mid	9.664	0.005	0.013	0.011	Weak Discharge
		Pz-Bot	9.659	0.006	0.008	0.012	no gradient
SPR_SLR	Stream	Land-Surface	9.764				
		WT	9.518	0.005	-0.246	0.005	

A.1.b. Shallow Peat Riparian Wetlands
Sampling Period: June (spring)

Wetland	Transect Distance (m)		Relative Elevation (m)	Error	Water Table Relative to Ground Surface (m), Potentiometric Head (m)	Error	Classification of Potentiometric Head
SPR_HR	3m	Land-Surface	9.207				
		WT	9.101	0.003	-0.106	0.003	
		Pz-Mid	9.103	0.006	0.002	0.009	no gradient
		Pz-Bot	9.127	0.005	0.026	0.008	Weak Discharge
SPR_HR	9m	Land-Surface	8.922				
		WT	8.834	0.005	-0.088	0.005	
		Pz-Mid	8.838	0.004	0.004	0.009	no gradient
		Pz-Bot	8.839	0.005	0.005	0.010	no gradient
SPR_HR	18m	Land-Surface	8.8				
		WT	8.776	0.051	-0.024	0.051	
		Pz-Mid	8.752	0.004	-0.024	0.055	no gradient
		Pz-Bot	8.766	0.004	-0.010	0.055	no gradient
SPR_HR	Stream	Land-Surface	8.800				
		WT	8.742	0.003	-0.058	0.003	
SPR_SLR	1m	Land-Surface	10.362				
		WT	10.355	0.005	-0.007	0.005	
		Pz-Mid	10.351	0.006	-0.004	0.011	no gradient
		Pz-Bot	10.391	0.005	0.036	0.010	Weak Discharge
SPR_SLR	5m	Land-Surface	10.29				
		WT	10.278	0.005	-0.012	0.005	
		Pz-Mid	10.275	0.006	-0.003	0.011	no gradient
		Pz-Bot	10.322	0.006	0.044	0.011	Weak Discharge
SPR_SLR	10.5m	Land-Surface	9.764				
		WT	9.675	0.006	-0.089	0.006	
		Pz-Mid	9.661	0.005	-0.014	0.011	Weak Recharge
		Pz-Bot	9.686	0.006	0.011	0.012	no gradient
SPR_SLR	Stream	Land-Surface	9.764				
		WT	9.575	0.005	-0.189	0.005	

A.1.c. Shallow Peat Riparian Wetlands
Sampling Period: August (summer)

Wetland	Transect Distance (m)		Relative Elevation (m)	Error	Water Table Relative to Ground Surface (m), Potentiometric Head (m)	Error	Classification of Potentiometric Head
SPR_HR	3m	Land-Surface	9.211				
		WT	8.759	0.005	-0.452	0.005	
		Pz-Mid	Below	~	~	~	~
		Pz-Bot	Below	~	~	~	~
SPR_HR	9m	Land-Surface	8.926				
		WT	8.606	0.003	-0.320	0.003	
		Pz-Mid	8.657	0.005	0.051	0.008	Weak Discharge
		Pz-Bot	8.612	0.004	0.006	0.007	no gradient
SPR_HR	18m	Land-Surface	8.803				
		WT	8.558	0.006	-0.245	0.006	
		Pz-Mid	Below	~	~	~	~
		Pz-Bot	8.499	0.004	-0.059	0.010	Weak Recharge
SPR_HR	Stream	Land-Surface	8.803				
		WT	8.461	0.005	-0.342	0.005	
SPR_SLR	1m	Land-Surface	10.362				
		WT	10.247	0.005	-0.115	0.005	
		Pz-Mid	10.243	0.006	-0.004	0.011	no gradient
		Pz-Bot	10.247	0.005	0.000	0.010	no gradient
SPR_SLR	5m	Land-Surface	10.29				
		WT	10.149	0.005	-0.141	0.005	
		Pz-Mid	10.180	0.006	0.031	0.011	Weak Discharge
		Pz-Bot	10.159	0.006	0.010	0.011	no gradient
SPR_SLR	10.5m	Land-Surface	9.764				
		WT	9.497	0.006	-0.267	0.006	
		Pz-Mid	Below	~	~	~	~
		Pz-Bot	9.512	0.006	0.015	0.012	Weak Discharge
SPR_SLR	Stream	Land-Surface	9.764				
		WT	9.399	0.005	-0.365	0.005	

A.1.d. Shallow Peat Riparian Wetlands
Sampling Period: September (pre-senescence)

Wetland	Transect Distance (m)		Relative Elevation (m)	Error	Water Table Relative to Ground Surface (m), Potentiometric Head (m)	Error	Classification of Potentiometric Head
SPR_HR	3m	Land-Surface	9.207				
		WT	8.709	0.003	-0.498	0.003	
		Pz-Mid	Below	~	~	~	~
		Pz-Bot	Below	~	~	~	~
SPR_HR	9m	Land-Surface	8.922				
		WT	8.567	0.005	-0.355	0.005	
		Pz-Mid	Below	~	~	~	~
		Pz-Bot	8.573	0.005	0.006	0.010	no gradient
SPR_HR	18m	Land-Surface	8.8				
		WT	8.470	0.051	-0.330	0.051	
		Pz-Mid	Below	~	~	~	~
		Pz-Bot	8.447	0.004	-0.023	0.055	no gradient
SPR_HR	Stream	Land-Surface	8.800				
		WT	8.412	0.003	-0.388	0.003	
SPR_SLR	1m	Land-Surface	10.362				
		WT	10.219	0.005	-0.143	0.005	
		Pz-Mid	10.221	0.006	0.002	0.011	no gradient
		Pz-Bot	10.233	0.005	0.014	0.010	Weak Discharge
SPR_SLR	5m	Land-Surface	10.29				
		WT	10.098	0.005	-0.192	0.005	
		Pz-Mid	Below	~	~	~	~
		Pz-Bot	10.142	0.006	0.044	0.011	Weak Discharge
SPR_SLR	10.5	Land-Surface	9.764				
		WT	9.464	0.006	-0.300	0.006	
		Pz-Mid	Below	~	~	~	~
		Pz-Bot	9.475	0.006	0.011	0.012	no gradient
SPR_SLR	Stream	Land-Surface	9.764				
		WT	9.366	0.005	-0.398	0.005	

A.1.e. Shallow Peat Riparian Wetlands
Sampling Period: November/December (post-senescence)

Wetland	Transect Distance (m)		Relative Elevation (m)	Error	Water Table Relative to Ground Surface (m), Potentiometric Head (m)	Error	Classification of Potentiometric Head
SPR_HR	3m	Land-Surface	9.207				
		WT	9.084	0.003	-0.123	0.003	
		Pz-Mid	9.086	0.006	0.002	0.009	no gradient
		Pz-Bot	9.101	0.005	0.017	0.008	Weak Discharge
SPR_HR	9m	Land-Surface	8.922				
		WT	8.769	0.005	-0.153	0.005	
		Pz-Mid	8.824	0.004	0.055	0.009	Weak Discharge
		Pz-Bot	8.777	0.005	0.008	0.010	no gradient
SPR_HR	18m	Land-Surface	8.8				
		WT	8.693	0.051	-0.107	0.051	
		Pz-Mid	8.679	0.004	-0.014	0.055	no gradient
		Pz-Bot	8.729	0.004	0.036	0.055	no gradient
SPR_HR	Stream	Land-Surface	8.800				
		WT	8.665	0.003	-0.135	0.003	
SPR_SLR	1m	Land-Surface	10.362				
		WT	10.361	0.005	-0.001	0.005	
		Pz-Mid	10.354	0.006	-0.007	0.011	no gradient
		Pz-Bot	10.412	0.005	0.051	0.010	Weak Discharge
SPR_SLR	5m	Land-Surface	10.29				
		WT	10.273	0.005	-0.017	0.005	
		Pz-Mid	10.269	0.006	-0.004	0.011	no gradient
		Pz-Bot	10.312	0.006	0.039	0.011	Weak Discharge
SPR_SLR	10.5m	Land-Surface	9.764				
		WT	9.689	0.006	-0.075	0.006	
		Pz-Mid	9.654	0.005	-0.035	0.011	Weak Recharge
		Pz-Bot	9.688	0.006	-0.001	0.012	no gradient
SPR_SLR	Stream	Land-Surface	9.764				
		WT	9.631	0.005	-0.133	0.005	

A.2.a. Deep Peat Riparian Wetlands
Sampling Period: April (end of snowmelt)

Wetland	Transect Distance (m)		Relative Elevation (m)	Error	Water Table Relative to Ground Surface (m), Potentiometric Head (m)	Error	Classification of Potentiometric Head
DPR_MR	1m	Land-Surface	8.937				
		WT	8.884	0.005	-0.053	0.005	
		Pz-Mid	8.884	0.003	0.000	0.008	no gradient
		Pz-Bot	8.877	0.003	-0.007	0.008	no gradient
	40.5m	Land-Surface	8.547				
		WT	8.510	0.006	-0.037	0.006	
		Pz-Mid	8.591	0.006	0.081	0.012	Weak Discharge
		Pz-Bot	8.827	0.005	0.317	0.011	Strong Discharge
	81m	Land-Surface	7.783				
		WT	7.828	0.007	0.045	0.007	
		Pz-Mid	7.840	0.005	0.012	0.012	no gradient
		Pz-Bot	8.036	0.005	0.208	0.012	Strong Discharge
	Stream	Land-Surface	7.783				
		WT	7.670	0.006	-0.113	0.006	
DPR_BR	1m	Land-Surface	9.478				
		WT	9.324	0.005	-0.154	0.005	
		Pz-Mid	9.281	0.005	-0.043	0.010	Weak Recharge
		Pz-Bot	9.415	0.004	0.091	0.009	Weak Discharge
	30m	Land-Surface	9.374				
		WT	9.288	0.003	-0.086	0.003	
		Pz-Mid	9.263	0.003	-0.025	0.006	Weak Recharge
		Pz-Bot	9.273	0.005	-0.015	0.008	Weak Recharge
	60m	Land-Surface	9.052				
		WT	9.045	0.004	-0.007	0.004	
		Pz-Mid	8.942	0.004	-0.103	0.008	Strong Recharge
		Pz-Bot	9.178	0.003	0.133	0.007	Strong Discharge
	Stream	Land-Surface	9.052				
		WT	8.855	0.003	-0.197	0.003	

A.2.b. Deep Peat Riparian Wetlands
Sampling Period: June (spring)

Wetland	Transect Distance (m)		Relative Elevation (m)	Error	Water Table Relative to Ground Surface (m), Potentiometric Head (m)	Error	Classification of Potentiometric Head
DPR_MR	1m	Land-Surface	8.94				
		WT	8.880	0.006	-0.060	0.006	
		Pz-Mid	8.877	0.003	-0.003	0.009	no gradient
		Pz-Bot	8.876	0.003	-0.004	0.009	no gradient
	40.5m	Land-Surface	8.545				
		WT	8.555	0.006	0.010	0.006	
		Pz-Mid	8.535	0.005	-0.020	0.011	Weak Recharge
		Pz-Bot	8.524	0.006	-0.031	0.012	Weak Recharge
	81m	Land-Surface	7.813				
		WT	7.865	0.006	0.052	0.006	
		Pz-Mid	7.855	0.006	-0.010	0.012	no gradient
		Pz-Bot	8.065	0.007	0.200	0.013	Strong Discharge
	Stream	Land-Surface	7.813				
		WT	7.700	0.008	-0.113	0.008	
DPR_BR	1m	Land-Surface	9.477				
		WT	9.338	0.003	-0.139	0.003	
		Pz-Mid	9.335	0.006	-0.003	0.009	no gradient
		Pz-Bot	9.383	0.005	0.045	0.008	Weak Discharge
	30m	Land-Surface	9.373				
		WT	9.273	0.004	-0.100	0.004	
		Pz-Mid	9.126	0.004	-0.147	0.008	Strong Recharge
		Pz-Bot	8.991	0.003	-0.282	0.007	Strong Recharge
	60m	Land-Surface	9.05				
		WT	9.045	0.004	-0.005	0.004	
		Pz-Mid	9.040	0.004	-0.005	0.008	no gradient
		Pz-Bot	9.297	0.005	0.252	0.009	Strong Discharge
	Stream	Land-Surface	9.050				
		WT	8.980	0.005	-0.070	0.005	

A.2.c. Deep Peat Riparian Wetlands
Sampling Period: August (summer)

Wetland	Transect Distance (m)		Relative Elevation (m)	Error	Water Table Relative to Ground Surface (m), Potentiometric Head (m)	Error	Classification of Potentiometric Head
DPR_MR	1m	Land-Surface	8.937				
		WT	8.848	0.005	-0.089	0.005	
		Pz-Mid	8.843	0.003	-0.005	0.008	no gradient
		Pz-Bot	8.845	0.003	-0.003	0.008	no gradient
	40.5m	Land-Surface	8.547				
		WT	8.487	0.006	-0.060	0.006	
		Pz-Mid	8.487	0.006	0.000	0.012	no gradient
		Pz-Bot	8.421	0.005	-0.066	0.011	Weak Recharge
	81m	Land-Surface	7.783				
		WT	7.807	0.007	0.024	0.007	
		Pz-Mid	7.821	0.005	0.014	0.012	Weak Discharge
		Pz-Bot	7.778	0.005	-0.029	0.012	Weak Recharge
	Stream	Land-Surface	7.783				
		WT	7.258	0.006	-0.525	0.006	
DPR_BR	1m	Land-Surface	9.478				
		WT	9.168	0.005	-0.310	0.005	
		Pz-Mid	9.170	0.005	0.002	0.010	no gradient
		Pz-Bot	9.084	0.004	-0.084	0.009	Weak Recharge
	30m	Land-Surface	9.374				
		WT	9.176	0.003	-0.198	0.003	
		Pz-Mid	9.096	0.003	-0.080	0.006	Weak Recharge
		Pz-Bot	9.085	0.005	-0.091	0.008	Weak Recharge
	60m	Land-Surface	9.052				
		WT	8.848	0.004	-0.204	0.004	
		Pz-Mid	9.795	0.004	0.947	0.008	Strong Discharge
		Pz-Bot	9.000	0.003	0.152	0.007	Strong Discharge
	Stream	Land-Surface	9.052				
		WT	8.721	0.003	-0.331	0.003	

A.2.d. Deep Peat Riparian Wetlands
Sampling Period: September (pre-senescence)

Wetland	Transect Distance (m)		Relative Elevation (m)	Error	Water Table Relative to Ground Surface (m), Potentiometric Head (m)	Error	Classification of Potentiometric Head
DPR_MR	1m	Land-Surface	8.94				
		WT	8.745	0.006	-0.195	0.006	
		Pz-Mid	8.748	0.003	0.003	0.009	no gradient
		Pz-Bot	8.656	0.003	-0.089	0.009	Weak Recharge
	40.5m	Land-Surface	8.545				
		WT	8.338	0.006	-0.207	0.006	
		Pz-Mid	8.429	0.005	0.091	0.011	Weak Discharge
		Pz-Bot	7.907	0.006	-0.431	0.012	Strong Recharge
	81m	Land-Surface	7.813				
		WT	7.766	0.006	-0.047	0.006	
		Pz-Mid	7.772	0.006	0.006	0.012	no gradient
		Pz-Bot	7.762	0.007	-0.004	0.013	no gradient
	Stream	Land-Surface	7.813				
		WT	7.612	0.008	-0.201	0.008	
DPR_BR	1m	Land-Surface	9.477				
		WT	9.141	0.003	-0.336	0.003	
		Pz-Mid	Below	~	~	~	~
		Pz-Bot	9.012	0.005	-0.129	0.008	Strong Recharge
	30m	Land-Surface	9.373				
		WT	9.066	0.004	-0.307	0.004	
		Pz-Mid	9.029	0.004	-0.037	0.008	Weak Recharge
		Pz-Bot	8.992	0.003	-0.074	0.007	Weak Recharge
	60m	Land-Surface	9.05				
		WT	8.784	0.004	-0.266	0.004	
		Pz-Mid	8.789	0.004	0.005	0.008	no gradient
		Pz-Bot	8.992	0.005	0.208	0.009	Strong Discharge
	Stream	Land-Surface	9.050				
		WT	8.736	0.005	-0.314	0.005	

A.2.e. Deep Peat Riparian Wetlands
Sampling Period: November/December (post-senescence)

Wetland	Transect Distance (m)		Relative Elevation (m)	Error	Water Table Relative to Ground Surface (m), Potentiometric Head (m)	Error	Classification of Potentiometric Head
DPR_MR	1m	Land-Surface	8.94				
		WT	8.863	0.006	-0.077	0.006	
		Pz-Mid	8.861	0.003	-0.002	0.009	no gradient
		Pz-Bot	8.864	0.003	0.001	0.009	no gradient
	40.5m	Land-Surface	8.545				
		WT	8.508	0.006	-0.037	0.006	
		Pz-Mid	8.508	0.005	0.000	0.011	no gradient
		Pz-Bot	8.531	0.006	0.023	0.012	Weak Discharge
	81m	Land-Surface	7.813				
		WT	7.852	0.006	0.039	0.006	
		Pz-Mid	7.853	0.006	0.001	0.012	no gradient
		Pz-Bot	7.913	0.007	0.061	0.013	Weak Discharge
	Stream	Land-Surface	7.813				
		WT	7.669	0.008	-0.144	0.008	
DPR_BR	1m	Land-Surface	9.477				
		WT	9.323	0.003	-0.154	0.003	
		Pz-Mid	9.299	0.006	-0.024	0.009	Weak Recharge
		Pz-Bot	9.374	0.005	0.051	0.008	Weak Discharge
	30m	Land-Surface	9.373				
		WT	9.241	0.004	-0.132	0.004	
		Pz-Mid	9.260	0.004	0.019	0.008	Weak Discharge
		Pz-Bot	9.277	0.003	0.036	0.007	Weak Discharge
	60m	Land-Surface	9.05				
		WT	9.039	0.004	-0.011	0.004	
		Pz-Mid	9.058	0.004	0.019	0.008	Weak Discharge
		Pz-Bot	9.314	0.005	0.275	0.009	Strong Discharge
	Stream	Land-Surface	9.050				
		WT	8.994	0.005	-0.056	0.005	

A.3.a. Headwater Wetlands
Sampling Period: April (end of snowmelt)

Wetland	Transect Distance (m)		Relative Elevation (m)	Error	Water Table Relative to Ground Surface (m), Potentiometric Head (m)	Error	Classification of Potentiometric Head
HW_P	1m	Land Surface	9.150				
		WT	frozen				
		Pz-Mid	frozen				
		Pz-Bot	frozen				
	45ma	Land Surface	9.005				
		WT	9.007	0.004	0.002	0.004	
		Pz-Mid	8.986	0.003	-0.021	0.007	Weak Recharge
		Pz-Bot	8.880	0.005	-0.127	0.009	Strong Recharge
	60m	Land Surface	8.997				
		WT	9.052	0.006	0.055	0.006	
		Pz-Mid	8.959	0.007	-0.093	0.013	Weak Recharge
		Pz-Bot	8.644	0.005	-0.408	0.011	Strong Recharge
	80m	Land Surface	9.000				
		WT	9.022	0.007	0.022	0.007	
		Pz-Mid	8.920	0.006	-0.102	0.013	Strong Recharge
		Pz-Bot	8.663	0.008	-0.359	0.015	Strong Recharge
	100m	Land Surface	8.903				
		WT	8.955	0.010	0.052	0.010	
		Pz-Mid	8.889	0.009	-0.066	0.019	Weak Recharge
		Pz-Bot	8.920	0.009	-0.035	0.019	Weak Recharge
	Outlet	Land-Surface	8.903	0.000			
		WT	8.995	0.01	0.092	0.010	
HW_H	1m	Land-Surface	9.041				
		WT	9.116	0.003	0.075	0.003	
		Pz-Mid	9.090	0.003	-0.026	0.006	Weak Recharge
		Pz-Bot	8.961	0.003	-0.155	0.006	Strong Recharge
	37.5m	Land-Surface	9.053				
		WT	9.122	0.004	0.069	0.004	
		Pz-Mid	8.996	0.004	-0.126	0.008	Strong Recharge
		Pz-Bot	8.628	0.005	-0.494	0.009	Strong Recharge
	75m	Land-Surface	9.026				
		WT	9.078	0.008	0.052	0.008	
		Pz-Mid	8.943	0.006	-0.135	0.014	Strong Recharge
		Pz-Bot	8.344	0.010	-0.734	0.018	Strong Recharge
	Outlet	Land-Surface	8.323				
		WT	8.256	0.015	-0.067	0.015	

A.3.b. Headwater Wetlands
Sampling Period: June (spring)

Wetland	Transect Distance (m)		Relative Elevation (m)	Error	Water Table Relative to Ground Surface (m), Potentiometric Head (m)	Error	Classification of Potentiometric Head
HW_P	1m	Land Surface	9.195				
		WT	9.204				
		Pz-Mid	9.131				
		Pz-Bot	9.153				
	45ma	Land Surface	9.005				
		WT	9.032	0.004	0.027	0.004	
		Pz-Mid	8.989	0.003	-0.043	0.007	Weak Recharge
		Pz-Bot	8.925	0.005	-0.107	0.009	Strong Recharge
	60m	Land Surface	8.997				
		WT	9.042	0.006	0.045	0.006	
		Pz-Mid	8.945	0.007	-0.097	0.013	Weak Recharge
		Pz-Bot	4.664	0.005	-4.378	0.011	Strong Recharge
	80m	Land Surface	9.000				
		WT	9.011	0.007	0.011	0.007	
		Pz-Mid	8.859	0.006	-0.152	0.013	Strong Recharge
		Pz-Bot	7.873	0.008	-1.138	0.015	Strong Recharge
	100m	Land Surface	8.903				
		WT	8.960	0.010	0.057	0.010	
		Pz-Mid	8.911	0.009	-0.049	0.019	Weak Recharge
		Pz-Bot	8.920	0.009	-0.040	0.019	Weak Recharge
	Outlet	Land-Surface	8.903	0.000			
		WT	8.96	0.01	0.057	0.010	
HW_H	1m	Land-Surface	9.039				
		WT	9.124	0.007	0.085	0.007	
		Pz-Mid	9.194	0.008	0.070	0.015	Weak Discharge
		Pz-Bot	9.095	0.005	-0.029	0.012	Weak Recharge
	37.5m	Land-Surface	9.057				
		WT	9.103	0.009	0.046	0.009	
		Pz-Mid	9.023	0.008	-0.080	0.017	Weak Recharge
		Pz-Bot	6.909	0.007	-2.194	0.016	Strong Recharge
	75m	Land-Surface	8.981				
		WT	9.064	0.008	0.083	0.008	
		Pz-Mid	8.993	0.008	-0.071	0.016	Weak Recharge
		Pz-Bot	7.764	0.008	-1.300	0.016	Strong Recharge
	Outlet	Land-Surface	8.323				
		WT	8.197	0.015	-0.126	0.015	

A.3.c. Headwater Wetlands
Sampling Period: August (summer)

Wetland	Transect Distance (m)		Relative Elevation (m)	Error	Water Table Relative to Ground Surface (m), Potentiometric Head (m)	Error	Classification of Potentiometric Head
HW_P	1m	Land Surface	9.195				
		WT	9.121				
		Pz-Mid	9.120				
		Pz-Bot	9.107				
	45ma	Land Surface	9.005				
		WT	8.986	0.004	-0.019	0.004	
		Pz-Mid	8.961	0.003	-0.025	0.007	Weak Recharge
		Pz-Bot	8.857	0.005	-0.129	0.009	Strong Recharge
	60m	Land Surface	8.997				
		WT	8.966	0.006	-0.031	0.006	
		Pz-Mid	8.941	0.007	-0.025	0.013	Weak Recharge
		Pz-Bot	8.544	0.005	-0.422	0.011	Strong Recharge
	80m	Land Surface	9.000				
		WT	8.970	0.007	-0.030	0.007	
		Pz-Mid	8.886	0.006	-0.084	0.013	Weak Recharge
		Pz-Bot	8.563	0.008	-0.407	0.015	Strong Recharge
	100m	Land Surface	8.903				
		WT	8.942	0.010	0.039	0.010	
		Pz-Mid	8.885	0.009	-0.057	0.019	Weak Recharge
		Pz-Bot	8.645	0.009	-0.297	0.019	Strong Recharge
	Outlet	Land-Surface	8.903	0.000			
		WT	8.942	0.01	0.039	0.010	
HW_H	1m	Land-Surface	9.041				
		WT	8.982	0.003	-0.059	0.003	
		Pz-Mid	8.979	0.003	-0.003	0.006	no gradient
		Pz-Bot	8.845	0.003	-0.137	0.006	Strong Recharge
	37.5m	Land-Surface	9.053				
		WT	8.970	0.004	-0.083	0.004	
		Pz-Mid	8.915	0.004	-0.055	0.008	Weak Recharge
		Pz-Bot	8.178	0.005	-0.792	0.009	Strong Recharge
	75m	Land-Surface	9.026				
		WT	8.951	0.008	-0.075	0.008	
		Pz-Mid	8.867	0.006	-0.084	0.014	Weak Recharge
		Pz-Bot	8.244	0.010	-0.707	0.018	Strong Recharge
	Outlet	Land-Surface	8.323				
		WT	8.105	0.015	-0.218	0.015	

A.3.d. Headwater Wetlands
Sampling Period: September (pre-senescence)

Wetland	Transect Distance (m)		Relative Elevation (m)	Error	Water Table Relative to Ground Surface (m), Potentiometric Head (m)	Error	Classification of Potentiometric Head
HW_P	1m	Land Surface	9.195				
		WT	9.027				
		Pz-Mid	8.987				
		Pz-Bot	9.006				
	45ma	Land Surface	9.005				
		WT	8.956	0.004	-0.049	0.004	
		Pz-Mid	8.926	0.003	-0.030	0.007	Weak Recharge
		Pz-Bot	8.803	0.005	-0.153	0.009	Strong Recharge
	60m	Land Surface	8.997				
		WT	8.928	0.006	-0.069	0.006	
		Pz-Mid	8.872	0.007	-0.056	0.013	Weak Recharge
		Pz-Bot	7.439	0.005	-1.489	0.011	Strong Recharge
	80m	Land Surface	9.000				
		WT	8.936	0.007	-0.064	0.007	
		Pz-Mid	8.820	0.006	-0.116	0.013	Strong Recharge
		Pz-Bot	4.014	0.008	-4.922	0.015	Strong Recharge
	100m	Land Surface	8.903				
		WT	8.900	0.010	-0.003	0.010	
		Pz-Mid	8.822	0.009	-0.078	0.019	Weak Recharge
		Pz-Bot	8.525	0.009	-0.375	0.019	Strong Recharge
	Outlet	Land-Surface	8.903	0.000			
		WT	8.9	0.01	-0.003	0.010	
HW_H	1m	Land-Surface	9.039				
		WT	8.973	0.007	-0.066	0.007	
		Pz-Mid	8.907	0.008	-0.066	0.015	Weak Recharge
		Pz-Bot	8.784	0.005	-0.189	0.012	Strong Recharge
	37.5m	Land-Surface	9.057				
		WT	8.963	0.009	-0.094	0.009	
		Pz-Mid	8.877	0.008	-0.086	0.017	Weak Recharge
		Pz-Bot	6.509	0.007	-2.454	0.016	Strong Recharge
	75m	Land-Surface	8.981				
		WT	8.937	0.008	-0.044	0.008	
		Pz-Mid	8.816	0.008	-0.121	0.016	Strong Recharge
		Pz-Bot	6.726	0.008	-2.211	0.016	Strong Recharge
	Outlet	Land-Surface	8.323				
		WT	8.027	0.015	-0.296	0.015	

A.3.e. Headwater Wetlands
Sampling Period: November/December (post-senescence)

Wetland	Transect Distance (m)		Relative Elevation (m)	Error	Water Table Relative to Ground Surface (m), Potentiometric Head (m)	Error	Classification of Potentiometric Head
HW_P	1m	Land Surface	9.195				
		WT	9.161				
		Pz-Mid	9.168				
		Pz-Bot	9.133				
	45ma	Land Surface	9.005				
		WT	9.005	0.004	0.000	0.004	
		Pz-Mid	9.011	0.003	0.006	0.007	no gradient
		Pz-Bot	8.961	0.005	-0.044	0.009	Weak Recharge
	60m	Land Surface	8.997				
		WT	9.005	0.006	0.008	0.006	
		Pz-Mid	8.992	0.007	-0.013	0.013	no gradient
		Pz-Bot	8.244	0.005	-0.761	0.011	Strong Recharge
	80m	Land Surface	9.000				
		WT	8.984	0.007	-0.016	0.007	
		Pz-Mid	8.906	0.006	-0.078	0.013	Weak Recharge
		Pz-Bot	no value	~	~	~	~
	100m	Land Surface	8.903				
		WT	8.918	0.010	0.015	0.010	
		Pz-Mid	8.906	0.009	-0.012	0.019	no gradient
		Pz-Bot	no value	~	~	~	~
	Outlet	Land-Surface	8.903	0.000			
		WT	8.918	0.01	0.015	0.010	
HW_H	1m	Land-Surface	9.039				
		WT	9.072	0.007	0.033	0.007	
		Pz-Mid	9.070	0.008	-0.002	0.015	no gradient
		Pz-Bot	8.948	0.005	-0.124	0.012	Strong Recharge
	37.5m	Land-Surface	9.057				
		WT	9.049	0.009	-0.008	0.009	
		Pz-Mid	8.994	0.008	-0.055	0.017	Weak Recharge
		Pz-Bot	7.083	0.007	-1.966	0.016	Strong Recharge
	75m	Land-Surface	8.981				
		WT	8.996	0.008	0.015	0.008	
		Pz-Mid	8.926	0.008	-0.070	0.016	Weak Recharge
		Pz-Bot	7.429	0.008	-1.567	0.016	Strong Recharge
	Outlet	Land-Surface	8.323				
		WT	8.195	0.015	-0.128	0.015	

APPENDIX B:

HYDROLOGIC CROSS SECTIONS

Hydrologic cross sections for each of six study wetlands during each of five seasonal sampling periods. Cross sections are separated by individual wetlands within each wetland type: shallow peat riparian wetlands (B.1.a,b,c,d,e,f,g,h,i,j), deep peat riparian wetlands (B.2.a,b,c,d,e,f,g,h,i,j), and headwater wetlands (B.2.a,b,c,d,e,f,g,h,i,j). Relative elevation of the ground surface, the water table, and the piezometric head potential, and the stream are shown for each wetland during each sampling period. For each individual wetland, one cross section representing a high flow regime and one cross section representing a low flow regime, are shown with approximate flow nets in addition to the water table and piezometer data.

Appendix B.1.a. Hydrologic cross section of a shallow peat riparian wetland, (Site SPR_HR), April (end of snowmelt).

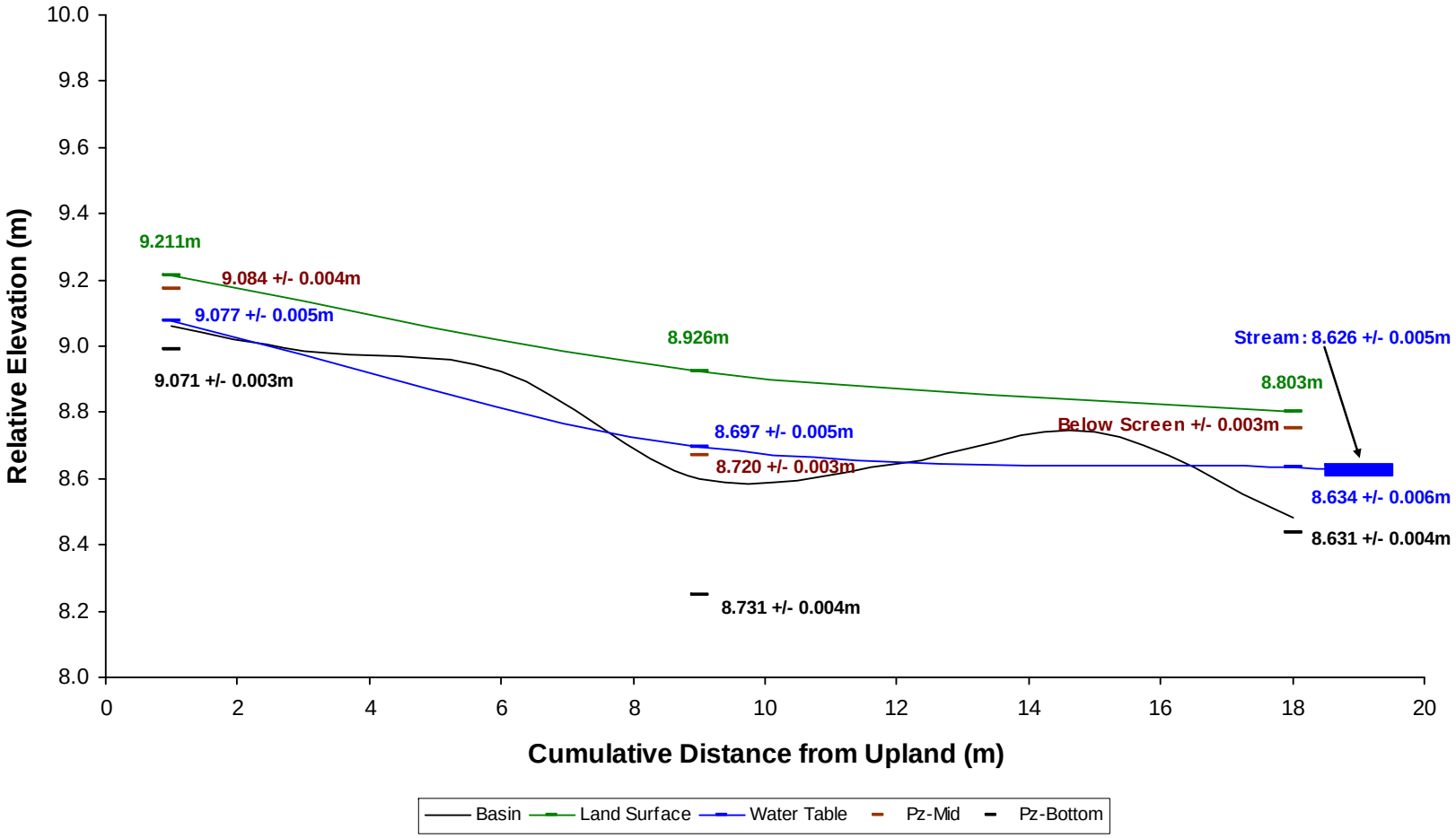

Appendix B.1.b.i. Hydrologic cross section for a shallow peat riparian wetland, (Site SPR_HR), June (spring).

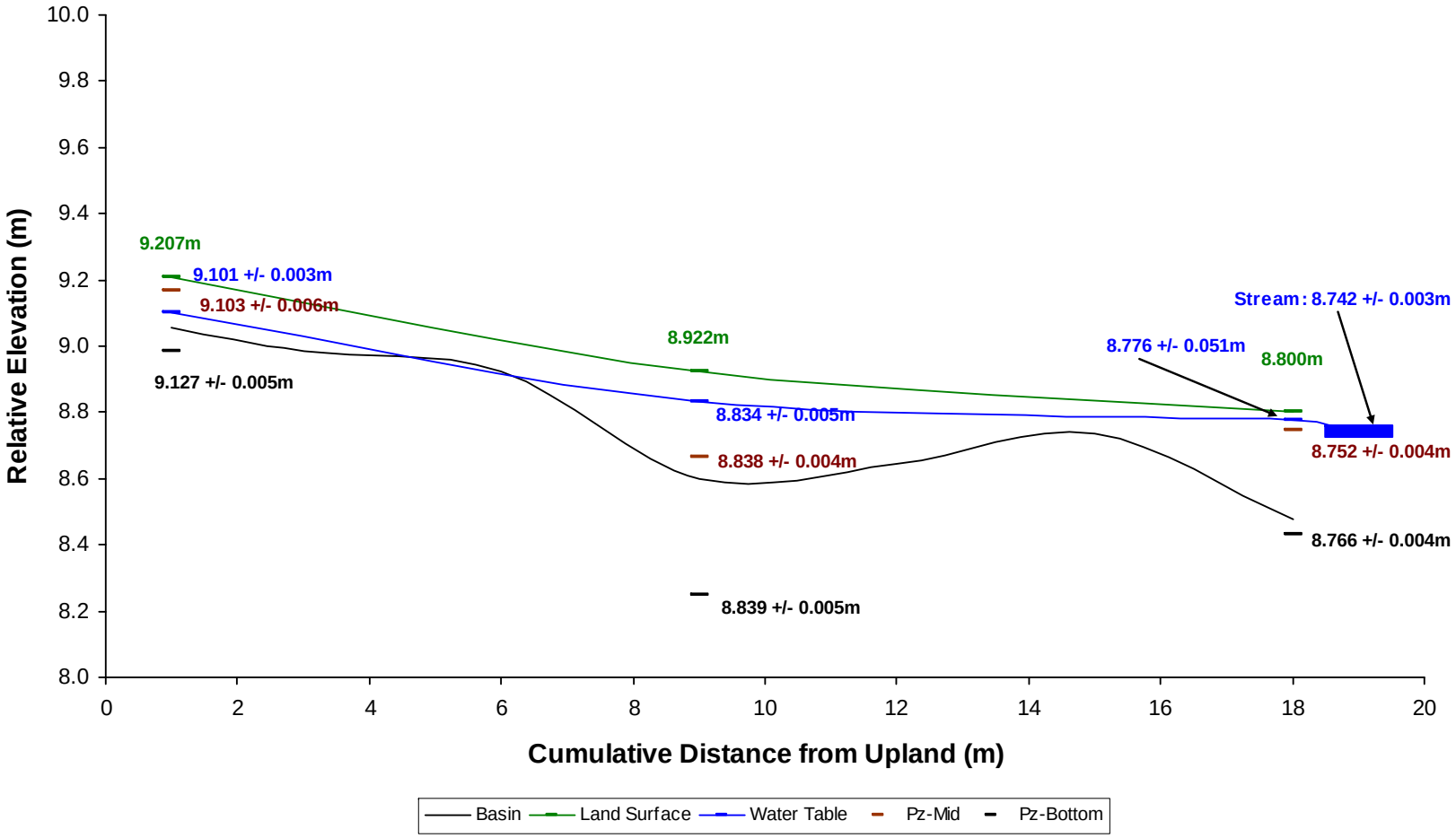

Appendix B.1.b.ii. Hydrologic cross section and flow net for a shallow peat riparian wetland, (Site SPR_HR), June (spring).

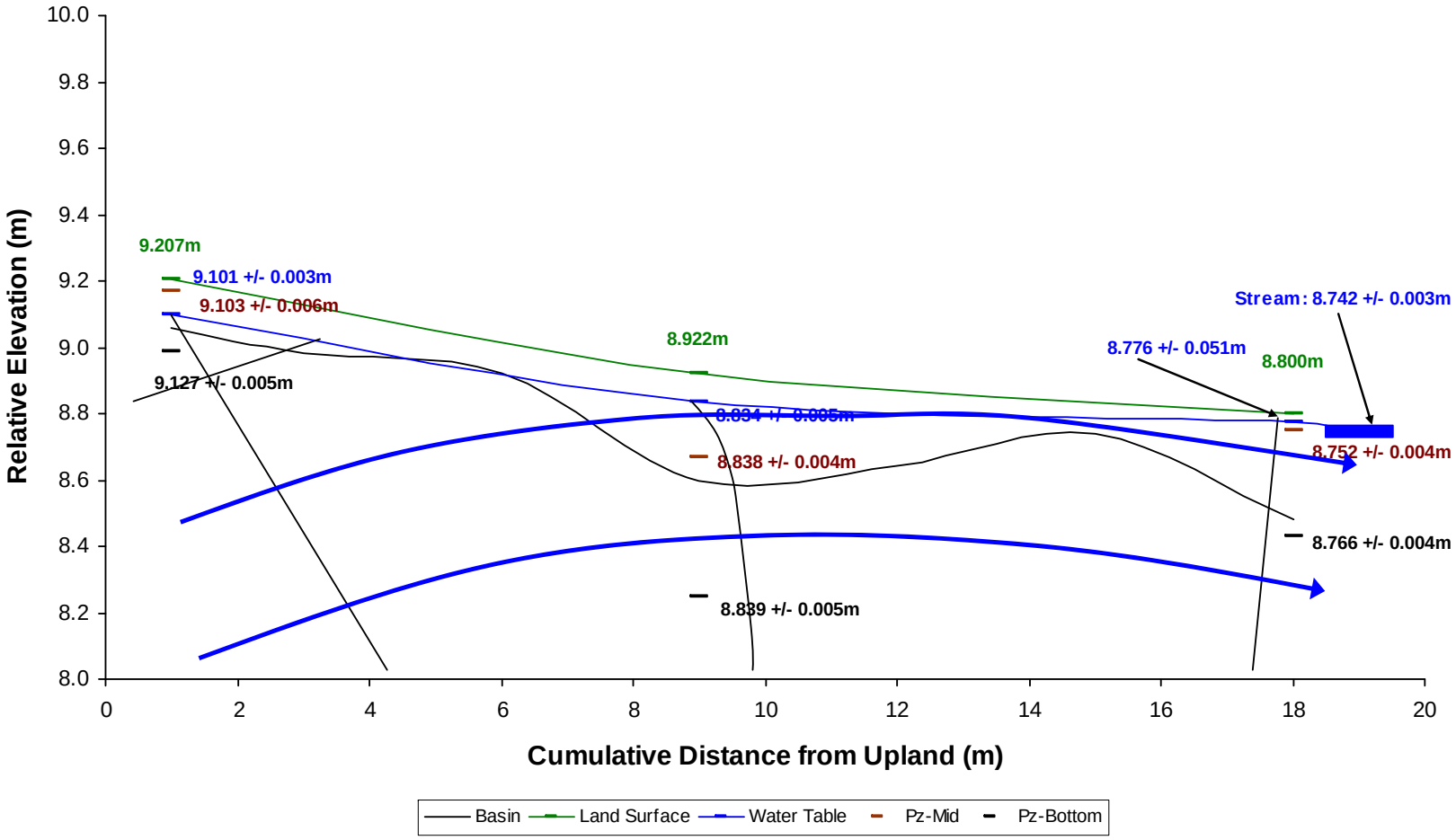

Appendix B.1.c. Hydrologic cross section for a shallow peat riparian wetland, (Site SPR_HR), August (summer).

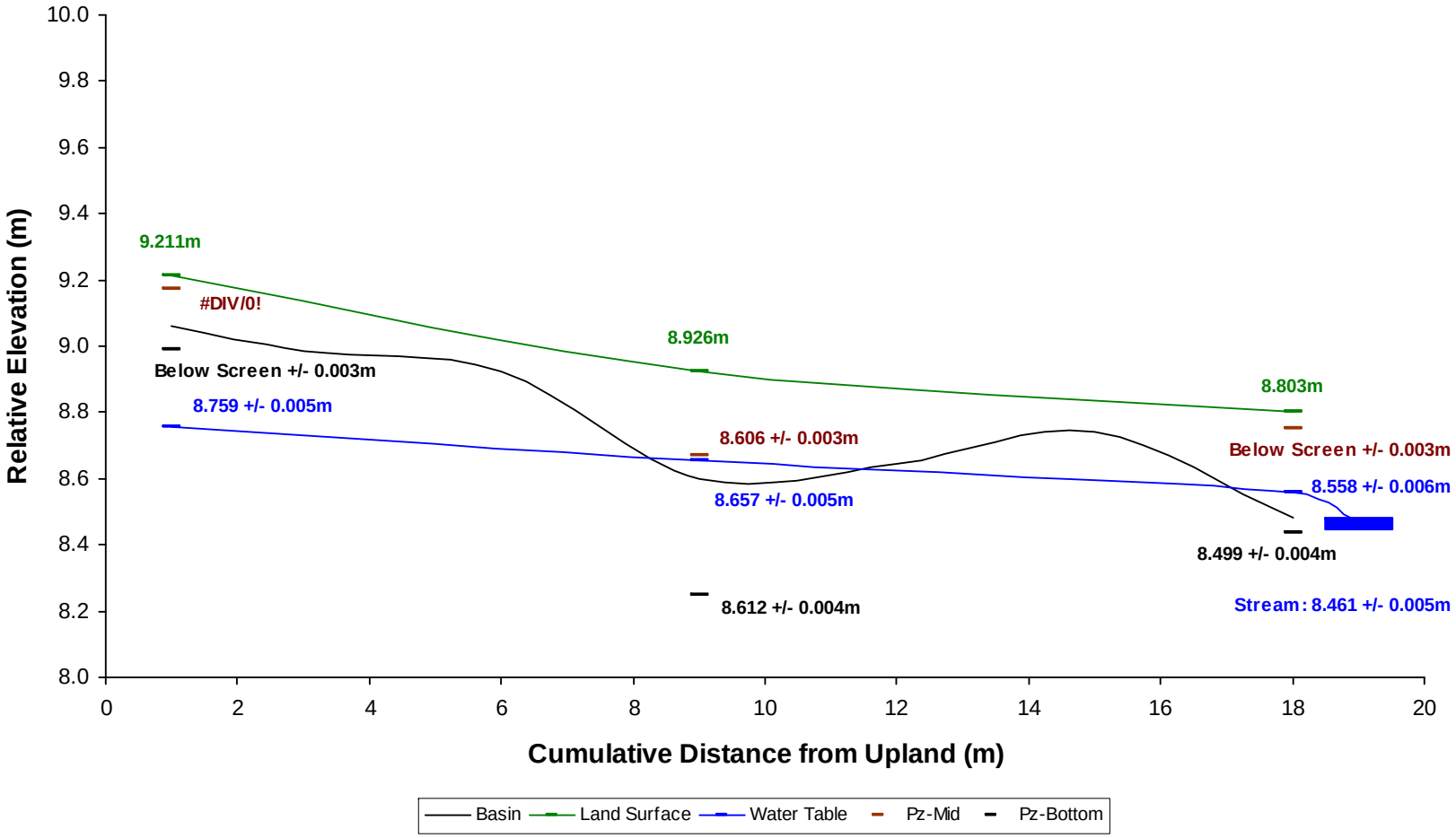

Appendix B.1.d.i. Hydrologic cross section for a shallow peat riparian wetland, (Site SPR_HR), September (pre-senescence).

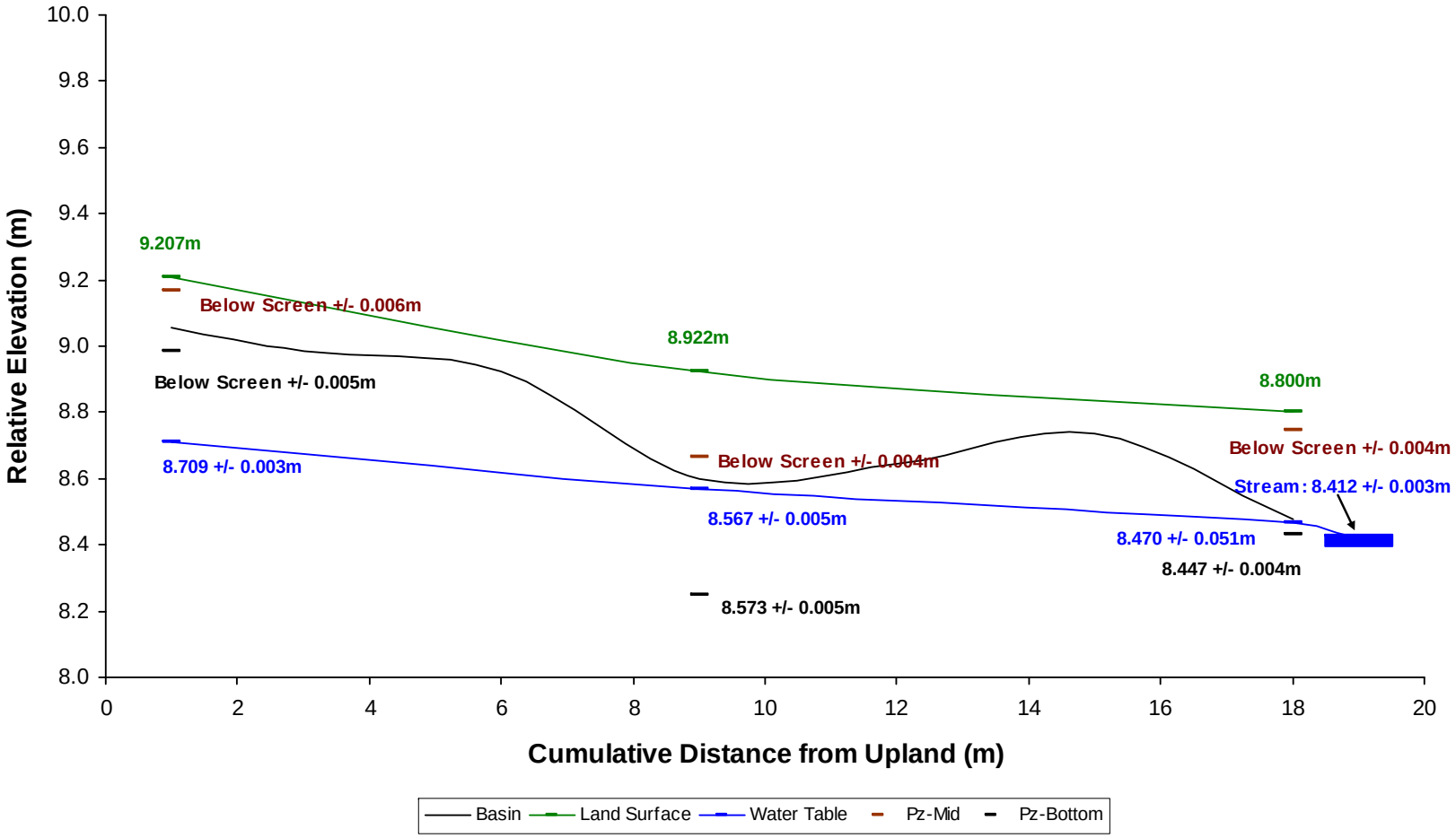

Appendix B.1.d.ii. Hydrologic cross section and flow net for a shallow peat riparian wetland, (Site SPR_HR), September (pre-senescence).

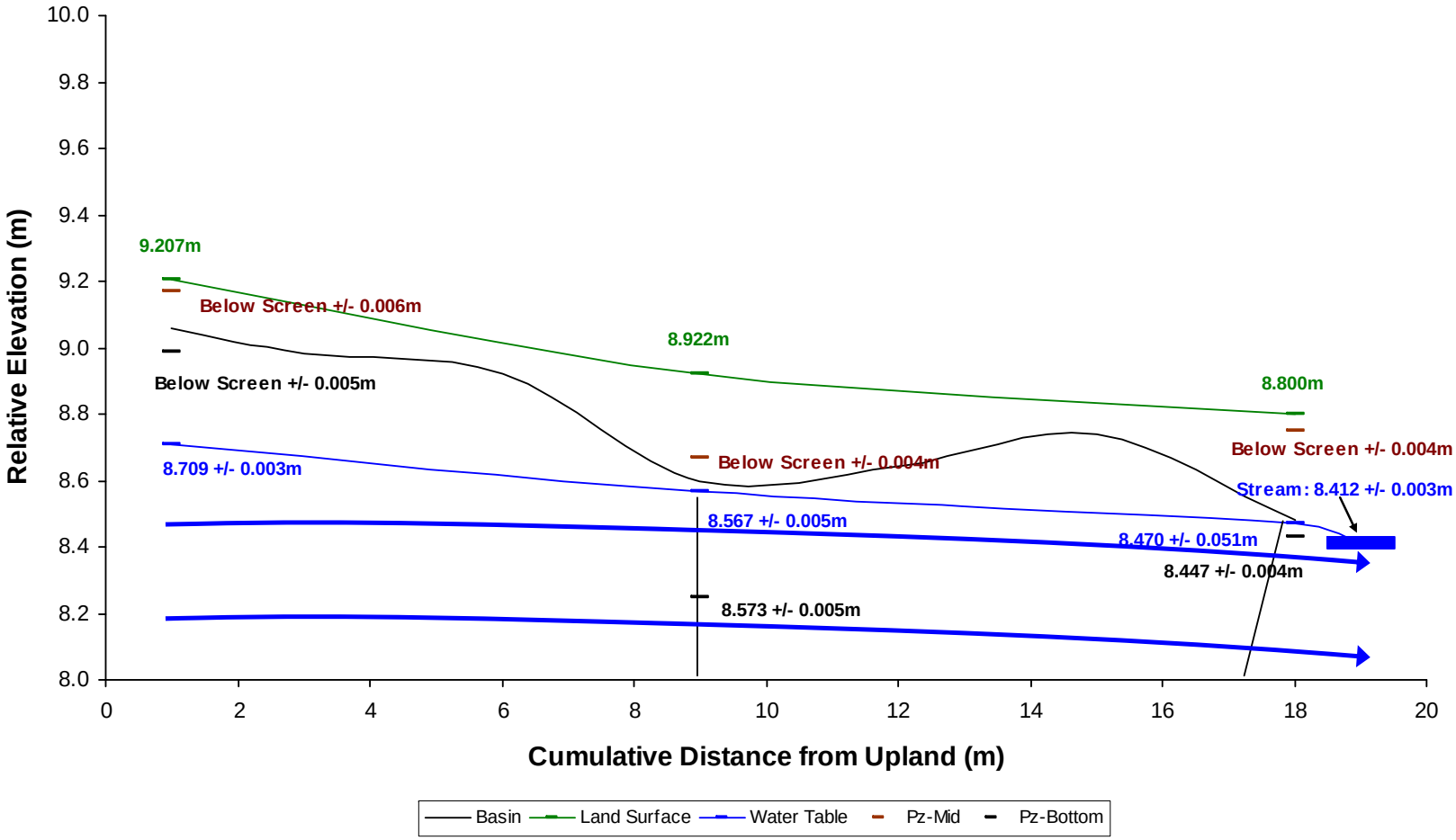

Appendix B.1.e. Hydrologic cross section for a shallow peat riparian wetland, (Site SPR_HR), November/December (post-senescence).

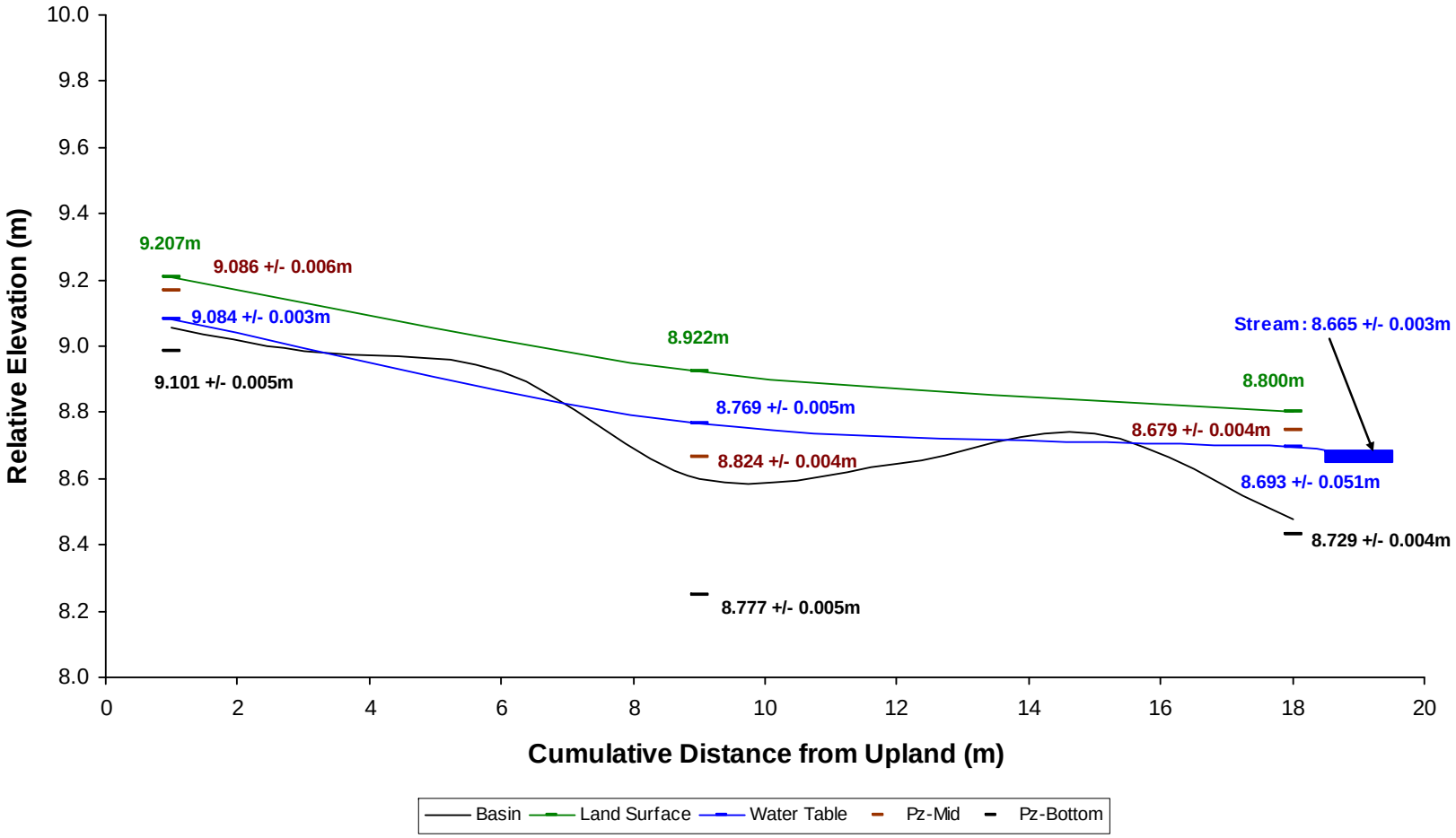

Appendix B.1.f. Hydrologic cross section for a shallow peat riparian wetland, (Site SPR_SLR), April (end of snowmelt).

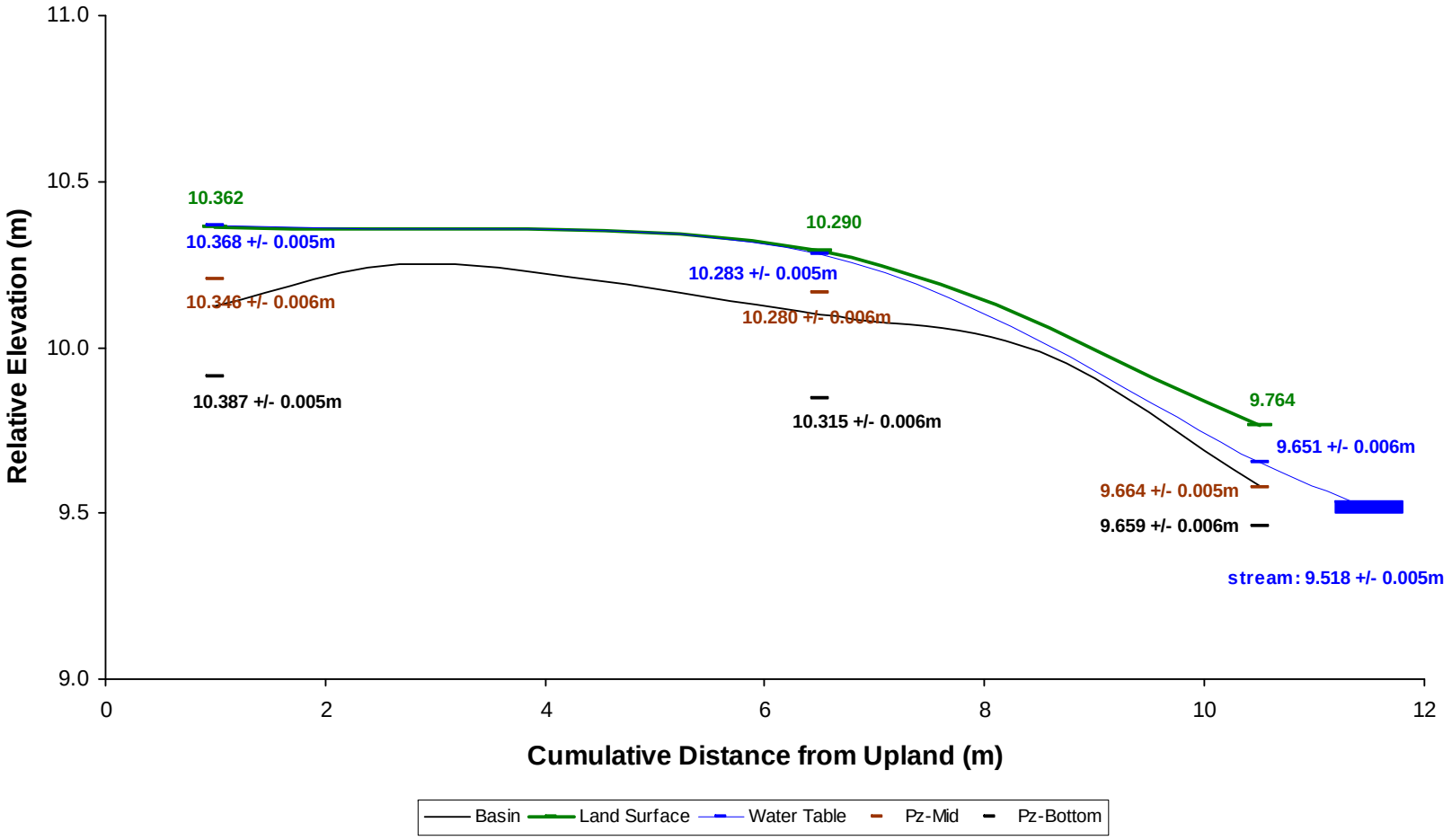

Appendix B.1.g.i. Hydrologic cross section for a shallow peat riparian wetland, (Site SPR_SLR), June (spring).

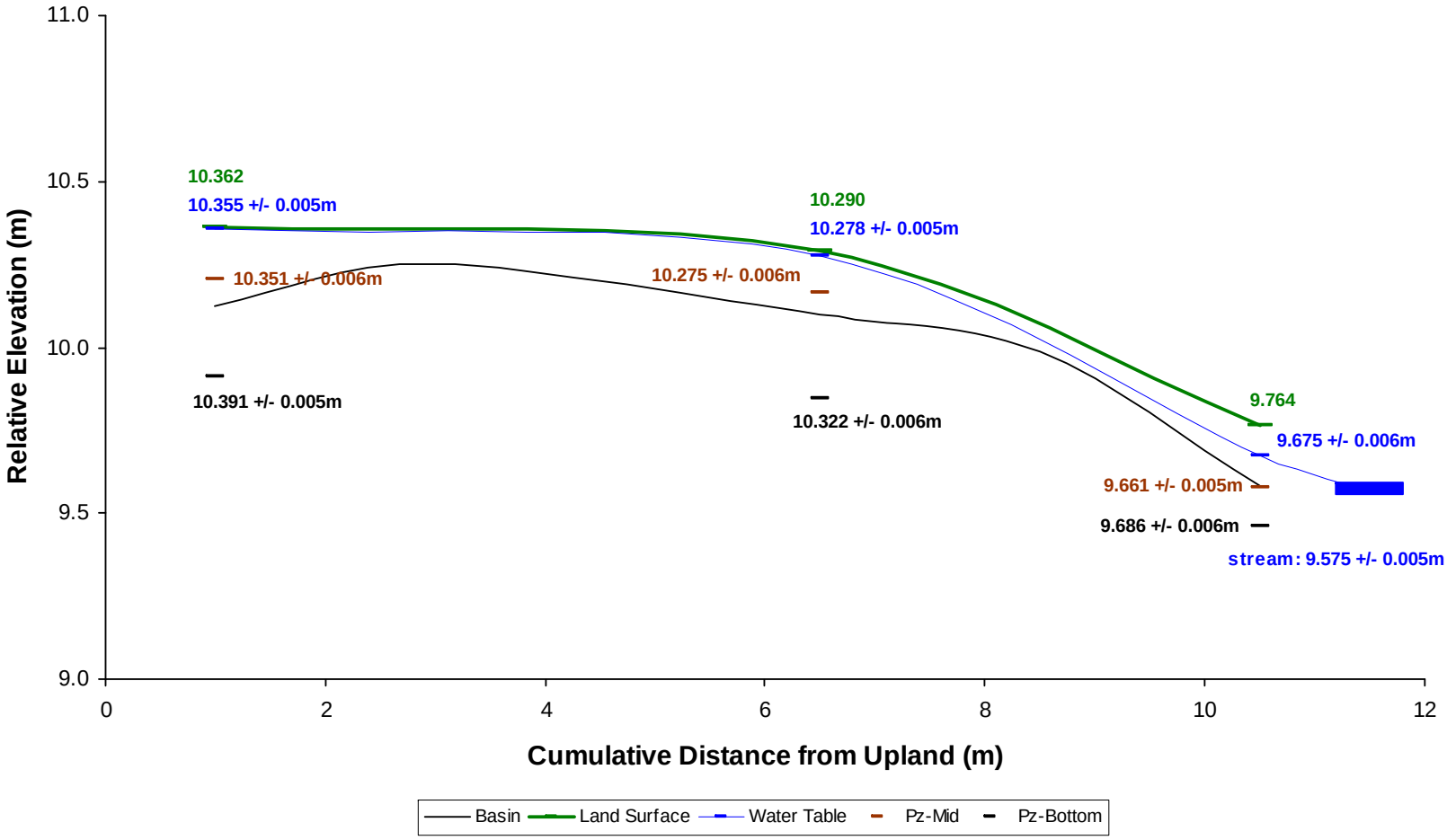

Appendix B.1.g.ii. Hydrologic cross section and flow net for a shallow peat riparian wetland, (Site SPR_SLR), June (spring).

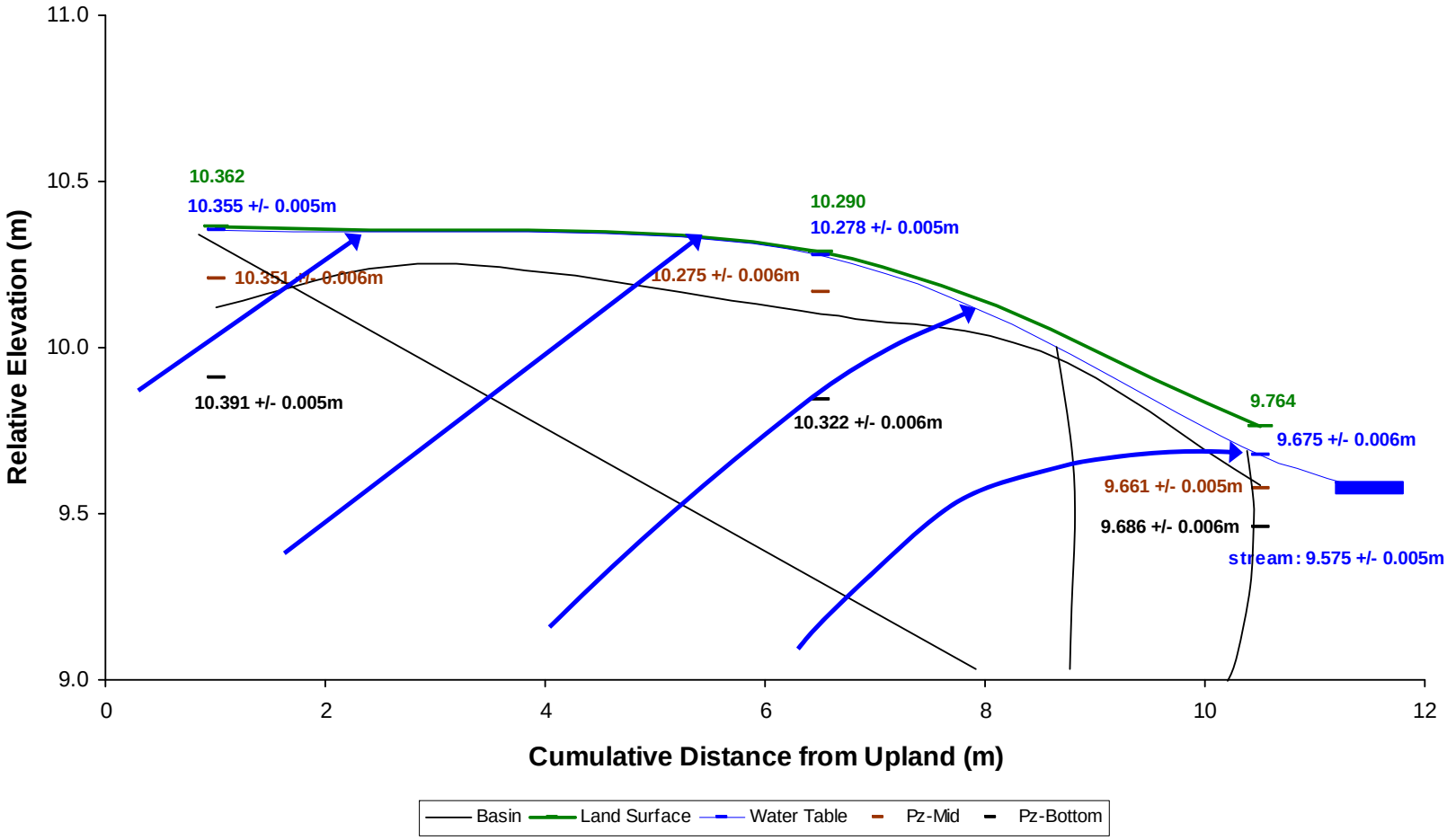

Appendix B.1.h. Hydrologic cross section for a shallow peat riparian wetland, (Site SPR_SLR), August (summer).

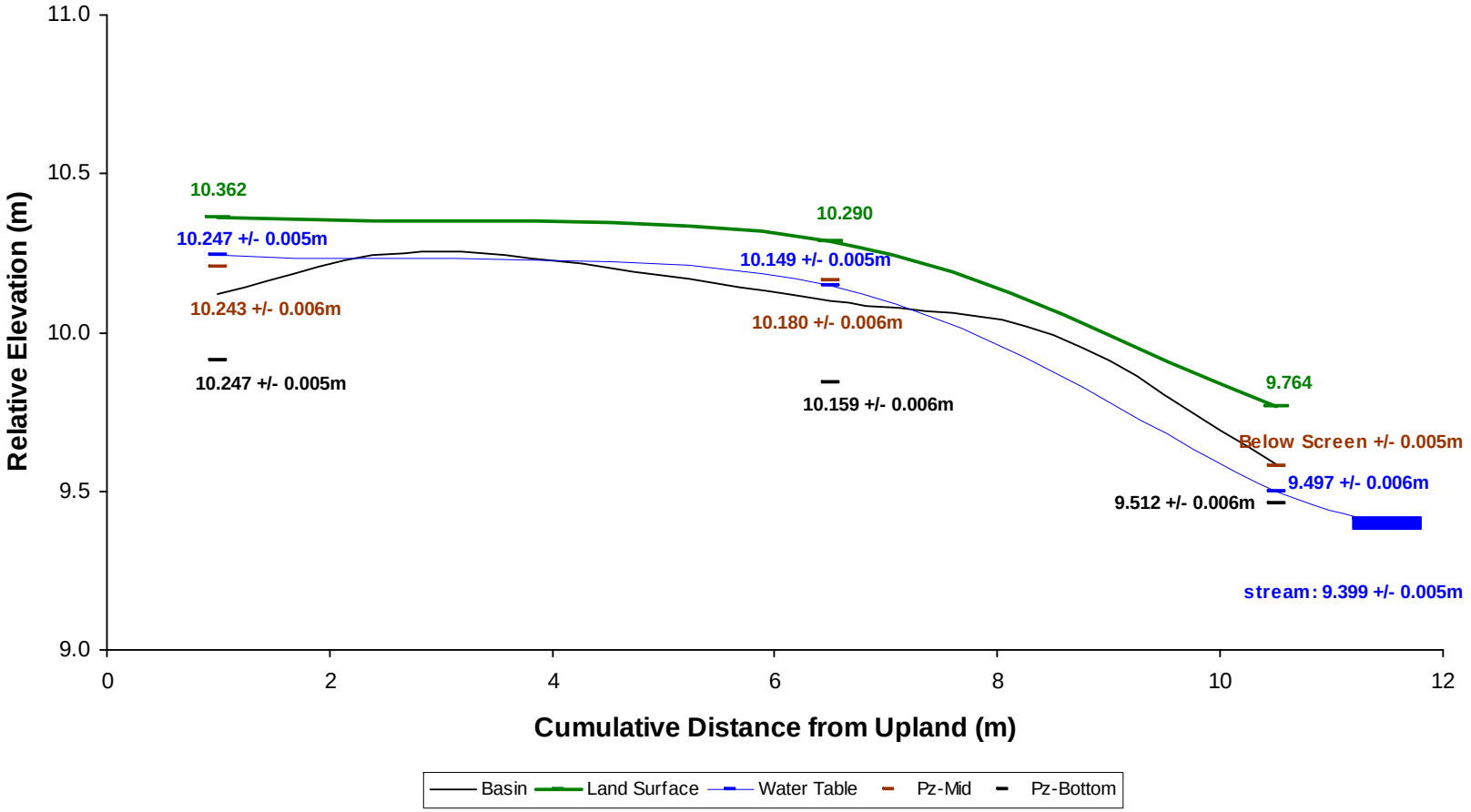

Appendix B.1.i.i. Hydrologic cross section for a shallow peat riparian wetland, (Site SPR_SLR), September (pre-senescence).

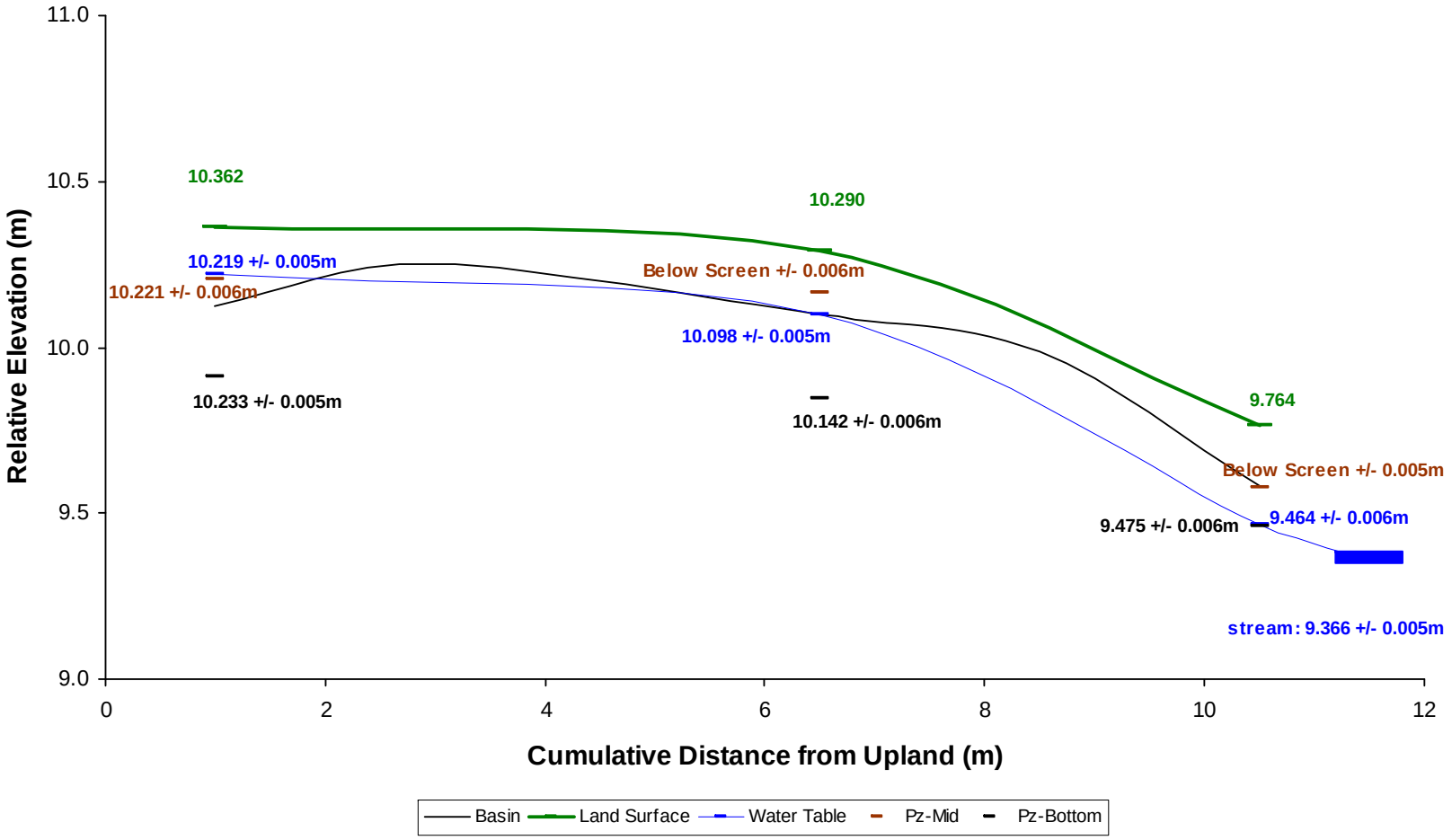

Appendix B.1.i.ii. Hydrologic cross section and flow net for a shallow peat riparian wetland, (Site SPR_SLR), September (pre-senescence).

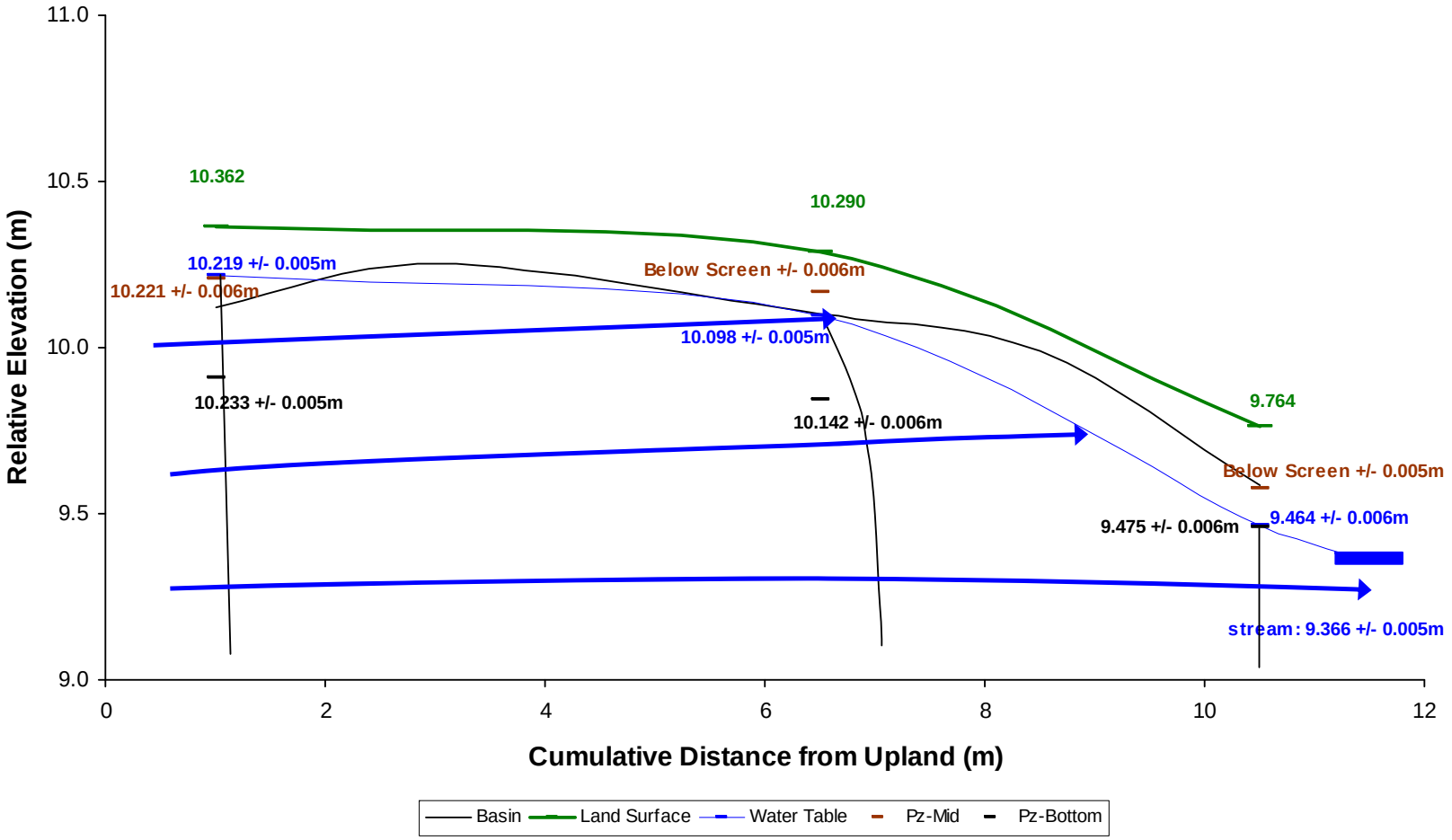

Appendix B.1.j. Hydrologic cross section for a shallow peat riparian wetland, (Site SPR_SLR), November/December (post-senescence).

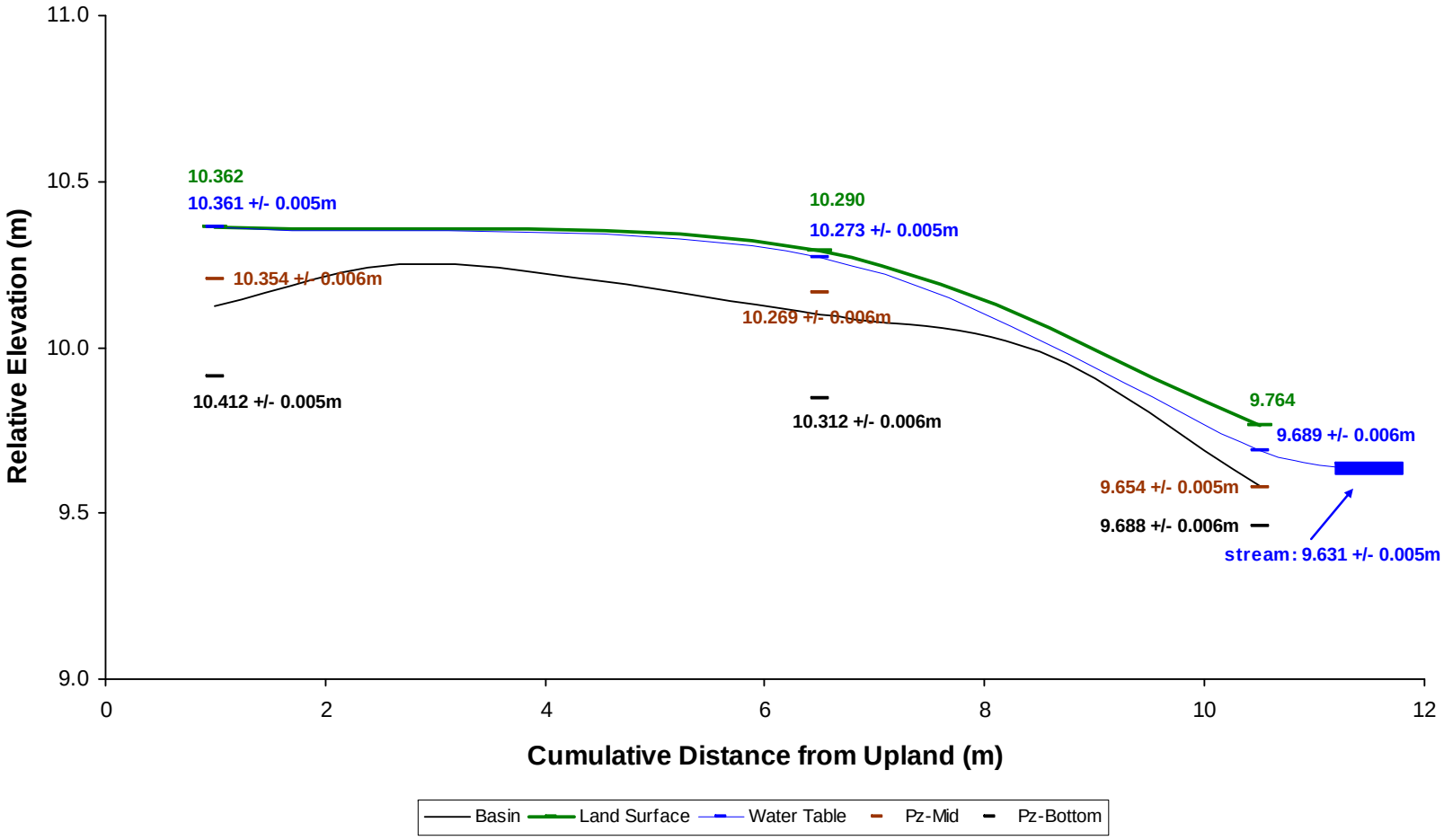

Appendix B.2.a.i. Hydrologic cross section for a deep peat riparian wetland, (Site DPR_MR), April (end of snowmelt).

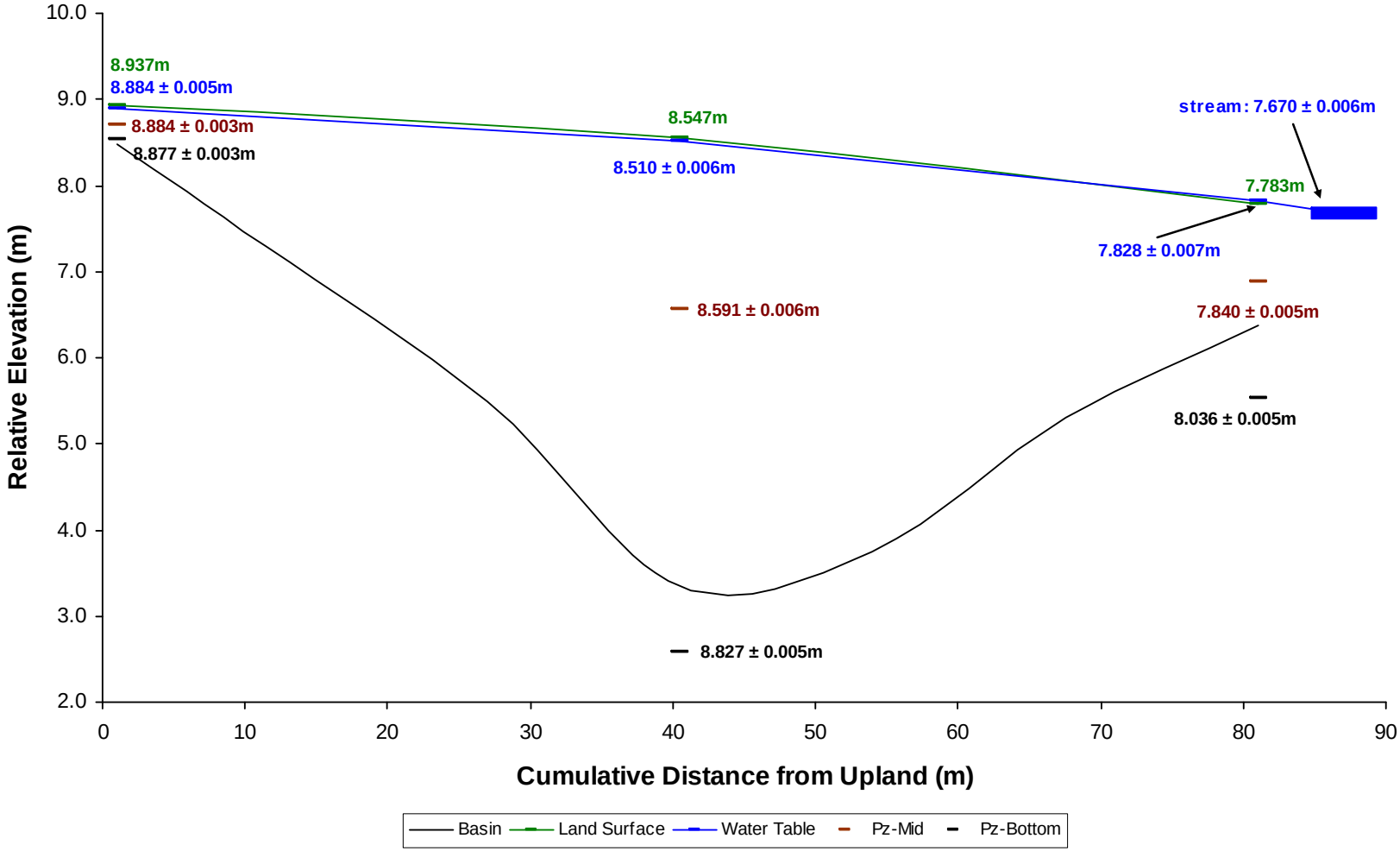

Appendix B.2.a.ii. Hydrologic cross section and flow net for a deep peat riparian wetland, (Site DPR_MR), April (end of snowmelt).

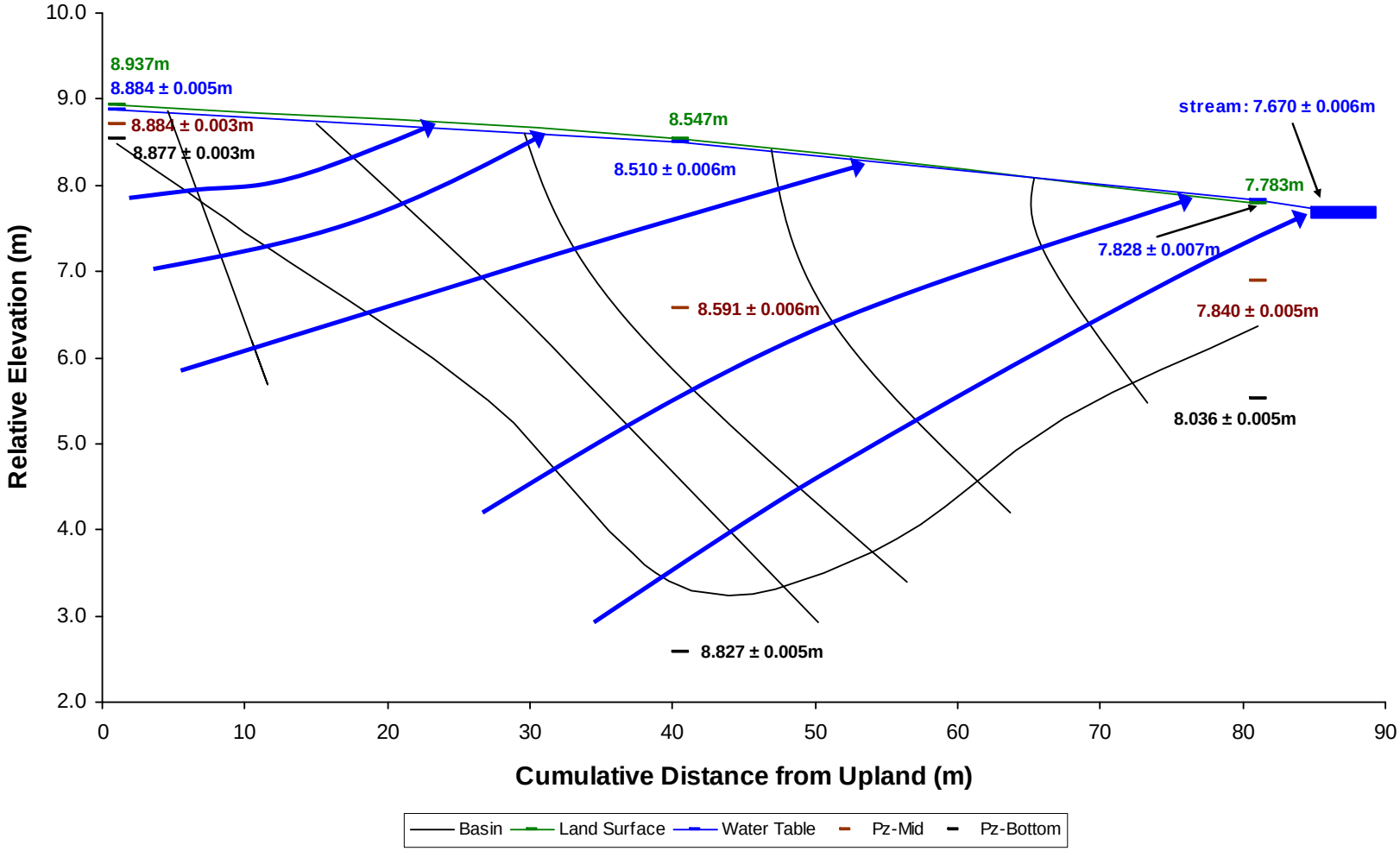

Appendix B.2.b. Hydrologic cross section for a deep peat riparian wetland, (Site DPR_MR), June (spring).

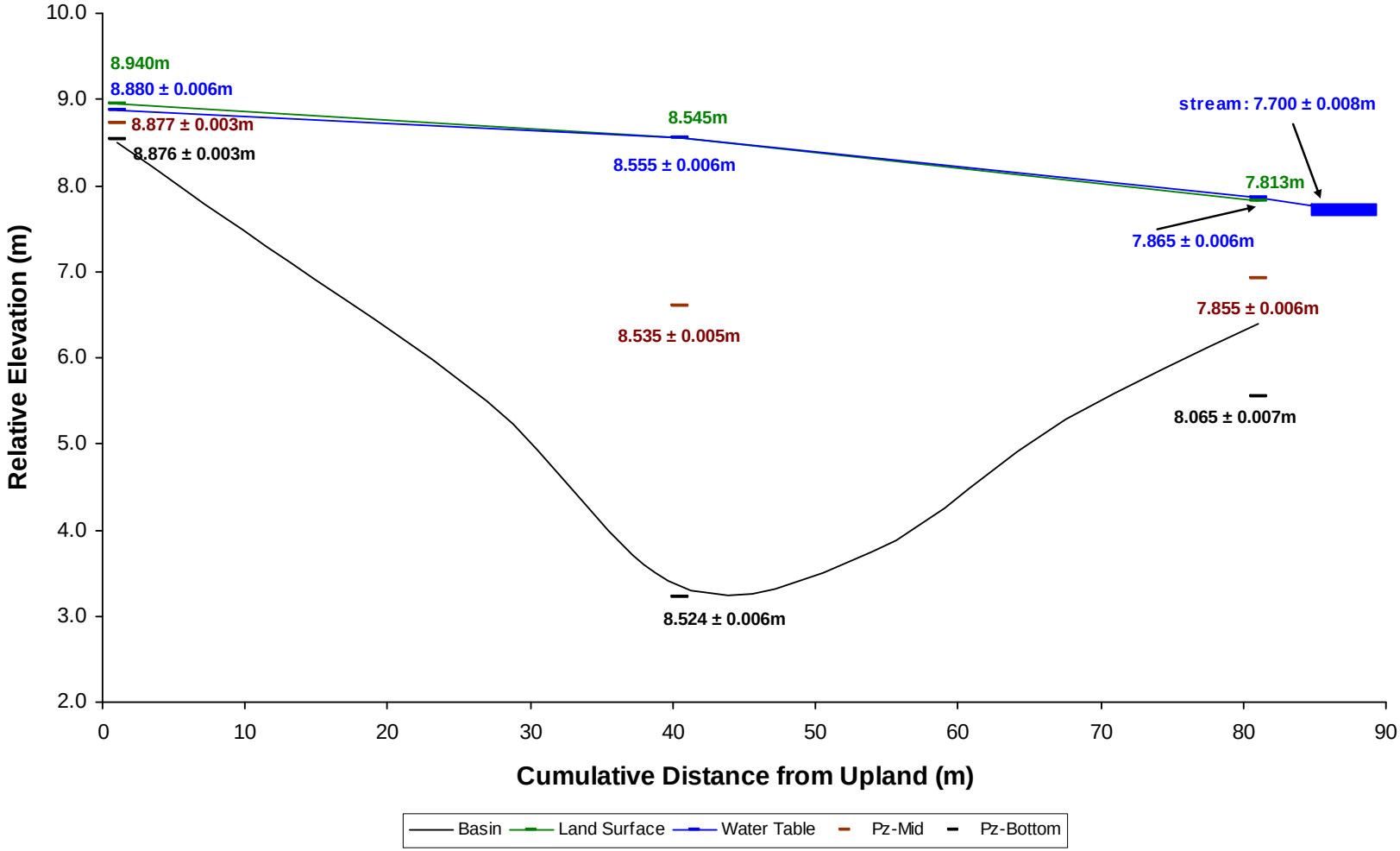

Appendix B.2.c. Hydrologic cross section for a deep peat riparian wetland, (Site DPR_MR), August (summer).

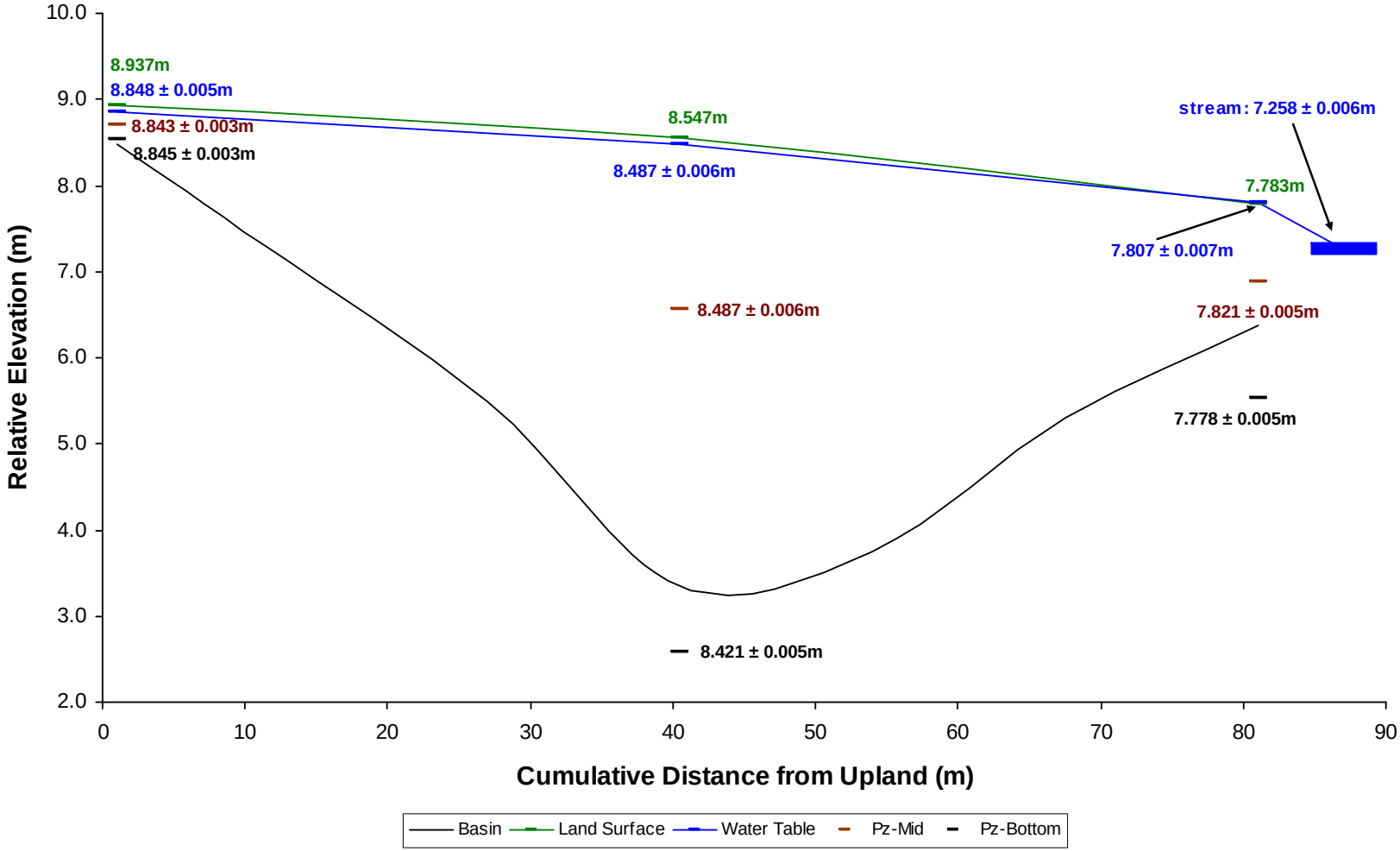

Appendix B.2.d.i Hydrologic cross section for a deep peat riparian wetland, (Site DPR_MR), September (pre-senescence).

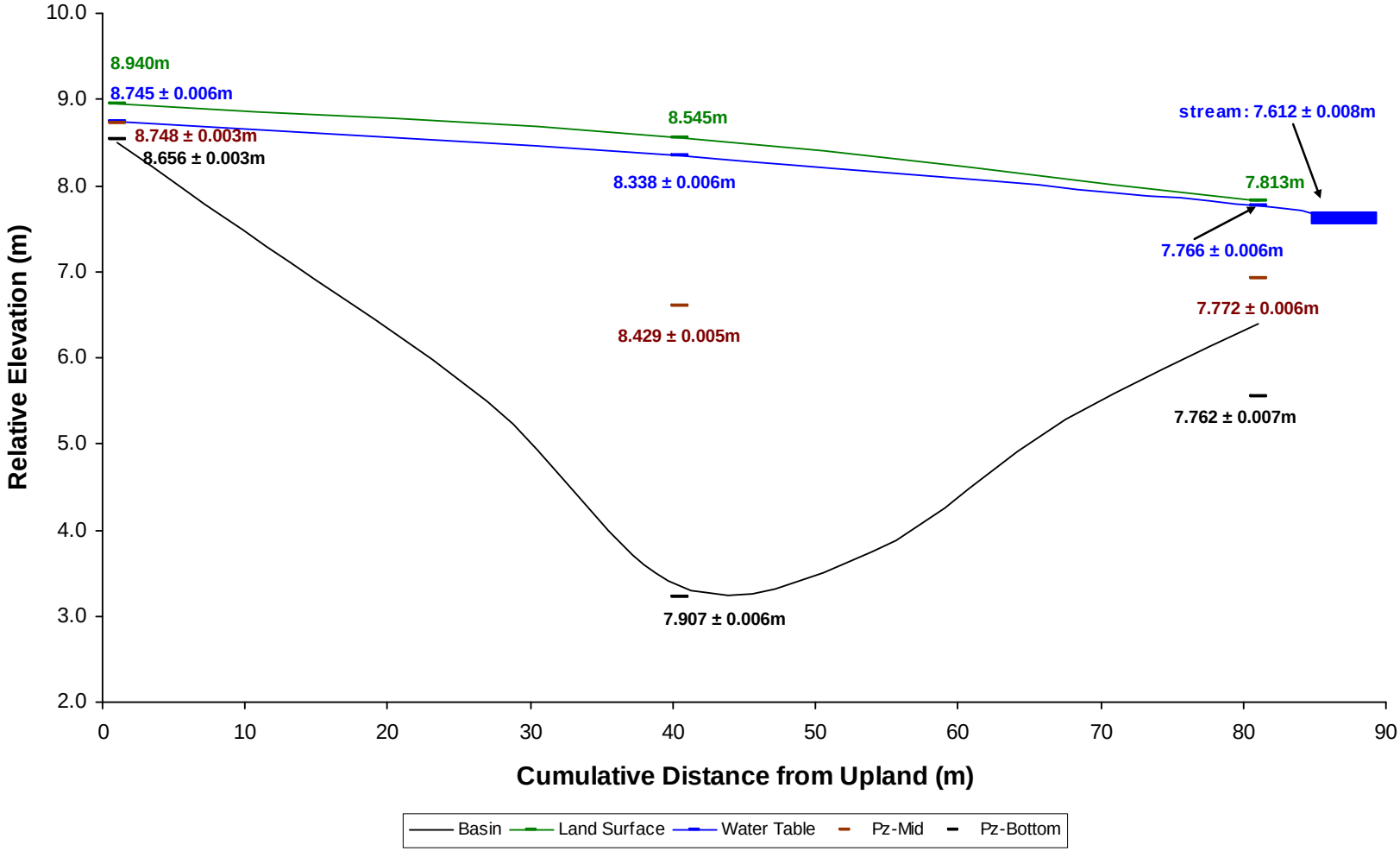

Appendix B.2.d.ii. Hydrologic cross section and flow net for a deep peat riparian wetland, (Site DPR_MR), September (pre-senescence).

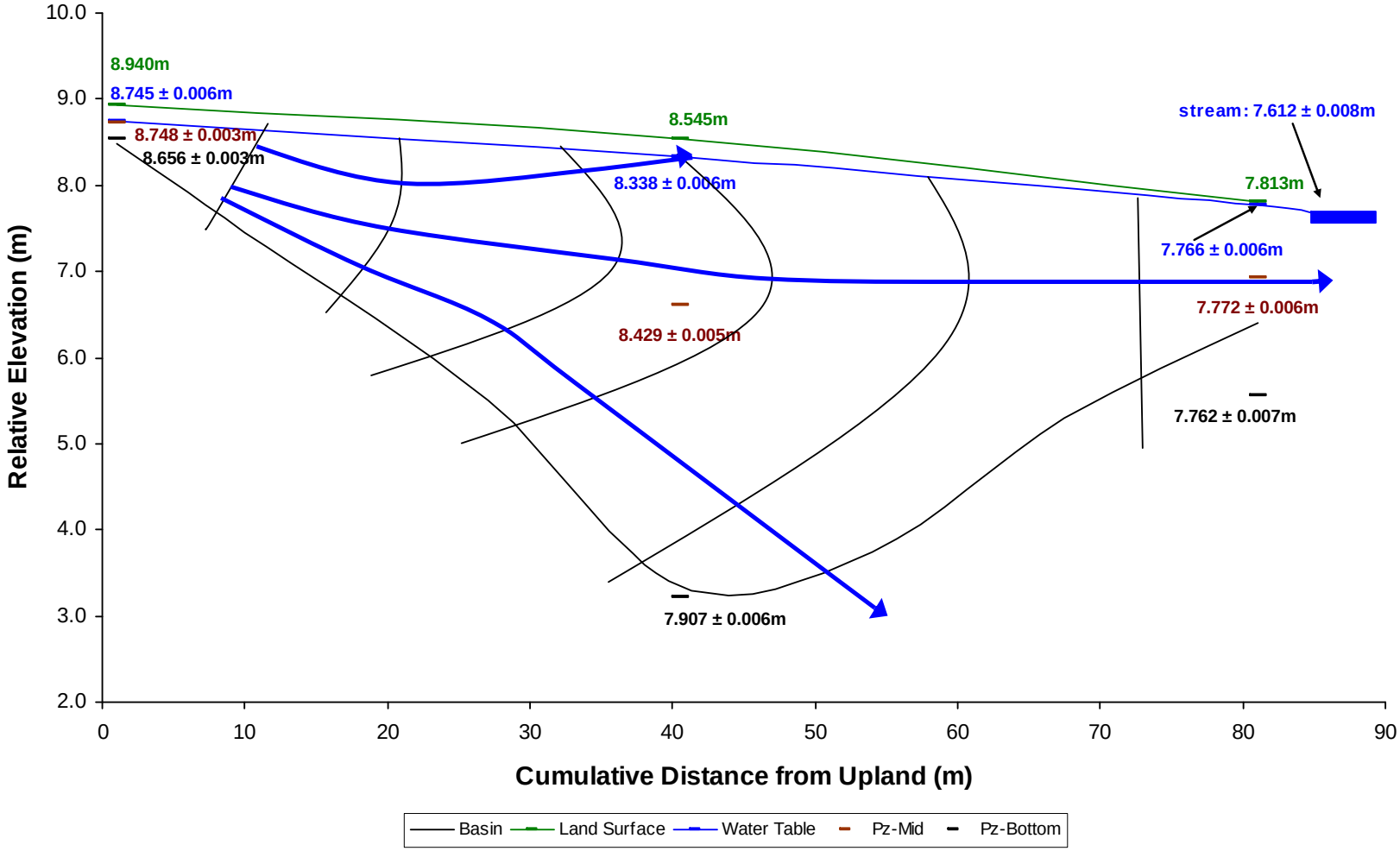

Appendix B.2.e. Hydrologic cross section for a deep peat riparian wetland, (Site DPR_MR), November/December (post-senescence).

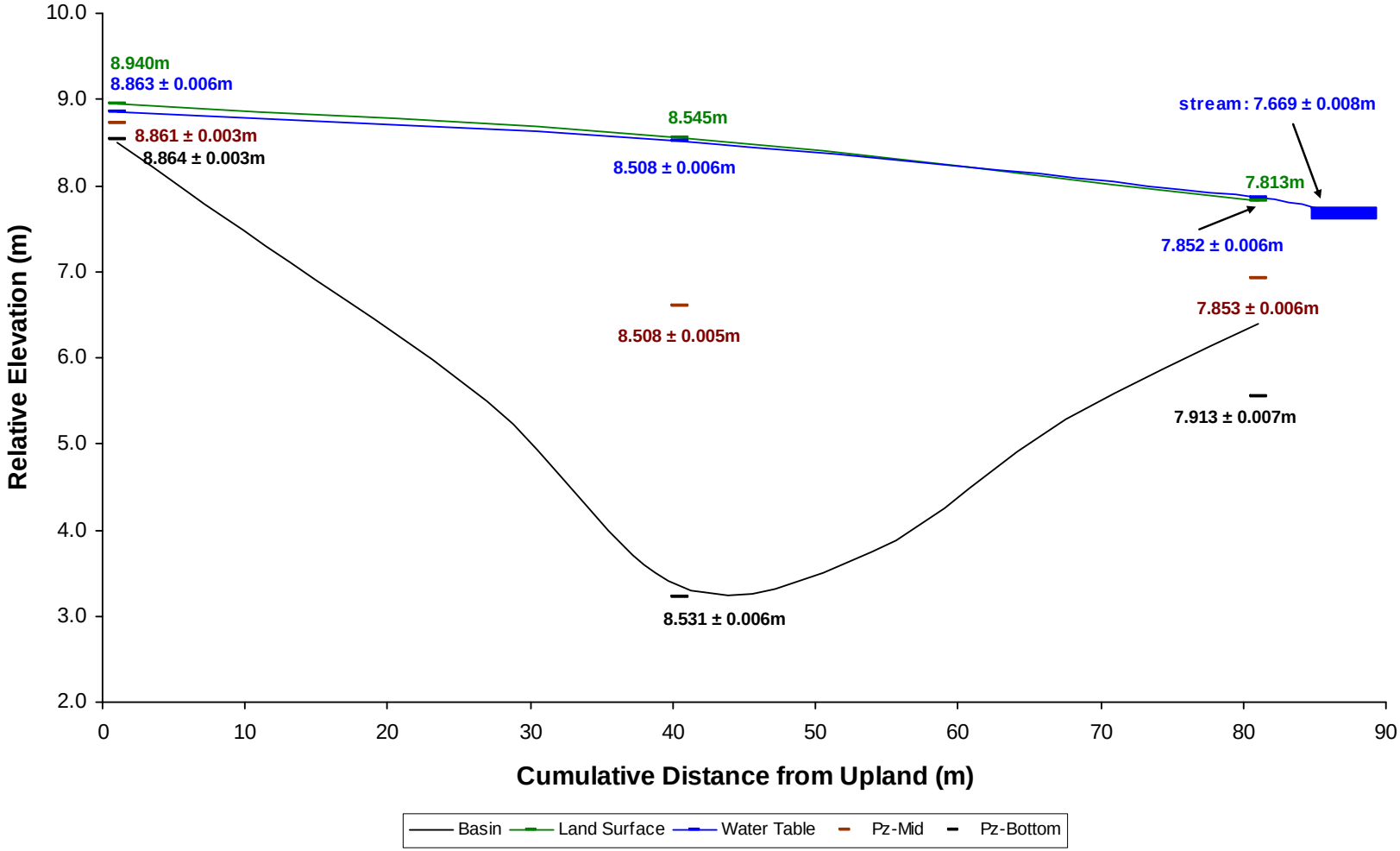

Appendix B.2.f.i. Hydrologic cross section for a deep peat riparian wetland, (Site DPR_BR), April (end of snowmelt).

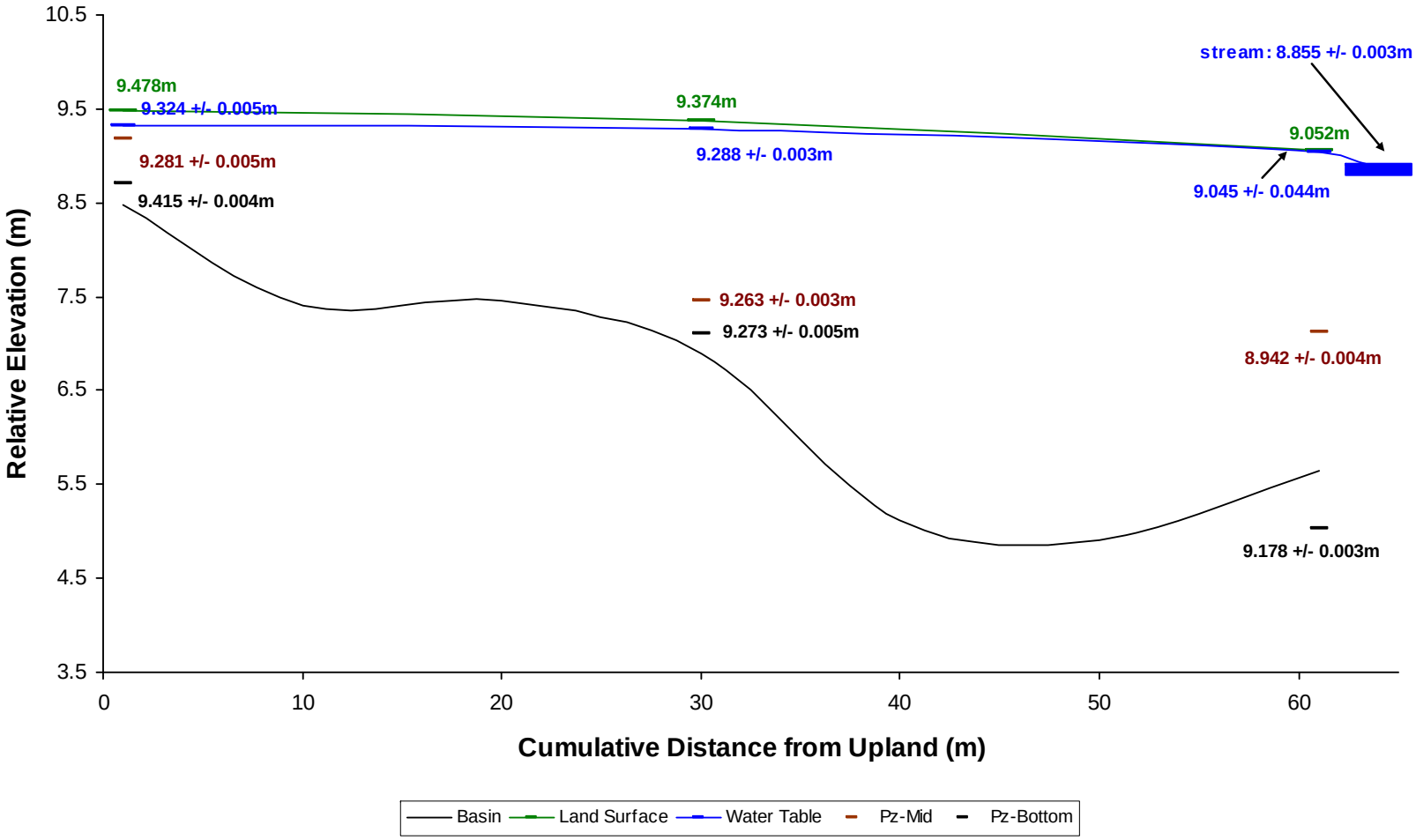

Appendix B.2.f.ii. Hydrologic cross section and flow net for a deep peat riparian wetland, (Site DPR_BR), April (end of snowmelt).

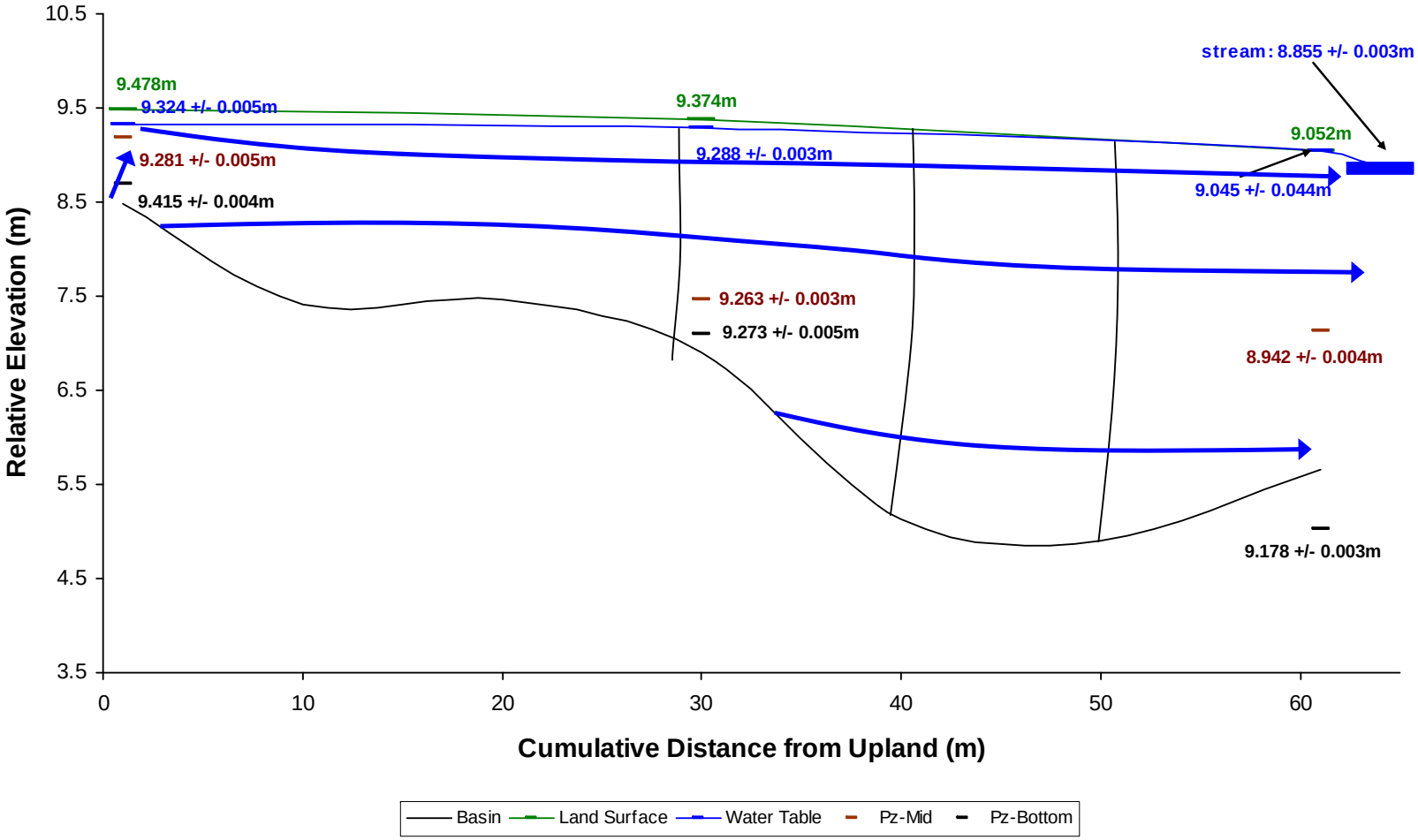

Appendix B.2.g. Hydrologic cross section for a deep peat riparian wetland, (Site DPR_BR), June (spring).

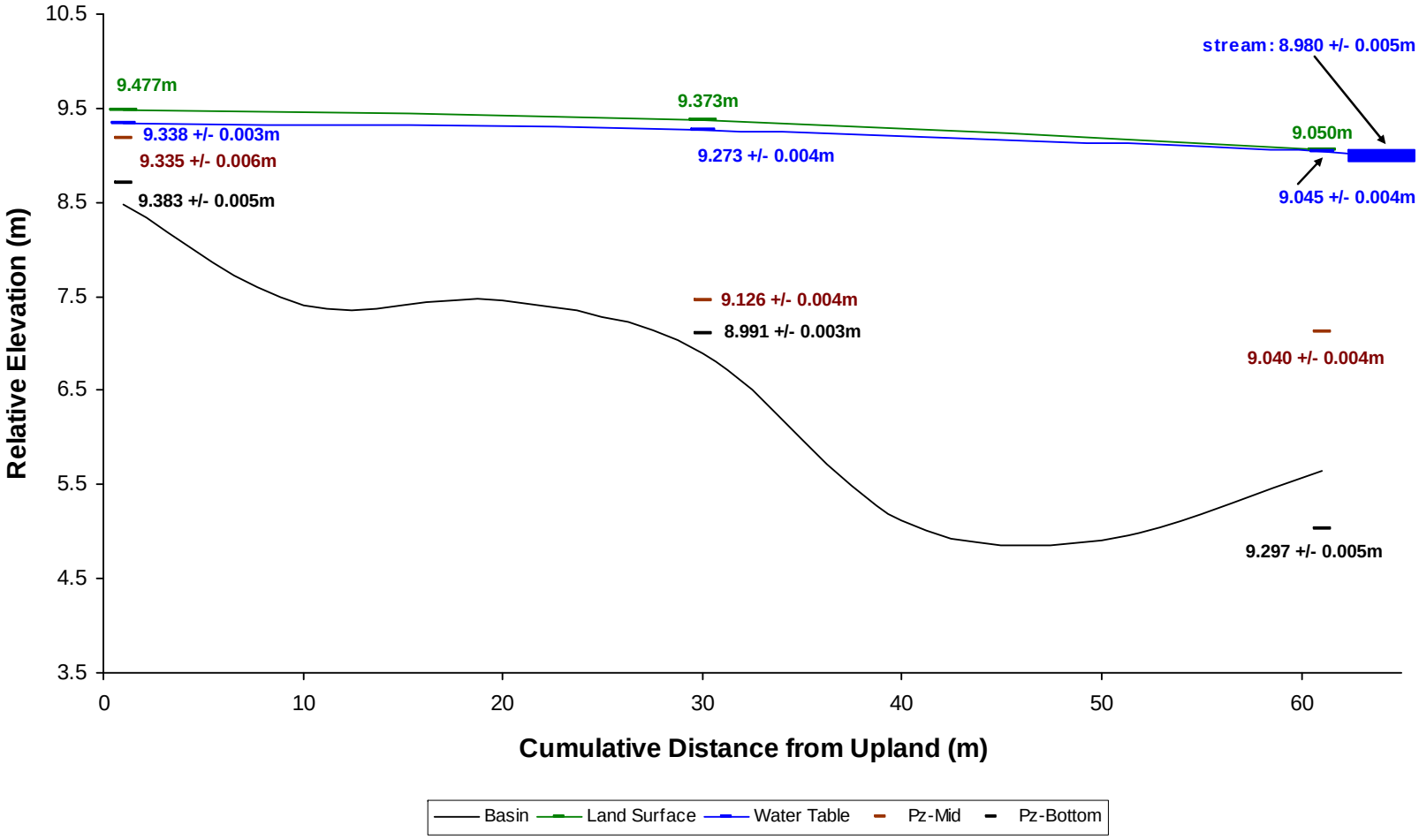

Appendix B.2.h. Hydrologic cross section for a deep peat riparian wetland, (Site DPR_BR), August (summer).

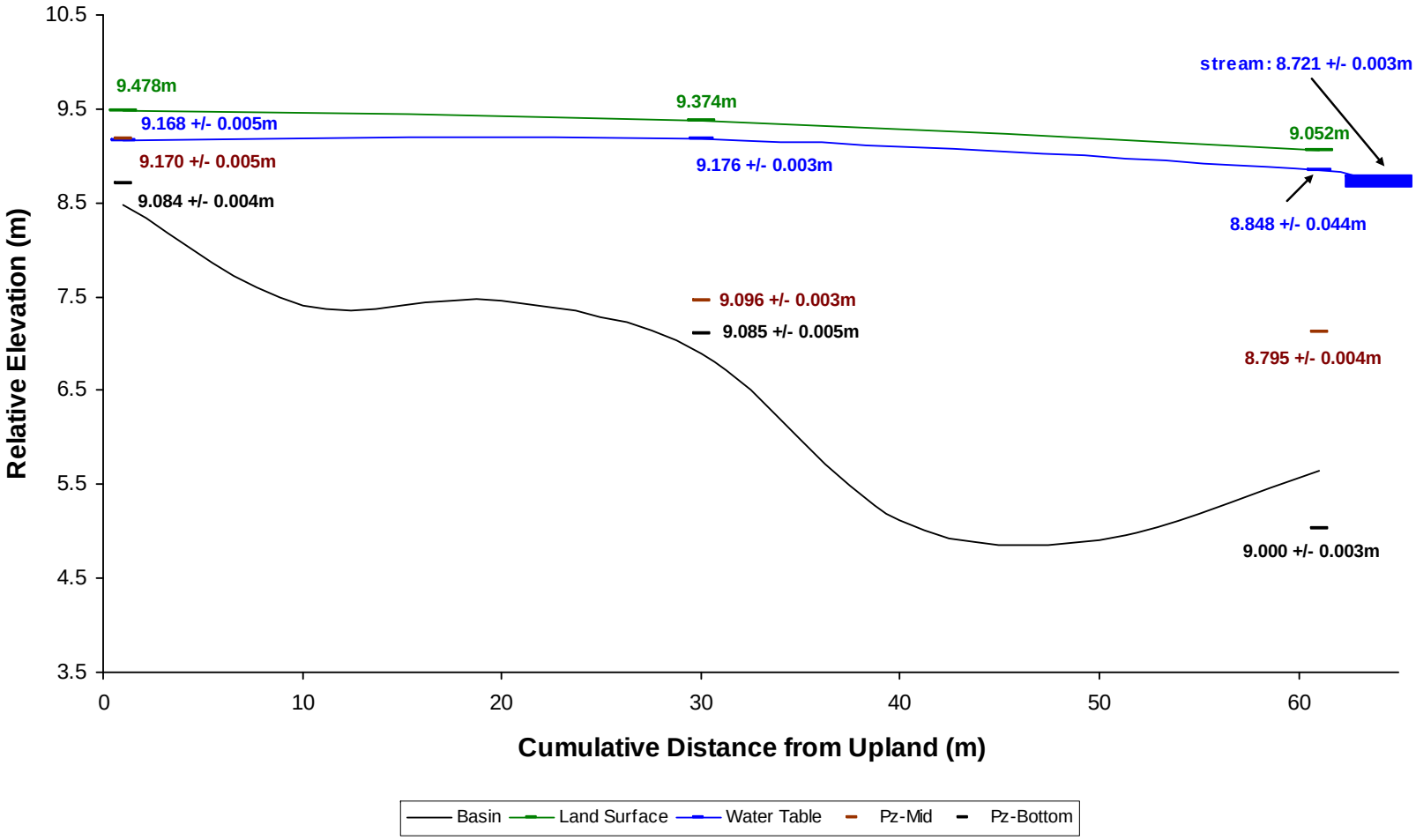

Appendix B.2.i.i. Hydrologic cross section for a deep peat riparian wetland, (Site DPR_BR), September (pre-senescence).

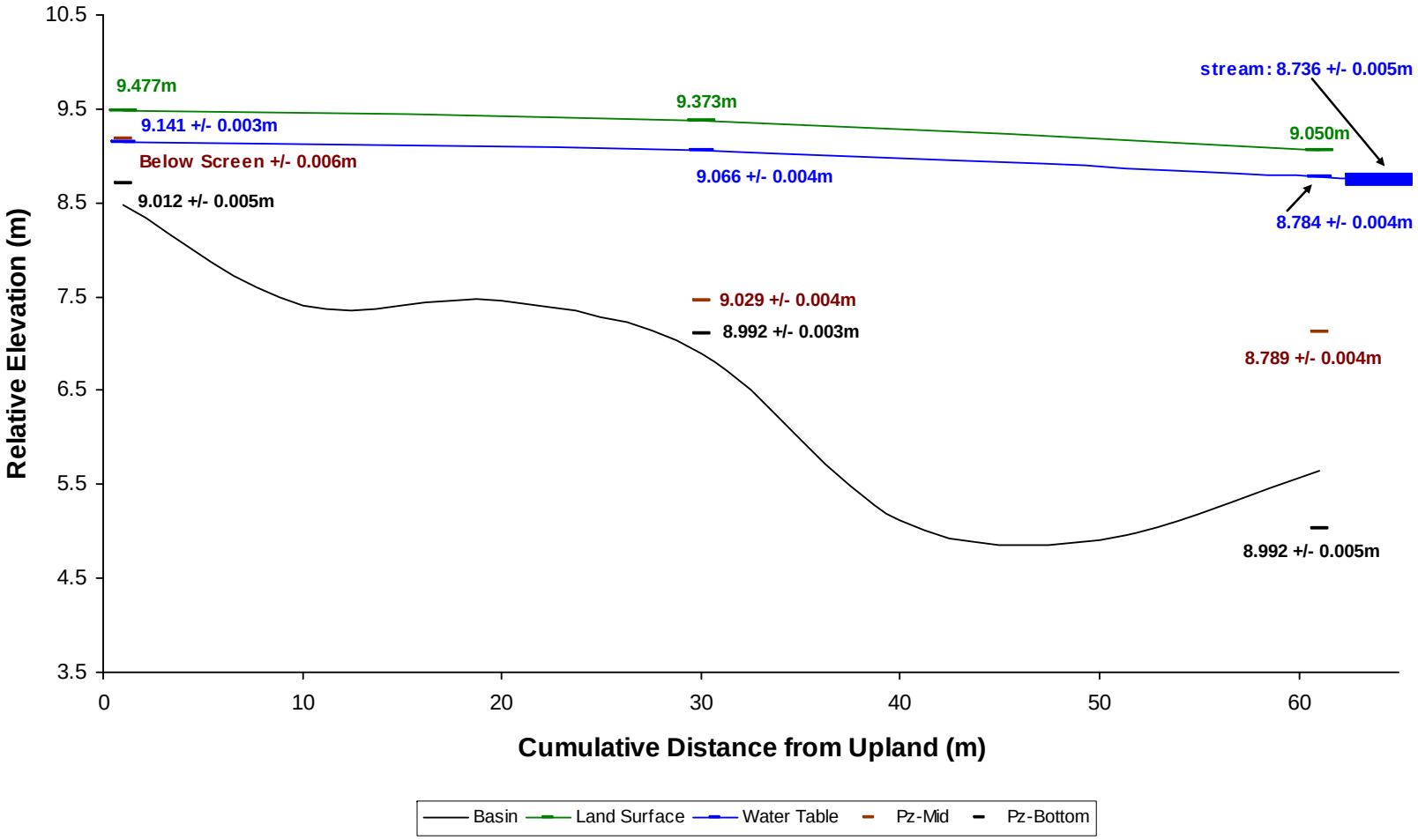

Appendix B.2.i.ii. Hydrologic cross section and flow net for a deep peat riparian wetland, (Site DPR_BR), September (pre-senescence).

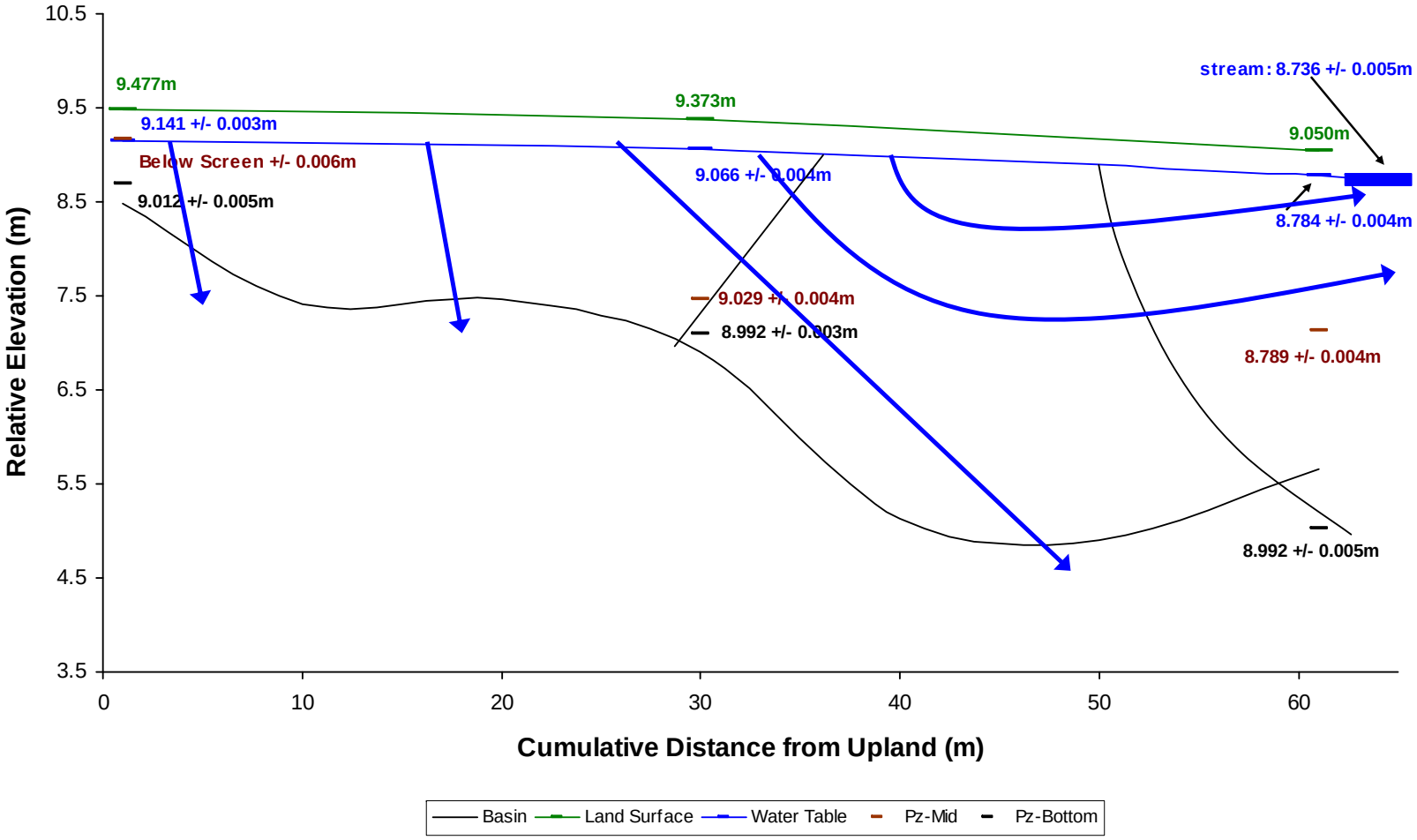

Appendix B.2.j. Hydrologic cross section for a deep peat riparian wetland, (Site DPR_BR), November/December (post-senescence).

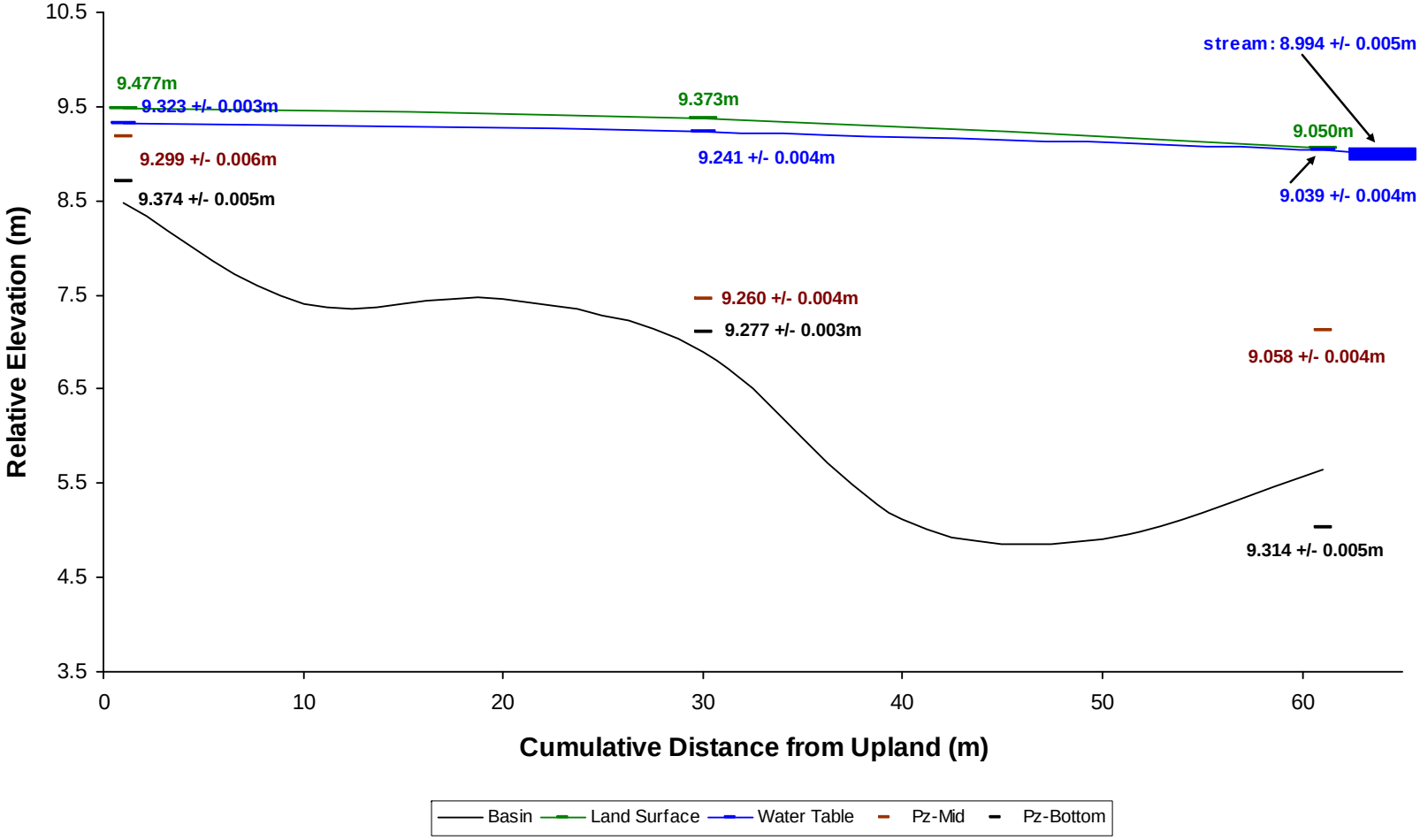

Appendix B.3.a. Hydrologic cross section for a headwater wetland, (Site HW_P), April (end of snowmelt).

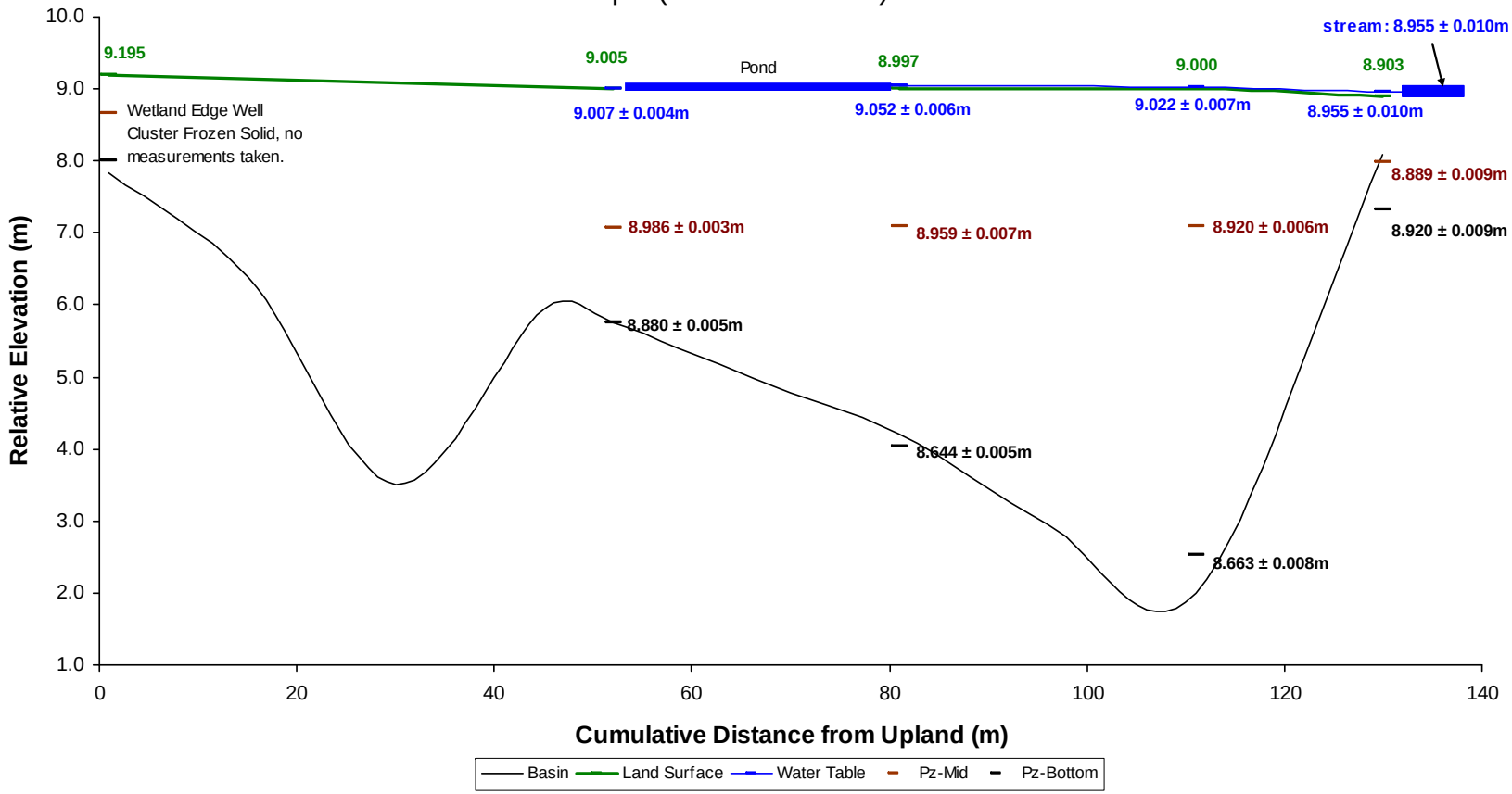

Appendix B.3.b.i. Hydrologic cross section for a headwater wetland, (Site HW_P), June (spring).

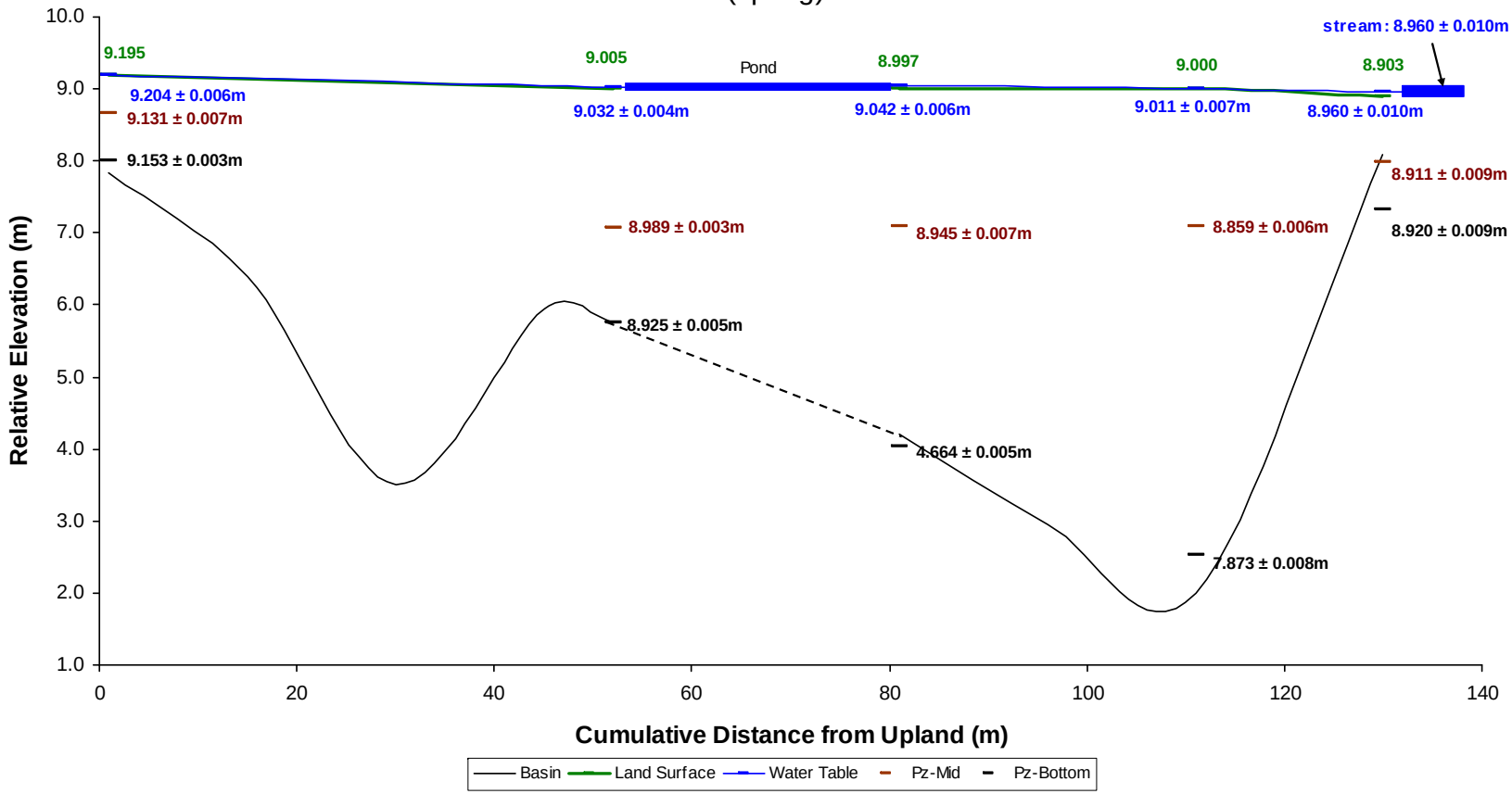

Appendix B.3.b.ii. Hydrologic cross section and flow net for a headwater wetland, (Site HW_P), June (spring).

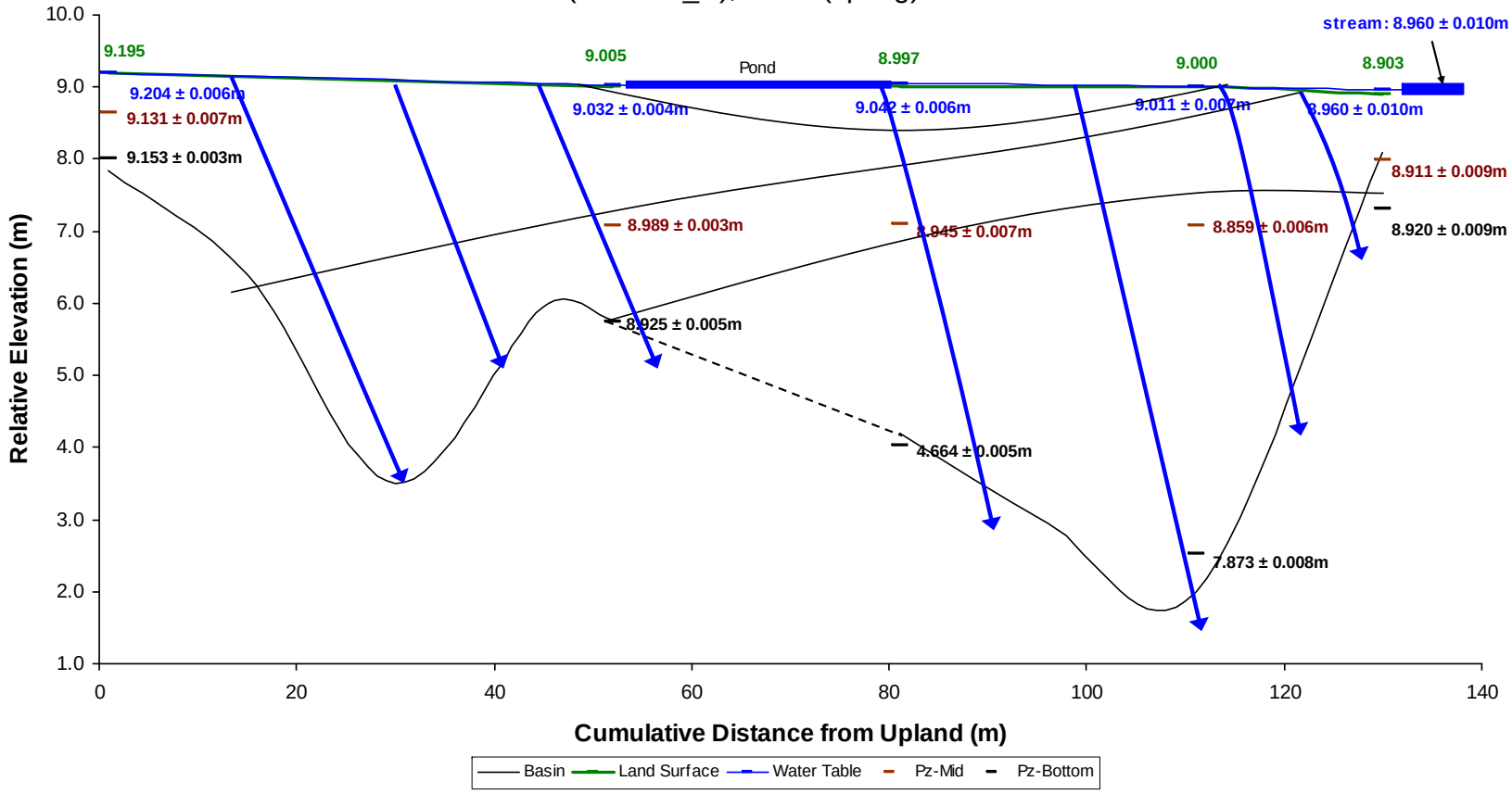

Appendix B.3.c. Hydrologic cross section for a headwater wetland, (Site HW_P), August (summer).

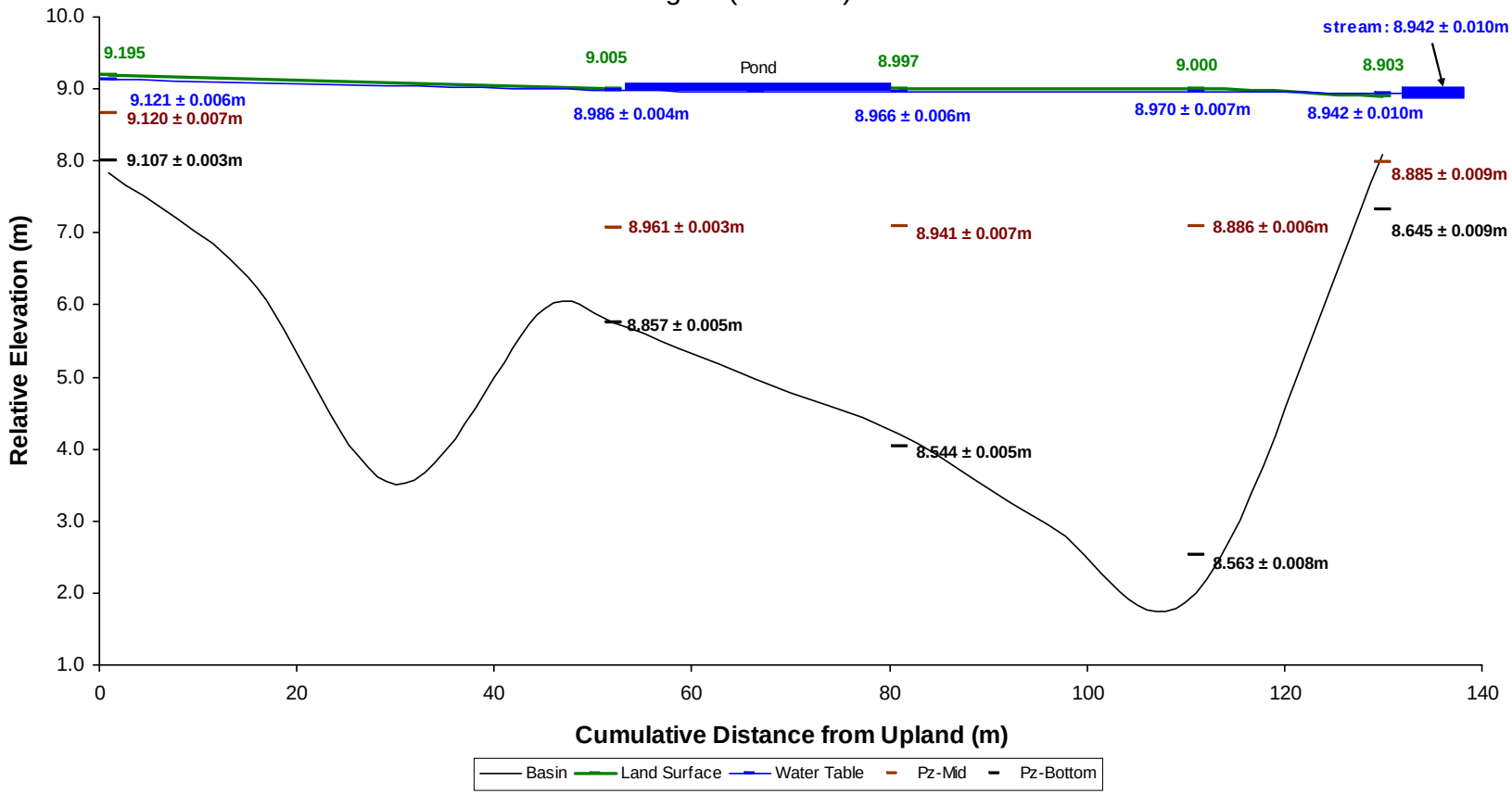

Appendix B.3.d.i. Hydrologic cross section for a headwater wetland, (Site HW_P), September (pre-senescence).

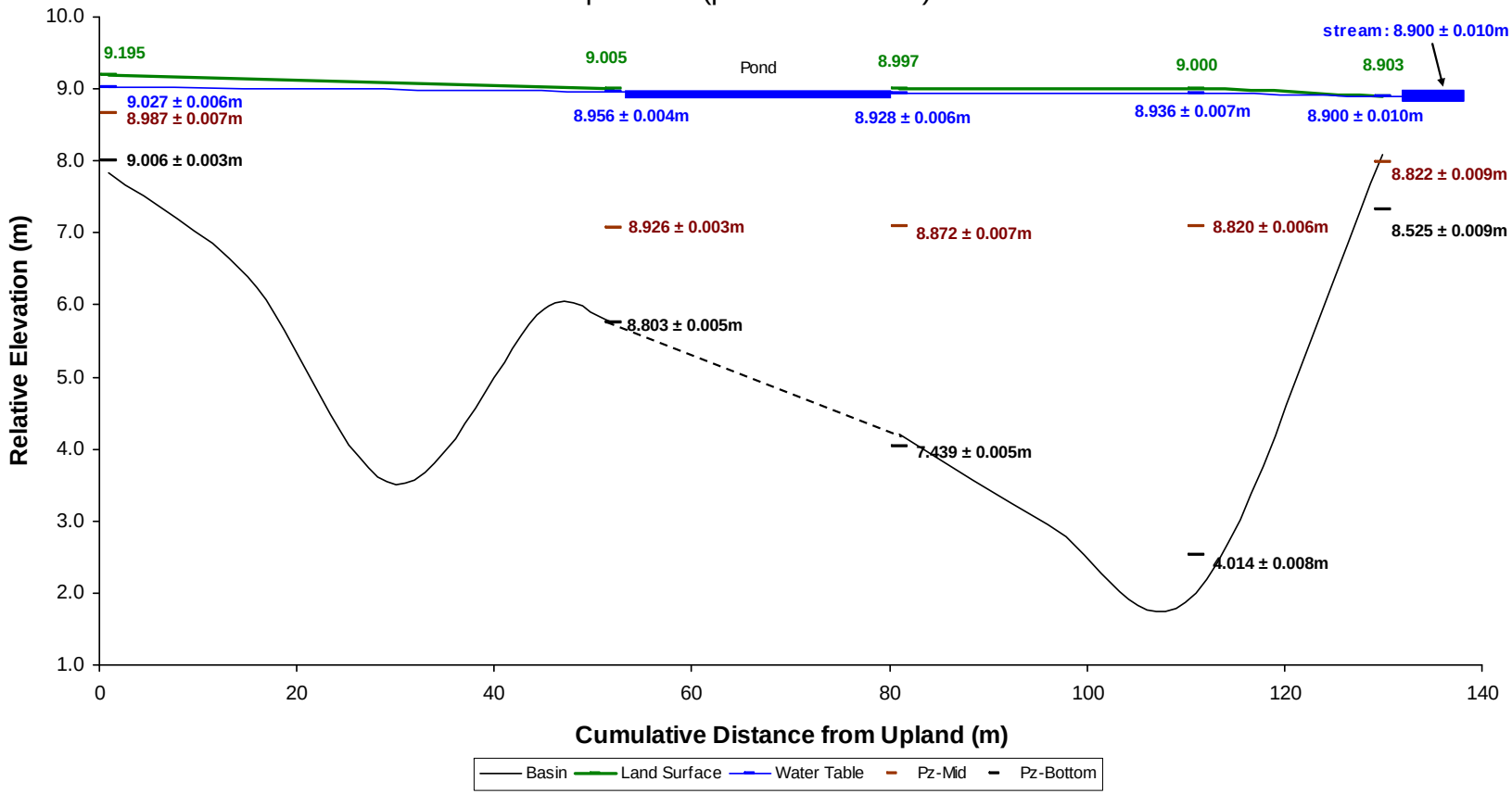

Appendix B.3.d.ii. Hydrologic cross section and flow net for a headwater wetland, (Site HW_P), September (pre-senescence).

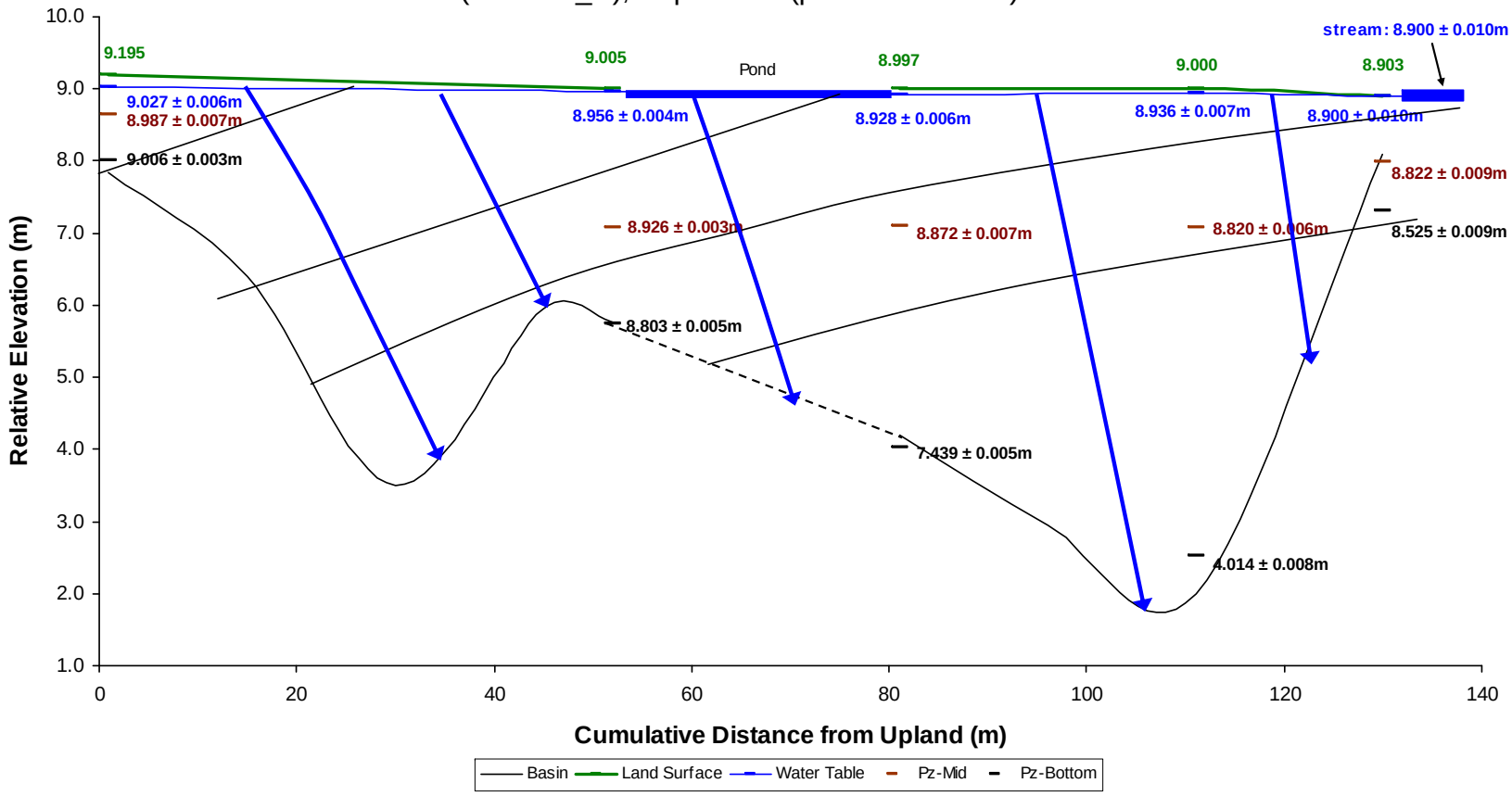

Appendix B.3.e. Hydrologic cross section for a headwater wetland, (Site HW_P), November/December (post-senescence).

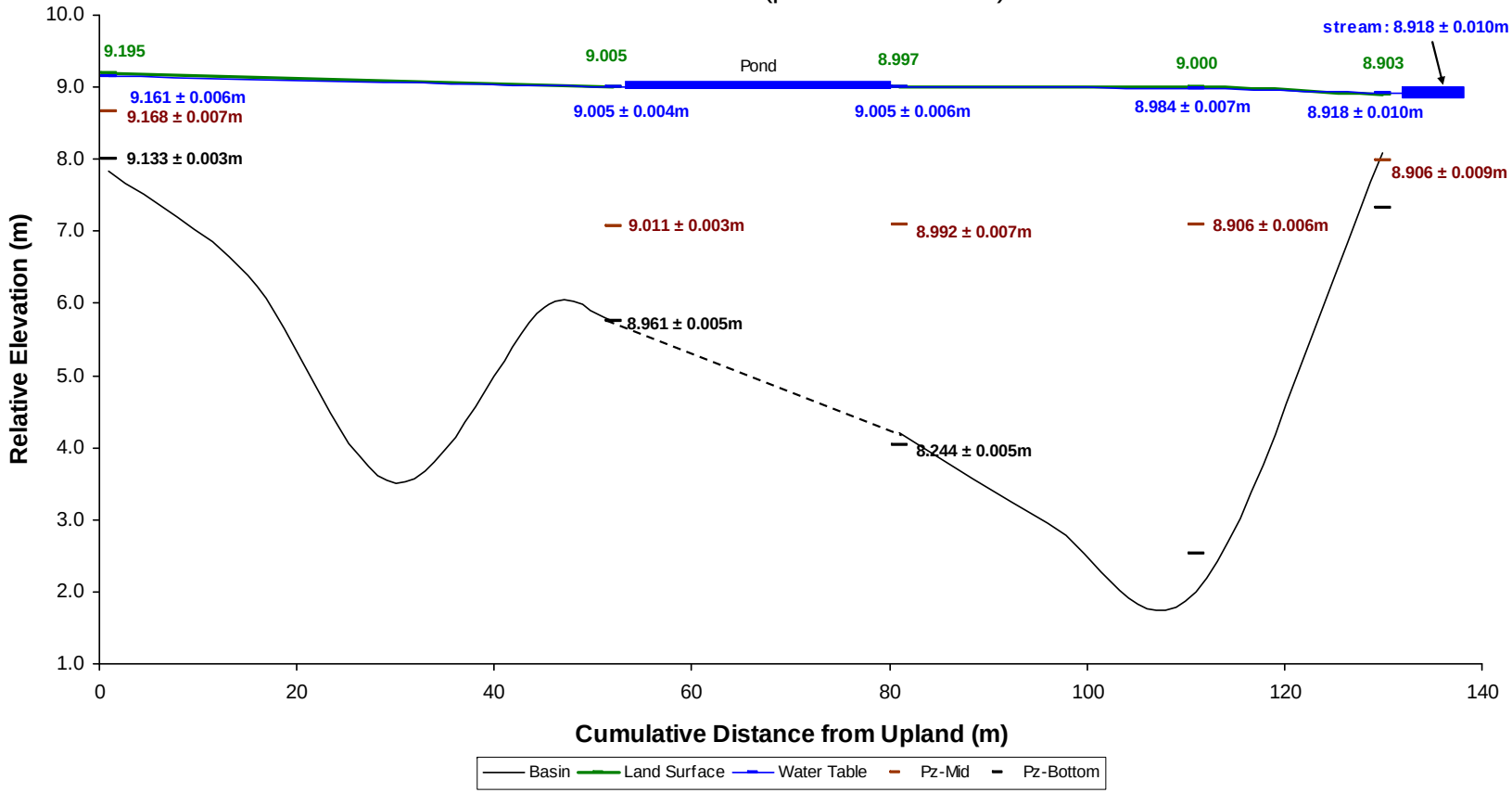

Appendix B.3.f.i. Hydrologic cross section for a headwater wetland, (Site HW_H), April (end of snowmelt).

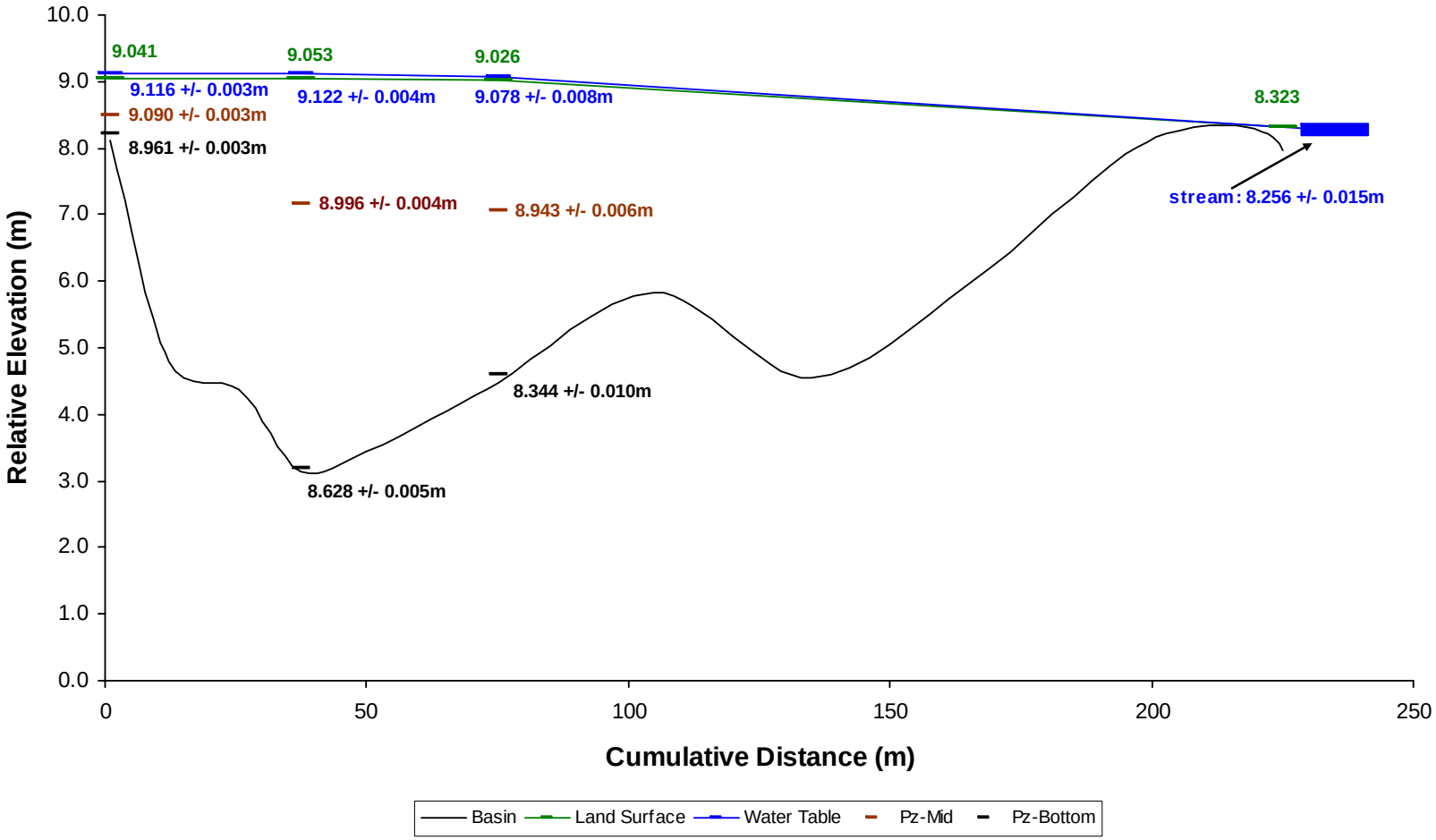

Appendix B.3.f.ii. Hydrologic cross section and flow net for a headwater wetland, (Site HW_H), April (end of snowmelt).

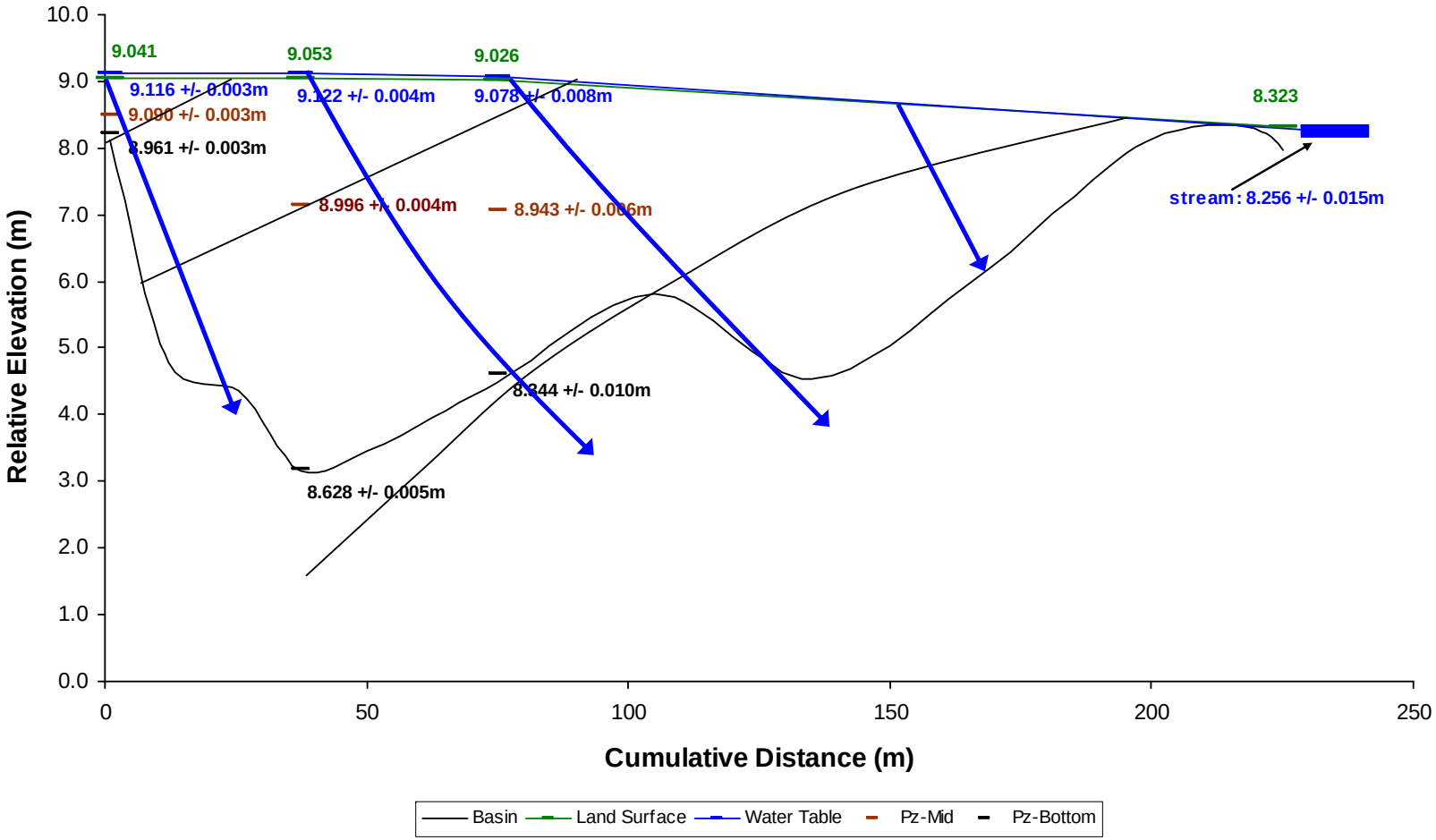

Appendix B.3.g. Hydrologic cross section for a headwater wetland, (Site HW_H), June (spring).

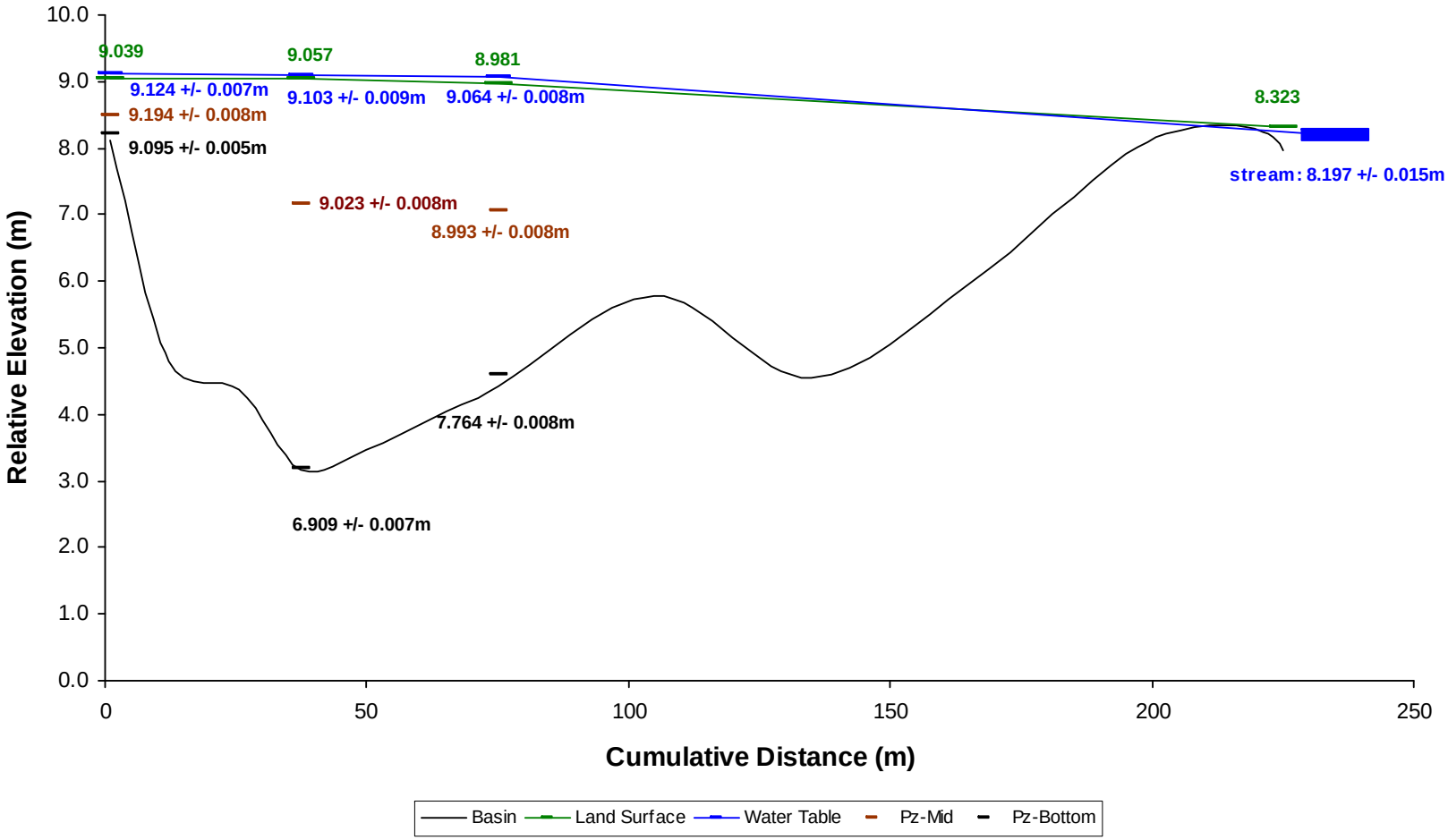

Appendix B.3.h. Hydrologic cross section for a headwater wetland, (Site HW_H), August (summer).

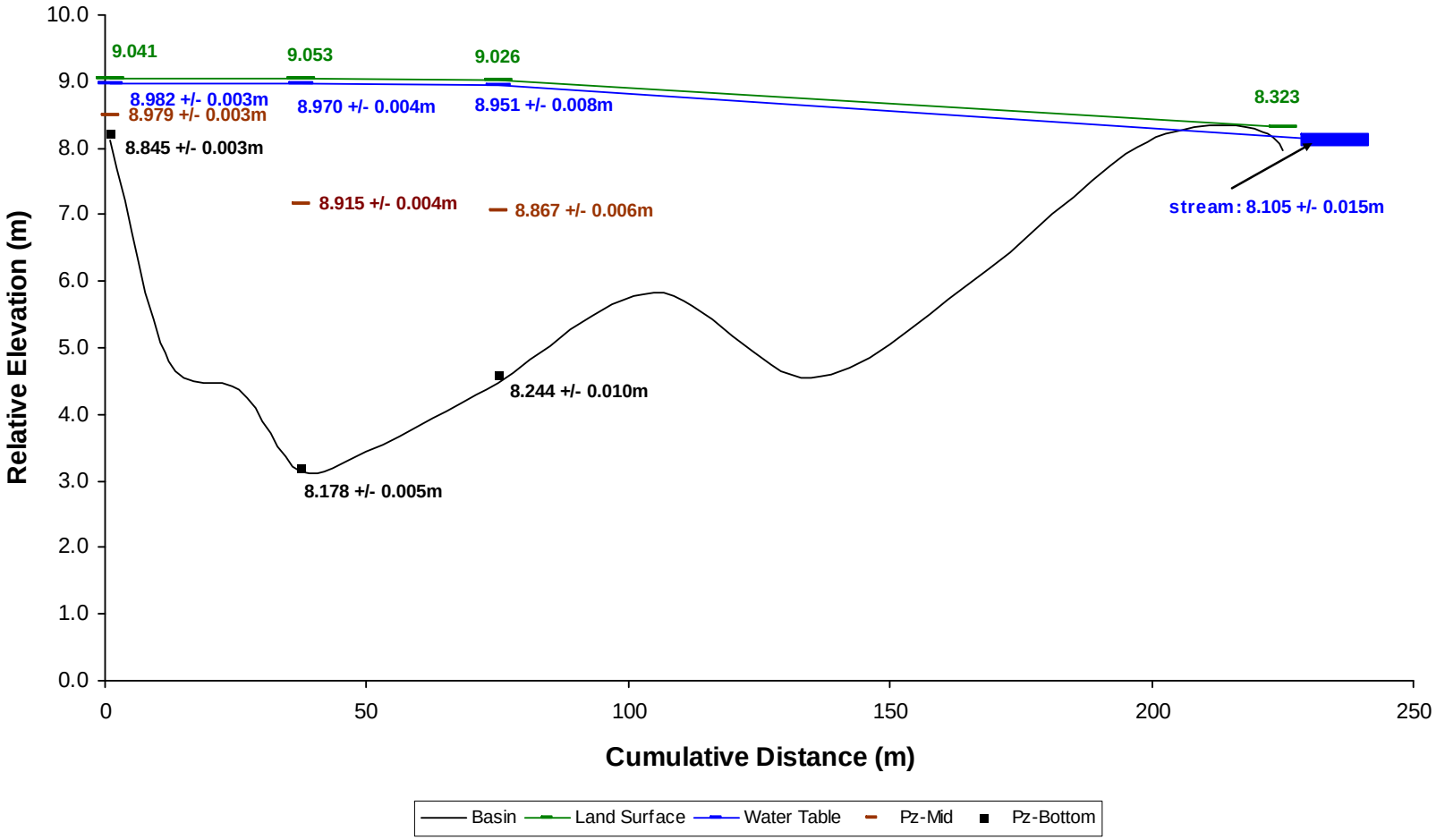

Appendix B.3.i.i. Hydrologic cross section for a headwater wetland, (Site HW_H), September (pre-senescence).

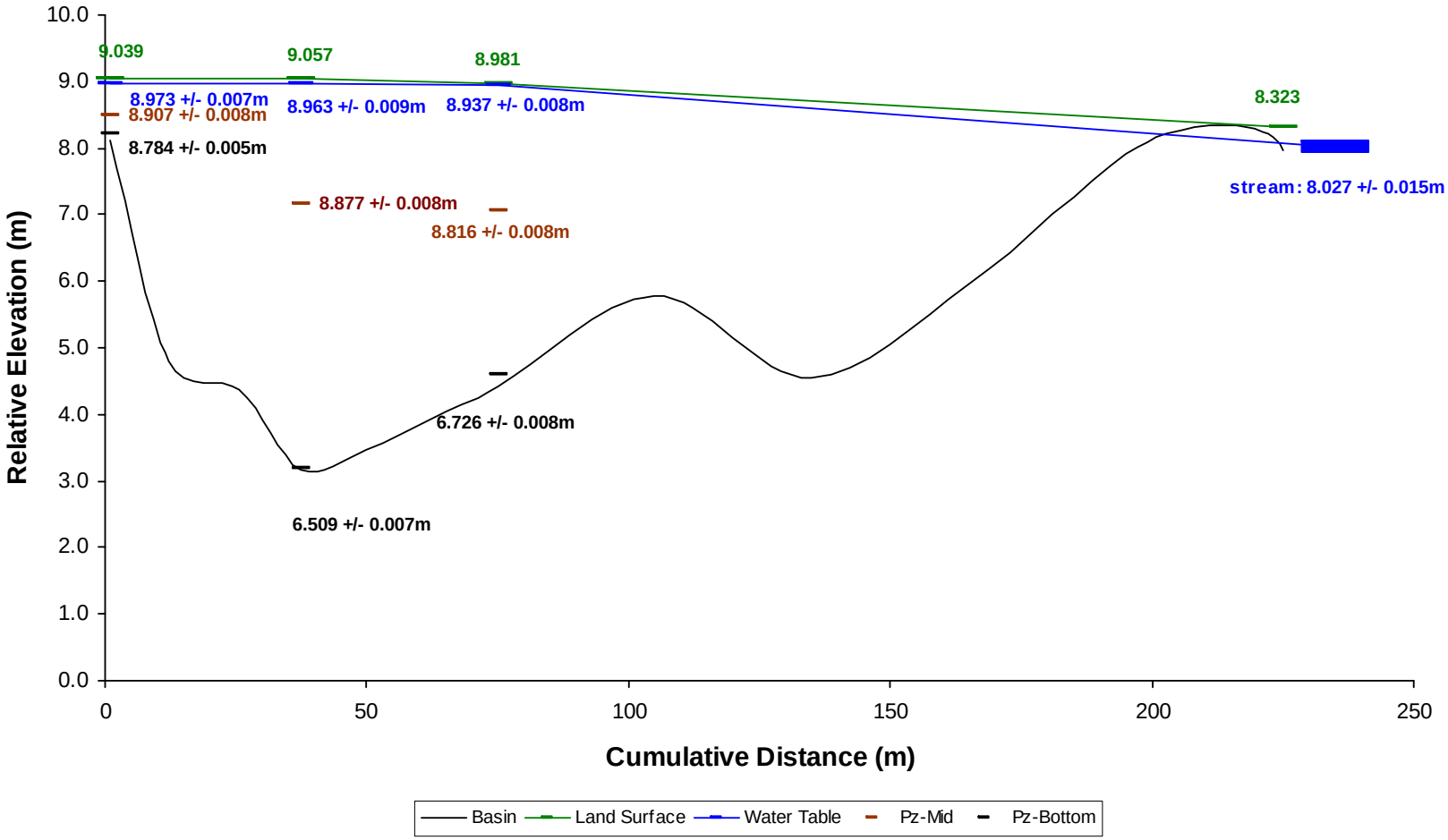

Appendix B.3.i.ii. Hydrologic cross section and flow net for a headwater wetland, (Site HW_H), September (pre-senescence).

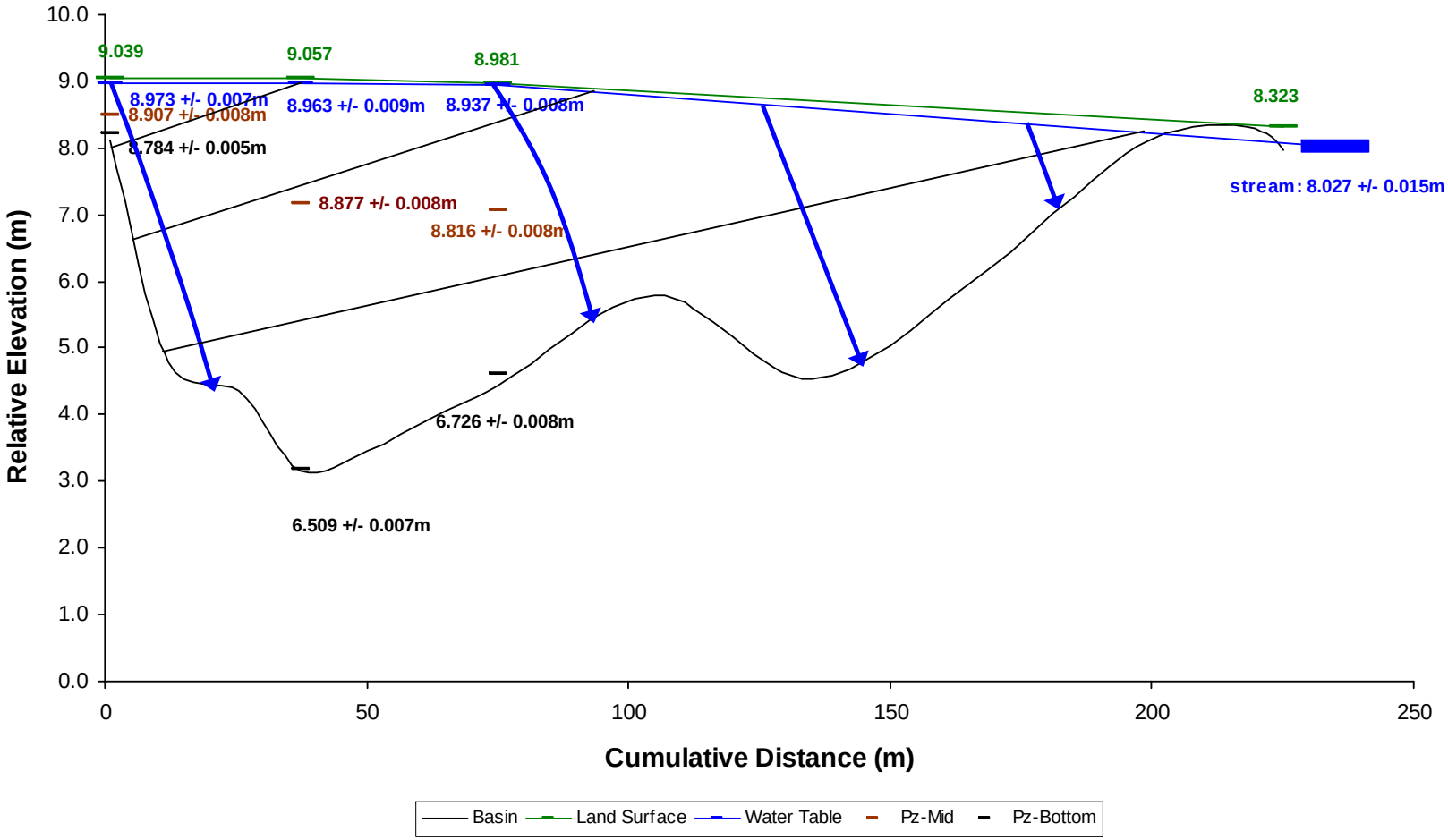

Appendix B.3.j. Hydrologic cross section for a headwater wetland, (Site HW_H), November/December (post-senescence).